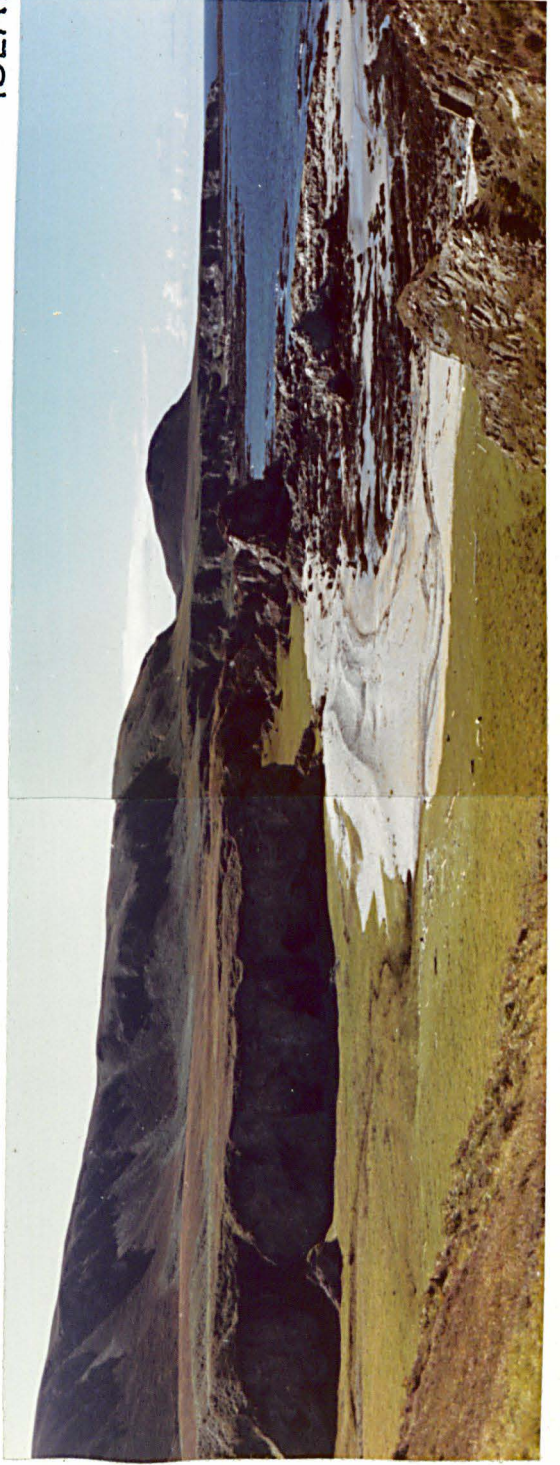


'SEDIMENTATION AND POST-DEPOSITIONAL HISTORY  
OF THE DALRADIAN BONAHAVEN FORMATION OF ISLAY'

by Ian Fairchild, B.Sc.

Thesis submitted to the University of Nottingham  
for the degree of Doctor of Philosophy,  
May, 1978

Rocks in plenty  
In cave, cliff and bay  
Reveal through study  
Another strand  
Long since passed away

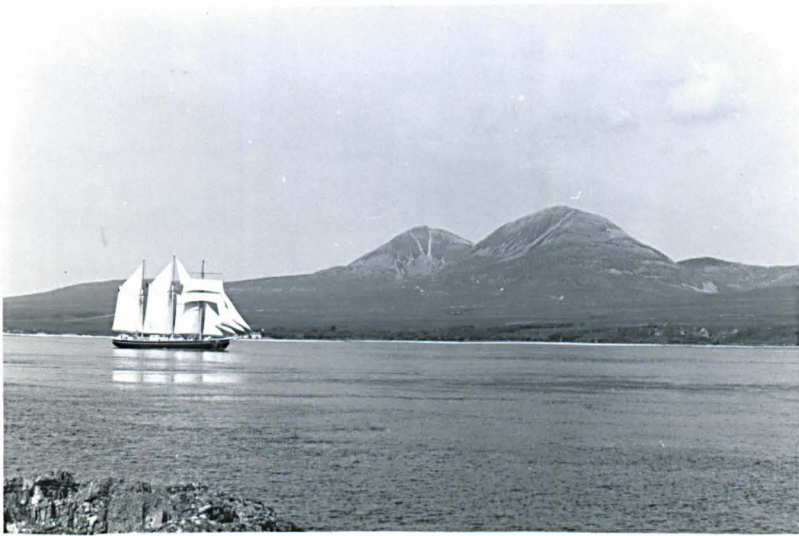




Holocene sedimentation at Bonahaven.

Ruvaal.





'Captain Scott' in the Sound of Islay.



Deer on the northern moors.

## ACKNOWLEDGEMENTS

This work was carried out at the Department of Geology, Nottingham University where facilities were provided by Professor The Lord Energlyn. Financial support was in the form of a Research Studentship from the National Environment Research Council from September 1974 to December 1976. The writing-up was largely carried out at the Department of Geology, Cambridge University during the tenure of a University Demonstratorship.

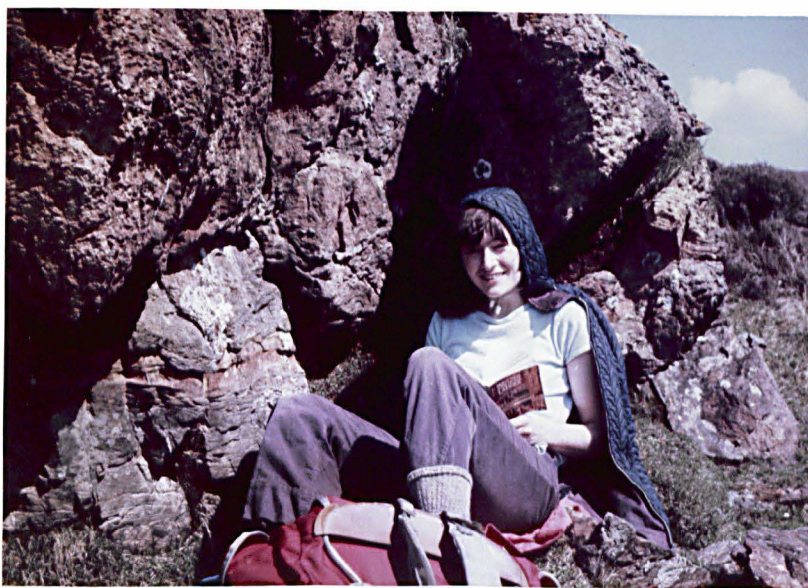
I would like to express my sincere gratitude to Dr. J.A.D. Dickson for his supervision of this work. Tony has always been ready to discuss observations and hypotheses and to provide me with authoritative comment and enthusiastic encouragement. My gratitude extends to all members of the Geology Department at Nottingham for their support and practical help, particularly Andy Swift and Colin Ferguson, and Peter Harvey, who gave many hours of microprobe instruction. David Jones efficiently processed the photographs in this thesis. In the Wolfson Institute, Pat O'Byrne provided able assistance and advice on microprobe work. I would like to thank the members of the Geology Department at Cambridge, particularly Peter Friend, for their encouragement and help during 1977.

Valuable criticism on drafts of various parts of this thesis was received from Dr. J.A.D. Dickson, Dr. C.C. Ferguson, Dr. P.K. Harvey, Dr. P. Bridges and Dr. R.J. Aldridge.

On Islay, the support and friendship of Kate Campbell, Kate MacGhie, and Lily and Dugie MacDougall was a great boon during fieldwork. I salute all the Ruvaal lighthouse keepers past and present that I have known: Jimmy, Billy,

Hamish, Bob, Robert, John, Angus and Malcolm, thanking them for their hospitality.

My family and friends have continually adjusted my perspectives and given me much delight during the course of this work. My wife Susan was a welcome assistant in the field and also pointed out the grave errors in my grammar. More importantly, she constantly renews in me the joy of living.



The outsitting field assistant and a woggler bed

(O.E.: stromatolite).

TABLE OF CONTENTS

CHAPTER 1: Introduction	1
1.1: Geological setting and the objects of research	1
1.2: Organization of the thesis and nomenclature used	3
1.3: History of research into the Bonahaven Formation	5
1.3.1: On the map: the Geological Survey	5
1.3.2: Stratigraphy and lithology	5
1.3.3: Structure	6
1.3.4: Fossils and age determinations	6
1.3.5: Sedimentology	7
1.4: Geography and outcrop	8
CHAPTER 2: Stratigraphy	10
2.1: Introduction	10
2.2: The lower and upper boundaries	11
2.3: The coastal localities	11
2.4: Lateral variations	12
CHAPTER 3: Structure of NE Islay	16
3.1: Historical development	16
3.2: Structural outline	17
3.3: The Islay Anticline	20
3.4: The Bonahaven Fault	22
3.5: Strain indicators and strain history	23
3.5.1: Deformed ooids	23
3.5.2: Cleavage and deformed sandstone dykelets	24
3.5.3: Deformed sedimentary structures	26
3.5.4: Pressure fringe lineations	28
3.5.5: Summary of strain history	31
CHAPTER 4: Sedimentology	32
4.1: Pre-Bonahaven sedimentology	32
4.1.1: Lithological description	32
4.1.1.1: Caol Ila road cutting	32
4.1.1.2: Member 5 of the Port Askaig Tillite	33
4.1.2: Environmental interpretation	33
4.1.3: Conclusions	34
4.2: Bonahaven Formation: members 1 and 2	35
4.2.1: Lithological sequence	35
4.2.2: Interpretation	39
4.2.3: Conclusions	45
4.3: Member 3	46
4.3.1: Introduction to the facies	46
4.3.2: The layered facies	48
4.3.2.1: Mineralogical composition of the sub-facies	48
4.3.2.2: Ripples and cross-lamination	49



6.3.3: Discussion	97
6.4: Member 3	99
6.4.1: Petrography	99
6.4.2: Chemistry	101
6.4.3: Discussion	103
6.5: Member 1	109
6.5.1: Type 1 dolomite	111
6.5.2: Type 2 dolomite	111
6.5.2.1: General feature	111
6.5.2.2: Replacements of mudstone and dolomicrite pebbles	112
6.5.2.3: Intergranular dolomite	115
6.5.3: Type 3 dolomite	121
6.5.4: Discussion	123
6.6: Dolomite in the Precambrian	125
6.7: Palaeotemperatures	126
 CHAPTER 7: Diagenesis and metamorphism	 127
7.1: Cementation	127
7.1.1: Calcite-plugged primary pores	127
7.1.2: Overgrowths on detritus	129
7.1.3: Intergranular calcite	131
7.2: Replacement and neomorphism	131
7.2.1: Ooids	132
7.2.1.1: Dolomite	132
7.2.1.2: Calcite	133
7.2.1.3: Quartz and albite	133
7.2.1.4: Pyrite	134
7.2.2: Replaceive calcite	134
7.2.3: Silicification	135
7.2.3.1: Microquartz	135
7.2.3.2: Glomerulotopes	136
7.2.4: Zoned dolomite rhombs and intergranular dolomite, member 3	137
7.2.4.1: Petrography	137
7.2.4.2: Luminescence and chemistry	139
7.2.4.3: Age of the rhombs	141
7.2.4.4: Causes of the zoning	141
7.2.4.4.1: Theoretical zonal patterns in a closed system	142
7.2.4.4.2: Application of the closed system to the rhombs	144
7.2.4.5: Conclusions	
7.3: Diagenetic solution	146
7.3.1: Intergranular solution	146
7.3.2: Stylolites	147
7.4: Deep burial: the diagenetic-metamorphic transition	148
7.4.1: Introduction	148
7.4.2: Pyrite	150
7.4.3: Albite	151





## ABSTRACT

The Bonahaven Formation is a wedge of shallow marine sediments overlying the late Precambrian glacial deposits of the Port Askaig Tillite. Siliciclastic back-barrier sediments (member 1) are succeeded by a transgressive quartzite (member 2). Probable glauconitized microfossils are present at the top of member 1. Member 3 is a mixed dolomitic-siliciclastic unit representing both wave-dominated submerged environments and tide-dominated sand flats. Stromatolites occur in both situations. The sedimentary facies show very little evidence of cyclicity. The formation of the penecontemporaneous dolomite relates to high or fluctuating salinities, perhaps assisted by stromatolitic algae. Its chemistry implies relatively reducing conditions. The member 4 environment consisted of siliciclastic tidal flats bordered by a dolomite-producing supra-tidal flat. A regression was followed by a transgression to the tidal shelf environment which typified the succeeding Jura Quartzite.

Diagenetic and metamorphic textures are distinguished, and microprobe analyses of the carbonate phases interpreted. Cementing textures are rare, but a long sequence of replacements, chiefly by calcite, dolomite, quartz and albite, can be recognized. Characterization of zoned dolomite crystals leads to clarification of criteria for distinguishing both cementing and replacive textures, and open and closed diagenetic systems. Inclusion-ridden quartz-albite mosaics seem to be a feature of deep burial of this mixed carbonate-clastic sequence. The syn-tectonic solution transfer phenomena, notably lamination-

parallel veins in stromatolites, are classified and interpreted. The biotite present in semi-pelites and sandstones is thought to be congruent with phlogopite forming in more calcareous and dolomitic rocks.

The NE-SW-trending shoreline of a NW landmass lay within, or near to north Islay during deposition of the Bonahaven Formation. Sediment provenance suggests that the Dalradian basin was intra-cratonic.

## CHAPTER 1: INTRODUCTION

### 1.1: Geological setting and the objects of research

The Dalradian Supergroup is a deformed assemblage, primarily of sedimentary rocks of Precambrian to Lower Palaeozoic age, which forms an important part of the Caledonides of Scotland and Ireland. Its place in plate tectonic reconstructions (e.g. Dewey, 1969) depends in part on deductions about sedimentary environments (e.g. Knill, 1963). These are most reliable where detailed sedimentological studies have been made, but such have only recently been attempted (Spencer, 1971a; Anderton, 1974, 1975, 1976). The most straightforward sections of the Dalradian lie in the archipelago, whose main islands are Islay and Jura, situated west of the SW Highlands of Scotland. Here the metamorphism is at its lowest grade and the fold style is open. The stratigraphic units represented here are shown in figure 1-1.

The Lower Dalradian (=Appin Group) has been subdivided by Rast & Litherland (1970) and Basahel (1971), but has not yet been studied sedimentologically in this area.

Anderton (1974) has provided a generalized palaeogeography for the Middle Dalradian (in particular the Islay and Easdale sub-groups). He described the evolution of the sedimentary basin and discussed the detailed sedimentology of the Jura Quartzite and higher horizons. Spencer (1971a) discussed the glacial sedimentology of the Port Askaig Tillite and its importance as a marker horizon throughout Scotland and Ireland. The intervening Bonahaven Formation had not, at the start of my research, been subjected to a detailed sedimentological study, except for some work by Klein (1970a) at the base of the sequence. It was chosen as the subject of this thesis

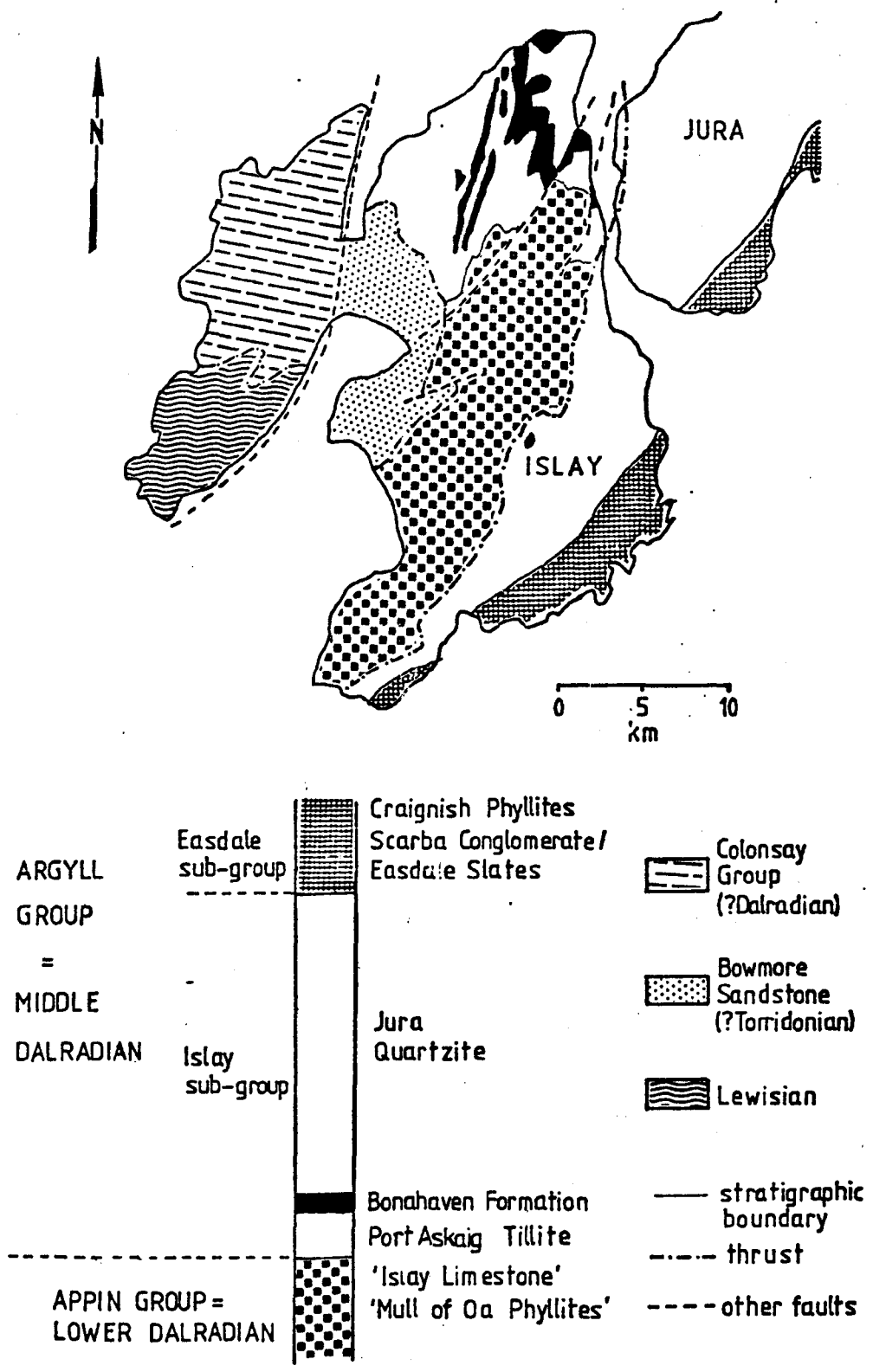


Figure 1-1: Principal solid geology of Islay, incorporating the work of Bailey (1917), Basahel (1971), Anderton (1974), Stewart (1975), Harris & Pitcher (1975), and personal observations.

because a stratigraphic framework existed (Spencer & Spencer, 1972) and good exposures were available.

The Bonahaven Formation consists of clastic rocks of widely varying grain size, most of which are dolomitic; in addition there are some fairly pure dolostones, some of which are stromatolitic. It is at the chlorite grade of regional metamorphism, and although penetratively deformed shows only open folds in general. The fundamental questions which this thesis attempts to answer are: how was this distinctive sedimentary sequence deposited, and how has it reacted to subsequent burial and tectonic stress?

Sedimentological studies need to be viewed in their stratigraphic context in order to obtain the most information. Therefore the major subdivisions (members) of the Formation have been traced over the inland outcrops to reconstruct their geometry. Sedimentary facies have been defined and their lateral persistence studied in the well exposed coastal outcrops. Thus a picture of the vertical sequence and horizontal distribution of the sedimentary environments has been built up and the general palaeogeography compared with the overlying and underlying Formations.

The second main product of my work is a detailed petrographic rock history of this low-grade metamorphic sequence, attempting to distinguish between diagenetic and metamorphic processes. Rather more information is available in the literature concerning mineralogical transformations in deeply buried rocks (Fuchtbauer, 1974; Winkler, 1976) than the textures which develop. In carbonate rocks and mineralogically mature clastic rocks such as those described here few predictable mineral reactions occur. Thus the nature of the described textures is the feature with potentially

Related to both the sedimentology and the subsequent history are chemical considerations. The most useful data obtainable were considered to be analyses of individual carbonate mineral phases using the microprobe, rather than whole rock analyses. This is because the partitioning of some elements between the modal mineral phases is not always clear from whole rock analyses. The results of the microprobe analysis have been used to characterize the depositional environments and, in conjunction with petrographic observations, to decipher the post-depositional history.

## 1.2: Organization of the thesis and nomenclature used

The order of treatment is set out in detail in the table of contents.

### Cross-references

Cross-references to other sections of the thesis are made by simply enclosing the section number in brackets without other explanation, e.g. (7.2.4.), (4.3).

### Figures

A separate numbering scheme for figures in each Chapter is used. Field photographs have a scale of either:

1. a hammer with 5cm markings            or
2. a 6" (15cm) ruler                            or
3. a magnetic compass whose base is 11cm.

### Microprobe analyses

These are detailed in Appendix A, tables A4 and A5. They are referred to in the text as analysis 2, analysis 27B etc.

### Stratigraphic names

The first reference to the Bonahaven Formation was

in the Survey memoir (Wilkinson, 1907) which referred to 'dolomitic beds' within the 'Islay Quartzite Series'. Bailey (1917) coined the name Dolomitic Group which persisted until Spencer & Spencer (1972) proposed a modern formal stratigraphic name, the Bonahaven Dolomite. The lithological term Dolomite is suppressed in this thesis because it gives a false impression of the lithological diversity of the sequence; also dolostone is used instead of the rock name dolomite.

Sections and bed numbers

The coastal sections are lettered as in Spencer & Spencer (1972), (see Enclosures), except that their Section E is here divided into the main Section E and a smaller Section F (see Chapter 2). Stromatolites are referred to to by a letter (Section) followed by a number (horizon) e.g. stromatolites in Section D are D1, D2, etc. Roman numerals are used for Section B to emphasize that these stromatolite horizons are not correlated with those in the other Sections - see enclosures 2 and 3. Bed numbers in member 3 are defined in Enclosures 2 and 3 and are referred to by their number followed by the Section letter, e.g. the lowest beds in Section D are 1D, 2D, 3D, etc.

Lithological terms

The rocks are generally described as they were before deformation, but if noticeably deformed this is also mentioned. Mud refers only to terrigenous material; (dolo-) micrite is used for fine-grained carbonate. The term quartzite is used as a convenient field term for silicic arenites lacking carbonate: many of these are fairly feldspathic (4.6). Dolarenites consist largely of sand-sized dolomicrite clasts. The suffix -topic is used for diagenetic fabric terms as suggested by Friedman (1965).

## Sedimentary structures

Cross-stratification and cross-lamination refer to cross-sets formed by megaripples and ripples respectively; massive refers to structureless. Other usage mostly conforms with that of Reineck & Singh (1973), in particular their bedding thickness nomenclature: medium laminated = 0.3-1cm, thick laminated = 1-3cm, thin bedded = 3-10cm, medium bedded = 10-30cm etc.

### 1.3: History of research into the Bonahaven Formation

#### 1.3.1: On the map: the Geological Survey

At the turn of the century Islay was mapped over a period of eight years by S.B. Wilkinson under the direction of B.N. Peach for the Geological Survey (Wilkinson, 1907). This was a great advance on previous knowledge, but the account had deficiencies in the stratigraphic and structural interpretation, which are discussed further in Chapter 3.

Peach was convinced that the Bonahaven Formation was to be correlated with the Cambrian succession of the NW Highlands. The 'dolomitic beds' were taken to be equivalent to the Cambrian Furoid Beds and were said to contain worm casts on the bedding planes. Furthermore, member 2 was reported to contain 'worm pipes' like that of the 'pipe rock' of the NW Highlands. It is clear now that the worm casts are syneresis crack casts (Spencer & Spencer, 1972) and that no remotely convincing worm pipes exist.

#### 1.3.2: Stratigraphy and lithology

The subdivisions now known as members 1, 2 and 3 (fig. 2-1) were originally made by the Survey (Wilkinson, 1907), who also gave a brief lithological description. Allison (1933)

separated out 'grey flags' at the top of the sequence (member 4) and divided member 3 into a lower unit of 'sandy dolomite' and an upper unit of 'fine-grained dolomite'. Spencer & Spencer (1972) defined the members, gave more detailed field descriptions and numbered the stromatolite horizons.

### 1.3.3: Structure

A survey of the literature relating to the structure of the Dalradian of Islay is given in Chapter 3. The only structural paper restricted in scope to the Bonahaven Formation is that of Borradaile & Johnson (1973) who made strain estimates in member 3.

### 1.3.4: Fossils and age determinations

The Survey reported no success in the search for Cambrian body fossils in the Formation, a situation which has not altered since; the trace fossils they reported in member 3 we now know to be inorganic structures. Klein (1970a) figured a drawing of supposed burrows from member 1, but I have been unable to confirm this: on the contrary the constant undisturbed sedimentary lamination implies that an infauna was not present.

Leggo & Pidgeon (1970) reported a Rb-Sr whole-rock isochron (a revised estimate of that of Leggo et al., 1969) of  $570 \pm 20$  m.a., from siltstones of member 1. They suggested that this figure probably represents a diagenetic age.

Downie et al. (1971) recorded acritarchs from member 3, which could be late Precambrian or early Cambrian in age.

Peach & Horne (1930) were the first to mention the stromatolite horizons in member 3 and expressed the hope that they might be used in age determinations. Hackman & Knill (1962) provided a limited account of the stromatolites.

Spencer & Spencer (1972) described the stromatolite horizons in more detail and compared a columnar stromatolite specimen with Jurusania which Russian workers regard as a characteristic group of the Vendian (latest Precambrian). However Jurusania is probably not an appropriate name for any of the stromatolites in the sequence (see Chapter 4).

Anderton (1974) suggested that as the Lower Cambrian succession in the NW Highlands records a transgression, the time-equivalent rocks in the SW Highlands should show an increasing depth of deposition at this time. The most likely horizon seems to be at the boundary of the Craignish Phyllites with the Crinan Grits, several thousand metres stratigraphically above the Bonahaven Formation.

In concurrence with the above weight of evidence, Harris & Pitcher (1975) concluded that the Formation is of Vendian age.

A.R. MacGregor of St. Andrew's University has recently been studying member 3, particularly with regard to stromatolite palaeoecology. Accordingly the stromatolites have been given a less comprehensive treatment in my work than would otherwise have been the case.

#### 1.3.5: Sedimentology

Klein (1970a) was the first to attempt a detailed sedimentological interpretation of part of the Bonahaven Formation. Although this paper is ostensibly concerned with the 'Lower fine-grained Quartzite' (Bailey, 1917; =member 5 of the Port Askaig Tillite, Spencer, 1971a) it mostly deals with the member 1 outcrops of the Bonahaven Formation at Caol Ila, but not at Bonahaven (see Spencer, 1971b). Klein recorded sub-tidal and inter-tidal flat environments which

he related to a general model of inter-tidal sedimentation. The application of this model to the rocks in this area is critically discussed in Chapter 4.

Spencer & Spencer (1972) produced some sedimentological information, but theirs was primarily a stratigraphic account.

#### 1.4: Geography and outcrop

Figure 1-2 shows selected geographic features of NE Islay. A fertile low-lying area in the south of the area, flanking the A846 Port Askaig-Bridgend road, is based on the slates and limestones of the Lower Dalradian. Northwards lie barren moorland hills with a shallow peat cover occasionally penetrated by outcrops of the Port Askaig Tillite, Bonahaven Formation and Jura Quartzite. The far eastern area, as far north as Bonahaven, is farmland, mostly rough pasture with reasonable exposure. Coastal areas are generally very well exposed. On the east coast there is a narrow foreshore and steep sea cliffs whereas on the north coast there is a wider foreshore with excellent exposure on the cliffs of the famous raised beaches.

All the exposures of the Bonahaven Formation are natural. Detailed stratal sequences can be established by large scale mapping of coastal exposures, the frequent Tertiary dolerite dykes (Walker, 1960) being very useful geographic markers. Inland exposures are scattered on steep hillsides, small hillocks and in some stream sections. These inland exposures are not only fragmentary, but biased as dolostones and quartzites are very much over-represented compared with the complete coastal sections.

The most accessible exposures are the coastal sections at Caol Ila and Bonahaven which are within a few hundred metres of the nearest road. Most of the inland exposures

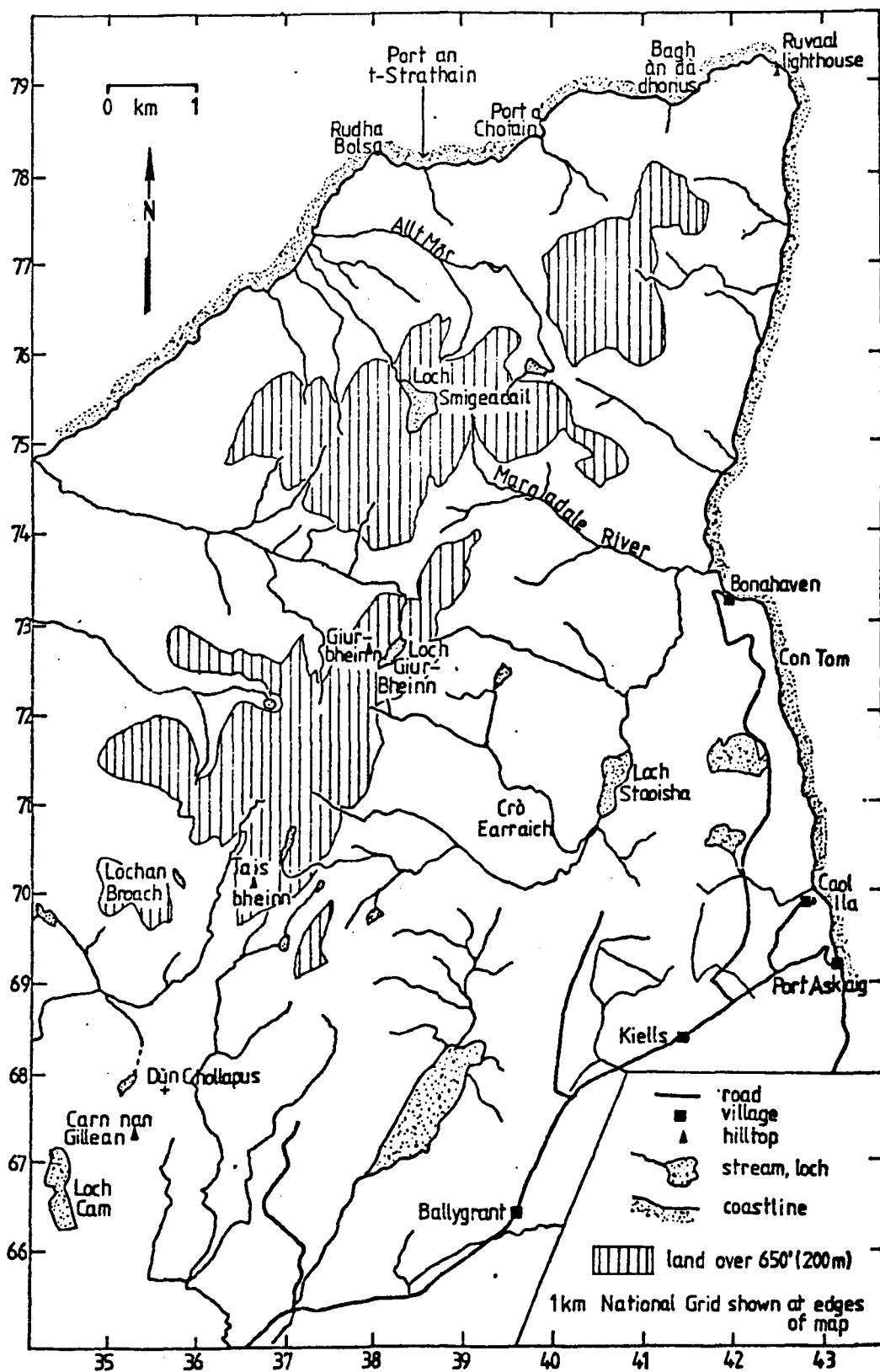


Figure 1-2: Selected geographic features of NE Islay, showing place names mentioned in the text of this thesis.

are several kilometres from the nearest road, but here are to be found the most accessible exposures of the dolostone in member 4 (fig. 2-1), north of Loch Cam. The best exposures of members 3 and 4 are on the north coast which may be reached either on foot from Bonahaven, or by small boat from Port Askaig or Caol Ila to Ruvaal Lighthouse and thence on foot. Approaching Section C from the east, the most direct route is to descend the cliff by a steep path which commences at the point where the telegraph wire passes over the cliff. Further west, the cliffs are lower and access to the shore may be gained at numerous points. The clearest exposures on both the north and east coasts are near to or above High Water Mark; access is hardly affected by the state of the tide at any point.

## CHAPTER 2: STRATIGRAPHY

### 2.1: Introduction

In this Chapter the lithological units that make up the Bonahaven Formation are introduced and important new information regarding their geometry is presented. This data will be used later in the palaeogeographic interpretation.

The Bonahaven Formation is essentially limited to northern Islay. Further north it is unexposed, lying beneath the sea for a considerable distance until the mainland is reached where its distinctive character is lost. Further south on Islay it is largely faulted out by the Beinn Bhan thrust (Basahel, 1971). It emerges from this fault line in only one locality: 1km. west of Beinn Bhan in central Islay where there are exposures on the banks of a lochan (grid reference NR 393 562).

The Bonahaven Formation rests on the Port Askaig Tillite and passes up into the Jura Quartzite (fig. 1-1).

The Port Askaig Tillite has been given an exhaustive stratigraphic treatment by Spencer (1971a) who divided it into 5 Members. It consists of a series of mixtites and some conglomerates, with interbeds of dolostones and quartzites.

The Bonahaven Formation was defined and divided into 4 informal members by Spencer & Spencer (1972). The use of these members is retained here.

The Jura Quartzite (Anderton, 1974, 1976) in this area consists of thick-bedded quartzite with rare beds of conglomerate or mudstone.

## 2.2: The lower and upper boundaries

The base of the Bonahaven Formation is easily recognized at two localities on the east coast. At Caol Ila (NR 4290 7020), the first of these, a series of thickly bedded, rather massive quartzites (Member 5 of the Port Askaig Tillite) pass sharply and conformably upward into a series of cleaved silty mudstones with thin lenticular silt or sand laminae. At the second locality, north of Con Tom (NR 4237 7270), a similar situation exists, but stratigraphically intermediate between the quartzites and the silty cleaved mudstones are 2m of thin parallel laminated fine-grained sandstone and mudstone which is included here with the Bonahaven Formation. The problems of establishing the base of the sequence inland will be mentioned later.

The upper boundary of the Bonahaven Formation is well exposed at several localities on the north coast (e.g. NR 4150 7895) where cleaved mudstones containing occasional thin beds of fine-grained sandstone pass sharply upward into quartzites of the Jura Quartzite Formation. There is an intercalation of mudstone 2m higher in the Jura Quartzite.

In each case way-up criteria are present in stratigraphically adjacent parts of the Bonahaven Formation and indicate that the sequences are uninverted.

## 2.3: The coastal localities

The top of the Formation is absent from the east coast exposures, whilst the bottom is unexposed on the north coast (see enclosure 1). Spencer & Spencer (1972) labelled five coastal sections A to E (a usage followed here, fig. 2-2), and figured the sequence from each of these sections. My more detailed work has shown their

observations to be generally valid except for Section E, where the presence of much minor folding and faulting make it more difficult to piece together the stratigraphy. Their member 3 section is largely erroneous here; also they apparently failed to recognise that there is a major fault near the western end of the section to the west of which the entire section from the base is repeated, although complexly folded. This is discussed further in Chapter 3. The extreme western section is here referred to as Section F (fig. 2-2).

Figure 2-1 shows a generalized complete sequence of the Bonahaven Formation based on sections A and B for the lower part and sections C and D for the upper part. Detailed lithological descriptions of the sequence are made in Chapter 4. The subdivisions ('units') of members 1 and 4 are made here for the first time. Spencer & Spencer (1972) numbered the stromatolite horizons in member 3. Their usage in Sections C, D and E has been adhered to as far as possible except where the new work has shown their correlations to be in error. The stromatolites in Section B have been re-numbered here with Roman numerals to emphasize the difference between this section and those on the north coast. In addition, all the beds in member 3 have been numbered (see enclosures 2 and 3), one scheme applying to Sections C, D and E together and another to Section B.

#### 2.4: Lateral variations

The thickness of two or more members of the Formation can be estimated at a number of inland localities (fig. 2-2). As exposure is relatively poor inland most of the columns in this figure represent traverses along as well as across

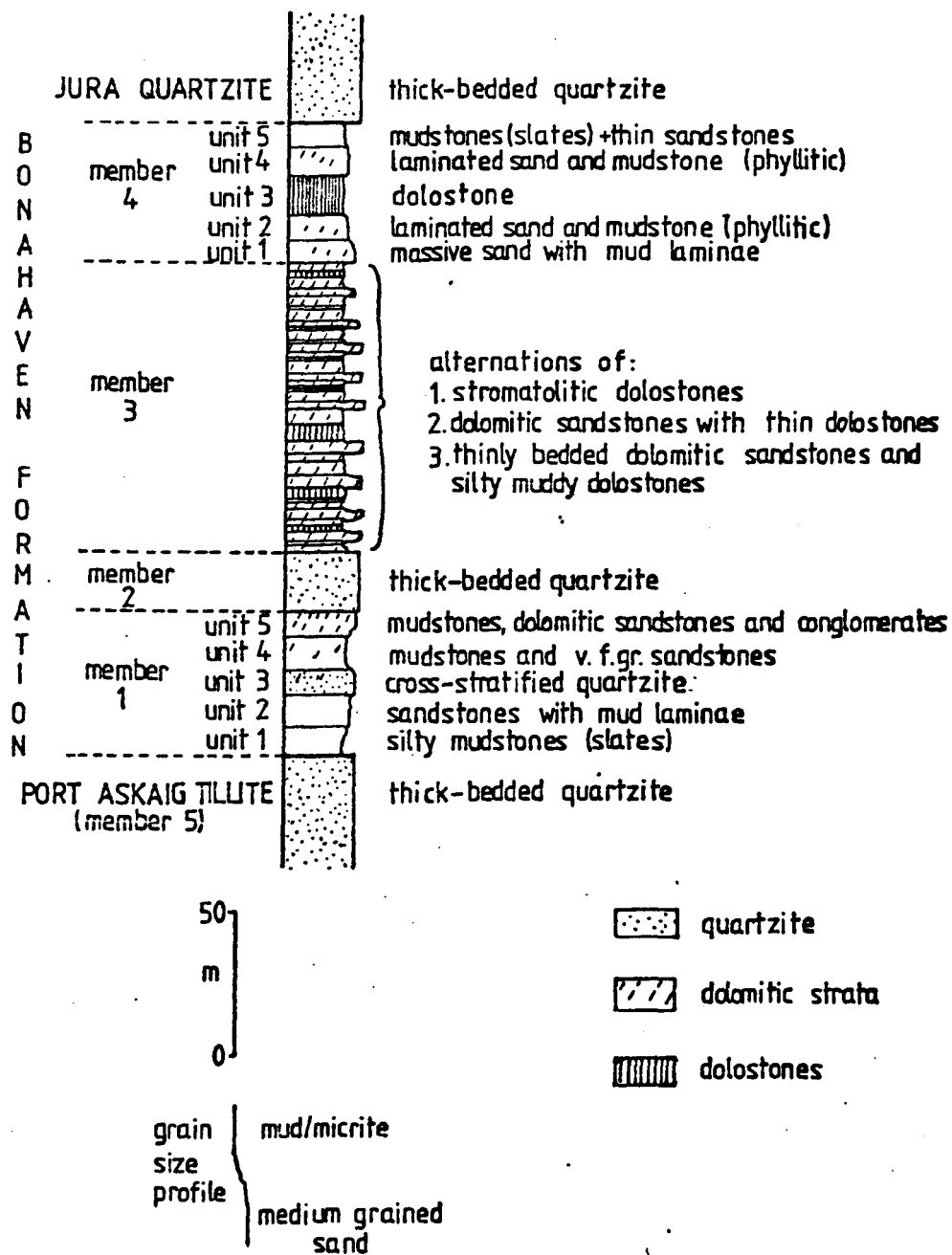


Figure 2-1: Generalized complete sequence of the Bonahaven Formation.

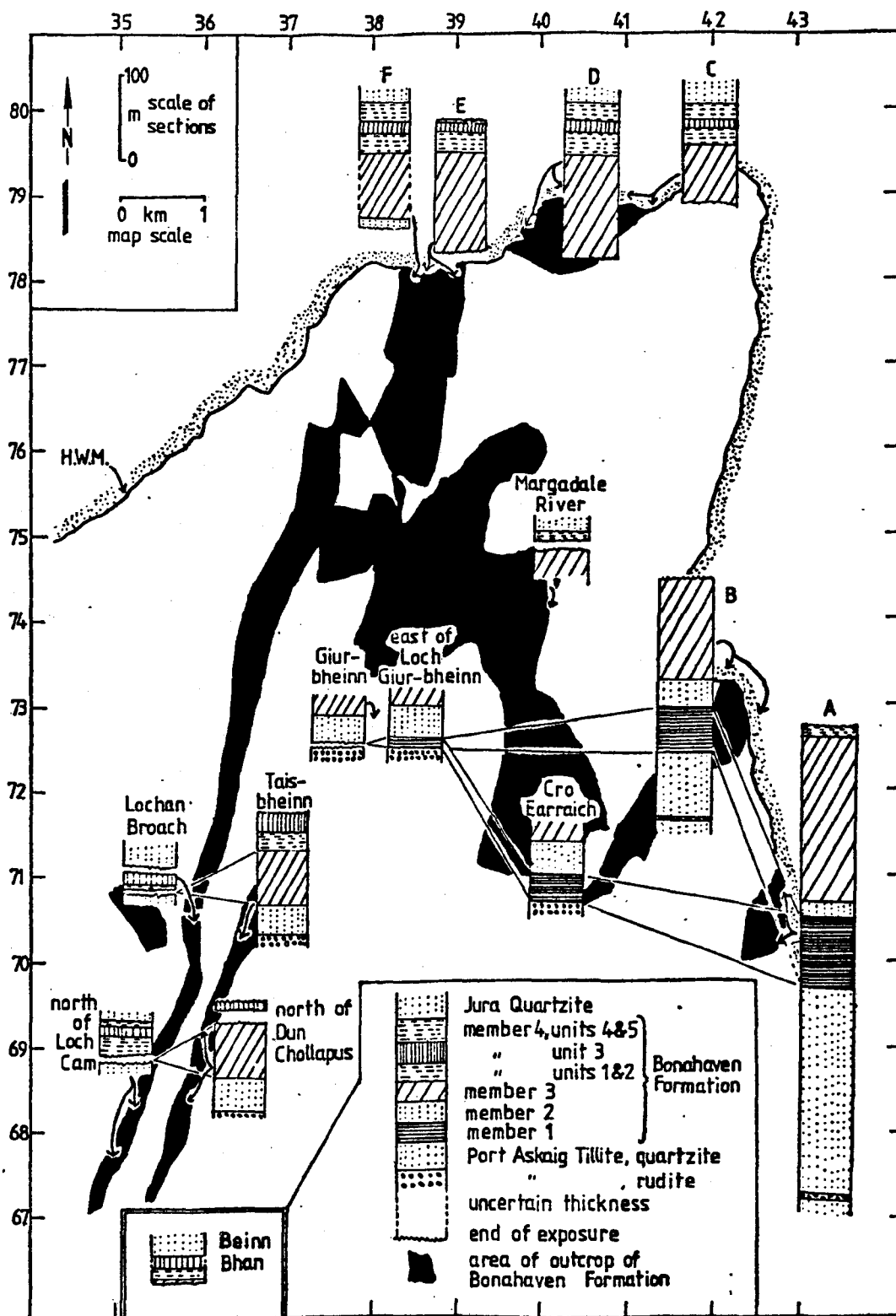


Figure 2-2: Stratigraphic sections of the Bonahaven Formation. Arrows indicate the location of the section in cases where the column is not directly over the location.

the strike in a given area. The inferred E-W changes in the sequence are illustrated in figure 2-3.

The top of the Port Askaig Tillite varies in facies. The east coast exposures at this horizon show a thick (200m) sequence of massive, thick-bedded quartzites with only thin boulder-bearing horizons (Spencer, 1971a). However further west, between Loch Giur-bheinn and Cro Earraich, there is usually a mixtite or pebbly quartzite several metres thick at the top of the Tillite. Further west still, there is a massive, slightly muddy sandstone with occasional granite pebbles.

The thickest section of member 1 of the Bonahaven Formation is at Caol Ila, where all five units are present. At the northern coastal crop south of Bonahaven, the sequence is thinner and unit 3 is apparently not present. Inland to the west the member thins and is not exposed at all west of a NNE-SSW line through Loch Giur-bheinn. It is the lowest parts of member 1 that seem to be lost first as the member is traced westwards. Thus in the Cro Earraich section (fig. 2-2) and all other localities west of Loch Staoisha, units 1, 2 and 3 are missing. Also, at the westernmost exposure of the member, immediately east of Loch Giur-bheinn, the sandstones and mudcracked mudstones exposed here (lithologically like unit 5 of the coastal outcrops) contain spherules (see Chapter 5) which occur only at the the top of member 1 on the coast.

Member 2 is present throughout the area, but changes from the massive, thick bedded quartzite of the east coast to a ripple-marked and cross-stratified quartzite particularly well exposed in Cro Earraich, the summit ridge

of Giur-bheinn and along the outcrop strips in the far west of the area. Where member 1 is absent in the western area it becomes impossible to prove that all of member 2 belongs to the Bonahaven Formation rather than with the Port Askaig Tillite as similar quartzites do occur within the Tillite. The problems of establishing time lines at the base of the Bonahaven Formation are discussed in Chapter 8.

Member 3, the characteristic stromatolite-bearing part of the Formation appears to be thickest at Caol Ila, thinner to the NW and absent in the far western outcrop strip from Loch Cam to Lochan Broach. Internally the numbered succession of beds (enclosures 2 and 3) correlates fairly well between Section E and Section C. However the top 15m of Section D, geographically intermediate between Sections C and E, does not correlate nearly so well. The fragments of the sequence which can be worked out in Section F do not correlate with section E and may be rather thinner. As mentioned earlier, individual beds are not correlatable between Section B and the north coast. Member 3 is poorly exposed in Section A, but seems to be very thick (150-200m), sandstone beds forming a smaller proportion of its thickness than in the north coast member 3 exposures. At Beinn Bhan in central Islay member 3 is represented by thinly bedded dolomitic sandstones and synaeresis-cracked mudstones.

Unit 1 of member 4 is seen to consist of a massive silty sandstone at Caol Ila, NW of Loch Staoisha, and on the north coast. On the north coast it is succeeded by thinly bedded (phyllitic) sandstones and mudstones (unit 2). Inland, exposures of unit 2 are poor, slates being

seen occasionally below unit 3. At Beinn Bhan there are thinly bedded sandstones and mudstones, ripple-marked and mud-cracked, below unit 3.

Unit 3 of member 4, a distinctive creamy-weathering dolostone is very well exposed on the north coast and in extensive outcrops inland in the western area. Some swallow holes also occur. Spencer & Spencer (1972) reported that it is present at the top of Section A (NR 428 714). However the dolostone at that locality occurs north of the fault upthrowing the Portaskaig Tillite to the north and is interbedded with slate and quartzite stratigraphically below the Tillite. In fact unit 3 is not exposed at all SE of Loch Smigeadail, although no complete member 4 sections are seen. The nearest to a complete section is the Margadale River sequence where less than 5m of the section are missing, but the dolostone is very unlikely to belong in the missing interval as even soft-weathering phyllites are exposed in the stream. Thus it is strongly suggested that unit 3 is absent in the eastern area, as is depicted in figure 2-3.

Heterogeneous phyllitic rocks (unit 4, member 4), probably originally thinly bedded sand and mudstone, are seen in the Margadale River and the north coast and are succeeded by slates with some thin sandstones (unit 5, member 4), seen at several inland localities as well as on the north coast immediately below the Jura Quartzite.

The most significant lateral changes in the sequence are depicted in figure 2-3. Note the overall thinning of the sequence to the west, but the thinning to the east of member 4, especially the absence of unit 3.

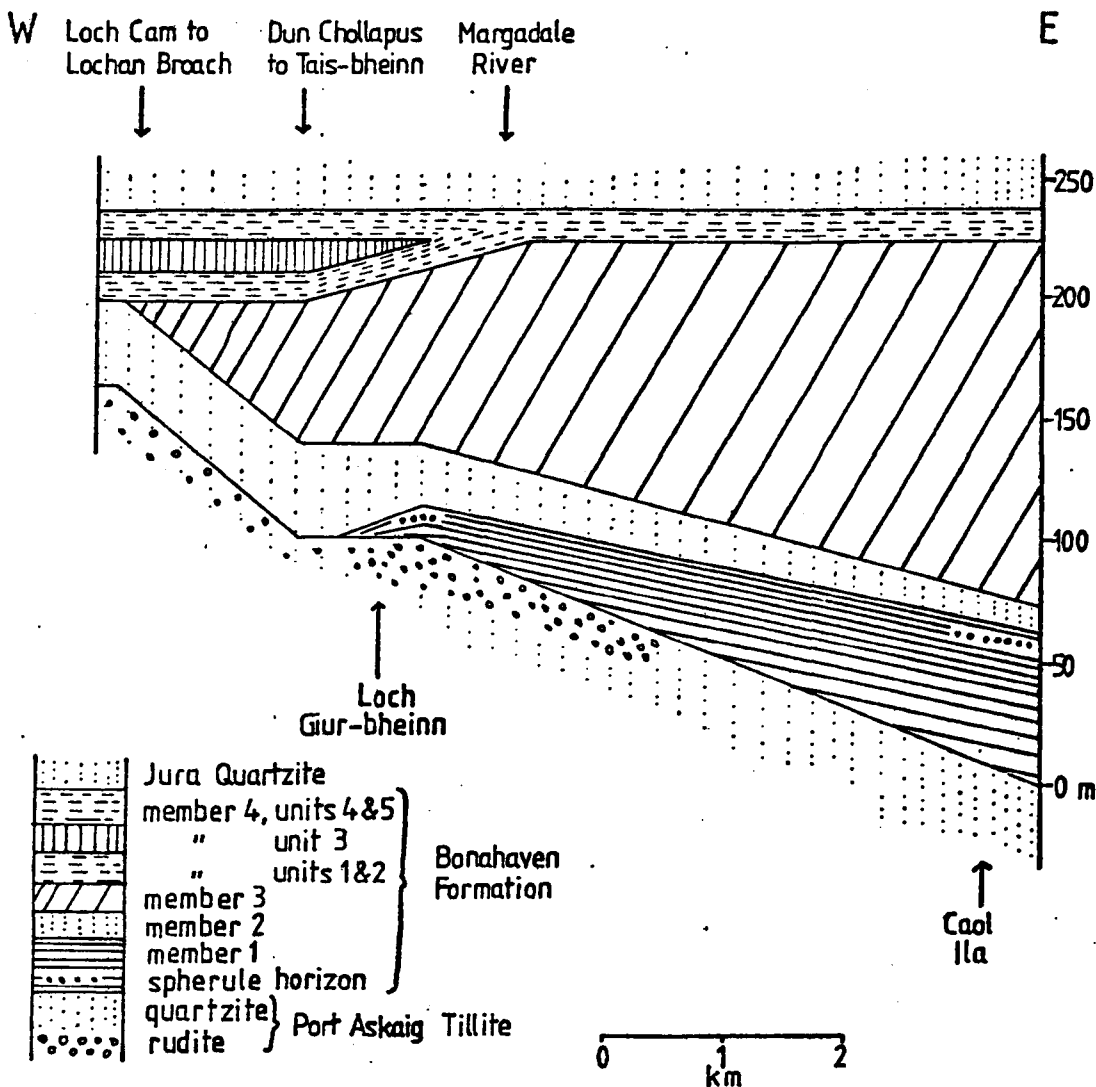


Figure 2-3: Schematic E-W palinspastic section of the Bonahaven Formation. The inferred changes are:

1. The top of the Portaskaig Tillite shows facies variations.
2. Member 1 (composed of various clastic lithologies) thins to the west by the wasting of its lower units and is absent altogether in the western area.
3. Member 2, a quartzite, thickens slightly from Caol Ila to the west (and NW).
4. Member 3, the distinctive dolomitic and stromatolite-bearing part of the sequence thins to the west (and NW) dying out altogether in the far western area.
5. Member 4 thins to the east chiefly by the loss of the unit 3 dolostone.

### CHAPTER 3: STRUCTURE OF NE ISLAY

#### 3.1: Historical development

The Geological Survey (Wilkinson, 1907) recognized the broad structure of Islay as anticlinal and more or less correctly interpreted the Dalradian stratigraphy from the Bonahaven Formation downwards. However the Jura Quartzite exposures on Islay were equated with those of Member 5 of the Port Askaig Tillite leaving the Bonahaven Formation as the stratigraphically highest rocks exposed. This necessitated a very complex structure in the north of the island and isoclinal folding was frequently mentioned, although it can never have been seen.

E.B. Bailey, in a brilliant work (1917), correctly interpreted the stratigraphy and introduced the concept of the Islay Anticline as it is accepted to-day. The discussion of his paper shows that his views were not accepted by many people at the time, although B.N. Peach (in Peach & Horne, 1930) later conceded those parts of Bailey's arguments that are relevant here.

Green (1924) proposed that Islay had a synclinal structure and equated the Port Askaig Tillite with the Bowmore Sandstone, considering that they were unconformable on a series of rocks which included the Bonahaven Formation. This was refuted by Bailey and others in discussion and later by Gregory (1928). Allison (1933) vindicated Bailey by the use of way-up structures in the Bonahaven Formation.

Basahel (1971) mapped a large part of southern Islay and produced a structural interpretation. He suggested that the major folding on Islay was the second phase and

recognized the presence of slides developed during the folding. However Roberts (1974), in his overall view of the structure of the SW Highlands of Scotland regarded the formation of the major folds on Islay as the first tectonic event ( $f_1$ ). This formed part of his 'primary deformation' during which the rock mass was penetratively deformed, with four separate phases of folding recognizable on the mainland. On Islay, there was movement to the NW (during formation of the Islay Anticline) along the line of the Loch Skerrols thrust which bounds the Dalradian outcrop to the west. Roberts correlated the late-stage, minor crenulation cleavage on Islay with similar structures on the mainland which form the second of four fold phases which constitute the 'secondary deformation'.

An attempt to quantify the amount of deformation was made by Borradaile & Johnson (1973). They estimated finite strain in thinly interbedded dolomitic sandstones and silty mudstones of member 3 by the degree of rotation of sandstone contraction crack casts toward parallelism with the main cleavage.

### 3.2: Structural outline

The structure is illustrated on the maps and section forming Enclosure 1 at the back of this thesis.

Although the rocks are penetratively deformed, the only significant folding is on a large scale. In the SE of the area, the beds dip uniformly northwards, their outcrop being determined by two major NE-SW trending faults. Proceeding westwards, there are a series of gentle folds followed by a tighter anticline with a faulted, near vertical, western limb.

### CHAPTER 3: STRUCTURE OF NE ISLAY

#### 3.1: Historical development

The Geological Survey (Wilkinson, 1907) recognized the broad structure of Islay as anticlinal and more or less correctly interpreted the Dalradian stratigraphy from the Bonahaven Formation downwards. However the Jura Quartzite exposures on Islay were equated with those of Member 5 of the Port Askaig Tillite leaving the Bonahaven Formation as the stratigraphically highest rocks exposed. This necessitated a very complex structure in the north of the island and isoclinal folding was frequently mentioned, although it can never have been seen.

E.B. Bailey, in a brilliant work (1917), correctly interpreted the stratigraphy and introduced the concept of the Islay Anticline as it is accepted to-day. The discussion of his paper shows that his views were not accepted by many people at the time, although B.N. Peach (in Peach & Horne, 1930) later conceded those parts of Bailey's arguments that are relevant here.

Green (1924) proposed that Islay had a synclinal structure and equated the Port Askaig Tillite with the Bowmore Sandstone, considering that they were unconformable on a series of rocks which included the Bonahaven Formation. This was refuted by Bailey and others in discussion and later by Gregory (1928). Allison (1933) vindicated Bailey by the use of way-up structures in the Bonahaven Formation.

Basahel (1971) mapped a large part of southern Islay and produced a structural interpretation. He suggested that the major folding on Islay was the second phase and

recognized the presence of slides developed during the folding. However Roberts (1974), in his overall view of the structure of the SW Highlands of Scotland regarded the formation of the major folds on Islay as the first tectonic event ( $f_1$ ). This formed part of his 'primary deformation' during which the rock mass was penetratively deformed, with four separate phases of folding recognizable on the mainland. On Islay, there was movement to the NW (during formation of the Islay Anticline) along the line of the Loch Skerrols thrust which bounds the Dalradian outcrop to the west. Roberts correlated the late-stage, minor crenulation cleavage on Islay with similar structures on the mainland which form the second of four fold phases which constitute the 'secondary deformation'.

An attempt to quantify the amount of deformation was made by Borradaile & Johnson (1973). They estimated finite strain in thinly interbedded dolomitic sandstones and silty mudstones of member 3 by the degree of rotation of sandstone contraction crack casts toward parallelism with the main cleavage.

### 3.2: Structural outline

The structure is illustrated on the maps and section forming Enclosure 1 at the back of this thesis.

Although the rocks are penetratively deformed, the only significant folding is on a large scale. In the SE of the area, the beds dip uniformly northwards, their outcrop being determined by two major NE-SW trending faults. Proceeding westwards, there are a series of gentle folds followed by a tighter anticline with a faulted, near vertical, western limb.

Stereographic projections of poles to bedding and cleavage are shown in figure 3-1. Readings taken east of Loch Giur-bheinn across the Giur-bheinn anticline (fig. 3-1a) indicate that this fold is cylindrical, with axial planar cleavage and a plunge of  $14^{\circ}$  to  $036^{\circ}$ . In contrast the Section D anticline on the north coast (fig. 3-1b) has an axis plunging  $9^{\circ}$  to  $214^{\circ}$ . Section E contains a number of folds (with wavelengths of a few or a few tens of metres) which plot out similarly (fig. 3-1c), although cylindrical folding is less clearly demonstrated here. The southerly plunge of the fold hinges on the north coast, although claimed to be a local effect by Borradaile & Johnson (1973), is matched by southerly plunging bedding-cleavage intersections to the north in the Garvellachs (data of Spencer, 1971a).

The strike of the slaty cleavage varies irregularly from  $030^{\circ}$  to  $060^{\circ}$  throughout the area and is fanned (fig. 3-1d) from a moderate NW dip on the east coast, through the vertical west of Loch Staoisha to a SE dip west of the line of the Giur-bheinn anticline. An anomalous area with non-Caledonoid trend is discussed in section 3.5.2..

In more highly deformed banded quartzite and phyllite (units 2 and 4, member 4) in various localities cleavage was developed parallel to bedding rather than in the regional orientation. The bedding in such cases is fairly uniformly dipping, although with minor buckles.

A second, crenulation cleavage, intermittently present in slaty lithologies throughout the area, dips at a moderate angle to the east in the SE area, and dips NW on the north coast, but is more variable here. It is axial planar to some minor folds of the first cleavage. It is possible

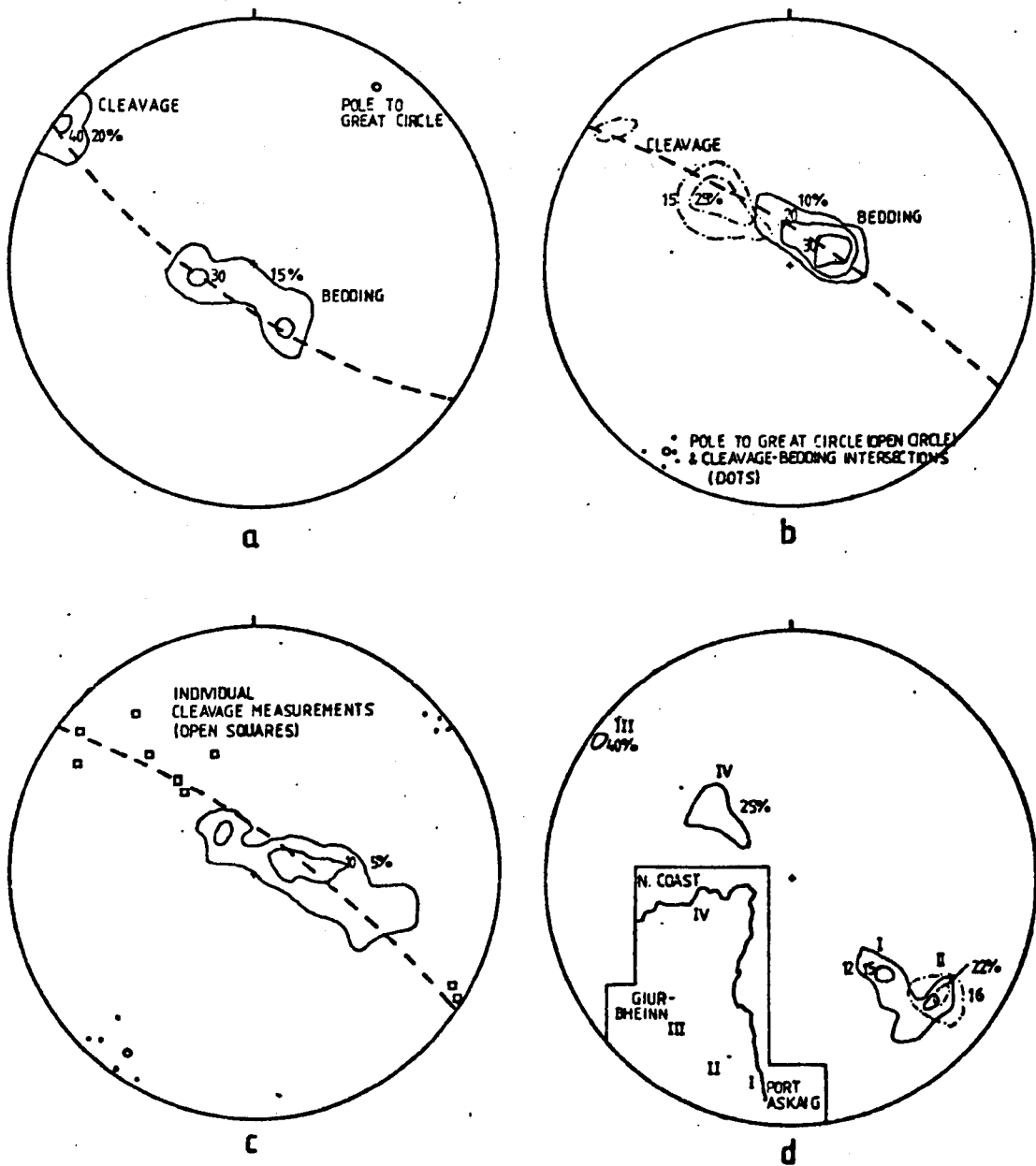


Figure 3-1: Stereographic projections of bedding and slaty cleavage poles. a. Giur-bheinn anticline (cleavage 19 readings, bedding 25 readings). b. Section D anticline (cleavage 24 readings, bedding 80 readings). c. Section E includes many folds of wavelength 10-100m (cleavage 9 readings, bedding 125 readings). d. Slaty cleavage measurements from four different areas in NE Islay. (shown on inset map). Number of readings: I(97), II(64), III(19), IV(24).

that its change in orientation was determined by the fanning of the first cleavage, crenulations being more readily developed with axial planes at a high angle to the first cleavage.

Henceforth the main cleavage is referred to as  $S_1$  (belonging to deformation  $D_1$ ) whilst the crenulation cleavage is termed  $S_2$  (formed during deformation  $D_2$ ).

Most of the faults in the area are regarded as post-tectonic, but one, here named the Bolsa fault, possesses some characteristics which suggest that it may have formed during  $D_1$ . The line of the Bolsa fault was mapped by Bailey (1917) from near Dun Chollapus in the south of the area, as far north as Loch Smigeadail. I have recognised its continuation to the north coast, giving a total length of 11km. On the north shore, the fault zone is very complex so the map (Enclosure 1) is almost certainly an oversimplification. However, there is clearly a major break separating Sections E and F with downthrow to the east. On the cliff-line the Section F strata show only a gradual steepening of their dip to the west away from the fault, but on the lower shore they are tightly folded, becoming vertical near the fault-line where there is much shearing and quartz veining. Inland the fault line can be closely fixed, although unexposed in the stream section Allt Mor and then is displaced 200m to the west by an E-W fault, before continuing southwards. In the SW area in particular, it is noticeable that the structure is approximately a strike fault, the bedding on either side of it varying from a steep normal to steep reversed dip, constantly younging to the west. Near Dun Chollapus it does cross-cut the bedding, truncating members 4 and 3 successively to the south.

As it is intimately associated with a zone of deformation much more intense than anywhere else in NE Islay away from the Loch Skerrols thrust, and cuts a long path parallel to the strike of a belt of near vertical rocks, I propose that the Bolsa fault was formed during  $D_1$ . However, the fault plane itself is not clearly folded, so the evidence is largely indirect. Basahel (1971) recognised three faults developed during the main folding in southern Islay with which the Bolsa fault may be analogous. The Beinn Bhan thrust is important here as it cuts out the Bonahaven Formation in central and southern Islay.

Other faults belong chiefly to two sets (NNW-SSE & WNW-ESE) and have a normal movement sense as deduced from exposed fault planes and mapped fault lines. At the eastern end of Section E, a major fault of the NNW-SSE set is offset by, and is thus probably earlier than, a minor fault of the other set. These faults seem to post-date the folding.

### 3.3: The Islay Anticline

The concept of the Islay Anticline, as illustrated in cross-section by Bailey (1917), is in accord with the work presented here, but it is felt that some clarification is required. Bailey did not show the line of the trace of the axial surface on his map and this has been the source of confusion later. The disposition of Lower and Middle Dalradian on Islay (fig 1-1) suggests at first sight a NNE plunging anticline reaching the coast near Bonahaven (fig. 3-2b; Roberts, 1974). However the outcrops in the Port Askaig-Bonahaven district are largely determined by faulting, the rocks being mainly uniformly dipping. Borradaile & Johnson (1973) show the axial trace of the Islay Anticline as joining the Section D anticline with the

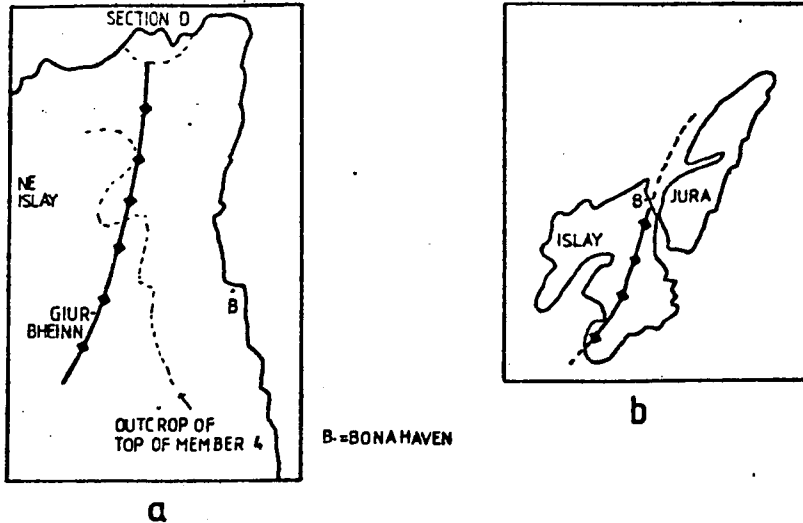


Figure 3-2: Axial trace of the Islay Anticline according to a) Borradaille & Johnson (1973) and b) Roberts (1974).

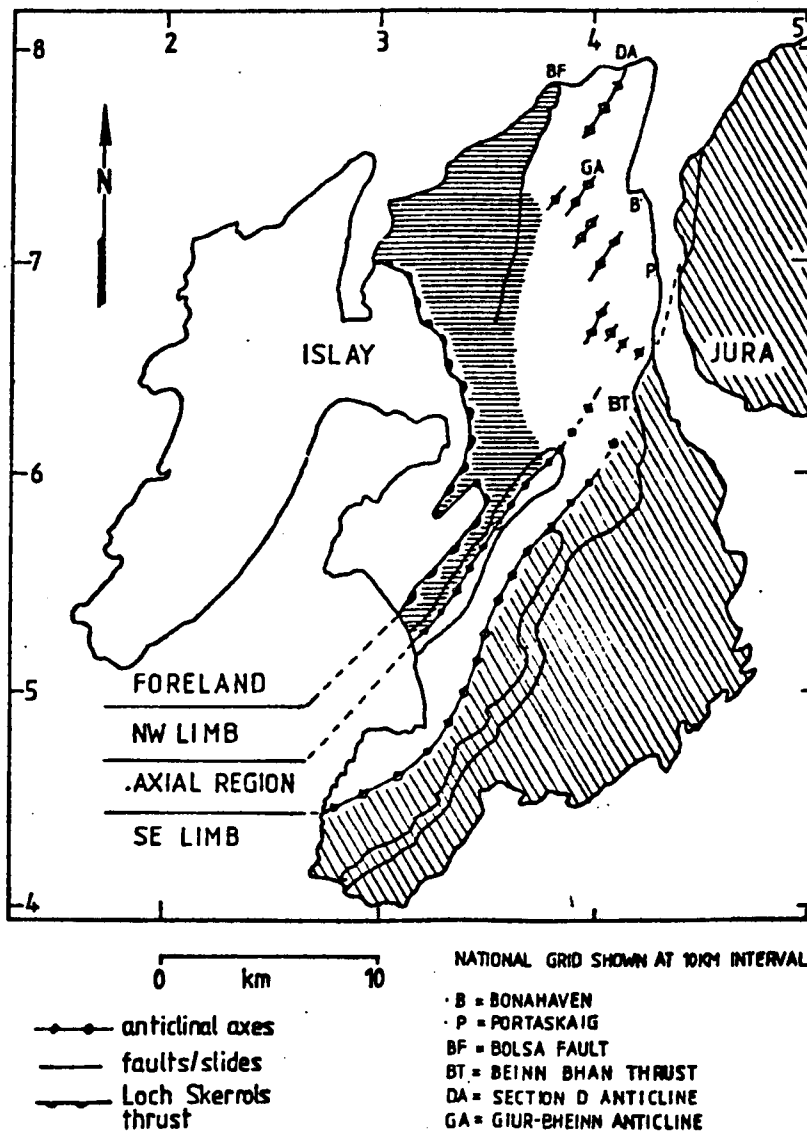


Figure 3-3: Structures of the primary Caledonian deformation (of Roberts, 1974) on Islay. Data from Wilkinson (1907), Bailey (1917), Basahel (1971), Digby (B.Sc. thesis Nottingham 1973) and personal observations.

Giur-bheinn anticline (fig. 3-2a). However the stereograms (fig. 3-1) show the fold axes to have low plunge and a constant azimuth of  $035^{\circ}$  which does not fit this line.

The trace of the axial surface of the Islay Anticline runs NE from Laggan Bay on the west coast of Islay through crucial, but poorly exposed ground. The Loch Skerrols thrust lies close by to the NW in this area. Rast & Litherland (1970) regarded the Islay Anticline in central Islay as an overturned fold with a moderate or steep northeasterly plunge. Basahel (1971) claimed that it is isoclinal, but presented no convincing evidence for this suggestion.

Following the trace of the axial surface NE towards the east coast of Islay, the strata on this line are unfolded, but to the NW folding does occur, the most westerly anticline clearly facing up to the NW as was the situation in central Islay. This implies that as the Islay Anticline is traced to the NE it becomes an en-echelon structure, each individual axis of the anticlinorium dying out to the NE, as depicted in figure 3-3. The stereograms (fig. 3-1a, b) thus represent cylindrical portions of an overall non-cylindrical structure. According to the definitions of Campbell (1958) the en-echelon arrangement is sinistral, but there is insufficient evidence to decide whether the structure is of the zig-zag type with doubly plunging folds or the elliptical type where all the folds have the same plunge. If the latter is the case the southerly plunge on the north coast could be explained as a transverse warping of the whole folded sheet.

The inferred en-echelon arrangement could be related to

the non-Caledonoid (N-S) trend of the Loch Skerrols thrust in northern Islay. The axial region of the Islay Anticline (fig. 3-3) appears roughly parallel to the thrust here, although the individual fold axes making up the anticlinorium were NE-SW, presumably perpendicular to the overall direction of shortening. This is consistent with the suggestion of Roberts (1974) that the non-Caledonoid trend of the Loch Skerrols thrust meant that the Port Askaig-Bonahaven district was relatively protected from deformation and so has a NW dipping cleavage, rather than the SE dip that is the normal case on Islay.

#### 3.4: The Bonahaven Fault

Islay is divided into two by the line of the Loch Indaal-Loch Gruinart transcurrent fault. Durrance (1976, and in correspondence) postulated, in discussing the results of a gravity survey of Islay, that the Bonahaven fault might also possess a transcurrent component. This would explain the bend in the Loch Indaal fault as the Bonahaven fault is nearly in line with the SW extension of the former (fig.1-1). However the Loch Skerrols thrust is apparently not offset along the line of the Bonahaven fault, and the latter's westerly downthrow is in opposition to the 1000m+ easterly downthrow of the Loch Indaal fault (Dobson et al., 1975). Also the evidence in the Bonahaven region does not support this hypothesis as the fault clearly bifurcates and rejoins south of Bonahaven, the sum of the downthrows of the twin faults being approximately the same (450m) as the downthrow of the undivided fault. Clearly in this area there is only a vertical component of displacement and so no adjustments are required along the fault line when

reconstructing the palaeogeography of the Bonahaven Formation on either side of it.

### 3.5: Strain indicators and strain history

Field observations of the inclination of bedding and cleavages described earlier indicate a major deformational event ( $D_1$ ) during which the bedding was folded and the main cleavage formed, and a later, minor episode ( $D_2$ ) forming crenulation cleavage in places. More information as to the deformational history is supplied by observations on deformed oöids and sandstone dykelets, the microscopic nature of the cleavages and the orientation of pressure fringes. This section is concerned with the orientation of tectonic fabrics rather than with deformation mechanisms which are treated in section 7.5. In the following discussion X, Y and Z are the principal axes of the finite strain ellipsoid, where  $X > Y > Z$ .

#### 3.5.1: Deformed oöids

Oöids in oölitic dolostones in member 3 show much variation in deformation partly because some of them show some replacement by quartz, but even comparing dolomicrite oöids there is undoubtedly some heterogeneity in the degree of deformation. Bed 54D displays prolate oöids (axial ratios 1.5:1:1; fig. 3-4) and beds 54E and 60E exhibit a similar degree of deformation. However oöids in beds 27B, 54C and 42E seem to be nearly undeformed (fig. 3-5).

The orientation of long axes of quartz grains and oöids in five dolostones is shown in figure 3-6. Four lie within the range of cleavage orientations whilst all are at a high angle to the bedding-cleavage intersection. This

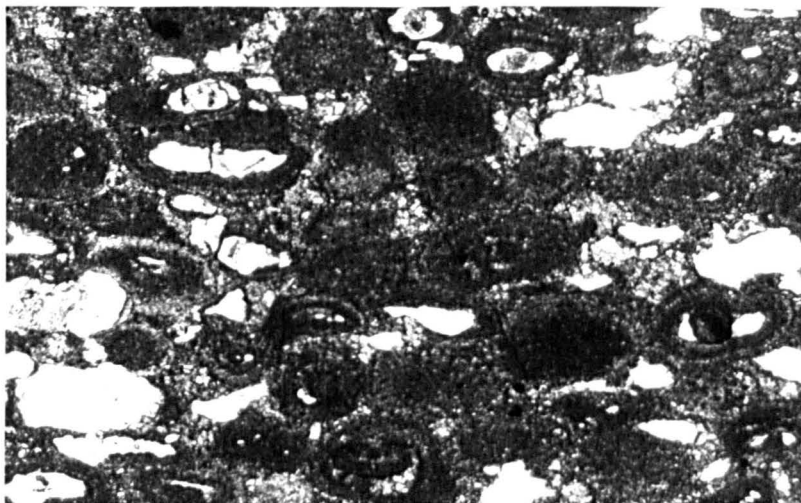


Figure 3-4: bed 54D, photomicrograph in plane polarized light of thin section cut perpendicular to cleavage. Ooids (some partly replaced by quartz) and quartz clasts are considerably deformed.

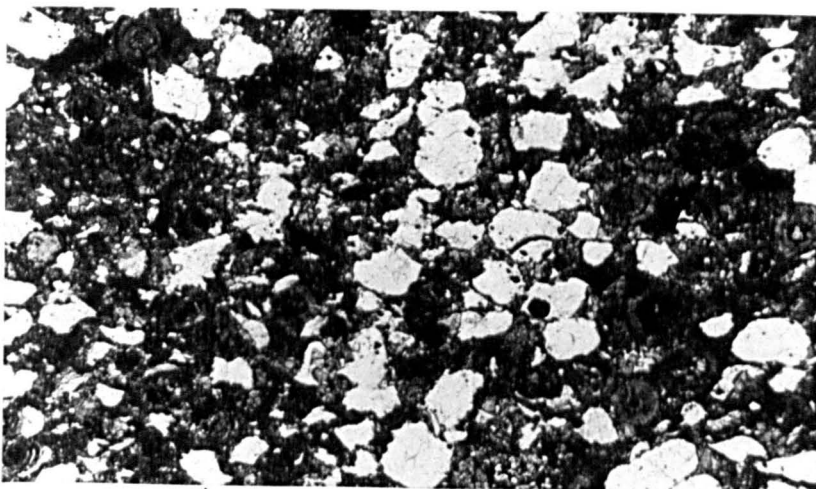
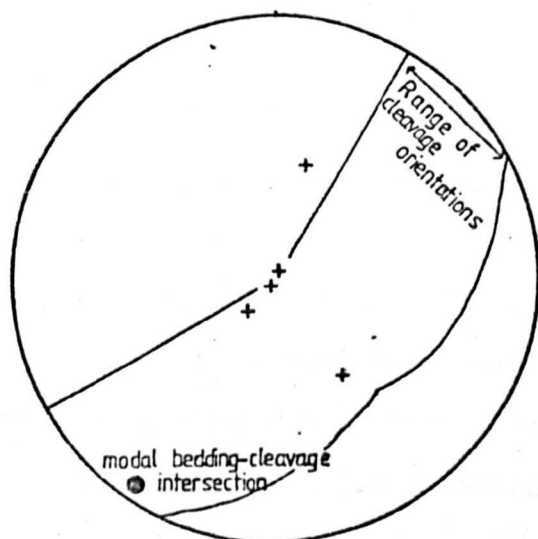


Figure 3-5: bed 42E, photomicrograph in plane polarized light of thin section cut perpendicular to cleavage. Quartz clasts and ooids appear nearly undeformed.



+ long axis of deformed ooids

Figure 3-6: Orientation of long axis of deformed ooids from the north coast compared with the cleavage orientation.

is a similar pattern to that shown by lineations described in section 3.5.4. There is clearly a lot of scope for strain determinations using ooids in both the Bonahaven Formation and the Islay Limestone.

### 3.5.2: Cleavage and deformed sandstone dykelets

The main cleavage is defined by a penetrative preferred orientation of white mica (phengite) and, as seen in thin sections cut perpendicular to the cleavage, by elongate quartz clasts and occasionally pyrite grains. Qualitatively the cleavage shows variable development, being weak in member 1 in Sections A and B (except at the base), most strongly developed in member 4 sediments on the north coast and to a variable and intermediate extent in member 3 sediments throughout the area. The poor development of cleavage beneath member 2 suggests that this unit may have acted as a shield during the deformation as do epidiorite sills elsewhere in the Dalradian (Anderton, 1975).

Borradaile & Johnson (1973) reported a lineation in the cleavage, taken to be the finite extension direction, visible (in the field) on the north coast, but not at Bonahaven. I could not detect such a lineation in the field, although a weak lineation is visible in thin sections cut parallel to cleavage (7.5).

That there was considerable flattening normal to the cleavage is beyond doubt. Borradaile & Johnson (1973) quantified this by assuming that the cleavage plane = XY and then deriving the strain ellipsoid by measuring how far sandstone contraction (synaeresis) crack-fills within dolomitic mudstone (sandstone dykelets) had rotated towards parallelism with the cleavage. They concluded that there

was a shortening normal to the cleavage of 33-66% and an extension within the cleavage of 25-157%. Because the method is subject to considerable errors these results do not imply that the deformation was this heterogeneous. The authors tentatively extended their results to the whole of the Formation indicating that present thicknesses are only 50-70% of those before deformation. However, the many competent sandstones and quartzites in the sequence may have suffered much less penetrative deformation. Also members 1 and 2 on the east coast appear nearly undeformed.

Observations on cleavage and deformed sandstone dykelets at the west end of Section D (fig. 3-7a) show that there is an anomalous area here as the dykelets are orientated in a non-Caledonoid direction (fig. 3-7c). In this area the bedding dips uniformly west or WSW at an angle of 12-18°. Approaching the anomalous area from the east, the dip of the cleavage and deformed contraction-crack casts swings round from SE to southerly (fig. 3-7a,b). Further SW, the dykelets dip SW whilst the most conspicuous cleavage dips SE (fig. 3-7c, 3-8). This section study shows that in the anomalous area the most conspicuous cleavage is not, as elsewhere, a penetrative slaty cleavage, but a discrete spaced cleavage that crenulates a pre-existing mica foliation (fig. 3-9). The latter, only indistinctly visible in the field, has a similar orientation to the deformed contraction crack fills. The spaced cleavage is not  $S_2$  because it in turn is crenulated, by a NW-dipping cleavage (=  $S_2$ , fig. 3-10). West of this area, member 4 sediments lacking sandstone dykelets occur; they have a penetrative Caledonoid-trending cleavage (fig. 3-7d) with no hint of an earlier fabric. In this small anomalous area then, the main deformational episode seems to have been composite. Most of the finite

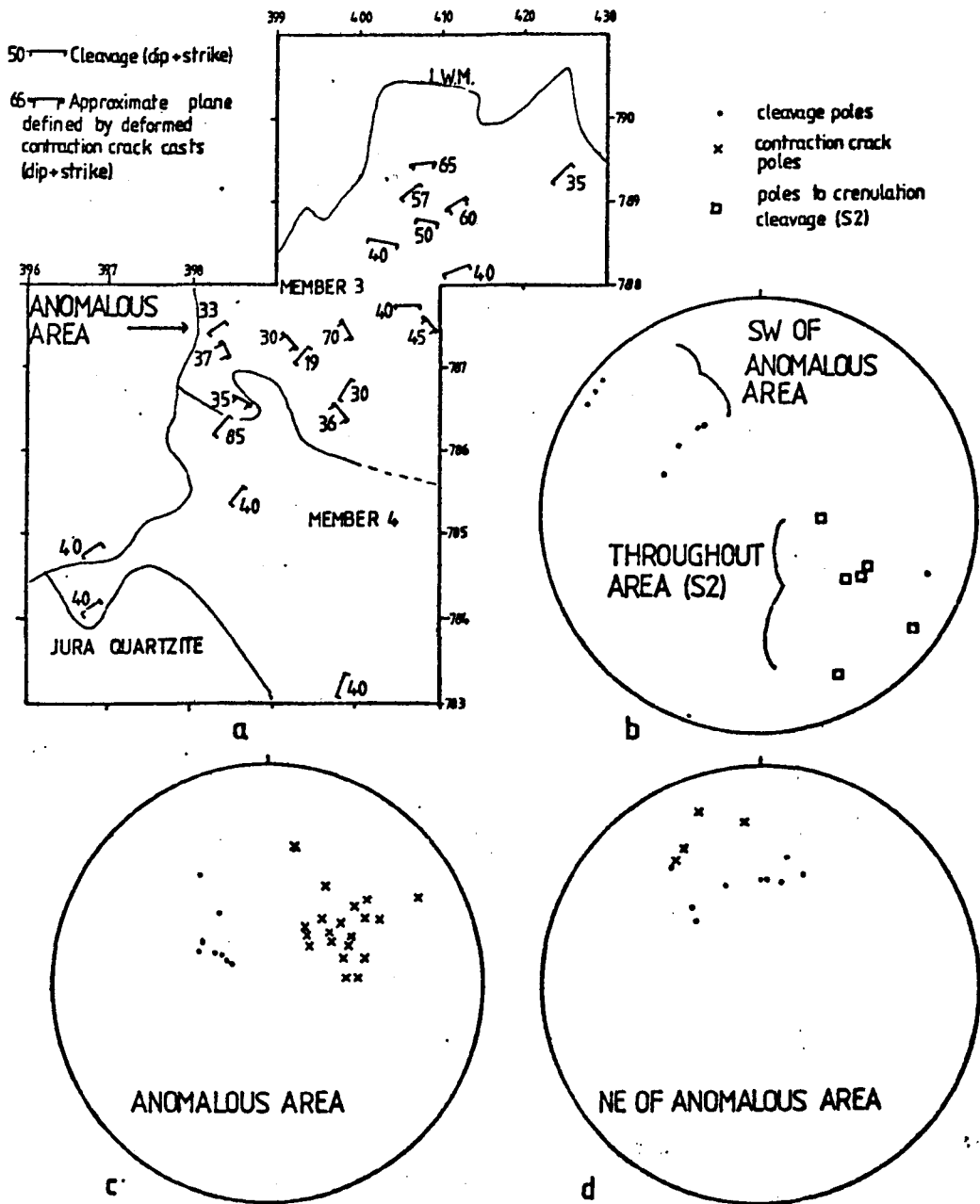


Figure 3-7: Anomalous area with non-Caledonoid trending deformation, western end of Section D. Bedding dips uniformly W or WSW at 12-18° throughout the area. a) map, with National grid (prefix NR omitted). b,c,d) stereographic projections.



Figure 3-8: Cleavage and deformed sandstone dykelets at the western end of Section D. The most conspicuous cleavage in the area (S1b) is visible in the lower half of the photograph, parallel to the hammer. Deformed sandstone dykelets (deformed towards S1a) dip in the opposite direction (visible in the upper half of the photograph).

500 $\mu$ m

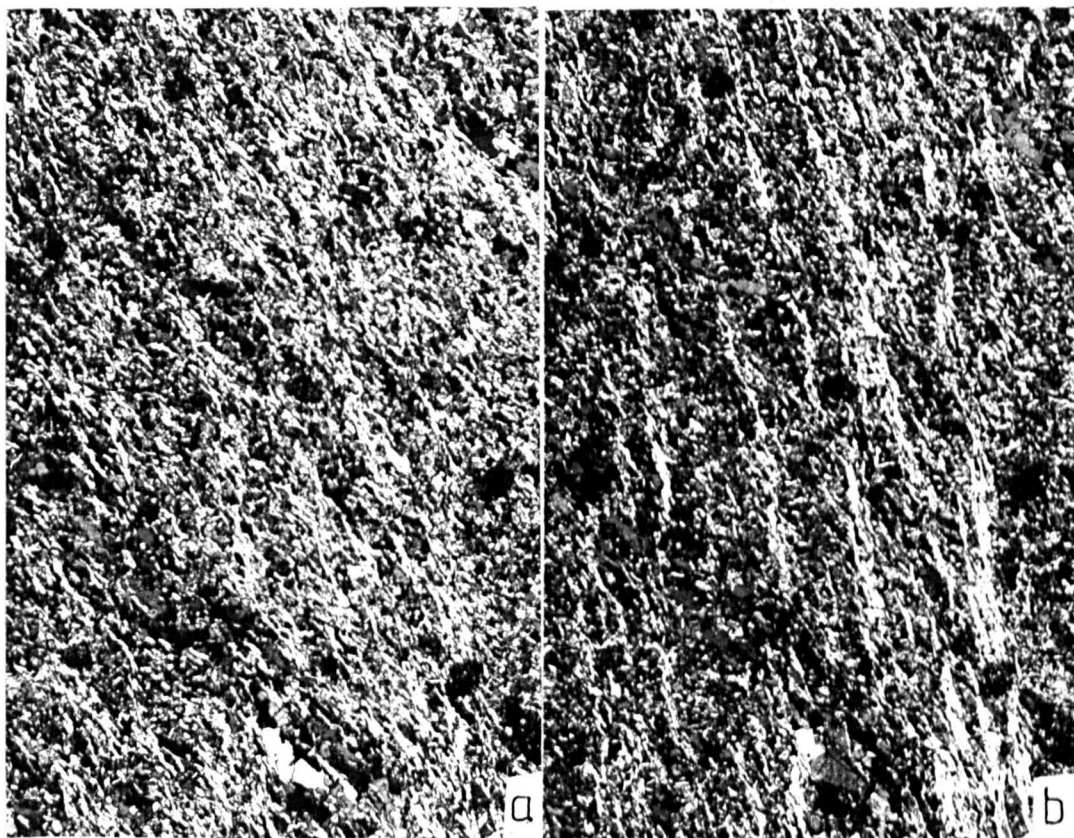


Figure 3-9: Photomicrographs under crossed polars of a sample from near the location of Figure 3-8. a) polars N-S and E-W; a penetrative cleavage (S1a) runs from top left to bottom right. b) polars NW-SE and NE-SW; same view as a); S1b is seen as a series of mica-rich microlithons running vertically in the photograph. Rotation of micas has occurred within the microlithons.

strain of the rocks was accomplished in a non-Caledonoid direction leading to the formation of a cleavage ( $S_{1a}$ ) towards which the sandstone dykelets rotated. It was only at a late stage that the Caledonoid-trending cleavage ( $S_{1b}$ ) became established everywhere; in the anomalous area  $S_{1b}$  adopted a spaced crenulation character as  $S_{1a}$  was already present. There seems no obvious reason why this area should exhibit this complex history as no nearby rigid blocks or syn-deformational faults have been recognised.

All the cleavages described above are considered to belong to the primary deformation of Roberts (1974). The secondary deformation is represented by  $S_2$ , described in sections 3.2 and 7.6.

### 3.5.3: Deformed sedimentary structures

The sandstone dykelets mentioned in the last section show the effects of the deformation especially well as they are set in an incompetent medium (dolomitic mudstone). However over-steepened cross-lamination and cross-stratification also occur, and bunched ripple form-sets (fig. 3-11) and stromatolite domes showing an elongation in plan parallel to the cleavage trace (fig. 3-12) can be seen. Quantification of the degree of deformation would be very difficult. However some discussion is needed on the validity of the palaeocurrents derived from the cross-strata.

For the member 1 and 2 cross-strata, there is little petrographic evidence of deformation in adjacent mudstones, let alone in the competent dolomitic sandstones and quartzites in which the cross-strata occur. Figure 3-13 purports to show that there has been negligible deformation of cross-strata in this part of the sequence. Note that this is not

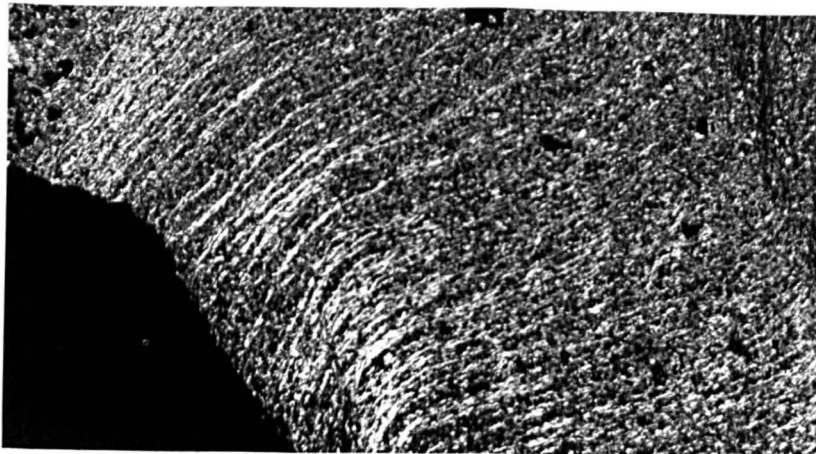


Figure 3-10: photomicrograph, crossed polars (same thin section as fig. 3-9). An  $S_2$  fold of  $S_1b$  microlithons is seen.



Figure 3-11: Bed 65D, showing bunched ripple form-sets (1), deformed sandstone dykelets (2), small loads (3) and a sandstone lamina showing minor folds.



Figure 3-12: Stromatolite bed D2 in plan showing elongation of stromatolite domes parallel to the hammer. As this is parallel to the cleavage trace, it is thought to be due to deformation rather than being an original sedimentary feature.

easy to prove because as the cleavage is not steeply dipping, the cross-strata may be flattened or steepened by the deformation, depending on their azimuth. In figure 3-13 both cross-strata and cleavage are plotted with the dip of the bedding removed by rotation about the bedding strike. The data are plotted as hypothetical lineations (currents) down the dip of the cross-strata. If we postulate a null hypothesis that the cross-strata have suffered a measurable amount of deformation (pure shear) tending to make them rotate towards coincidence with cleavage then we would expect the dip angles of the cross-strata to show a degree of scatter which would be reduced to a minimum (with average dip  $25-30^{\circ}$  assuming all are avalanche sets) when the appropriate deformation had been removed.

The arrows on each measurement show how its orientation would change if we remove a hypothetical deformation increment. However, most of these arrows point away from the range  $25-30^{\circ}$  dip for a given azimuth. Therefore even removing a small hypothetical amount of deformation increases the scatter of the results. The scatter will increase more, the further the points are rotated. It can be concluded that the null hypothesis is invalid and that the dip angles of the cross-strata tend to show the best clustering around  $25-30^{\circ}$  if we consider that they are undeformed.

In member 3, deformation is more noticeable generally, but the variation in the dip of the bedding make it more difficult to perform the same exercise as above. Only near the top of Section D are dominantly oversteepened cross-strata the rule (dips of  $35-40^{\circ}$  being common). Bunched ripple form-sets, deformed loads and some small-scale folds also occur here. Plotting all the cross-strata from member 3

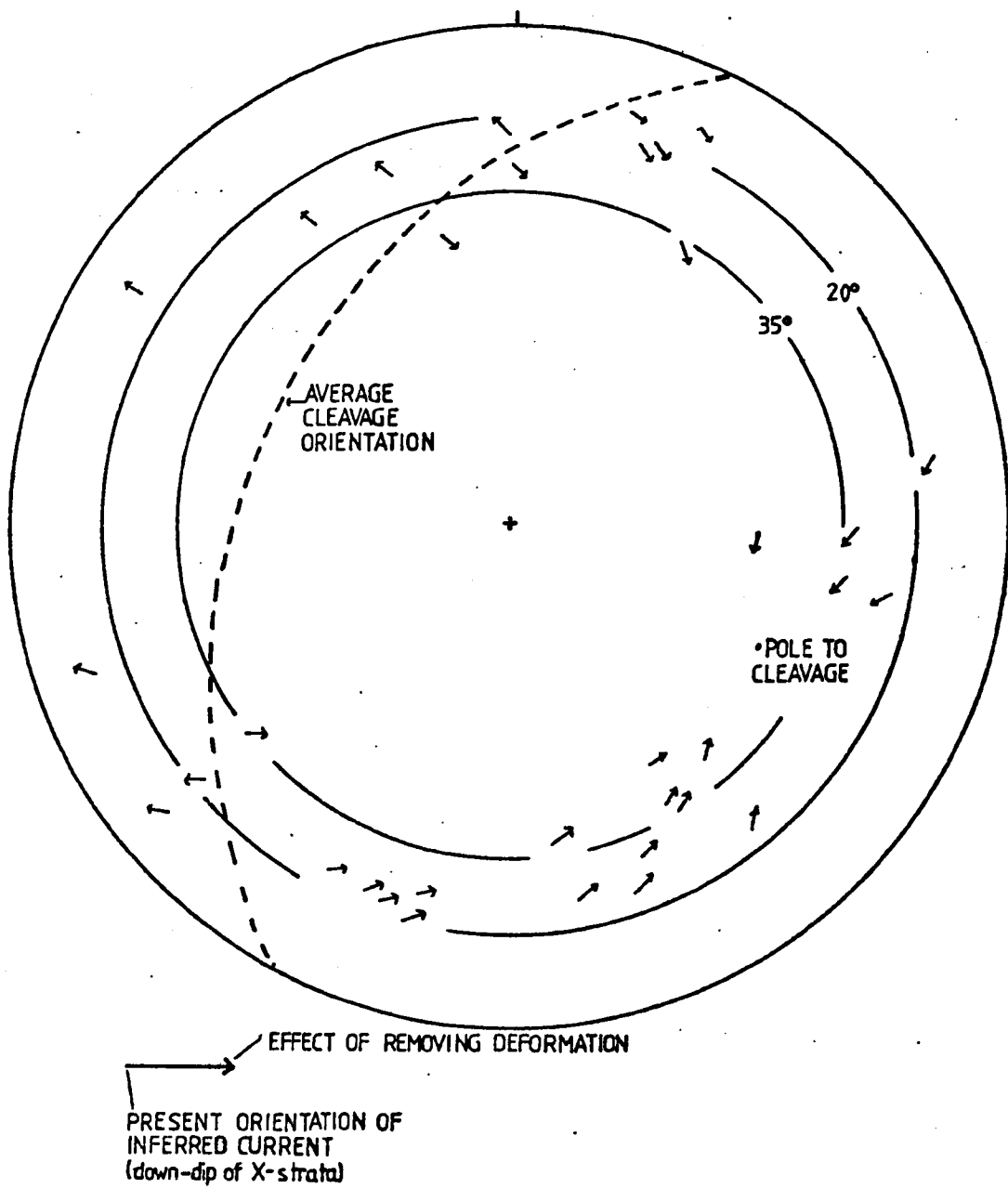


Figure 3-13: Deformation and member 1 cross-strata. The latter are plotted as lineations down the dip of the cross-strata (= currents). Discussion in the text suggests that the cross-strata are undeformed.

together (fig. 4-37) there is no overall preferred orientation, yet bimodal distributions in various orientations occur at individual localities. It is considered likely that the strike of the cross-strata have not been altered more than a few degrees from their original orientation.

#### 3.5.4: Pressure fringe lineations

Lineations are defined by the orientation of elongate quartz and calcite within pressure fringes, principally around pyrite cubes and in bedding-parallel veins in stromatolites (figs. 3-14, 3-15 & 3-16).

Fringes around pyrite (e.g. Pabst, 1931; Spry, 1969) and detritus occur in a number of lithologies, principally dolomitic mudstones and some calcareous sandstones. For fringes around pyrite and bedding-parallel mica they are best developed on pyrite crystal faces which are normal to the cleavage trace, in sections perpendicular to the cleavage (fig. 3-15). The orientation of the long axis of the fringe in three dimensions defines X in a coaxially accumulated deformation (Elliott, 1972) and this was always observed to be parallel to the cleavage trace in sections perpendicular to the cleavage.

In the field, stromatolitic bedding is generally displayed by veins, here called seams, of quartz and calcite, which have closely similar textures to the pressure fringes around pyrite: a similar origin is proposed (7.4). Growth was either in a single direction, or in two diverging directions away from a central parting. The mineral lineation may be at any angle to the seam walls (fig. 3-15b, 3-16; cf. Durney & Ramsay, 1973). Curved crystals (sense of Shearman et al., 1972) occur in some seams (figs. 3-15c,

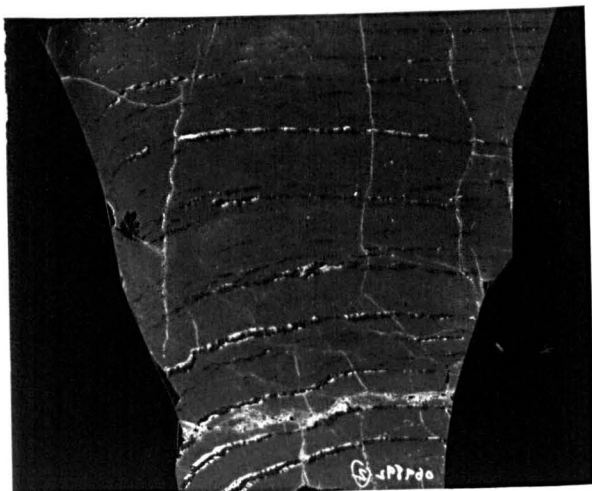


Figure 3-14: negative print (x1) of domal stromatolite with quartz seams (within seams quartz is black and calcite light coloured). Calcite veins are also present.

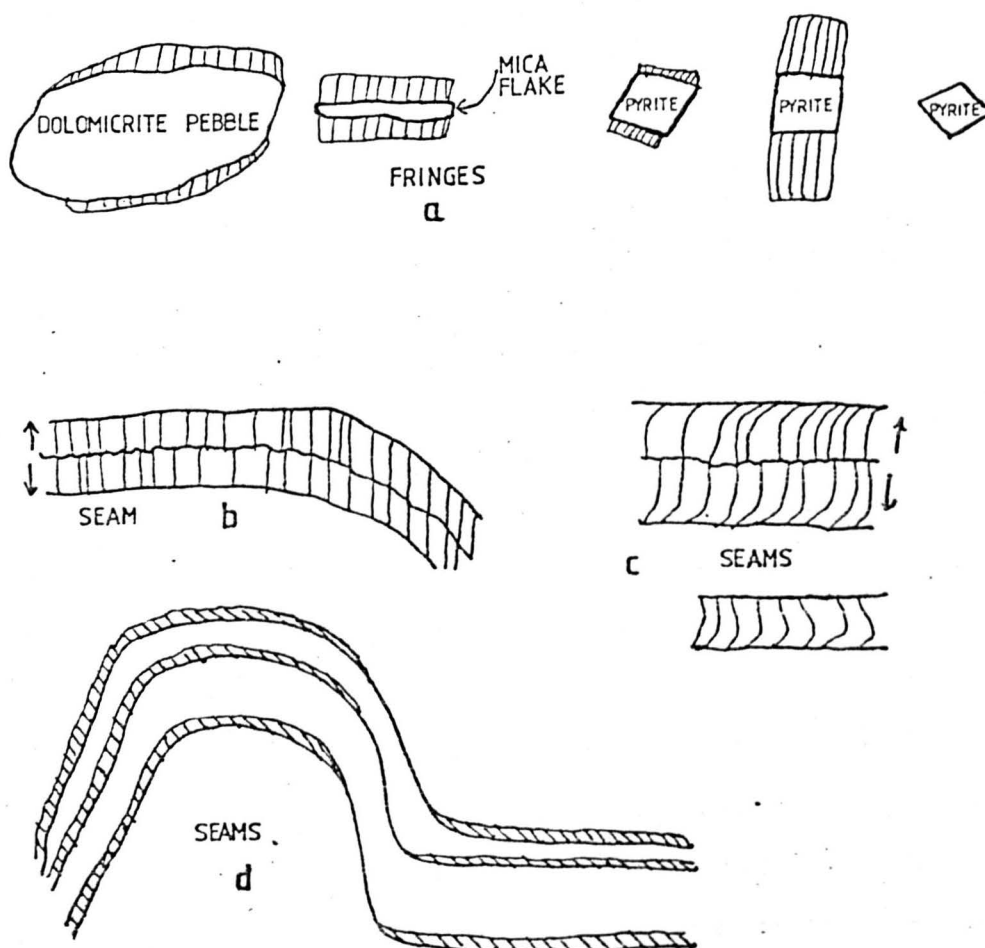


Figure 3-15: Some geometrical relationships of seams and pressure fringes (see Chapter 7 for a discussion of their genesis).

a) Fringes (principally of elongate quartz) occur around dolomicrite pebbles, large mica flakes (clasts) and pyrite grains. For the latter crystal elongation is perpendicular to the growth surface; fringes do not develop on surfaces at a low angle to the extension direction.

b) sketch of a quartz seam such as those commonly found in stromatolites; arrows indicate growth directions. (A pronounced crystal elongation is not always present - see Chapter 7).

c) seam with curved crystals indicate changing orientations of incremental strains.

d) seams in domal stromatolite only occur on the side of the dome more nearly perpendicular to the extension direction. The same structure is shown by seams containing unelongate crystals.

3-17) which indicates variation in the incremental strain with time (Durney & Ramsay, 1973). A crystal elongation is not always present within the seams (see 7.5). The geometry of domal stromatolites sometimes requires that seams grow on one side of the domes only (fig. 3-15d). Thus where an internal fabric is absent, the direction of extension can be deduced approximately by the distribution of seams in domed stromatolites.

For some hand specimens, observations have been made in two planes using sawn surfaces and thin sections to work out the three-dimensional orientation of the pressure fringe lineation. Similar observations were taken on stromatolites in the field, although curved crystals cannot be detected here. The results are shown in figure 3-18a.

Orientations of quartz lineations from seams and pyrite fringes lie within the same field supporting the interpretation of these as analogous structures. The results show considerable scatter, part of which can be explained as a result of the variable orientation of the cleavage. Thus the pressure fringe lineations from Section D show a progressive change from southerly or easterly plunge through to westerly on reaching the anomalous area, paralleling the change in strike of  $S_{1a}$  from NE to SE. Thus the bulk of the extensions lie in the cleavage orientation of the slatier lithologies, with high, southerly angles of pitch in general. This constant relationship of the bulk of the points indicates that the incremental strains which they represent do parallel X.

Can the relative age of the fringes with respect to the folding be established? This is not easy to demonstrate because the bedding only dips at low angles as a rule.

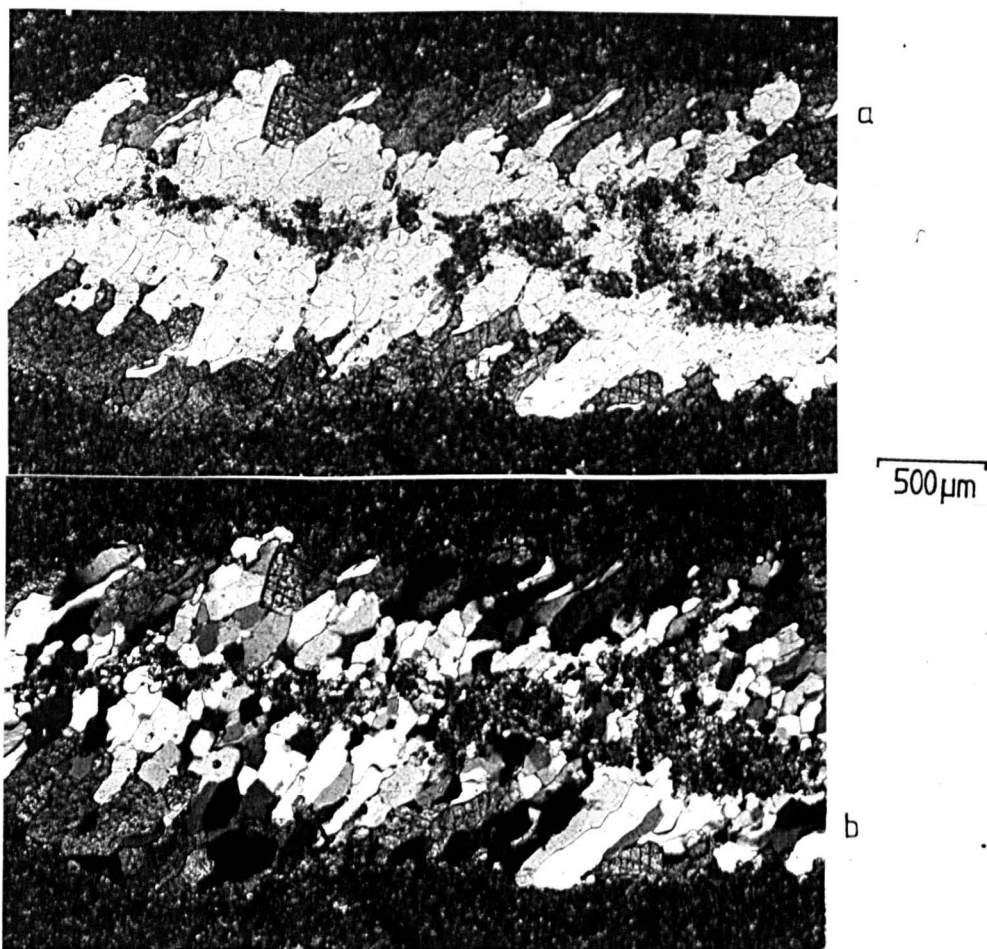


Figure 3-16: Photomicrographs of quartz-calcite seam in stromatolitic dolostone (D4); a) plane polarized light b) crossed polars. Note central parting of dolomicrite (this continues as a stylolite at the end of the seam outside the field of view). Crystal size increases away from the central parting. Calcite (cleaved) only occurs near the seam margins. Crystal elongation is oblique to the seam walls. For a discussion of genesis see Chapter 7.



Figure 3-17: Photomicrograph, crossed polars of quartz seam with curved crystals (stromatolite C8). Increase in crystal size downwards suggest growth was from top to bottom in the photograph.

However, the data points show a less dispersed distribution when plotted in their present orientation (fig. 3-18a) than when plotted with the dip of the bedding removed (fig. 3-18b). Also the points show a much more consistent relationship to the change in cleavage strike in figure 3-18a. This suggests that most of the folding was accomplished before the fringes were formed. The presence of some curved crystals might indicate that the bedding was being rotated as the structures formed (Wickham & Anthony, 1977), but the sense of curvature is usually opposed to this. Bedding plane slip during folding might produce a different sense of curvature, but there is no other evidence that this has occurred. The suggested relationship of extensional veins developing after folding, but within the same stress field, has been recognised elsewhere (Phillips, 1975).

That the mineral lineation represents growth during only part of D1 is suggested by:

1. the apparent bedding rotation before the lineation formed
2. the presence of curved crystals in some, but not all, samples
3. the variable direction of curvature
4. the presence of some lineations which depart considerably from the overall clustering of points on fig. 3-18a.

The incremental strains were thus to some extent variable in orientation, although not so much that X was not clearly defined by the bulk of the preserved mineral lineations.

Lineations are also defined by elongate nodules dipping at moderate angles to the SW for the most part. Their origin is uncertain because their orientation is different from that of nearby deformed ooids or mineral lineations in most cases.

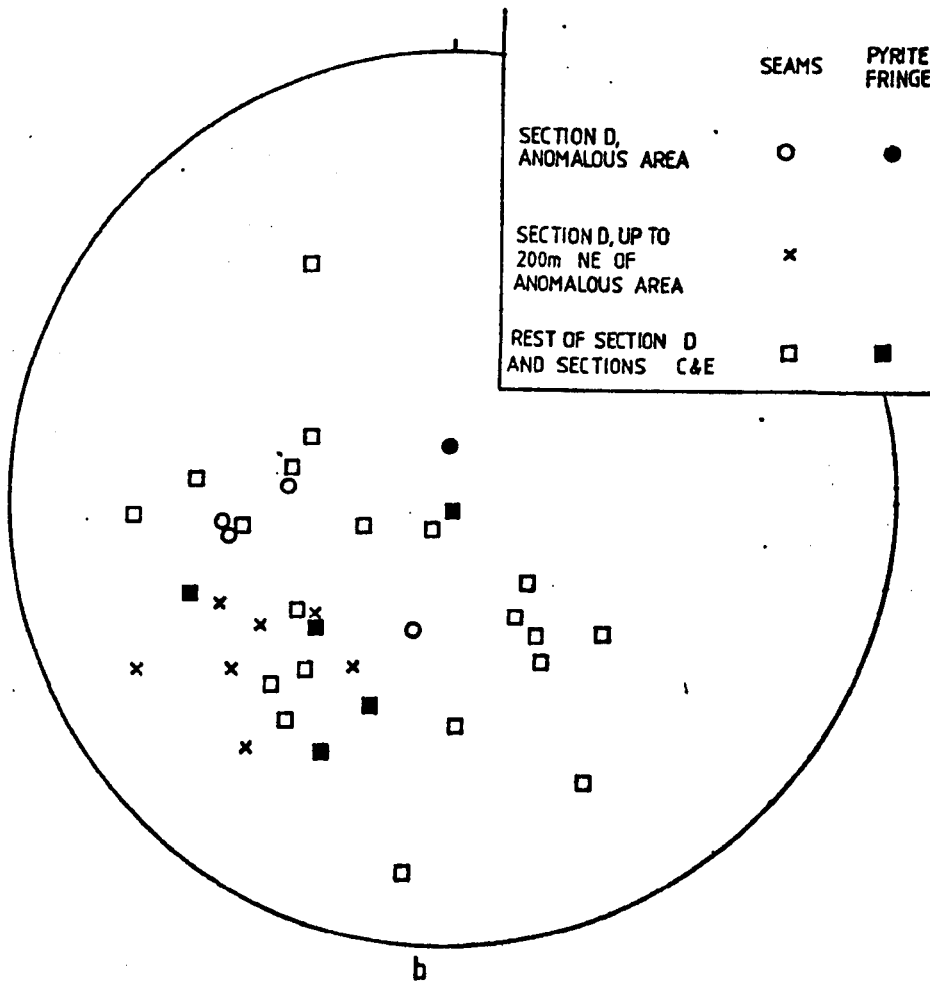
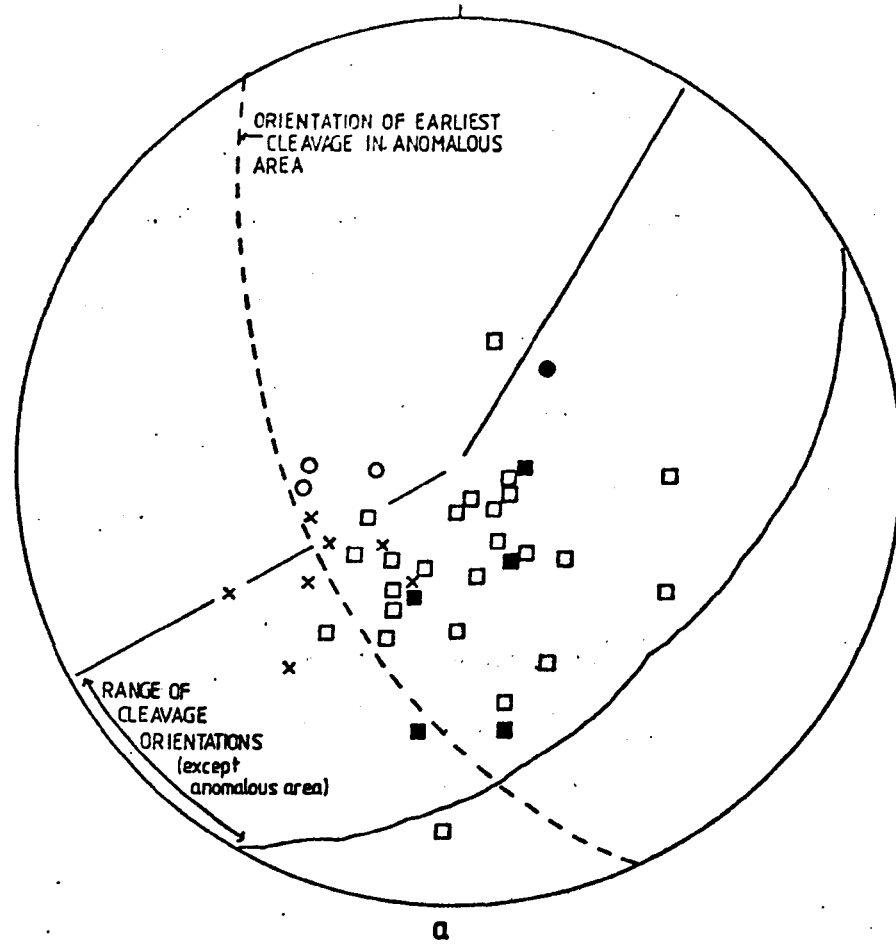


Figure 3-18: Orientation of mineral lineations in seams and pyrite fringes a) in their present orientation and b) with the dip of the bedding removed. The lineations show a less dispersed and more readily explicable distribution in a).

### 3.5.5: Summary of strain history

The rocks suffered nearly all their finite strain during the primary deformation which produced folds (and probably the Bolsa fault), with movement to the west producing the Loch Skerrols thrust (Roberts, 1974). The deformation seems rather inhomogeneous, but increased in intensity overall from the east to the north coast, and westwards along the north coast (evidence from degree of development of cleavage and presence of pressure fringes only sporadically on the east coast).

The slaty cleavage represents the XY plane, within which the X direction may be expressed by a mineral lineation. Pressure fringes and deformed ooids from the north coast show that extensions here generally pitched in the XY plane at angles of 35-85° from the bedding-cleavage intersection in a southerly sense. This contrasts with the northerly plunge of X in the northern Loch Awe district NE of Islay, where the fold axes are also sub-horizontal (Borradaile, 1973). On the north coast of Islay, there is some evidence that the incremental strains were variable in orientation from time to time (curved crystals).

The folding may have been inhibited after an early stage by the fact that much deformation was being achieved by solution transfer, the tangible results of which are the mineral lineations (see section 7.5).

Penetrative deformation was not in a Caledonoid direction near the western end of Section D at the start of the primary deformation, but by its conclusion a Caledonoid-trending cleavage was established over the whole region.

The secondary deformation contributed little to the finite strain, being manifested as thin crenulation bands scattered sparsely across the area.

## CHAPTER 4: SEDIMENTOLOGY

### 4.1: Pre-Bonahaven sedimentology

Consideration of the sedimentology of the higher parts of the Port Askaig Tillite will provide a useful introduction to the sedimentation history of the Bonahaven Formation.

Spencer (1971a) considered the Port Askaig Tillite of Islay and the Garvellach islands to consist essentially of a series of grounded-ice tillites (mixtites) with interbeds of shallow marine sediments. He provided evidence for the origin of the latter in the higher parts of the Tillite (Members 3,4 and 5) by citing the abundance of 'white sandstones' (quartzite) and cross-stratification with poly-modal or radial distribution of azimuths, and the presence of ?beach conglomerates and wave-generated ripples (with NE-SW crestlines).

#### 4.1.1: Lithological description

##### 4.1.1.1.: Caol Ila road cutting

In the Port Askaig district most of the interbeds are rather massive quartzites which yield little sedimentological information. However a new road cutting (made since 1971) at Caol Ila in Member 4 of the Tillite, is more helpful (fig. 4-1). Here 17m of sandstones are seen, without any mixtite contacts. They are fine to medium grained, thick bedded and feldspathic, showing either no internal structure or parallel lamination. Groups of parallel silt laminae also occur and there is a tendency to fine upwards into a 2-10mm mudstone lamina, which commonly forms the top to a bedding plane. These mud laminae are seen to be composite

## CAOL ILA ROAD CUTTING

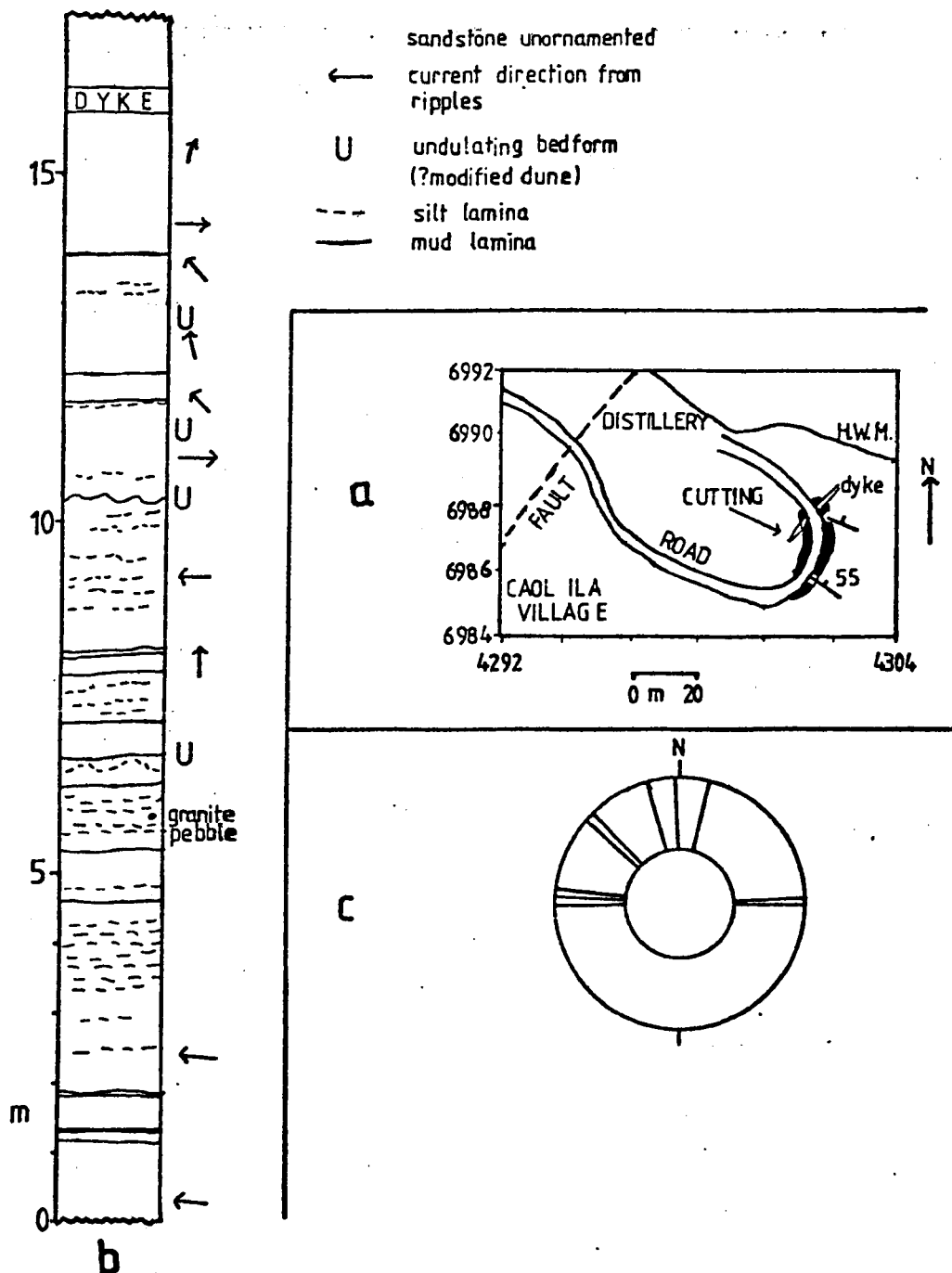


Figure 4-1: Caol Ila road cutting. a) locality map with the National Grid. All sediments are within the Port Askaig Tillite: Member 4 to the east of the fault and Member 5 to the west. b) stratigraphic section through the road cutting. These sediments are absent from the nearby shore section where only mixtite is exposed. It is not clear whether this is an original feature, or due to faulting. c) summary of current directions deduced from current ripples.

in thin section, i.e. they are made up of several thinner mud laminae. The former presence of bedforms is shown by some mud laminae which exhibit a series of regularly spaced rounded undulations, varying from 0.5m spacing and 3cm height to 3m spacing and up to 40cm height. The sand underneath such mud laminae is structureless. In addition, ten bedding planes show straight crested ripples which have wavelengths of 5-7cm, height of 5mm and an asymmetry (symmetry index 2.5-6) which indicates a current, rather than a wave origin.

#### 4.1.1.2: Member 5 of the Port Askaig Tillite

Some 200m of fine to medium grained pure sandstones (quartzites) with only thin mixtite or conglomerate horizons form the highest beds in the Tillite in the Caol Ila and Bonahaven districts (Spencer, 1971a). The sandstones are thickly bedded, usually massive, but sometimes parallel-laminated. There are rare bedding plane undulations similar to those described in the last section, rare mudstone laminae, wedge-shaped beds and wave-formed ripples.

Inland mixtite and especially pebbly sandstone occur at the top of the Tillite as was described in Chapter 2. Their significance is discussed in Chapter 8.

#### 4.1.2: Environmental interpretation

The interbeds in the higher parts of the Tillite (Members 3, 4 and 5) show none of the characteristic features of glacial outwash in braided streams or lakes described by Church & Gilbert (1976) and Gustavson et al. (1976). Although the sediment supply may partly have been fluvially derived from a nearby glaciated land surface, it seems likely that the interbeds formed during inter-glacials

(Spencer 1971a) and in a marine situation.

The cross-stratification recorded by Spencer (1971a) appears similar to that in the Jura Quartzite (Anderton, 1976) deposited as dunes and sand waves in a tidal sea. Klein (1970a) regarded the parallel-laminated quartzites of Member 5 as forming in a shallow sub-tidal, tide-dominated situation, and suggested that the bedding plane undulations are modified dune bedforms. The latter do seem to be constructional rather than erosional bedforms because they are smoothly rounded, regularly spaced and constructed of medium sand which would have been non-cohesive originally. Internal lamination is not recognizable because of the purity of the sand and lack of carbonate cement. The undulations could have been produced either by wave action (Clifton et al., 1971) or by tides (Klein, 1970b), but the nature of the small fining-upward sequences with a thin, often composite mud layer is more in keeping with tidal processes (Reineck, 1967) than with wave or storm action (Reineck & Singh, 1972). The current ripples also suggest tidal processes, perhaps forming during emergence of an inter-tidal sand bar (although superimposed ripples might be expected here). As they are low in the hierarchy of possible bedforms it is not thought that the orientations of the ripples are directly related to overall tidal flow directions.

#### 4.1.3.: Conclusions

Although much more work could be done on the interbeds in the Port Askaig Tillite as a whole, the higher interbeds seem to have been deposited in a shallow marine environment, under tidal influence. Glacial sediments are totally subordinate in Member 5 in the east coast sections.

#### 4.2: Bonahaven Formation: members 1 and 2

These sediments, which are more heterogeneous than those lower in the sequence, represent a range of sub-environments within a general very shallow marine setting.

##### 4.2.1: Lithological sequence

Comparative sections through members 1 and 2 at Caol Ila (A) and Bonahaven (B) are illustrated in figure 4-2. The environmental interpretations made there may be compared with Klein's (1970a) model for the sequence (fig. 4-3).

Unit 1 consists of silty mudstones (slates) with sharply defined thin laminations of silt and fine sand which are strictly parallel and traceable for a metre or more to the limits of the exposure.

Unit 1 grades up through lenticularly bedded sand and mudstone to a series of very fine-grained sandstones (unit 2), commonly rippled, and containing delicate anastomosing thin silty mud laminae (fig. 4-4). Characteristically sand laminae less than 2mm thick alternate with bundles (up to 4mm thick) of mud laminae individually 50-300µm thick. Thicker sand layers develop straight-crested ripples, wavelength about 8cm, displaying an indistinct low profile with no marked asymmetry. The orientation of their crestlines is dominantly NW-SE (fig. 4-6a). Internal cross-lamination is marked by mud flasers in some cases, but is usually difficult to discern. However transport seems to have been both to the NE and SW (fig. 4-5). Two bedding planes have superimposed ripples (interference ripples of Klein, 1970a) orientated NE-SW and NW-SE which, if one or both of the sets are current ripples, is suggestive of sub-aerial exposure. All the ripples in unit 2 are rather indistinctive (it is not clear from their form whether they are current or wave-

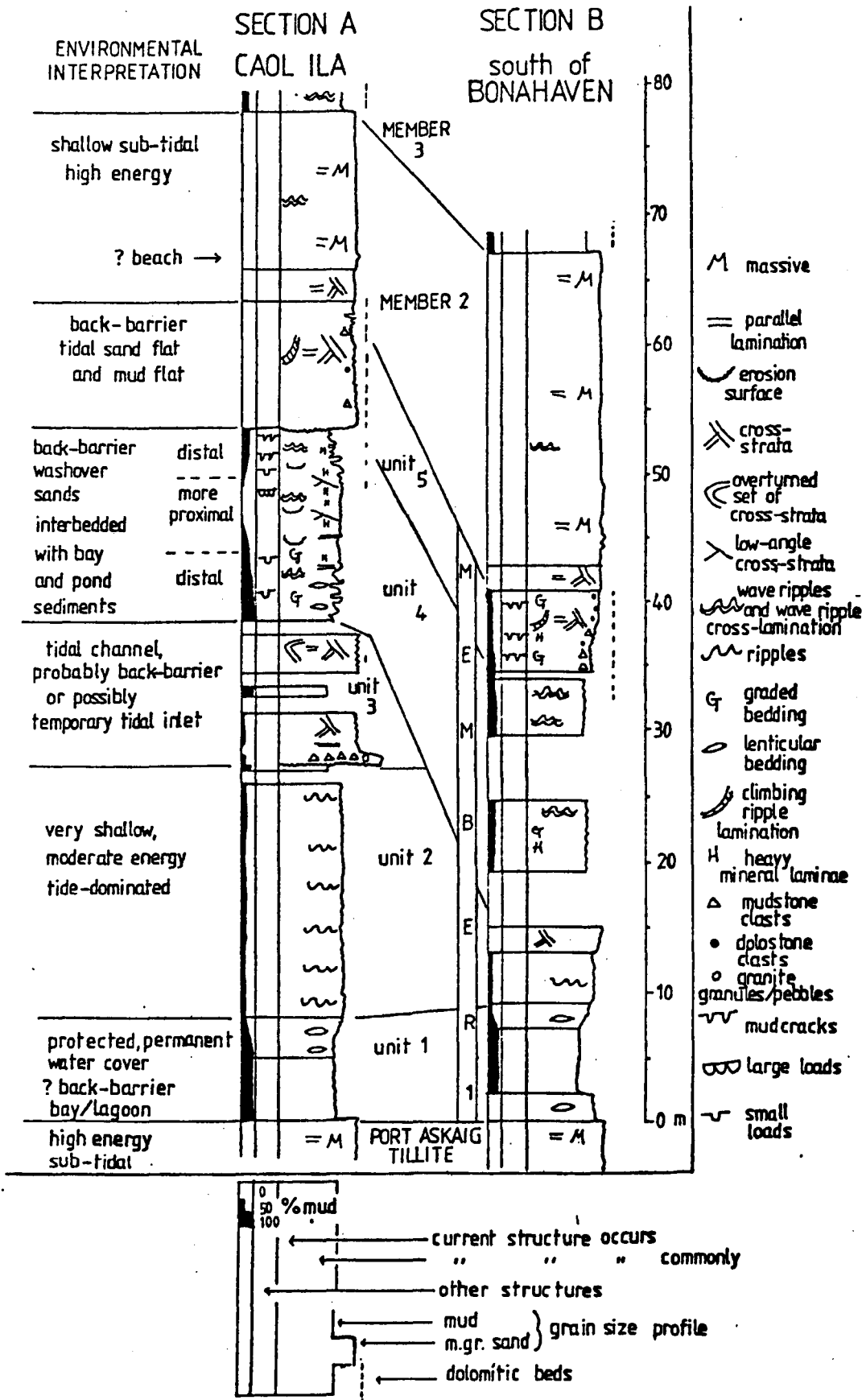


Figure 4-2: Sections through members 1 and 2 of the Bonahaven Formation

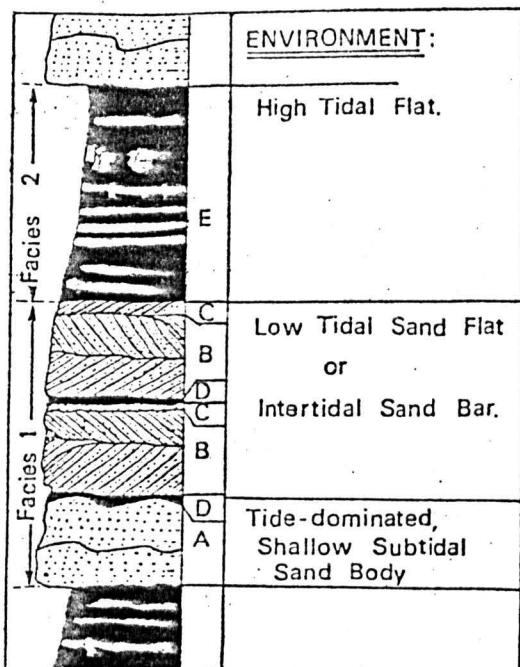


Figure 4-3: Klein's (1970a) model of inter-tidal sedimentation as applied to Member 5 of the Port Askaig Tillite and members 1 and 2 of the Bonahaven Formation.

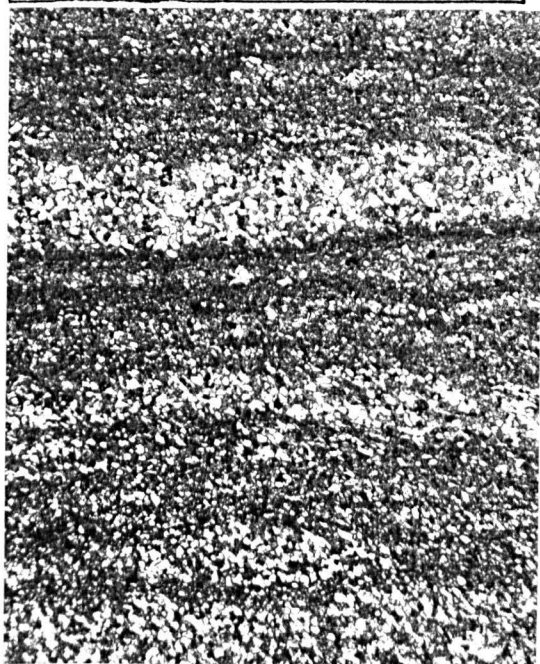


Figure 4-4: photomicrograph, plane polarized light, unit 2. Very fine-grained sandstones with thin silty mud laminae.

1mm

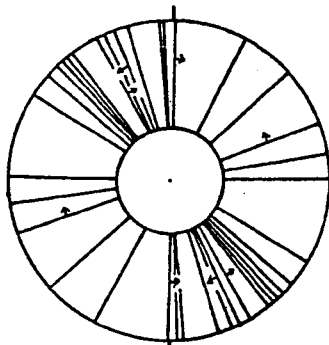


Figure 4-5: unit 2, member 1; cross-section through rippled bed. Ripple is seen to be composite with transport in two directions. Klein (1970a, fig. 4) termed this structure a dune, but its wavelength is much too small for a dune. Parallel laminae below the ripple probably formed by lamina by lamina accretion, like that of fig.4-4, rather than being upper-flow regime laminations.

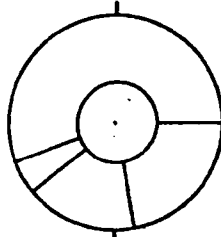
generated ripples) and have probably been degraded soon after their formation.

Unit 3, exposed only at Caol Ila, rests erosively on silty mudstone in a small exposure on the modern shore; the erosion surface is overlain by a very coarse pebbly feldspathic sandstone. In an exposure on the cliff there is a conglomerate of tightly packed mudstone fragments with interstitial coarse sand. Granite fragments like those in the Port Askaig Tillite occur. These lithologies pass upward into parallel-laminated medium-grained sandstones, then to a dominantly cross-stratified sandstone, with erosional tabular sets 5-15cm in thickness. Most of the bed tops are planar however and are capped by a mud lamina (fig. 4-7). An intervening set of cross-lamination (Klein, 1970a, fig. 4-3) is by no means always present. The mud laminae are commonly composite, consisting of several, one millimetre thick, laminae. One set of cross-strata is overturned which, considering <sup>the</sup> textural maturity and environmental setting of these sediments, indicates contemporary earthquake activity (Allen & Banks, 1972) rather than overhead passage of a dense slurry (Hendry & Stauffer, 1975). The orientations of the cross-strata (fig. 4-6b,c) show much variation, but in the 35-37m interval are clearly bi-modal north-south, suggestive of a tidal origin. Occasionally upper set boundaries are rounded and compare with re-activation surfaces (Klein, 1970b).

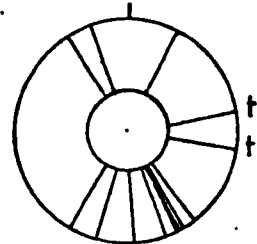
The dominant lithology at the base of unit 4 is a purplish mudstone with lenses of greenish sand and silt. Some of the lenses have internal cross-laminae marked by concentrations of heavy minerals. Thinner silt layers grade up into mudstone. Interbedded with these sediments are well-sorted, very-fine grained sandstones (50-100µm grain size) with



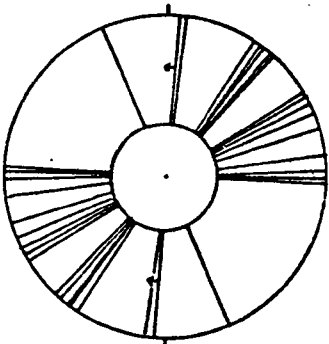
a ripple crestlines: unit 2



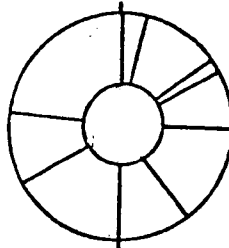
b cross-strata:  
unit 3  
28-32m



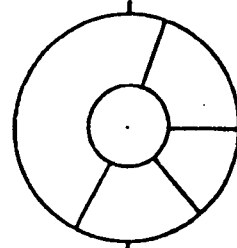
c cross-strata:  
unit 3  
35-37m (t=37-38m)



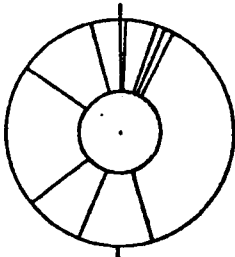
d ripple crestlines: units 4&5



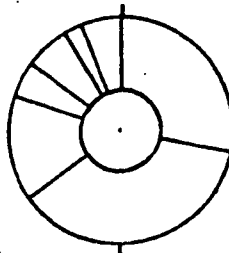
e low-angle cross-strata  
unit 4



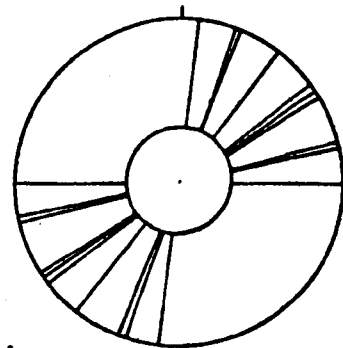
f cross-strata  
unit 5 (lower part)



g cross-strata unit 5 (upper)  
and member 2:  
Caol Ila



h cross-strata  
unit 5 and  
member 2:  
Bonahaven

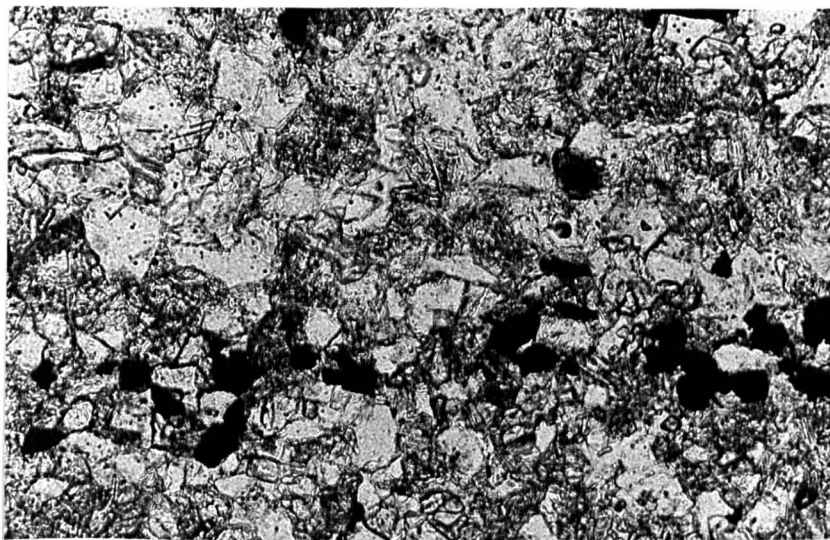


i ripple crestlines,  
member 2

Figure 4-6: Palaeocurrents from members 1 and 2.



Figure 4-7: Unit 3 (36m) Caol Ila. Cross-stratified sandstone (quartzite) overlain by a planar mud lamina. An intervening set of cross-lamination may be present.



200  $\mu$ m

Figure 4-8: Heavy mineral lamination in unit 4 sandstone (photomicrograph, plane polarized light). Opaque grains are magnetite; clear grains, quartz; and turbid grains, sericitized feldspar. This is the only level in the Bonahaven Formation where clastic textures are so well preserved in very fine grained sand material.

parallel heavy mineral laminae (fig. 4-8). The fine grain size of these sandstones coupled with the excellent sorting indicates that these parallel laminae formed under upper flow regime conditions. There are also erosional co-sets of cross-lamination (set thickness up to 4mm) marked by heavy mineral laminations. No palaeocurrent measurements could be obtained on these. These various lithologies are shown in figure 4-9, where a small irregular erosion surface overlain by silts occurs, perhaps suggestive of sub-aerial exposure.

The 45-50m interval within unit 4 at Caol Ila (fig. 4-2) consists of the parallel laminated very fine grained sandstones which are arranged into a series of wedge-shaped cross-sets (fig. 4-10), each set being of height 10-50cm and lateral extent greater than 10m. The dip angle of the lamination is in the range 6-16° with a wide scatter of dip azimuths (fig. 4-6e). Klein (1970a) apparently mistook the heavy mineral laminae for mud laminations, concluding that the unit was dominated by 'tidal bedding' (Reineck & Wunderlich, 1968). Small scours within, and at the base of the sets of low angle cross-strata are filled initially with medium sand or cross-laminated fine sand, grading up to very fine sand (fig. 4-11). One level shows structures which compare with large loads (Brenchley & Newall, 1977) consisting of concave upward bulbs 0.5-1m wide separated by cusps. Small scale loads, with maximum penetration of about 1cm occur frequently in unit 4.

The top 5m of unit 4 at Caol Ila consists of thickly laminated to medium bedded mudstones and parallel laminated very fine-grained sandstones. The mudstones are almost invariably mudcracked, sometimes with two orders of polygons (fig. 4-12). Eroded mud fragments in the sands

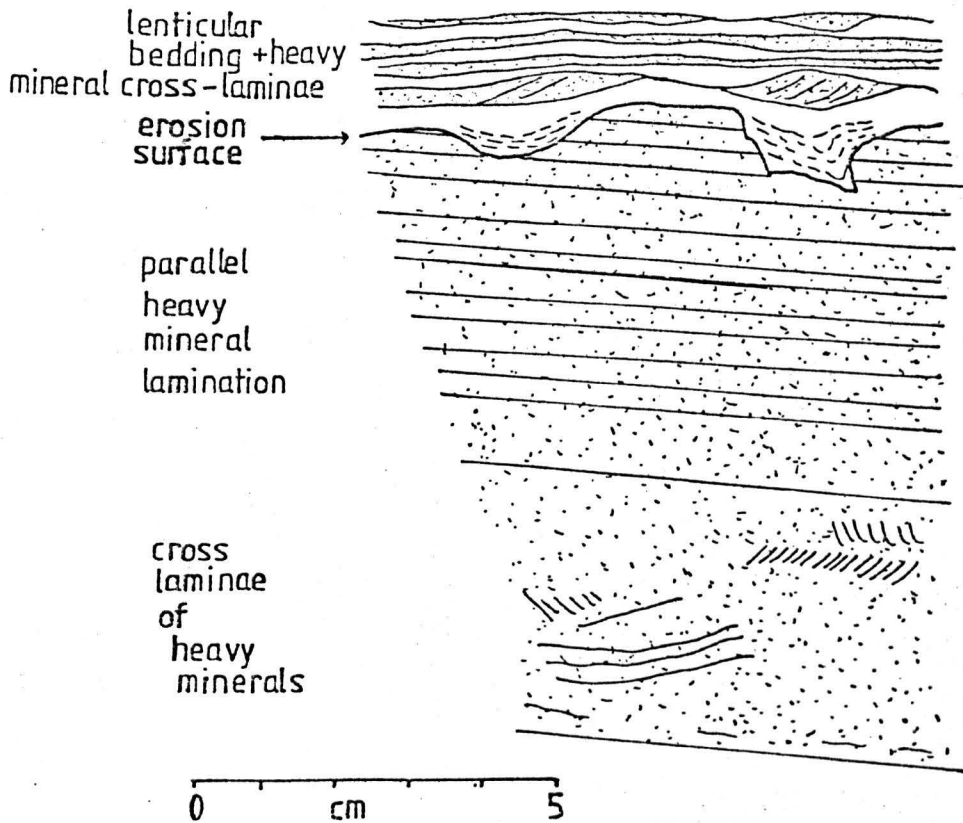


Figure 4-9: sketch from tracing of polished surface of hand specimen, unit 4 (42m) from Caol Ila. Sand layers are stippled.



Figure 4-10: Unit 4, Caol Ila (50m). Low angle cross-sets: the topmost set dips to the left with a slightly irregular set base. The central set dips to the right forming a wedge thickening to the right. The lowest 'set' represents horizontal parallel lamination.

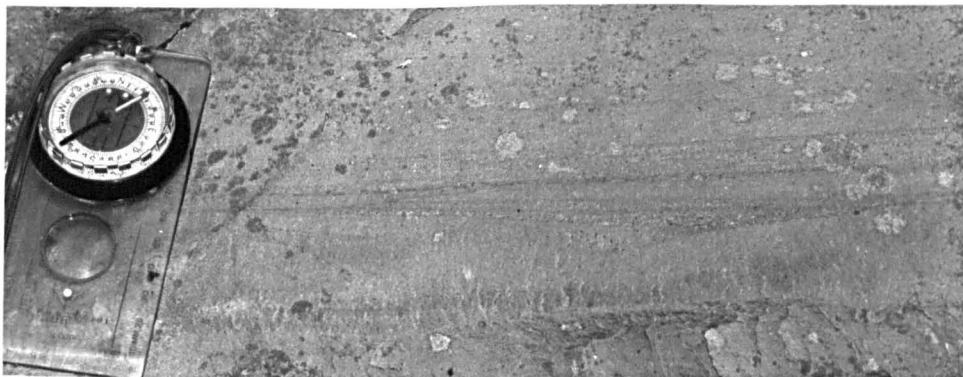


Figure 4-11: Unit 4 (48m) at Caol Ila. Scour in very fine grained sandstone overlain initially by medium grained sand, fining upwards.

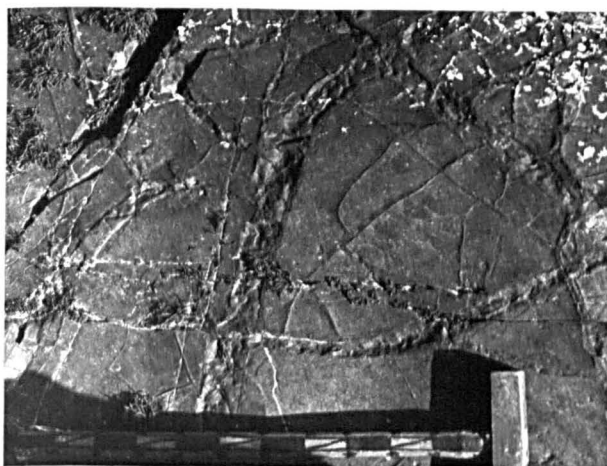


Figure 4-12: Unit 4 (50m) at Caol Ila. Mudcracks, with two orders of polygons visible.



Figure 4-13: Unit 5 (40m) at Bonahaven. Interbedded dolomitic sandstones (smooth weathering), the lowest of which is parallel laminated, and conglomerates of dolostone fragments (rough or holey weathering). Many of these fragments are secondary replacements of mudstone clasts.

are visible in thin section, although not in the field. These observations indicate that the mudcracks have a sub-aerial origin, rather than being sub-aqueous synaeresis cracks as postulated by Spencer (1971b) and Spencer & Spencer (1972), although genuine synaeresis cracks do occur in member 3. Symmetrical wave ripples are also common near the top of unit 4; they have wavelengths averaging 3.2cm (10 readings), crestlines being orientated NE-SW (fig. 4-6d).

Unit 5 is readily distinguished from the lower units by the presence of dolostone clasts and dolomitic sandstones. At Caol Ila it is dominantly medium-grained sandstone, but at Bonahaven it contains mudstone beds. The base of the unit at Caol Ila has an irregular erosion surface with relief up to 10cm. In both areas the sandstones are parallel-laminated and cross-stratified, fine to medium grained and dolomitic. The parallel laminae are marked by concentrations of mud clasts or by variation in the quantity of intergranular dolomite. The cross-strata form sets up to 15cm thick, similar to those seen in unit 3 at Caol Ila. Two examples of climbing ripples occur, featuring sets 1.5-2cm thick and angles of climb varying from 5 to 20°. Wave-ripple form-sets (3 readings) average less than 3cm in wavelength. The sandstones bear mudstone and dolostone pebbles, scattered throughout, but also concentrated at some levels. At Bonahaven there are abundant mud beds, mostly mudcracked; some are now only represented by horizons of mudstone pebbles. Some show internal silt laminations with low angle truncations, probably resulting from deposition on gently undulating surfaces. The uppermost mud beds bear spherules (Chapter 5)

which are thought to be microfossils. In the field dolostone beds appear to be present, but on laboratory examination these invariably prove to be dolomitic sandstones or tightly packed conglomerates of dolostone fragments (fig. 4-13). Graded sequences a few cm thick, from sand or silt to silt or mud, are common, followed upward by an erosion surface overlain by a dolomitic sandstone or conglomerate. Thus many mud beds are partly or wholly eroded (see Chapter 5, figure 5).

Member 2 consists of medium grained pure sandstones (quartzites) which contrast with the dolomitic sandstones beneath. There is a basal 2m cross-stratified interval of erosional tabular sets each up to 25cm thick. At Caol Ila, although not clearly at Bonahaven, current directions from these cross-strata show a bimodal pattern (fig. 4-6g,h). Some parallel laminae marked by coarse sand occur a metre or so higher in the section. Most of member 2 is structureless, but can be parallel laminated or more often thickly bedded by joints. Thus it is lithologically very similar to Member 5 of the Port Askaig Tillite. Inland to the west (Cro Earraich) member 2 shows abundant wave rippling (fig. 4-6i) with 3-6cm wavelengths and NE-SW crestlines. In the far western area it is commonly cross-stratified (15cm thick sets) and wave rippled.

#### 4.2.2: Interpretation

Klein (1970a) worked on Member 5 of the Tillite and member 1 of the Bonahaven Formation, interpreting them purely in terms of tidal processes, and proposed a simple regressive model (fig. 4-3). Two such regressive sequences were recognised by Spencer (1971b): tidal flat deposits

(units 1 and 4) succeeding shallow sub-tidal and inter-tidal sands (top of Port Askaig Tillite and units 2/3). Klein has demonstrated the importance of tidal processes in these rocks, but his model is not particularly appropriate for this sequence.

The re-interpretation below (summarized in figure 4-2) is based on the vertical sequence and sedimentary sequences of the east coast exposures and will be expanded in Chapter 8 when discussing the consequences of the wedging out inland of member 1.

Unit 1 of member 1 probably does not represent tidal flat deposition as envisaged by Klein (1970a). Instead, the regular plane silt laminae and lack of mudcracking and channelling indicate a sheltered, permanently submerged environment, either lagoonal, or some way offshore. However the gradational relationship to unit 2 which is interpreted below as inter-tidal/very shallow sub-tidal supports a lagoonal origin for unit 1.

Unit 2 is coarser, indicating an overall more energetic environment. The regularity and fineness of the mud laminae suggests they originated by repeated slack-water deposition (i.e. tidally influenced, Reineck, 1967) rather than during calm water episodes during storms (Reineck & Singh, 1972), although Raaf et al. (1977) show that flaser bedding can form in wave-dominated sequences. The interpretation that the sands were deposited from tidal currents is supported by the orientation of ripples in unit 2 which are at right angles to definite wave ripples found in the Port Askaig Tillite and numerous levels in the Bonahaven Formation, which implies that they are current ripples. The prevalence of such bedforms indicates very shallow water which may have been inter-tidal at times

judging by the occurrence of superimposed ripples.

Unit 3 is a coarse deposit which has an erosional (probably channeled) lower boundary, resting on mudstone. The basal conglomerate represents a lag gravel of local and exotic fragments followed upward by the cross-stratified sands deposited by reversing (tidal) currents. The rare sets of cross-lamination (Klein, 1970a) cannot be regarded as proof of exposure (representing late stage run-off) because it cannot be demonstrated that their orientation is at right-angles to that of the cross-strata as Klein claims. The cross-lamination could well represent ripples produced by rather weak flow in one part of the tidal cycle in an inter-tidal or sub-tidal situation. The mud laminae which overlie the cross-laminae or cross-strata are generally planar. Thus the mud, and underlying sand were not deposited during a single tide (cf. Klein, 1970a), but there was an interval during which the bedforms were wiped out. The fact that some of the mud laminae are too thick to have been deposited during one slack tide was shown by McCave (1971) and is confirmed by the composite nature of the mud laminations in thin section. Thus they were deposited from a series of slack water episodes, probably during neap tides.

Unit 3 obviously represents a tidal channel of some kind in an estuarine, deltaic or tidal flat situation (Straaten, 1954b, Oomkens, 1974), a tidal delta (Hubbard & Barwis, 1976) or an inlet in a barrier island (Terwindt, 1971; Kumar, 1973; Kumar & Sanders, 1974). Although very large bedforms (sand waves) are present commonly in the lower reaches of a tidal inlet, the resulting sets of cross-strata may have thicknesses of only about 10cm (Kumar, 1973) similar to that

of unit 3. Parallel lamination only occurs in the shallower (4-5m depth) parts of the inlet described by Kumar (1973), but occurs at the base of the channel at Caol Ila, suggesting that the latter cannot have been deeper than about 5m, shallower than a fully-fledged inlet would be. The channel certainly must have been the site of relatively high current velocities: compare unit 3 with the deposits of low discharge channels in tidal flats described by Evans (1965) and Bridges & Leeder (1976). Such a channel could occur in a variety of settings but the interpretation of back-barrier sedimentation in unit 4 (see below) implies that unit 3 is likely to represent part of a tidal delta or temporary inlet. The mudstone in the poorly exposed central part of unit 3 probably indicates that two separate channel sequences are present.

The basal part of unit 4 is not a regressive continuation of unit 3 sedimentation as neither tidal flat deposits (tidal channel model) nor spit platform deposits (tidal inlet model) are present. The basal mudstones may instead be an abandoned channel-fill deposit. (Goodwin & Anderson, 1974).

The mudcracks in the top part of unit 4 indicate an intermittently exposed situation for at least part of unit 4. The best clue as to the nature of this situation comes from the parallel laminated very fine grained sandstones, rich in heavy minerals, which are characteristic of unit 4. The mere presence of heavy mineral laminae is not diagnostic of any particular environment as they occur in beach sediments (Clifton, 1969), washover sands (Schwartz, 1975) and deep sea contourites (Bouma & Hollister, 1973). It seems that any heavy mineral-rich sediment acted on by a sorting

process will exhibit heavy mineral laminations.

Kumar (1973) described parallel-laminated channel deposits of medium sand with a heavy mineral-enriched silt fraction occurring at depths of about 4m in a tidal inlet. However these sediments are of limited occurrence in the inlet sequence, so the sheer abundance of parallel-laminated sediment at Caol Ila rules this out. The arrangement into low-angle cross-sets, the occurrence as isolated medium beds in mudstone, the absence of associated cross-stratification and thin mud laminae argues against a tidal origin for the unit 4 parallel-laminated sediments.

Sediments showing parallel lamination arranged in low-angle cross-sets have been described in beach, washover and shoreface situations. Although the sediments are finer than usual for such environments, suitable analogies are furnished by Davies et al. (1971).

The type of stratification and dip angles of the low-angle cross-sets are consistent with beach sedimentation (Hayes et al., 1969), although the large range in orientation of the Caol Ila sets (fig. 4-6e) would not be expected. Shoreface sediments deposited on sub-aqueous bars exhibit landward and seaward-dipping low-angle cross-sets, horizontal lamination, co-sets of current ripple laminae, wave ripples and lenticular bedding (lower and middle shoreface; Davies et al., 1971; Davidson-Arnott & Greenwood, 1976). However the presence of desiccated mud beds is a major difficulty in either of these interpretations.

A viable alternative is provided by washover sedimentation which characteristically produces parallel-laminated sands (Andrews, 1970; Schwartz, 1975). Individual washover (hurricane) events produce thicknesses of sediment from a few cm

to 1.5m (Schwartz, 1975) with a sharp scoured base (Andrews, 1970) comparable with the unit 4 sandstones. The lamination tends to have very low landward dip, although can be variable (Schwartz, 1975). Andrews (1970) records seaward-dipping lamination produced during the storm ebb.

On the washover interpretation, the lower part of unit 4 would represent back-barrier bay sediments (silt and mud) with permanent water cover, interfingering with the distal end of a washover fan (parallel-laminated sands). The central part of unit 4 would represent slightly more proximal parts of the fan, reverting to distal in the upper part where the interbedded mudcracked, internally unlaminated mudstones would be deposited in ponds which eventually dried up (Andrews, 1970). Tidal re-working of washover sediments would form the sets of ripple lamination (fig. 4-9). Wave action between hurricanes in back-barrier ponds or flats (Barwis, 1976) would form the wave-generated ripples, whose very low average wavelength (3.2cm) suggests a very restricted fetch (Tanner, 1971) as one would expect in such a situation (e.g. Hobday & Horne, 1977).

Unit 5 is consistent with a continuing record of back-barrier sedimentation. At Caol Ila, being dominantly cross-stratified sands with intraclasts, it probably represents the deposits of a tidal sand flat (Klein, 1970b; Hayes et al., 1969), possibly as a tidal delta (Hubbard & Barwis, 1976). The climbing ripple lamination caused by rapid sediment fall-out from suspension, and the graded sequences in the Bonahaven section could form on the flood tide following a storm (Anderton, 1975). The preserved wave-generated ripples are, as in unit 4, of very small wavelength suggestive of restricted wave fetch. Remnants of

mud flats are represented by the desiccated mud beds at Bonahaven. Some pure dolostone was being formed in the area, but is preserved now only as clasts; it could be that it was forming close to H.W.M. and so was likely to have been eroded.

The base of member 2 is similar to the unit 5 sandstones, except that the former is not dolomitic. The tidal origin of this cross-stratified material is not in doubt, but the significance of the somewhat thicker sets is not clear.

The higher parts of member 2 compare with the top of the Port Askaig Tillite: a similar high energy sub-tidal environment seems most likely. Another possibility is a washover deposit, but its thickness and uniform lithology over a wide area argue against this. Given a sub-tidal origin, then a transgression over the whole of northern Islay is indicated. One would expect to see the passage of a surf zone preserved (Fischer, 1961): there are some parallel laminations of coarse sand fairly low in the member which could represent beach deposits, but this is not conclusive.

Shallower water in the western area may be indicated by the more diverse sedimentary structures here compared with the east coast exposures.

4.2.3: Conclusions

Following deposition of the high-energy sub-tidal sediments at the top of the Port Askaig Tillite there is a regression at the start of Bonahaven times with the inferred emergence of a barrier island offshore. All the member 1 sediments are consistent with a back-barrier, commonly inter-tidal situation, although direct evidence for the existence of a barrier only comes from unit 4.

There is no cyclicity (cf. Klein 1970a), rather a vertical sequence of sub-environments are seen, which are not repeated. Member 2 records a transgression, returning the area to the type of sedimentation characteristic of the top of the Port Askaig Tillite.

#### 4.3: Member 3

There is an abrupt change in sedimentation type from the pure sandstone at the top of member 2 to the distinctive sedimentary assemblage which constitutes member 3. The latter is constantly dolomitic and contains large numbers of pure dolostone laminae and beds, some of which are clearly stromatolitic. Stratigraphic logs of member 3 in Sections B,C,D and E are illustrated in Enclosure 2. Three sedimentary facies are recognised, and are described below.

##### 4.3.1: Introduction to the facies

The layered facies consists of thickly laminated to thin bedded very fine to medium grained dolomitic sandstones and muddy dolostones. The latter range in composition from pure dolomicrites to silty, slightly dolomitic mudstones. This is considered to be a primary feature.

Three sub-facies are designated as follows:

The standard sub-facies has abundant contraction (syn-aeresis) cracks and wave-generated cross-lamination.

The lenticular-graded sub-facies exhibits lenticular and/or graded bedding.

The marginal sub-facies is characterised by frequent irregularly-topped dolostone beds, often with pockets of edgewise dolostone flakes within sharp depressions on the bed top.

The sandstone facies consists of individual beds (0.2-3m thick) of cross-stratified, medium grained dolomitic sandstone, commonly bearing ooids. There are abundant dolostone clasts and laminae and thin beds of dolostone showing contraction (probably desiccation) cracks.

The stromatolite facies refers to stromatolite bioherms and biostromes.

Table 4-1 shows the relative abundance of the various sedimentary structures in the sandstone and layered facies.

TABLE 4-1

Percentage of beds of the layered and sandstone facies which show various sedimentary and other structures

structure	symbol	standard	lent-grad	marginal	sandstone facies
		layered facies			
Lenticular bedding		0	75	0	0
Graded bedding		20	54	25	0
Wave-generated ripples and cross-lamination		72	14	43	35
Dolostone conglomerates or pebbles		20	14	29	72
Nodules		28	46	25	12
Loads		8	11	32	6
Contraction cracks		87	25	71	17
Scoured + desiccated dolostone		13	21	46	0
Flake pockets		7	7	46	0
Cross-stratification		8	4	0	73
Low-angle bedding		0	0	11	0
Small erosion surfaces		0	0	7	-
Silicified sandstone matrix	SIL	0	0	0	8
Oölitic	OOL	3	0	0	27
Parallel lamination	=	3	0	0	17
Massive (structure-less)	M	0	0	0	19

4.3.2: The layered facies

This facies makes up most of the thickness of member 3. Its various attributes are described below.

4.3.2.1: Mineralogical composition of the sub-facies

Figures 4-14, 15 and 16 show the variation in mineralogical composition of each sub-facies, based on visual estimates, and some point counts, of abundance of minerals within homogeneous domains in thin sections. The thin section examination was carried out independently of considerations of the sub-facies to which each sample might belong and so the diagrams should not show any systematic bias in this respect i.e. are accurate, although imprecise.

The standard sub-facies shows a wide range in composition with few points in the corners of the triangle indicating availability of sand, silt and clay as well as conditions appropriate for the precipitation of carbonate. In addition, many of the finer laminae are noticeably carbonaceous. In contrast the lenticular-graded sub-facies contains on average less quartz, and tends to be dolomitic. The marginal sub-facies is notable for its paucity of clay: most of the fine-grained laminae here are very dolomite-rich.

Thus the designation of facies primarily by sedimentary structures also carries with it a distinction in terms of mineralogical composition.

Most beds can be readily assigned to a given sub-facies, although there are some cases, usually where a bed is poorly exposed, where this is more difficult. Intermediate cases do occur however indicating that the subfacies are to some extent gradational.

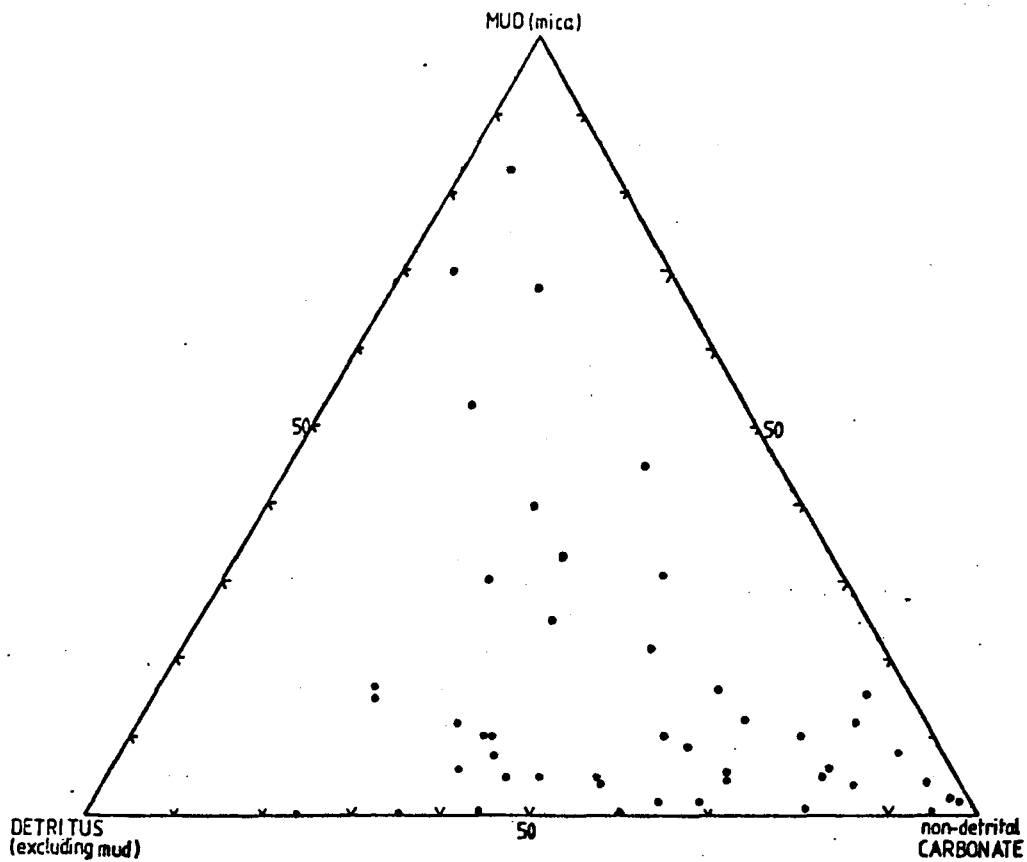


Figure 4-14: Composition of individual laminae within the lenticular-graded sub-facies (mostly from visual estimates in thin section).

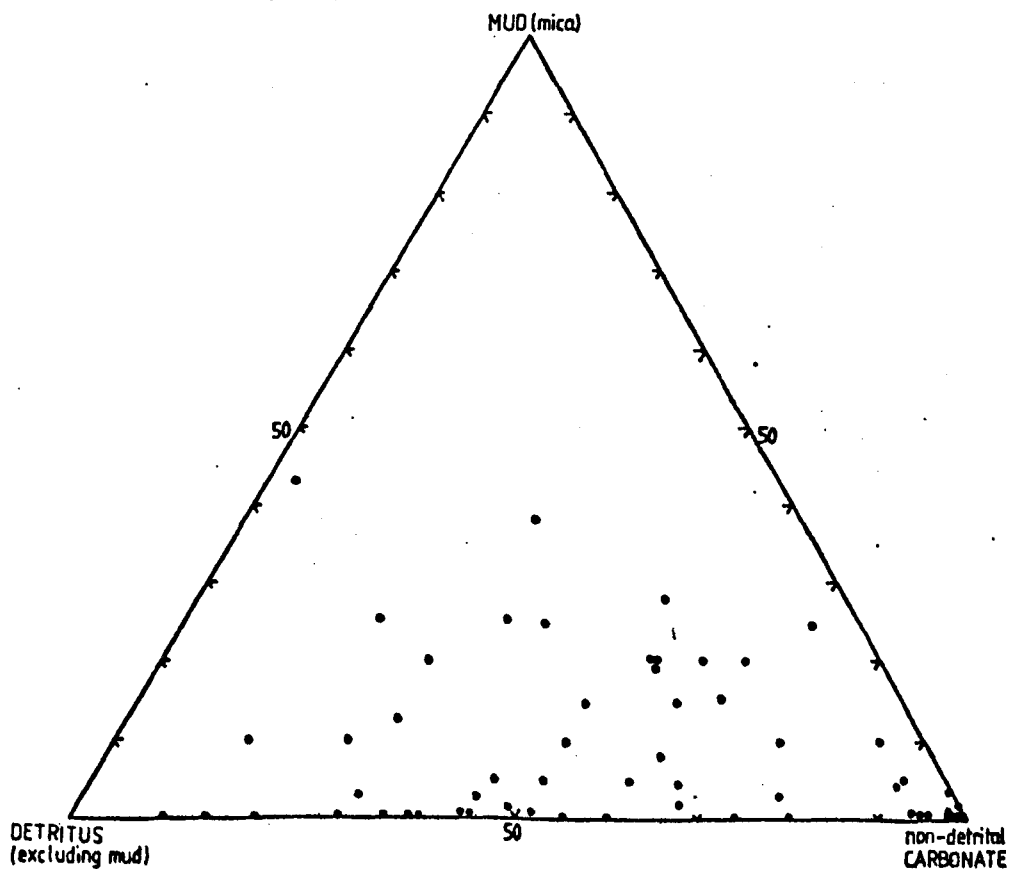


Figure 4-15: Composition of individual laminae within the marginal sub-facies (mostly from visual estimates in thin section).

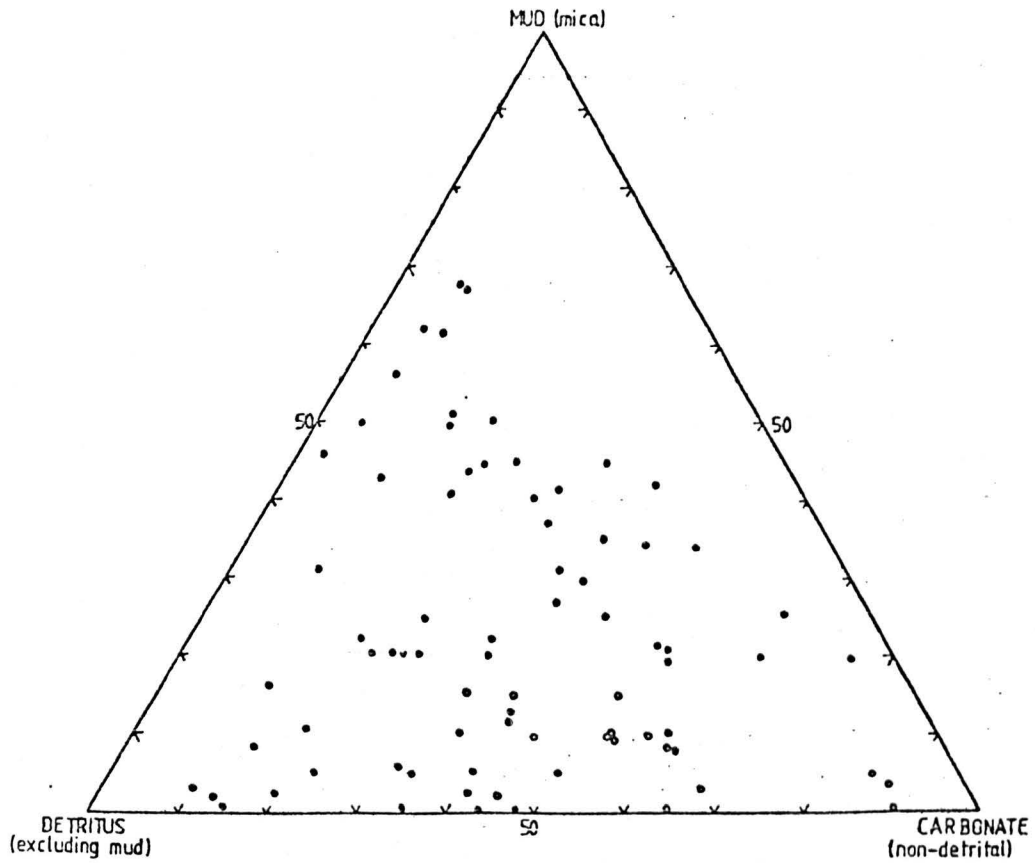


Figure 4-16: Composition of individual laminae within the standard sub-facies (mostly from visual estimates in thin section)..



Figure 4-17: Bed 37/90; cross-lamination from wave-generated ripples.

#### 4.3.2.2: Ripples and cross-lamination

Cross-lamination in the layered facies is characteristically composed of wavy laminations, symmetric or asymmetric (fig. 4-17), associated with preserved form sets. These preserved ripple marks range in wavelength from 2.5 to 22cm and have a ripple index (wavelength/height) of 10. Crestlines are straight to slightly sinuous with occasional tuning fork junctions (Tanner, 1967), and are either symmetric or asymmetric with ripple symmetry index (stoss length over lee length) of less than about 2. This indicates that the ripples are wave-generated. The cross-lamination compares with the wave-generated cross-lamination described by Raaf et al. (1977).

The orientation of the ripple crestlines is dominantly ENE-WSW (fig. 4-18). This direction can be taken to be perpendicular to the prevailing winds and to lie roughly parallel to the shoreline (Hobday & Horne, 1977) or at least within  $65^{\circ}$  of the shoreline orientation (Davis, 1965). Asymmetric wave ripples indicate shoaling waves with a net translation which is dominantly onshore. In member 3, 8 wave ripples are asymmetric to the NW and 3 to the SE which suggests the shoreline lay to the NW. Some ripples with a symmetry index greater than 2 occur; they show diverse transport directions (fig. 4-19). Several of these may be true current ripples, but they are unimportant in comparison to the wave-generated ripples.

Tanner (1971) has devised an empirical numerical method for estimating the fetch of the waves producing a given ripple-mark field, based on the argument that if ripples are preserved which show a wide range in wavelength and have a stable average value for the wavelength, then this

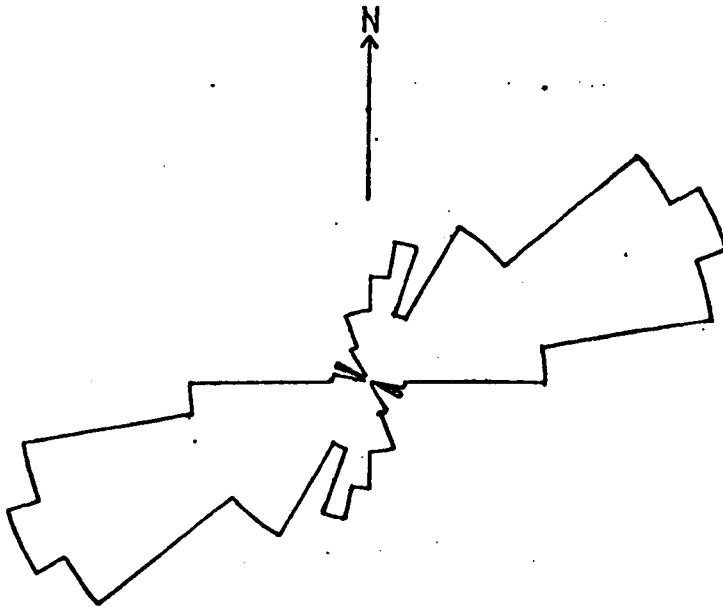


Figure 4-18: Crestline orientations of member 3 wave-generated ripples. (total 62 readings).

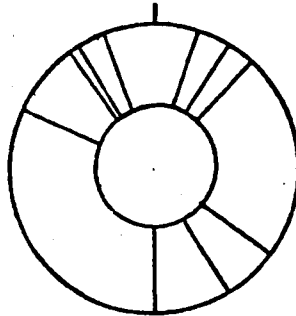


Figure 4-19: Current directions from member 3 ripples with ripple symmetry index greater than 2 (10 readings).

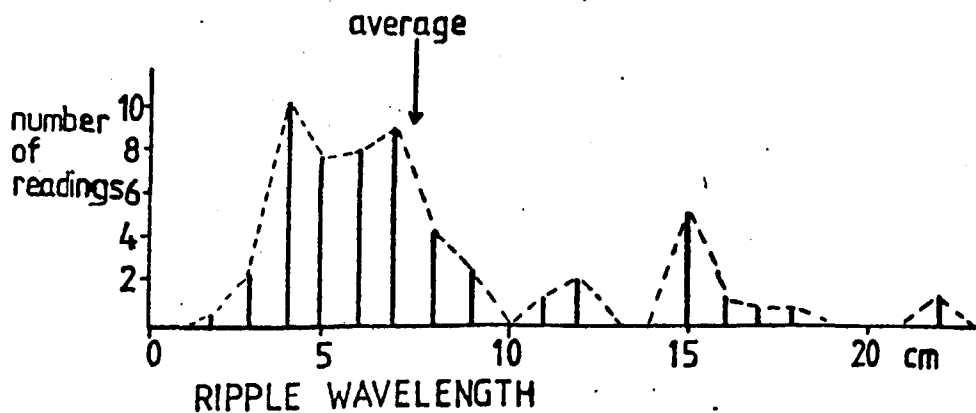


Figure 4-20: Wavelengths of ripples used in wave fetch estimates (56 readings).

average represents the product of 'average' wave conditions. The longer the fetch of the waves, the greater will be the wave height under 'average' conditions and the average wavelength of the resulting ripple marks. Komar (1974) indicated shortcomings in estimates of wave parameters of ancient rocks if oceanic rather than very shallow water conditions prevailed: the result is that values of water depth and fetch, if inaccurate, are underestimates.

In member 3, 56 ripple marks are available with symmetry index 1.5 or less to estimate ancient wave parameters. They show a wide range in wavelength (fig. 4-20) so that the above conditions are met, although the number of readings is somewhat low. The results (Table 4-2) indicate an order of magnitude water depth of 80cm and a fetch definitely in excess of 100km. This length of fetch precludes there having been a sub-aerial barrier nearby offshore.

TABLE 4-2

Estimates of ancient water depth and wave fetch from member 3 ripples

INPUT: 56 measurements  
 Average wavelength= 7.5cm  
 Average grain size= 150 $\mu$ m

OUTPUT: 1. "simplest" method of Tanner (1971)  
 Wave height= 17cm  
 Water depth= 80cm  
 Fetch= 224km.

2. other estimates of fetch, solving pairs of equations from Tanner 1971 .

		equation			
		17	18	19	
equation	21	180	1400	160	(note: equation 17 tends to under-estimate) fetch).
	20	50	220	140	
	10	52-74	204-276	142-170	

CONCLUSION: Fetch is in excess of 100km

Superimposed and interference ripples occur at three horizons: both sets in bed 9D are wave-generated, of large wavelength and probably contemporaneous with one another: they are probably sub-tidal (Tanner, 1960; Davis, 1965). Those in bed 6D are of indeterminate origin, whilst in bed 63C both sets are current ripples: extremely shallow water can be inferred here.

#### 4.3.2.3: Lenticular and graded bedding

Lenticular bedding is characteristic of the lenticular-graded sub-facies and indicates a shortage of sand-sized detritus (as seen in the compositional triangle of figure 4-14) leading to the formation of lensing sand layers. Graded bedding is linked with this in that it is most conspicuous in very thin lenticular sand layers (fig. 4-21) of the lenticular-graded sub-facies, although also occurs in the other sub-facies. In the graded lithologies the coarsest grain size is very fine to medium grained sand which grades up over a few millimetres to a (muddy) dolostone (1-5cm thick) with some quartz silt. Graded units on this scale in shallow water environments could be generated by slackening of tidal currents or by the waning of a storm. Tidal slack-water laminae were noted in units 2 and 3 of member 1: as the tidal cycle is short, the laminae are very thin there. Storms are much less frequent so a relatively thick inter-storm deposit would be expected. Thus the dominance of wave-generated ripples over current ripples in this facies and the relatively thick and undivided nature of the fine-grained layers indicates that storms were responsible for the graded bedding. Exposed (proximal) areas would receive much sediment falling out rapidly to give the sinusoidal ripple lamination characteristic of the standard sub-facies, whilst more sheltered



Figure 4-21: Bed 50E; graded bedding. Abundant quartz-calcite nodules also visible.

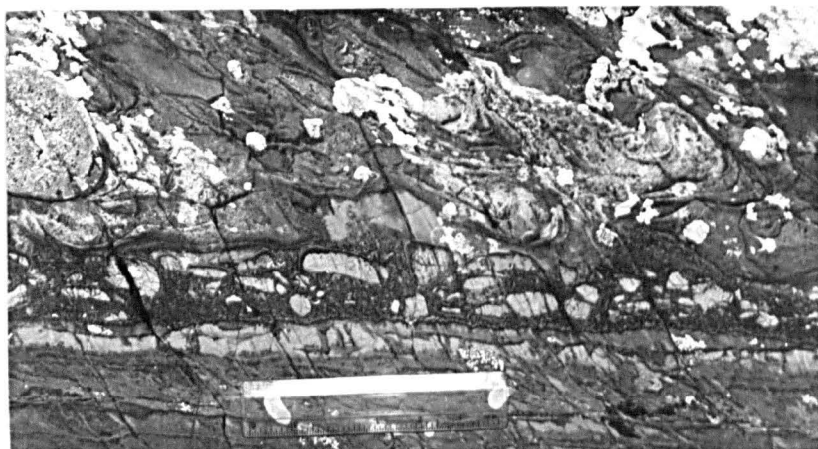


Figure 4-22: Conglomerate of dolostone pebbles and flakes; bed 64/5C. A liquefied sand layer occurs higher up.

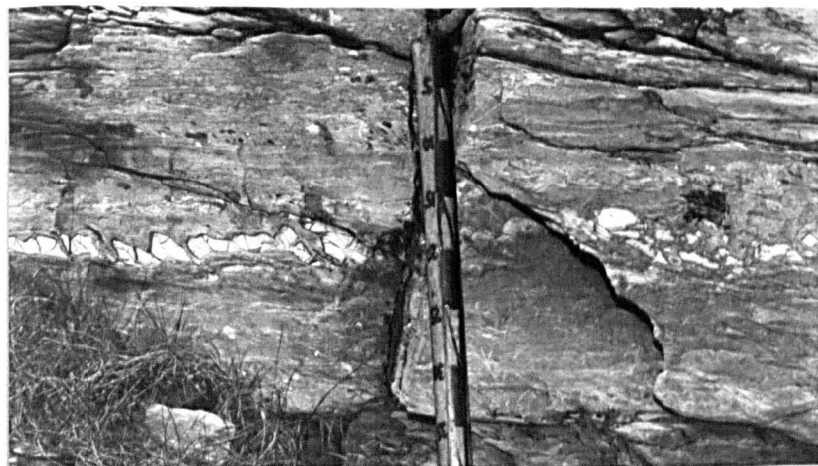


Figure 4-23: Bed 18D; dolostone with wavy top surface and probable desiccation cracks changing laterally to a conglomerate of dolostone pebbles.

(distal) areas would receive only a thin, often lenticular sand layer which would grade up to muddy dolostone.

#### 4.3.2.4: Parallel lamination and cross-stratification

Parallel lamination, probably of the upper-flow regime because of the absence of mud, and cross-sets up to about 8cm thick occur occasionally in the layered facies. The cross-strata, by analogy with the sandstone facies (4.3.3) were formed from tidal currents, whilst the parallel lamination formed from high energy wave action or swift tidal currents. This evidence, together with the few current ripples present indicates a certain amount of tidal activity during deposition of parts of the layered facies. However, apart from beds 61C and 61E which seem to show intermediate characters, all beds can be confidently assigned to the wave-dominated layered facies or the tide-dominated sandstone facies.

#### 4.3.2.5: Low-angle bedding

Beds 70C and 72C, belonging to the marginal sub-facies, show low-angle ( $5^{\circ}$ ) cross-bedding of thin silt laminae in dolostone, changing laterally to horizontal bedding by thinning of the dolostone. This superficially resembles point-bar deposits of inter-tidal creeks of low discharge (e.g. Bridges & Leeder, 1976). However cross-sets do not truncate one another, so the structure is essentially accretional rather than erosional. Dolomite formation was apparently inhibited in localised areas, perhaps due to local variations in tidal flow velocities. The structure could form inter-tidally or sub-tidally (P.Bridges pers.comm.).

#### 4.3.2.6: Conglomerates and breccias of dolostone clasts

These lithologies occur in three geometrical forms (in addition to the breccias in the sandstone and

stromatolite facies).

1. thin, fairly continuous beds 2-40cm thick
2. lenses up to 20cm thick, which have a lateral persistence of only a few metres.

3. as edgewise flake pockets (see 4.3.2.8).

1. The thin beds have a lateral persistence of less than 100m up to several hundred metres or more and most are less than 10cm thick (fig. 4-22). They are composed of fine to coarse-grained quartz sand, dolomicrite pebbles which are usually fairly well rounded, and occasionally centimetre sized dolomicrite flakes (aspect ratio of 2 to 20). The sand and rounded dolostone pebbles were probably derived by storm transport of sandstone facies material. High energy is indicated by an occasional edgewise arrangement. Some of these conglomerates could actually be thin representatives of the sandstone facies, but are too thin to show the characteristic cross-stratification. The small flakes of dolostone were presumably derived by rip-up of desiccated dolostone layers (see also 4.3.2.8).

2. The less continuous conglomerate layers are probably all storm-generated deposits; they contain more angular flat dolostone clasts than the more continuous beds so were presumably less transported. Some are clearly generated by the break-up of desiccated dolostone beds (fig. 4-23). One conglomerate lens occupies a small channel (a few centimetres deep) in bed 73E, but other lenses appear simply to fill up local depressions with only minor erosion. Scour following storms is probably also responsible for the small channels a couple of centimetres deep which occur in the marginal sub-facies at the top of Section C.

#### 4.3.2.7: Dolarenites

Dolarenites occur in beds 41B, 46B and 68-70E. They contain a high proportion of fine to medium-grained sand-sized dolomicrite fragments, often associated with flakes of dolomicrite which have an aspect ratio of usually 4-5, ranging up to 40(20mm x 250 $\mu$ m). The flakes were presumably generated by erosion of a desiccated dolostone surface and were abraded to the sand-sized fragments (peloids). Peloids occur sparsely in many sandstones in member 3 and were probably more abundant than can now be seen because of the effects of compaction and recrystallization. The occurrence of dolarenites near the top of Sections B and E reflects the abundant of dolostone, often desiccated, at this level. The generation of intraclasts there was much more important at times than the influx of terrigenous detritus.

#### 4.3.2.8: Flake pockets and irregularly-topped dolostone beds

Many dolostone beds have an upper surface which displays relief of 2-5cm, exceptionally up to 15cm. Some of these are clearly the result of loading of an overlying sand layer (see 4.3.2.10), but others are characterised by rounded convex-up areas separated by sharp downward points which could not be the result of loading. Often dolostone flakes rest in the downpoints, having an edgewise arrangement because they are in a confined space: these structures are here called flake pockets (figs. 4-24, 25 and 26) and are very common in the marginal sub-facies.

Flake pockets are considered to have resulted from a combination of scouring and desiccation. Desiccation was certainly a contributory factor because in bed 70E, the only locality where these structures are seen in plan,

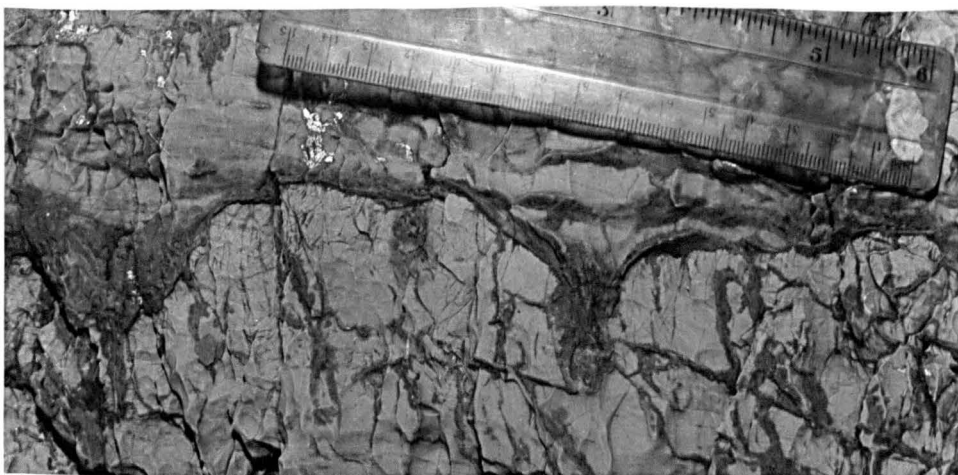


Figure 4-24: Bed 70C; irregularly-topped dolostone bed with flake pockets.

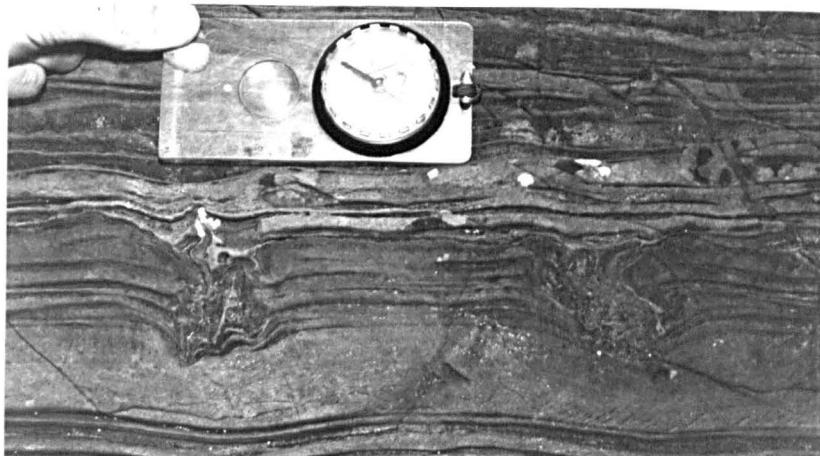


Figure 4-25: Bed 20B; two well-developed flake pockets. Deflection of sedimentary laminae around pockets is due to compaction.



Figure 4-26: Bed 70E; flake pocket showing clear edgewise arrangement of flakes. The pocket connects with the sand layer at the 9cm mark on the ruler. Higher sand layers are graded, but the lowest one shows indistinct sinusoidal ripple lamination.

the flake pockets form a linked network of large polygons (diameter 20cm). Flakes are concentrated in the furrows (pockets) at the margins of the polygons and have their length parallel to the edges of the polygons. However the present form of the dolostone upper surface is not simply that of mudcrack profiles, so some erosion must have taken place. Probably the flakes were generated locally by spalling of desiccated flakes and transported a short distance to rest in erosively modified desiccation cracks. There are however no exposures showing flakes preserved in the process of being formed.

Where an irregularly-topped dolostone bed does not have flake pockets, desiccation need not have been involved, merely scouring of a soft sediment surface. This is indicated by examples in beds 70C (fig. 4-27), 16B and 53D where small contraction cracks occur orientated uniformly at right-angles to an irregular surface presumably produced by scouring. The distribution of the contraction cracks indicates that they must have post-dated the scouring, which therefore must have been on a water-rich, i.e. non-desiccated, surface.

#### 4.3.2.9: Contraction cracks

Spencer & Spencer (1972) showed that sand-filled contraction cracks are common in member 3 and attributed them all to syneresis, operating sub-aqueously. The present study confirms the presence of syneresis cracks, although it seems that desiccation cracks are present at at least one horizon.

The cracks are up to 4cm deep by a few millimetres wide, with a variable degree of linking in plan view. In sections at a low angle to cleavage they show a parallel-sided, but

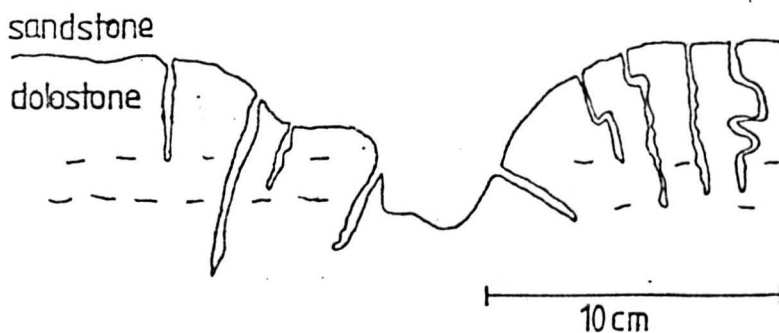


Figure 4-27: Bed 70C; top of dolostone bed showing an irregular (scoured) surface and contraction cracks which appear to post-date the irregular surface because their orientation varies with the dip of this surface. Bedding in the dolostone is undisturbed showing that no element of loading is involved. (Traced from photograph with the aid of a field sketch.)



Figure 4-28: Bed 36/9C; synaeresis cracks in plan view; no complete polygons are formed.

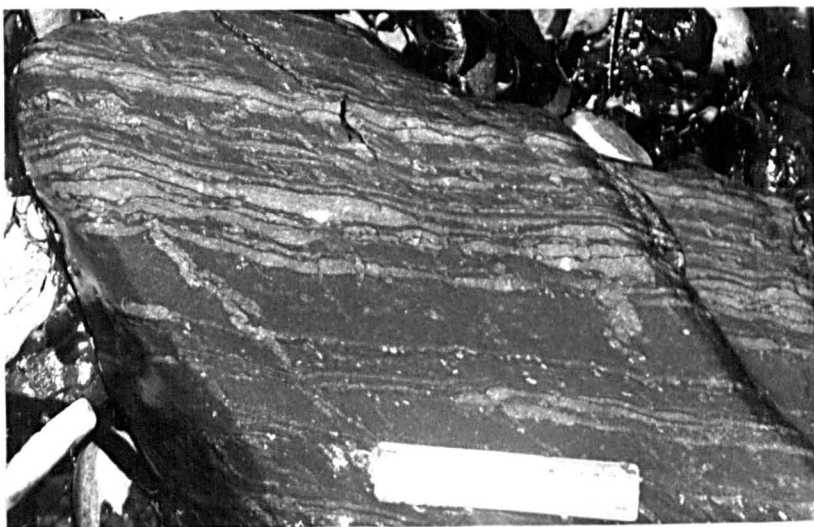


Figure 4-29: loose block from bed 43D; well-developed synaeresis cracks show some pygmatic (compacted) forms and some rotation towards the cleavage. The host lithology for the cracks is carbonaceous dolomitic mudstone.

ptygmatic, form caused by differential compaction of sandy crack-fill and host muddy dolostone. Restoring the cracks to their original length gives a relative compaction factor of 2.3, a result similar to that of Shelton (1962). In sections perpendicular to cleavage the structures are more nearly linear and parallel to one another as a result of deformation (fig. 3-11, fig. 4-29, Borradaile & Johnson, 1973).

Evidence for a syneresis, rather than desiccation origin is summarized below.

1. In cross-section they are parallel-sided, rather than strongly tapering (White, 1961).

2. They have relative compaction factors greater than those of desiccation crack-fills in member 1 (hence the shrinkage process was not as efficient at expelling water as desiccation).

3. They are not associated with mudflake breccias or clasts.

4. A few examples of upward-terminating cracks occur indicating injection, which is more likely for syneresis structures (Spencer & Spencer, 1972), but passive infilling from above is the general rule.

5. The incomplete polygonal structure in plan view (fig. 4-28) tends to indicate a sub-aqueous, rather than sub-aerial origin (Straaten, 1954a, b). However, there is no indication of a parallel alignment of cracks such as that described by Donovan & Foster (1972).

One common effect in cross-section is an upturning of mud laminae next to the cracks; this superficially resembles desiccation mud curling, but in this case is clearly the result of compaction and tectonic deformation.

(Bed 45D)  
At one horizon there are definite desiccation cracks.

These form polygons up to 25cm across with cracks 2cm wide in a partly eroded dolostone lamina with some intraclasts. Complete polygons on a smaller scale are fairly common: <sup>in other beds</sup> it is difficult to rule out a desiccation origin for these, although they are much smaller than both the structures just described and the modified desiccation structures represented by the flake pockets.

In conclusion, most of the cracks in the layered facies appear to be of synaeresis origin.

The most likely cause of synaeresis is an increase (Burst, 1965) or a decrease (White, 1961) in salinity. The cracks are ephemeral (White, 1961), so that periodic influxes of coarser sediment are needed to preserve them (Donovan & Foster, 1972). Sporadic introduction of storm-derived sediment enabled the preservation of the member 3 cracks.

Cracks in pure dolostone present a problem in that a content of flocculated (White, 1961) or swelling (Burst, 1965) clay thought to be necessary for synaeresis to occur, is absent. However a process of osmotic dewatering (Füchtbauer & Tisljar, 1975) caused by salinity increase in overlying water seems feasible. Mukherji & Young (1973) also postulated that certain contraction cracks in micrite were of synaeresis origin. Experimental work to verify this suggestion would be useful. Certainly the fact that spectacular loads can form on dolostone beds (see next section) indicates that the dolostones were very water-rich originally and so had good potential for forming shrinkage cracks.

#### 4.3.2.10: Loads

Loading of coarser into underlying finer sediment with a penetration of 1-4cm occurs at a number of levels. This

demonstrates that the underlying layer was plastic and presumably water-saturated. The most spectacular example, with very deep penetration (fig. 4-30) and occasional development of load balls, is in the marginal sub-facies. Although loads can occur in an inter-tidal setting (Schwarz, 1975) they do not occur in supra-tidal sediments, thus a supra-tidal origin for the marginal sub-facies is ruled out.

#### 4.3.2.11: Nodules

A.R. MacGregor (1975, talk at B.S.R.G. meeting) suggested that quartz-calcite nodules in member 3, especially noticeable in the uppermost 20m of Section B, represent replaced anhydrite nodules. He cited their 'cauliflower' margins and incipient 'chicken-wire' texture where two or more nodules occur together to support this idea. The occurrence of pyrite-rich rims in some nodules might also indicate the former presence of sulphate (Milner, 1976). Originally the nodule-bearing rocks would have been buried beneath a supratidal sequence, which was subsequently eroded, with more abundant anhydrite nodules.

In Section 7.4.5 the nodules are discussed in detail and it is concluded that, contrary to MacGregor's hypothesis, the nodules seem to be of secondary origin.

#### 4.3.2.12: Summary of the significance of the layered facies

During deposition of the layered facies, influx of sand-grade detritus was only intermittent and thought to be related principally to storm action. Where sufficient sediment was supplied wave-ripple lamination was generated, otherwise lenticular and/or graded sand laminae were formed. Tidal currents were unimportant.

Very shallow water is indicated by evidence of desiccation in some beds. However desiccation seems to have been the

exception rather than the rule even in these beds. The abundant synaeresis cracks present in most of the layered facies strata indicate a permanent water cover. The absence of birds-eye vugs (Shinn, 1968) tends to confirm this view.

Varying salinities are indicated by the synaeresis cracks and a high salinity or varying salinity is indicated by the presence of dolomite (see Chapter 6). However the wave fetch seems too long for there to have been a nearby sub-aerial barrier to have caused this situation.

This discussion is continued in Section 4.3.5.3 when the other facies and the vertical transitions and lateral persistence of beds have been described.

#### 4.3.3: The sandstone facies

##### 4.3.3.1: Bed geometry

The beds of this facies are fairly continuous, many being correlatable across the 2-2.5km distance from Sections C to E with very little change in thickness (Enclosure 3). Only in one case was it possible to observe the lateral margin of one of these beds: bed 34D passes laterally into marginal sub-facies by a gradual decrease in sand content and increase in continuity and thickness of dolostone beds until the sand layers become only a few centimetres thick and are no longer cross-stratified.

This sheet-like geometry with inter-fingering lateral margins argues against any strongly channelised forms being present. Indeed erosion at their bases seems minimal, at most a few centimetres.

##### 4.3.3.2: Composition

The facies has a bimodal composition of medium-grained sand and micritic material. Sand grade material is mainly

quartz with some microcline, dolomicrite oöids and intraclasts. Oöids are locally extremely abundant (e.g. beds 54C, 54D, 54E, 25B), but were not generated in their present location because oölitic coats on siliciclastic detritus are extremely rare: the oöids have a microcrystalline core in general.

Thick laminae and thin beds of dolostone are common. The triangular diagram (fig. 4-31) shows these beds to be remarkably pure, i.e. clay-free. Dolostone laminae drape over bedforms (figs. 4-34 and 4-35) and hence formed during periods of little current activity.

#### 4.3.3.3: Sedimentary structures of the sandstones

Parallel lamination, cross-stratification and cross-lamination occur commonly in the sandstone facies. Most of the cross-lamination is related to the generation of wave ripples which have very similar characteristics to those in the layered facies. Their orientations are included in figure 4-18. Parallel lamination is restricted to well-sorted medium-grained sandstones and so is regarded as a structure of the upper flow regime.

Cross-stratification is the commonest structure, set thickness (fig. 4-38) ranging up to 20cm with a mode of about 5cm. The palaeocurrents (see next section) and the pure (siliceous) nature of the original sands indicate an origin from tidal currents. The sets of cross-strata are erosional and tabular, although the laminations are typically tangential at the set base (fig. 4-32). The cross-strata are marked by variations in the proportion of intergranular dolomite and sometimes by dolostone pebbles lying on the foresets (fig. 4-33). Some distorted (liquefied) cross-strata occur (e.g. bed 29D), probably indicating contemporary

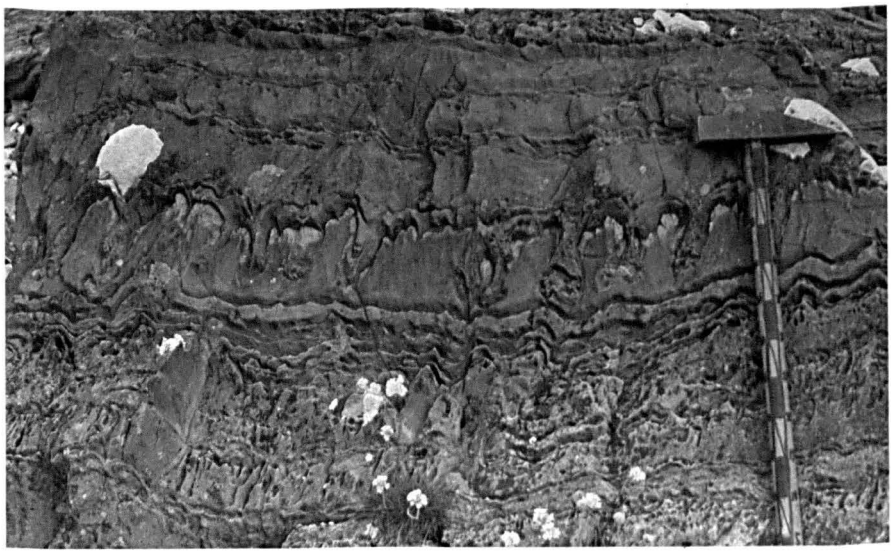


Figure 4-30: Bed 73B; load casts, some nearly detached from the source bed.

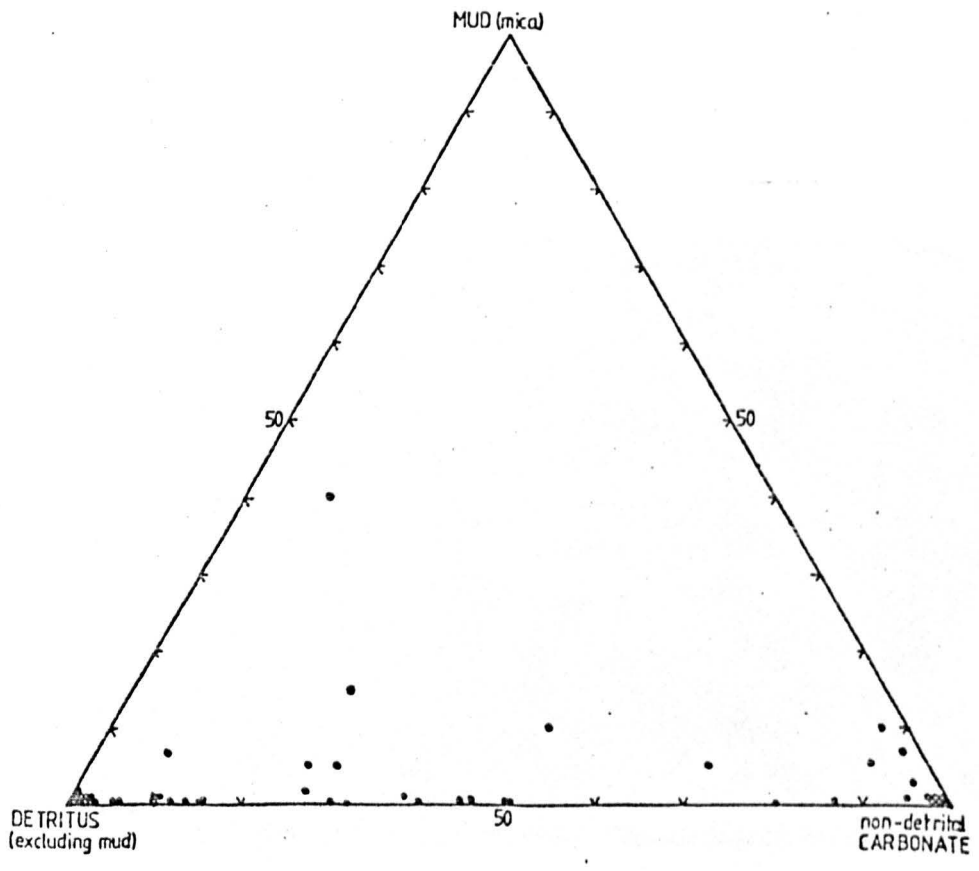


Figure 4-31: Mineralogical composition of individual laminae within the sandstone facies (mostly from visual estimates in thin section).

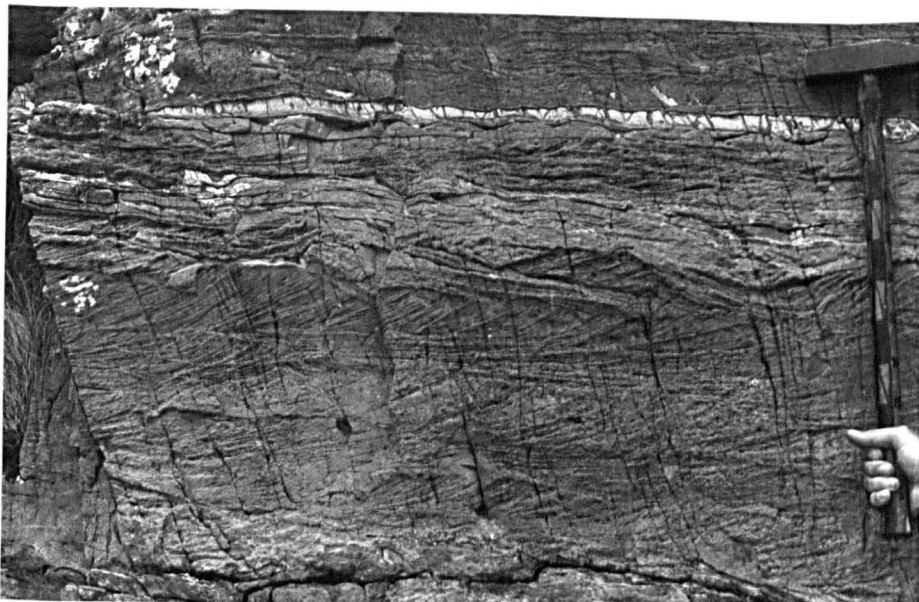


Figure 4-32: Bed 21D; dolomitic sandstone, cross-stratified in the lower part with erosional tabular sets which are tangential at their bases. Current directions are unimodal within the area photographed, but see Enclosure 2 for summary of current orientations in this bed. The upper part of the photograph shows more cross-lamination including some wave-generated ripple form sets and a dolostone lamina with contraction cracks.



Figure 4-33: Bed 46D; cross-stratified dolomitic sandstones with dolostone clasts on the foresets, especially noticeable in the set which runs from left to right just above centre.

earthquake activity, but are uncommon.

The shape of the cross-sets, and the tangential nature of the lamination at the set base, suggests deposition from moderately straight-crested bedforms under relatively high current velocity with much sediment in suspension (Beek & Koster, 1972, Goodwin & Anderson, 1974). Reactivation surfaces can be recognized occasionally (e.g. beds 60D, 62D) indicating the intermittent nature of the tidal flow. In bed 68E, none of the cross-sets is thicker than 3cm: here the deposition seems to have been from current ripples. In all other beds the set thickness is almost invariably greater than 3cm, too thick to have been deposited from current ripples. Bedforms of suitable size are preserved in three cases:

1. On the top of bed 62E (at 39017825) occur preserved straight crested, fairly symmetric bedforms of wavelength 60cm. Their form has been at least slightly modified by later superimposed wave ripples. Even so, the wavelength and symmetry of these bedforms would be rather unusual if produced by unidirectional flow, so they could be of wave origin.

2. A preserved dune in profile is seen in bed 21D (at 40467886; fig. 4-34) draped by a dolostone lamina; its wavelength is 120cm (stoss 90cm, lee 30cm) and is 11cm high.

3. In bed 60D (at 39987866) there is a preserved flat-topped bar (fig. 4-35).

Comparison with modern shallow tidal areas (e.g. Klein 1970b) suggests that asymmetric dunes like that of figure 4-34 were responsible, on migration, for the production of most of the cross-stratification in the sandstone facies.



Figure 4-34: Bed 21D; a preserved dune is visible to the right of the hammer-head and is capped by a dolostone lamina.

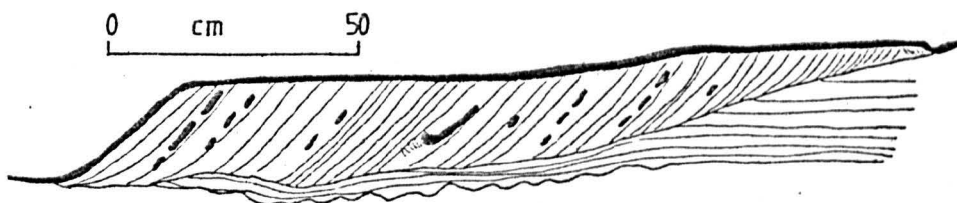


Figure 4-35: Bed 60D; preserved flat-topped bar. Note the wave ripples below the lower surface, composite nature of the cross-stratification, dolostone pebbles on foresets, backflow eddies and the dolostone lamina draping the whole structure (dolostone shown in black). Cross-strata are oversteepened due to deformation. Drawn from a photograph and a field sketch.



Figure 4-36: Bed 68E; dolomitic sandstone with dolostone laminae which show abundant contraction (desiccation) cracks leading to the break-up of laminae in places e.g. on the right hand side of the lowest dolostone lamina.

#### 4.3.3.4: Dolostone beds

The dolostone beds formed during periods of low current velocity as can be judged from their draping over bedforms. They generally show no internal lamination. They commonly display contraction cracks which form linked polygons up to 15cm across. There are all transitions from continuous dolostone beds, through broken-up beds (fig 4-36), to horizons of dolostone pebbles and isolated pebbles, quite well rounded in some cases. The pebbles were somewhat plastic as they are occasionally slightly bent, but brittle fracture occurred on more severe bending. A few pebbles of oölitic dolostone occur, demonstrating some early lithification.

The dolostone beds seem to have formed by steady accretion by precipitation of carbonate. They were easily fragmented because they were thin, underlain by an unconsolidated sand layer and dissected by contraction cracks. The size and complete nature of the polygons formed by the contraction cracks and the brittle nature of the pebbles (cf. Füchtbauer & Tisljar, 1975) suggests an origin of the cracks by desiccation.

#### 4.3.3.5: Palaeocurrents

Current directions from the cross-strata are shown on Enclosure 2. At any one locality the cross-stratal distribution within each bed often shows two widely spaced modes (e.g. beds 21D, 29D, 62D, 68E) or is multi-modal (beds 21D, 60D, 62E), demonstrating the action of reversing tidal currents, rather than unidirectional currents. Considering the palaeocurrents as a whole (fig. 4-37), there is a very wide spread of current directions. The vector mean is  $253^{\circ}$  with standard deviation  $\pm 121^{\circ}$  and the

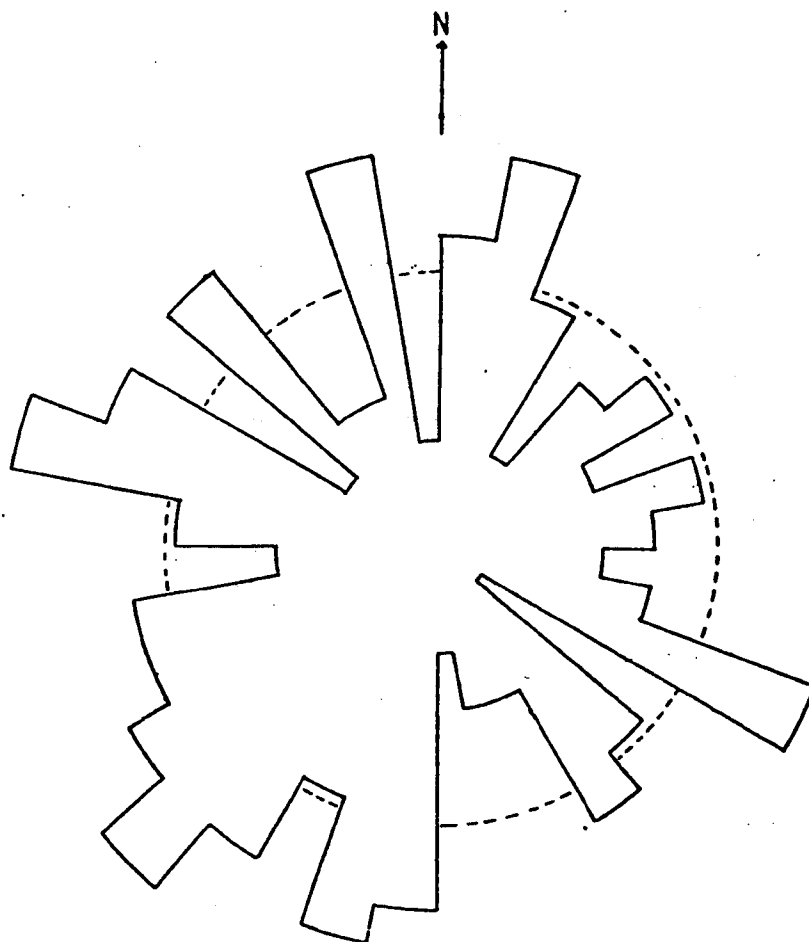


Figure 4-37: Summary rose diagram of the palaeocurrents from cross-strata of the sandstone facies in member 3 (181 measurements). Dotted line represents the equivalent uniform distribution of azimuths.

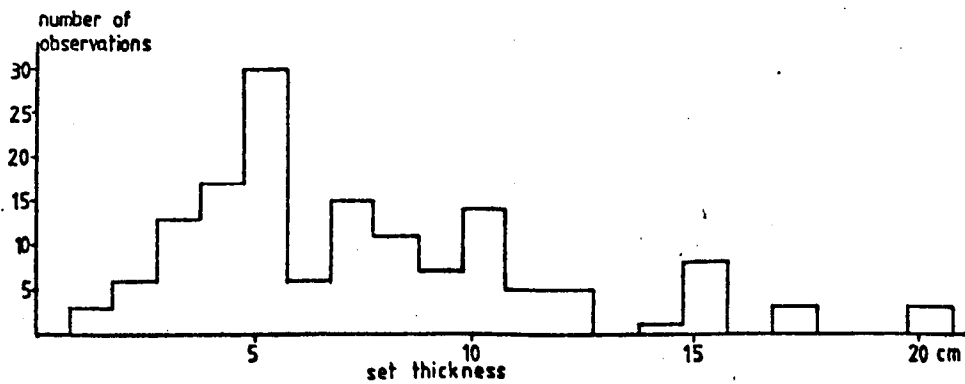


Figure 4-38: Cross-stratification set thickness, sandstone facies, member 3.

magnitude of the vector is 10.7%. This vector is statistically significant (Rayleigh Test) at the 90% level, but not the 95% level (method of Curray, 1956) or not significant even at the 90% level (method of Mardia, 1972). The overall distribution is thus best regarded as random.

The extreme local variations in current directions are well shown in bed 21D where, proceeding eastwards a N-S bi-polar distribution is replaced by a probable quadrimodal N-S-E-W distribution, then by a bi-polar E-W current system.

#### 4.3.3.6: Environment of deposition

The sheet-like geometry of each bed with very little erosion at the base, the erosional sets of cross-stratification, and absence of metre-sized fining-upward cycles suggests deposition in very shallow, poorly confined channels. The manner of deposition would have been analogous to a braided stream (Allen, 1970): a marine origin in this case being clearly shown by the palaeocurrent distribution. The dolostone beds formed on the equivalent of braid bars. The desiccation cracks which they contain implies an intertidal situation, at least at times. The situation is thus similar to a tidal sand flat (Straaten, 1954b, p13; Klein, 1970b), although the size of the bedforms and resulting sets of cross-strata was rather smaller than in modern examples described. This could be due to a smaller tidal range in the member 3 environment. As for other tidal flats, its existence would have depended on some sheltering effect from wave action (Reineck, 1969), thought in this case to be due to a sub-aqueous bar (see 4.3.5.3). A mud flat was apparently not formed in the area: practically no detrital argillaceous material seems to have been available in the depositional environment.

The current directions were very variable because they would have been controlled by minor, local variations in topography. This may ultimately be related to an extremely irregular configuration of the coastline. The currents were apparently not separated into ebb and flood channels as unimodal distributions within one bed are rare. No deductions as to the overall trend or position of the coastline can be made from the palaeocurrents.

4.3.4: Stromatolite facies

Spencer & Spencer (1972) have described and illustrated the geometry of the stromatolite beds in fair detail and described some general features of their internal lamination. The new information here clarifies their use as stratigraphic markers (Chapter 2 and enclosures), enables deductions to be made regarding the relationship of their form to environmental and algal growth factors, and explains the nature and significance of their microstructure.

The literature on stromatolites is becoming vast and is not reviewed systematically here. General summaries and a glossary of terms appear in Walter (1976).

4.3.4.1: Macrostructure

The form that stromatolites take can be fashioned both by the physical environment (Logan et al., 1964) and by algal growth factors (Walter, 1972). In particular the isolation of the algal mat into discrete masses can occur by severance by wave action (Logan et al., 1964) or by the preferential growth of algal clones (Monty, 1967; Golubic, 1973; Gebelein, 1974). Columnar types have been used as bio-stratigraphic indicators in various parts of the world (Walter, 1972, 1976), possibly indicating a degree of biological control on column form.

When stromatolites directly overlie layered facies sediments (which were deposited under relatively quiescent environmental conditions) they formed either a stratiform lamination or low domes (e.g. horizons D2, D3, D4, C8). Domes developed where the algal mat draped over dolostone pebbles or an irregular sediment surface (e.g. D4) or perhaps where there was lateral growth expansion of the mat. The process of preferential sediment trapping on high points seems not to have operated as the domes commonly give way upwards to cryptalgalaminites (e.g. D3; D4, fig. 4-39; E4, E8, BI, BIII). In some beds there is an influx of medium-grained sand, that is increasing energy of the environment after the mat has been established. This results in the severance of the continuous mat leading to the growth of discrete columns (C8, D8; figs. 4-40, 4-46) and/or the production of a breccia of stromatolite flakes (e.g. C9). When stromatolite growth commenced in an already high energy environment (e.g. BIII, D5, D7) the structures formed were irregular in shape. In two cases (D5 and BV) the mat subsequently became continuous, but with a very ragged structure of small domes reflecting a high sediment influx. These observations show that there is an empirical relationship of stromatolite form to environmental energy as seen for modern examples in Shark Bay, Western Australia (Logan et al. 1974).

On the other hand, there are many isolate stromatolitic masses forming oblate spheroids and ellipsoids (BVI, D5 upper, C5, E5, D6, E6, E7, C9, E9, fig. 4-41) encased in layered facies sediments. These forms cannot have been induced by physical separation of the mat under harsh environmental conditions. Instead it seems to be a growth feature of

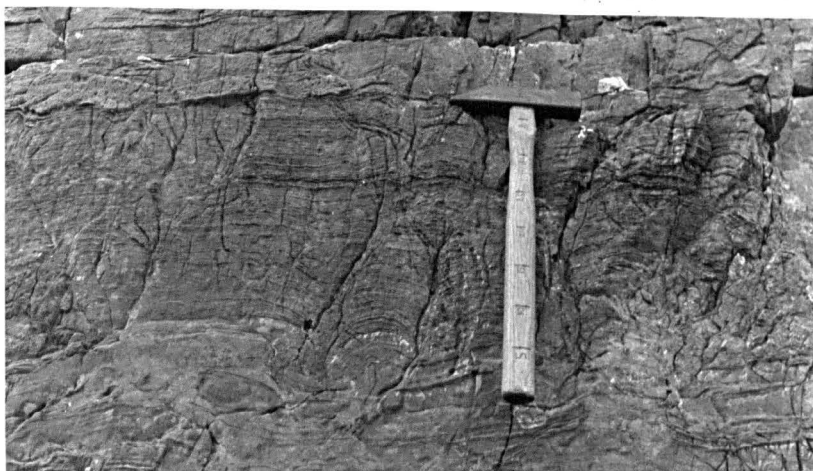


Figure 4-39: Stromatolite horizon D4; stromatolitic lamination doming over irregularities in the substrate (dolostone) passes upwards into cryptalgalaminites overlain by sandstone.



Figure 4-40: stromatolite horizon D'8'; cryptalgalaminite followed upward by columnar stromatolite with medium grained sand and flake debris between the columns. These are overlain by a purplish silty sandstone.



Figure 4-41: Stromatolite horizon E9; oblate spheroidal stromatolite bioherm, in detail consisting of many small linked domes; lamination is overturned on the bioherm margins.

the algae. The bioherms show a structure of concentric layers with small laterally-linked domes or columns within each layer and vertical, or overturned bedding on their margins. This is apparently a common form of sub-tidal stromatolite bioherms in the Precambrian (Serebryakov, 1976). Another point is that even where the algal mat was separated by environmental factors leading to the development of discrete columns, these columns have a definite shape which may be of taxonomic significance (see 4.3.4.3).

#### 4.3.4.2 Microstructure

The interpretation of the microstructures of ancient stromatolites is difficult (Hubbard, 1972; Bertrand-Sarfati, 1976) because of their susceptibility to post-depositional alteration (Bathurst, 1971) and because of the polygenetic origin of laminations in Recent stromatolites (Monty, 1976; Park, 1976). In member 3, the lamination defining the stromatolites occurs in nine modes described below, only the first four of which are 'primary'.

1. Clastic layers. There may be discrete layers of clastic material up to millimetre scale thickness. The detritus is mainly silt- or very fine-grained sand-sized quartz, microcline and mica, although dolomite peloids sometimes occur (BY, E9; fig. 7-13). The detritus usually occurs in fairly even layers, independent of the slope of the surface, suggesting that it was agglutinated by the algal mat. In some cases medium-grained sand is concentrated in hollows or inter-stromatolitic areas, suggesting that it was only the finer material that was bound into the stromatolite (Frost, 1974). In other cases this detritus appears to be uniformly scattered throughout the stromatolite without forming distinct layers. Sediment-rich layers,

where they do occur, would have been deposited when suspended sediment was particularly abundant, e.g. following a storm. They are analogous to the sand layers in the layered facies. Commonly stromatolitic lamination is truncated by scour and healed over by later growth.

2. Dolomite grain size alternations. Nearly all the stromatolites show an alternation of finer and coarser-grained dolomite on a scale from 100 $\mu$ m to several mm (fig. 4-42). Such a structure is very common in ancient stromatolites (Henderson, 1975; Horodyski, 1976), but no general statement as to its significance has been made. In member 3, the finer mode, in different cases, lies in the range 3-50 $\mu$ m whilst the coarser mode ranges from 5-10 to 125 $\mu$ m. It is thought that the finer end of these ranges are closest to the original grain sizes. The coarser domains often contain a variable amount of detritus ranging from silt to very fine-grained sand. This detritus is low in concentration compared to the dolomite, but it is not clear whether this is an original feature, or whether some of the detritus has been removed diagenetically. Thus the coarser laminae are, broadly speaking, clastic. The finer laminae, on the other hand, appear to be the product of early precipitation of carbonate. Evidence for this is best seen in a sample from BYI (figs. 4-43, 4-44) which shows the development of rounded masses of fine-grained dolomite, occasionally coalescing to form more continuous bands. This structure seems identical to early calcified areas in stromatolites from Baffin Bay, Texas described by Dalrymple (1966) and also recognized in ancient stromatolites by Leeder (1975). In the Baffin Bay examples, bacterial decay of organic matter in algal-rich layers forms ammonia which induces

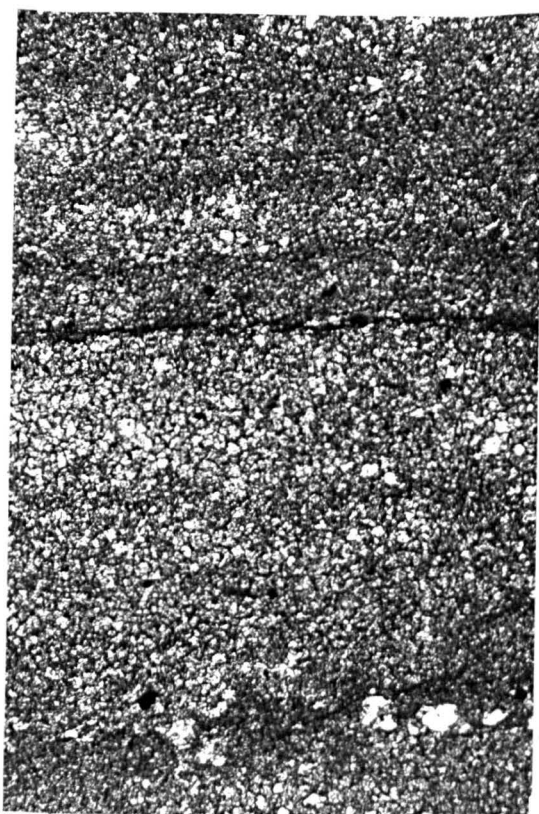
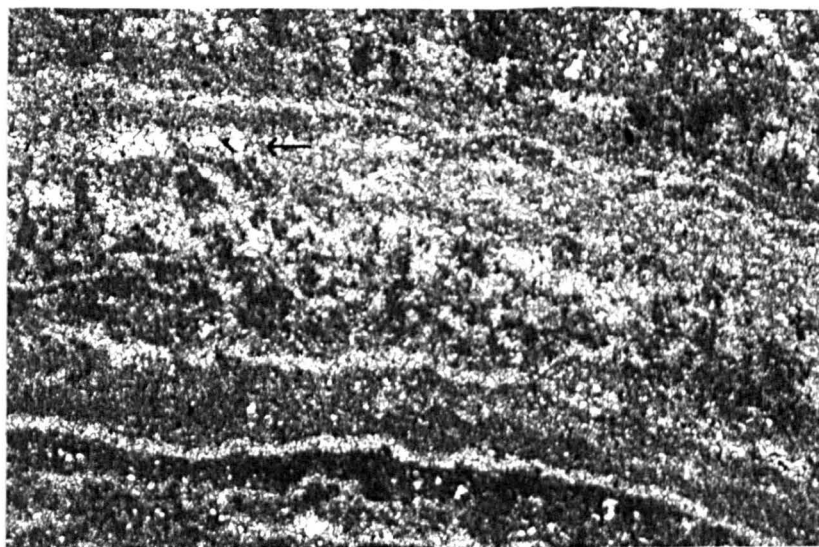


Figure 4-42: Photomicrograph, plane polarized light, stromatolite horizon D2. Stromatolite consists of a dolomite mosaic with scattered terrigenous silt. Stromatolitic lamination is shown by alternations in the grain size of the mosaic (dark=fine-grained) and by bedding-parallel stylolites (black lines e.g. just above centre).

500 $\mu$ m



500 $\mu$ m

Figure 4-43: Photomicrograph, plane polarized light, stromatolite horizon BVI; shows rounded coalescing masses of (dark) fine-grained dolomite interpreted as penecontemporaneous calcification of the stromatolite. Light areas may all be fenestrae, but this is only certain when their centres are of calcite (see 7.1.1), as in the arrowed area, rather than of dolomite.

carbonate precipitation. Cathodoluminescence (fig. 4-44) shows that detrital material (microcline) is absent from the fine-grained domains. Other, poorer examples of this texture occur in beds BIII, D2 and D4.

3. Fenestrae. Associated with microstructures exhibiting clear early calcification are discrete patches of dolomite and calcite microspar which are interpreted as fenestrae (7.1.1). They are either equant, 100-300 $\mu$ m in diameter, or elongate (fig. 4-43), paralleling the stromatolitic lamination defined by grain size variations and clastic layers. Such fenestrae could originate as sheet cracks formed by removal of organic matter, or by desiccation (Fischer, 1975; Bertrand Sarfati, 1976) or by lateral growth expansion (Monty, 1976). Because these fenestrae occur in bioherms which are considered (4.3.4.1; 4.3.4.4) to be sub-tidal, and because early calcification would have provided a relatively firm framework, it is thought that the most likely explanation for the formation of the fenestrae relates to decomposition and removal of organic matter. The voids were maintained by the early precipitation of fine-grained carbonate.

4. Radial-calcite laminae. Within domes in the calcitic stromatolite BIII occur discrete laminae of calcite with a pronounced preferred dimensional and optical orientation of individual crystals perpendicular to the lamination surface. They are very smooth and continuous and display a poorly defined median line with small calcite inclusions. They are certainly pre-tectonic because they are cross-cut by quartz seams (see 9, below).

The laminae compare with the radial-fibrous-calcite laminae described from the Middle Proterozoic by Horodyski (1975) which he ascribed to early calcite precipitation

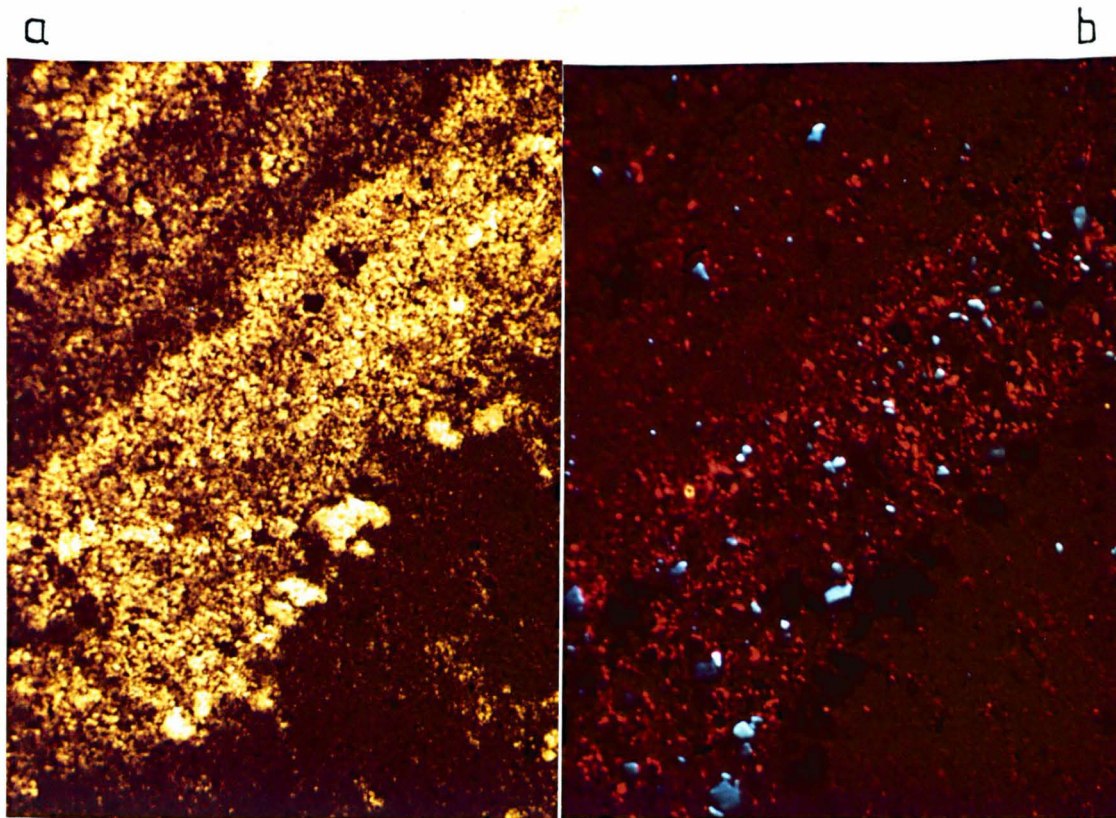


Figure 4-44: Photomicrographs in a) transmitted light and b) under luminescence, stromatolite horizon BVI. Distribution of detritus is clearly shown by the occurrence of blue-luminescing microcline. The microcline-free areas represent early-calcified domains.



Figure 4-45: Photomicrograph, plane polarized light, stromatolite horizon BV. Detritus (white) contains a high proportion of microcline with overgrowths giving rise to rectangular outlines. The stromatolitic lamination is expressed by alternations of coarse calcitic domains and finer dolomitic domains, the latter containing some internal lamination.

200 $\mu$ m

immediately beneath a living algal mat. This would explain the smooth, continuous nature of the laminations reflecting the uniform conditions beneath the mat, compared with the more variable conditions within the mat as exemplified by the patchy nature of within-mat calcification (fig. 4-43). The presence of inclusions only along a poorly defined median line may indicate that the calcite has a displacive mode of growth.

5. Calcite-dolomite alternations. Parts of stromatolite horizons BIII, BIV, BV, C9 and D6 show an alternation of calcitic and dolomitic laminae on a millimetre, or finer, scale (fig. 4-45). Such a structure has been interpreted by Gebelein & Hoffman (1973) to be related to original alternations of calcium carbonate detritus and organic layers, the latter being preferentially dolomitized because of the capacity of blue-green algae to concentrate Mg relative to Ca in their sheaths. Whilst this might help to explain the dolomitic nature of the stromatolites in member 3 as a whole, the calcite-dolomite alternations as now seen are not thought to relate directly to original structure. The original detritus was originally dominantly terrigenous, not calcitic so the calcite layers are not simply clastic layers. The calcite forms a coarse mosaic within which no lamination is preserved, so it is thought to be a diagenetic replacement after dolomite (see also Chapter 7). The exception is BIII which does show some grain size variation within calcite laminae as well as exhibiting type 4 (radial-fibrous) laminae: the calcite here may well be primary.

6. Stylolites. Low relief stylolites, concentrating mica and other impurities, occur frequently parallel to

stromatolitic lamination, as seen elsewhere by Henderson (1975). Although largely opaque in transmitted light they are yellowish in reflected light and so are not to be confused with bituminous films (representing remains of algal mats: Laporte, 1967; Hofmann, 1975a) which do not occur in the Bonahaven Formation.

7. Clay-rich bands. Bands of nearly pure mica occur parallel to bedding in domal stromatolites. They may, like the stylolites, signify solution of carbonate.

8. Quartz-albite bands More common than 7. are bands of secondary quartz and albite (30-150 $\mu$ m) at 200 $\mu$ m to 2mm intervals, especially in domal and columnar stromatolites. They do not seem to represent a transformation of original detritus because they never contain microcline (see also 7.4). Where they are diffuse, however, they may not always be distinguishable from detrital layers: thus it is not always possible to recognize the nature and distribution of original contained detritus in the stromatolites.

9. Quartz-calcite seams. The most spectacular demonstration of the mobility of quartz and carbonate in the stromatolites are the ubiquitous tectonic quartz seams by which the stromatolites are usually recognized in the field (see also Chapters 3 and 7). Similar structures occur in Proterozoic stromatolites of the Transvaal Series of South Africa (Button, 1973).

There is no evidence from the microstructures of a differentiation of algal communities to produce different growth forms as all the primary microstructural types (except 4) occur in all of the macrostructural types. Entire laminae are generally smooth in the Bonahaven

Formation. This is a distinctive microbiological feature in the Recent (Logan et al., 1974), but may not be so for fossil stromatolites (Bertrand-Sarfati, 1976).

The controls on microstructure appear to be variation in the rate of sediment influx perhaps coupled with seasonal differentiation of the algal coenose (Bertrand-Sarfati, 1976). The first control leads to the formation of clastic laminae following storms under layered facies-type conditions or typically a more scattered and constant influx of sand under sandstone facies conditions. The second control refers to different species becoming dominant in the mat at different times of the year; these different species may have different sediment trapping and carbonate-precipitating abilities which could produce a seasonal lamination. As was noted for the macrostructure, both environmental and algal growth parameters are potentially important in determining the microstructure.

#### 4.3.4.3. Classification

The nomenclature, classification, or taxonomy of stromatolites is still much in dispute (Walter, 1976). Hofmann (1975b) doubted the accuracy of three-dimensional reconstructions and many authors have questioned the criteria used to assign names to stromatolites. Columnar stromatolites in C8 (fig. 4-46), D6 and D8 are named here according to the classification of Cloud & Semikhatov (1969). These have smooth walls, maximum column diameter of about 5cm, show bifid parallel branching with some expansion of the columns just below a branch. The laminae are moderately to strongly convex. Successive laminae envelop one another at the column margins, so the name Jurusania given to these stromatolites by Spencer & Spencer (1972) is inappropriate. However the group name Gymnogolen fits the description just

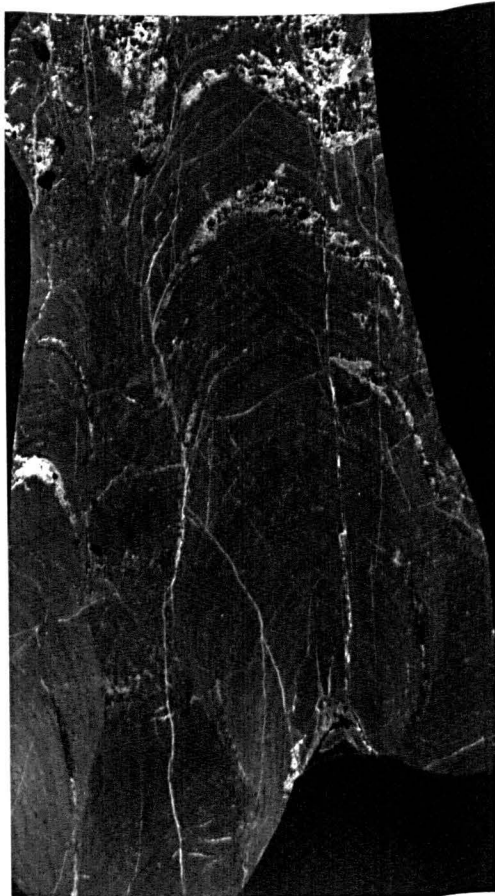


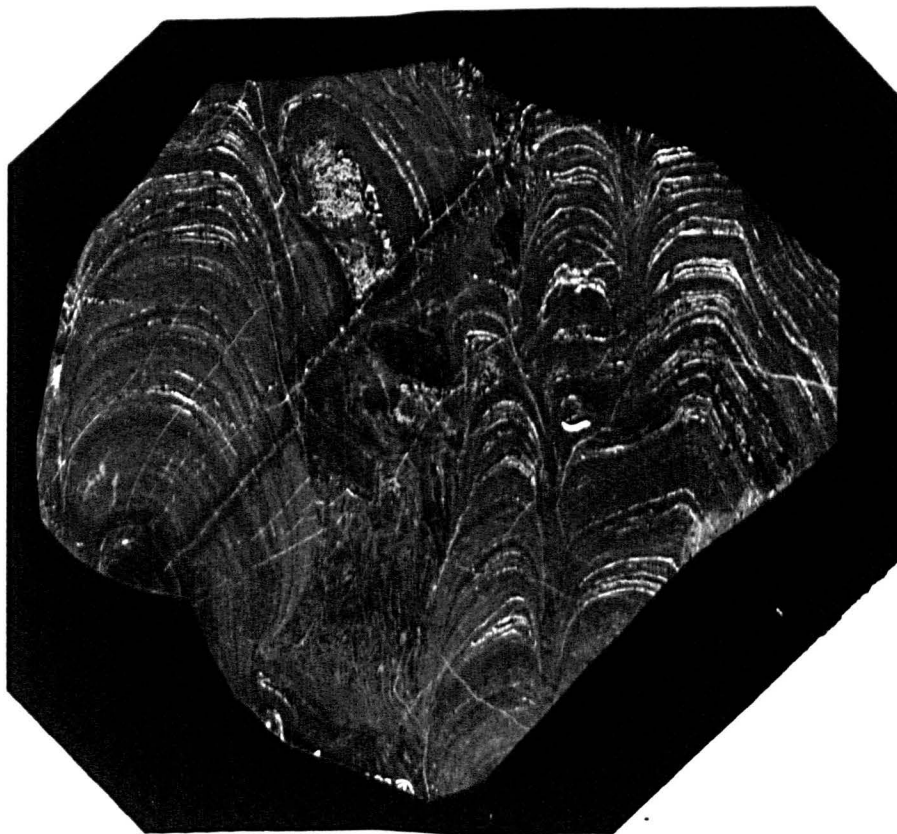
Figure 4-46: negative prints of peels of polished surfaces of stromatolites (x1).

a) well developed columnar stromatolites from horizon D'8'.

Thin quartz seams occur and larger nodular areas.

b) columnar stromatolites from horizon C8; flake breccia between columns is well shown.

Quartz seams and one nodular area (top) occur.



given. This group is restricted to the Upper Riphean according to Cloud & Semikhatov (1969) and Krylov & Semikhatov (1976), although Hofmann (1973) allowed a Vendian age, which would be more appropriate here. I cannot take this classification entirely seriously however until the effects of depositional environment on stromatolite form have been fully elucidated.

#### 4.3.4.4: Environmental deductions

There is no clear evidence of sub-aerial exposure from the stromatolites. The rare fenestrae do not seem to be of the 'birds-eye' type; the stromatolite flake breccias can easily be generated underwater (Monty, 1967; Gebelein, 1969), and there are no polygonal forms like those of Kendall & Skipwith (1968). Rather the conclusion of very shallow water conditions comes from study of the associated sediments. In the case of the biohermal types a minimum water depth equal to the height of the bioherm (which is 3m in parts of E9) is indicated. This will apply also to the layered facies sediments deposited between the bioherms.

The relationship between stromatolite form and environment was outlined in section 4.3.4.1.

#### 4.3.4.5: Controls of development of stromatolite beds

There is no overall cyclicity or set pattern in the development of the stromatolite beds. It is considered in the next section (4.3.5) that there is in fact only weak evidence for overall cyclicity in member 3.

The reasons why stromatolite growth was instigated at each horizon is not clear: there is certainly no constant sedimentological factor. One is forced to appeal to unknowns such as the supply of nutrients (Monty, 1973) or other parameters that are not directly determinable from the sediments. Cessation of growth might be influenced by the same parameters, but there is evidence for a sedimentological

factor also. It might be expected that an influx of coarse detritus might cause cessation of growth. Although this is so at horizon D3, this is the only horizon where this occurs. At other horizons (e.g. D5, BIII) stromatolite growth took place under sandstone facies conditions. Rather, in many cases the lithology immediately overlying the stromatolites is a lamina of coarse silt or very fine-grained sand, weathering slightly purplish, contrasting with the yellow-orange of the stromatolites. Thus a relatively severe storm bringing in an abundance of choking fine sediment into the area caused deposition of a sediment layer sufficiently thick for the algae to be unable to move through it to re-establish a mat at the sediment surface.

#### 4.3.5: Facies and sedimentary environment

##### 4.3.5.1: Lateral facies variation

There seems no correlation between Section B and the north coast sections. Along the north coast, Enclosure 3 shows that most beds of a given facies persist throughout the extent of the outcrop. The variations in stromatolite bed geometry laterally are generally related to the development of bioherms which do not have any relation to environmental changes, as was discussed in the last section.

Sandstone facies beds 5D; 44C,E; 56E; 58E and 68E are missing from adjoining sections; 19E appears as standard sub-facies in Section D, and bed 34D changes laterally to marginal sub-facies by a process of smooth transition. The average lateral persistence of the sandstone facies beds is greater than 3km as all such beds in Section C can be matched in Section E; the limited evidence available suggests that where they do wedge out, they pass by transition

into marginal sub-facies sediments.

Lateral transitions between the sub-facies of the layered facies occur in beds 17, 35, 38, 45, 56/9, 65 and 68 on the north coast, but are not actually observed in continuous sections. The closest is bed 35D which changes from lenticular-graded to marginal sub-facies in less than 300m. The existence of different sub-facies at the same time in the same area is therefore indicated. Conversely, most of the beds show no change and so have a lateral persistence in terms of kilometres.

Stromatolite horizon 9 and the marginal sub-facies sediments above it are absent from Section D. Presumably this area had a slower rate of subsidence than to the east and west. The thin dolostone conglomerates, particularly the one at the top of member 3 are the only possible evidence for an actual hiatus in sedimentation at the top of Section D. It is unlikely that the member 3/member 4 boundary is diachronous to any extent because member 4 sediments could not be lateral equivalents of those of member 3 on sedimentological grounds.

#### 4.3.5.2: Vertical facies transitions

The sequence of vertical facies changes in the north coast outcrops of member 3 have been examined using a transition probability matrix (Table 4-3a) where each element  $P_{ij}$  represents the probability of the transition of the facies in row  $i$  to the facies in column  $j$  occurring. (The numbers in brackets are the actual numbers of transitions involved).

As there is no objective criterion such as well-developed bedding planes for subdividing units of one facies, transitions must be from one facies or sub-facies to another, thus

the main diagonal consists of zeroes. Schwarzacher (1975) has shown that this way of structuring the matrix cannot be objectively tested against an independent random process. The only alternative would be to record the facies present at fixed interval throughout member 3, but this assumes that the sedimentation rate was the same for each facies which is probably not the case. In fact all geological sequences which have been analysed quantitatively are non-random (Schwarzacher, 1975) but they may or may not show cyclicity. As the amount of data is limited and the proof of cyclicity is difficult, no statistically rigorous observations can be made here.

Nevertheless, it is useful to calculate the 'trial matrix' (Table 4-3b; Gingerich, 1969) which gives the expected transition probabilities allowing for the fact that some facies occur more frequently than others. Each element is obtained by dividing the number of transitions in column  $j$  by the total number of transitions in all the columns except  $i$ . The differences between Tables 4-3a and b are shown in Table 4-3c (=differences from random). Although not proving that any particular cyclicity or preferred arrangement of beds occurs, it does indicate where unexpectedly large or small numbers of transitions occur and thus limits the hypotheses which can be put forward.

There does not seem to be any overall cyclicity in the sequence, although preferred transitions do occur.

Stromatolite beds are more likely to be preceded by lenticular-graded sub-facies sediments than followed by them and vice-versa for standard sub-facies sediments. This can be taken to mean that stromatolite beds are more easily established when sediment influx is low

TABLE 4-3

Transition matrices

(a) Transition probability matrix (transition frequency matrix in brackets)

	St	Sa	S	L	M
St	0	0.47(12.5)	0.15(4)	0.23(6)	0.15(4)
Sa	0.46(13)	0	0.13(3.5)	0.33(9.5)	0.08(2)
S	0.50(6)	0.25(3)	0	0.17(2)	0.08(1)
L	0.37(6.5)	0.43(7.5)	0.20(3.5)	0	0
M	0.50(2)	0.25(1)	0.25(1)	0	0

(b) Independent random matrix

	St	Sa	S	L	M
St	0	0.40	0.20	0.29	0.11
Sa	0.43	0	0.19	0.27	0.11
S	0.36	0.32	0	0.23	0.09
L	0.39	0.34	0.17	0	0.10
M	0.34	0.30	0.15	0.21	0

(c) Differences from random (x100)

	St	Sa	S	L	M
St	0	+7	-5	-6	+4
Sa	+3	0	-6	+6	-3
S	+14	-7	0	-6	-1
L	-2	+9	+3	0	-10
M	+16	-5	+10	-21	0

## Abbreviations:

St= standard sub-facies

Sa= sandstone facies

S= stromatolite facies

L= lenticular-graded sub-facies

M= marginal sub-facies

(lenticular-graded sub-facies) and more easily killed off by influx of abundant suspended sediment (standard sub-facies).

Sandstone facies beds tend to be bounded above and below by stromatolite beds less often than in the 'random' case and are bounded above and below more often than random by lenticular-graded sub-facies sediments. The interpretation of these observations remains obscure: the difference from 'random' is anyway rather small.

The preferred associations of the marginal sub-facies are uncertain because there are only a few of these beds. Although they are not found vertically adjacent to the lenticular-graded sub-facies at all, a lateral transition between them occurs in bed 45D. In addition it is sometimes difficult to assign a bed to one or other of these sub-facies, which suggests that they are gradational.

Overall, explanation of vertical facies variation in terms of sequential changes in the overall environment, rather than cyclic superposition of laterally equivalent facies, seems most appropriate.

#### 4.3.5.3: The member 3 environment

Klein (1970a) suggested that member 3 might represent an inter- and supra-tidal flat assemblage such as those described by Laporte (1967), Schenk (1967), Kahle & Floyd (1971) and many others. However Gebelein (1977), working on modern sediments in Florida states that the supra-tidal analogy may have been over-played and that very little of the sediments described by Laporte and others is really supra-tidal. Indeed the mere presence of dolostones (Zenger, 1972; Hoffman, 1975) or stromatolites (Hoffman, 1972) says nothing about water depth or general environment.

The depositional environment envisaged for member 3 in

the present work involves a generally shallow sub-tidal setting with occasional emergence in the marginal sub-facies and perhaps more widespread inter-tidal conditions during deposition of the sandstone facies.

In the layered facies, synaeresis cracks imply changing salinities, and a high salinity, at least at times, is suggested by the abundant fine-grained (dolomitic) carbonate. Therefore a general 'lagoonal' environment is postulated, i.e. a fairly permanent water body to some extent isolated from the open sea. The word 'lagoonal' is placed in inverted commas because there was clearly a great deal more sediment movement even in the layered facies, than in a completely isolated lagoon. In fact there was no sub-aerial barrier nearby off-shore because the wave fetch was so long, as was deduced earlier. However there may have been a submerged barrier, possibly an oöid shoal to judge from the occasional presence of oöids in the layered facies and their common occurrence in the sandstone facies. Salinity increases would have been caused by evaporation, salinity decreases by influx of sea water, especially during storms, by rainfall, and possibly by fluvial influx, although there is no direct evidence for rivers draining into the area.

The dominant depositional processes in the layered facies were storms alternating with quiet water carbonate and clay deposition, tidal currents being unimportant. Most beds are continuous along the north coast, but cannot be correlated with Section B.

The standard sub-facies was deposited under a permanent water cover during conditions of fairly abundant supply of terrigenous detritus (abundant wave-rippled sands, Table 4-1) and frequent salinity changes (abundant synaeresis cracks, Table 4-1).

The lenticular-graded sub-facies represents deposition either in areas more remote from sediment influx, or, to

judge from the considerable lateral extent of these beds, at times when wide areas of the 'lagoon' were receiving less sediment. Table 4-1 shows that wave-rippling and synaeresis cracks are low in proportion compared with the other two sub-facies suggesting conditions of uniform salinity and fairly quiet water.

The marginal sub-facies is characterized by a lack of fine-grained terrigenous detritus and indications of occasional emergence. It would have been deposited in shoaling areas within or at the margins of the 'lagoon'.

The sandstone facies contains cross-stratification generated by tidal currents as well as wave ripples. The dominance of tidal currents here indicates a slightly different palaeogeographic situation from the layered facies as tidal currents were unimportant in the latter. Most beds of the sandstone and layered facies are continuous along the north coast, but cannot be correlated with Section B. This suggests that discrete depositional areas existed, although it is not clear to what extent they were gradational. This may be related to an extremely irregular coastline or perhaps to shoaling areas of little subsidence separating depositional areas. Although lateral passage of sandstone facies into marginal sub-facies was observed in one case, it is not possible to say whether sandstone facies deposition in e.g. the north coast area was contemporaneous with, say, standard sub-facies deposition in e.g. the Bonahaven area. That is, it is not possible to prove whether a vertical transition from sandstone facies to lenticular-graded or standard sub-facies reflects merely a geographic change of local significance or whether large stretches of the Dalradian coastline was affected by a change, perhaps in tidal range. However the apparent decrease in the number

of sandstone facies beds from the north coast to Sections A and B (Chapter 2 and Enclosure 2) favours the former alternative.

The conclusions of this section are combined with information on sediment provenance (4.5) and palaeogeography (8.1) to produce some palaeogeographic cartoons (figure 8-2), which illustrate the environment envisaged.

#### 4.3.5.4: Modern and ancient analogues of member 3

Comparison with modern coastal environments, made more difficult because of the abundant bioturbation in modern sediments, reveals some analogies, but no environment exactly equivalent to member 3.

The Laguna Madre-Baffin Bay area of Texas (Rusnak, 1960; Behrens & Land, 1972; Miller, 1975) shows salinity fluctuations, absence of diurnal tidal activity and some formation of dolomite, which compares with some features of the layered facies. However, as the Laguna Madre has a sub-aerial barrier separating it from the ocean, the effects of wave activity are confined to the production of washover fans and the winnowing of sediment on the landward lagoon shore, which clearly does not tally with the layered facies.

The Trucial Coast of the Persian Gulf (Kendall & Skipwith, 1968; Purser & Seibold, 1973; Purser & Evans, 1973; Loreau & Purser, 1973) displays a shoal/barrier island system, linked in places to the mainland and associated with oölitic tidal deltas. Similarities with member 3 include the presence of dolomite, the prevalence of sub-tidal sedimentation behind the barrier (over hundreds of square kilometres in any one area) with only narrow tidal flats and the regional importance of both waves and tides, but the abundant bioturbation obscures any further similarities. Algal mats are restricted

to highly saline, inter-tidal areas because of predation, but this would not have applied in Precambrian times. The presence of a sub-aerial barrier along much of the shoreline and the abundant oöid-coated detritus are two significant differences.

The Shark Bay area of Western Australia (Hagan & Logan, 1974) may provide a closer analogy to member 3 sedimentation, and on an areal scale perhaps ten times larger than the present-day outcrops of member 3 (excluding Beinn Bhan). Restricted circulation and hyper-saline conditions are produced by the growth of sea-grass banks (Read, 1974) at the entrance to long indentations in the coastline. Although a micro-tidal area (less than 2m tidal range, Hayes & Kana, 1976), tidal currents are important around the margins of these indentations due to shoaling of water and restriction of flow (?= sandstone facies). In the centres of the indentations (basins) the bottom sediments are usually only disturbed by storms (?= layered facies). Oöids develop nearshore (Hagan & Logan, 1974) as in the Laguna Madre (Rusnak, 1960), but this is not thought to be the case in member 3 because of the extreme rarity of coated detritus. Well differentiated stromatolites develop in shallower water (Logan et al., 1974). A more detailed comparison does not seem to be warranted because of the bioturbation in the modern environment and the lack of information on the basinal sediments.

In ancient sedimentary sequences, barrier-lagoon models are frequently developed in the literature (Truswell & Eriksson, 1975; Button, 1976; Rees et al., 1976; Kendall, 1969; Bridges, 1976; Akhtar & Srivastava, 1976). The first three of these compare closely with member 3 in that a sub-aqueous

barrier was proposed in each case. Storm-generated rudites (Rees et al., 1976) or ripple-marked dolostones (Truswell & Eriksson, 1975) may be present, but wave action seems much less noticeable overall, than in member 3. Marginal muddy tidal flats are a feature of many of these models, but are not present in member 3.

Finally a comparison may be made with another Vendian dolostone sequence, the Porsanger Dolomite of Norway (Tucker, 1977), which occurs immediately beneath a Tillite sequence. The Porsanger Dolomite is mostly sub-tidal, although some is inter-tidal as demonstrated by desiccated dolostone beds; other similarities include the presence of abundant stromatolites, dolostone conglomerates and ooids. However, there is no terrigenous mud in the Porsanger sequence and there are more differentiated stromatolite horizons and several metre thick flakestone horizons. Tucker attributes the presence of dolomite to a hot climate and lack of terrigenous influx (apart from wind-blown sand): presumably restricted circulation in the depositional area would also have to be involved. Cyclic sequences are present which Tucker attributes to progradation by tidal flats and periodic eustatic sea level changes. In member 3 of the Bonahaven Formation no such cyclic sequences are recognizable except that the sandstone facies-layered facies alternations could be regarded as cyclic in some sense. The subtle geographic changes invoked to explain these alternations could also be controlled by eustatic sea level changes, although local fault-related tectonism (e.g. Beukes, 1977) may be more likely.

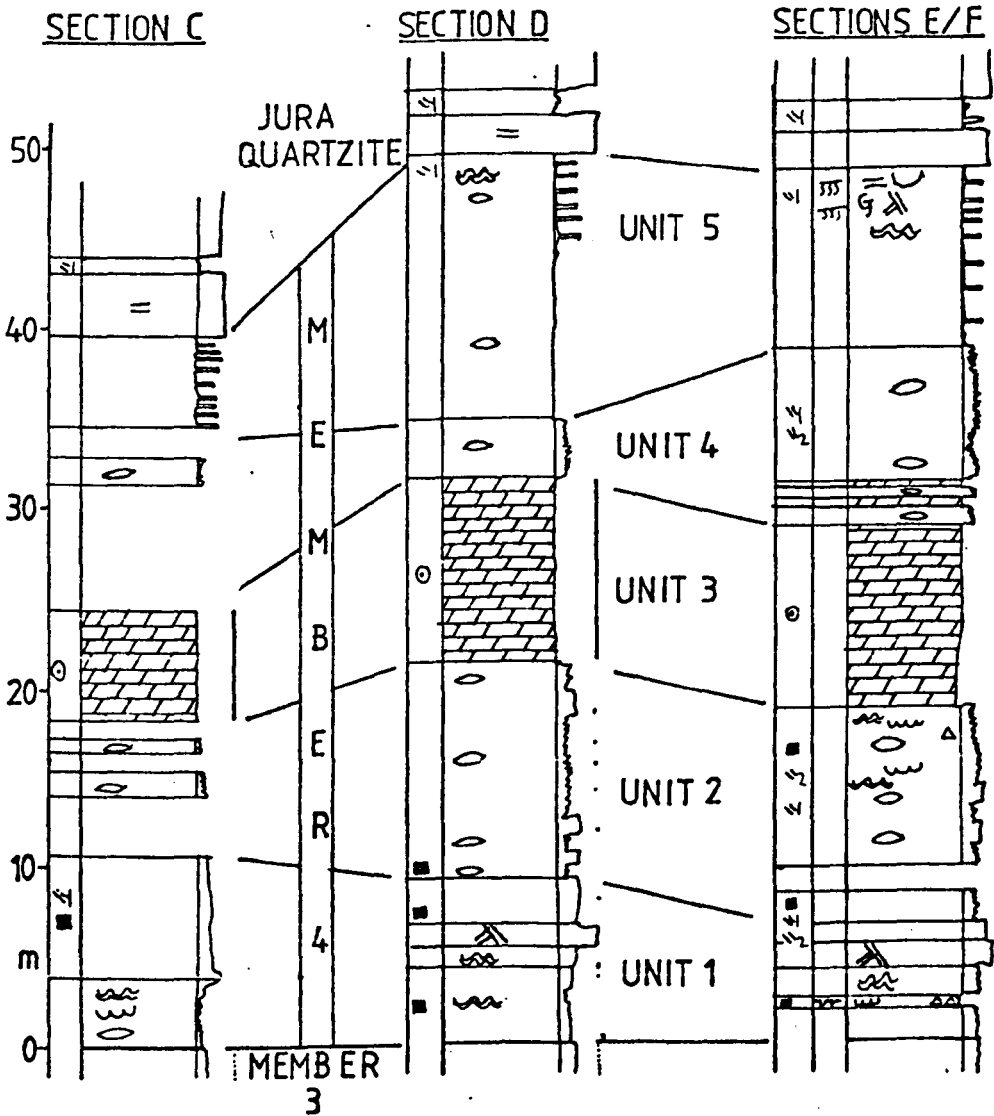
#### 4.4: Member 4

This member is generally rather deformed and some rocks possess true metamorphic textures. As a result sedimentary structures are less well preserved than lower in the sequence. The five sub-divisions of the member introduced in Chapter 2 are represented at each of the north coast sections (fig. 4-47). Features of sedimentological interest are described below.

##### 4.4.1: Unit 1

The change from dolomitic sedimentation of member 3 to dominantly terrigenous deposition in unit 1 of member 4 is sharp. The carbonate-poor nature of units 1, 2, 4 and 5 is clearly shown in figure 4-48. Much of unit 1 appears in the field as a massive, poorly cleaved silty sandstone. Sedimentary structures are recognizable in places (fig. 4-47). Wave-generated ripples show similar orientations to those of member 3 (fig. 4-49), with slightly smaller dimensions (average wavelength 6.3cm, range 3-10cm). Cross-strata occur in one quartzitic bed in Sections D and E and are also similar to those in member 3. The presence of two, widely spaced current orientations (fig. 4-50) suggests a tidal origin for the cross-strata. In thin section, much of the massive silty sandstone is seen to consist of fairly well-sorted coarse silt and very fine-grained sand with thin mud wisps which are thought to be primary flaser laminae. There are silt-sized heavy minerals which define trains bounding sets of cross-lamination (?current-ripple lamination). Thicker (cm size) mud laminae are common at some horizons, for example at the base of the unit in Section C, so that lenticular and 'tidal' bedding are formed.

A very minor part of the unit is dolomitic. Mudcracks



- CROSS-STRATA
- PARALLEL LAMINATION
- SMALL EROSION SURFACE
- GRADED BEDDING
- FLASER BEDDING
- LENTICULAR BEDDING
- WAVE RIPPLE FORM SETS & WAVE RIPPLE LAMINATION
- MUDCRACKS
- MUDSTONE CLASTS
- CONTRACTION CRACKS
- CONSPICUOUS S1
- S2
- NODULES
- LARGE PYRITE CUBES

- CURRENT STRUCTURES
- OTHER PRIMARY STRUCTURES
- SECONDARY STRUCTURES
- SILT
- V.F.G.R SAND
- M.G.R SAND
- CREAM-WEATHERING DOLOSTONE
- DOLOSTONE
- DOLOMITIC STRATA

Figure 4-47: Member 4 sections on the north coast.

with derived muddy dolostone clasts were seen in one specimen. The dolomite is ferroan and thus resembles that of member 3, rather than that of the massive dolostone, unit 3 of member 4.

#### 4.4.2: Unit 2

Unit 2 contains similar lithologies to unit 1, but with a higher proportion of mudstone and lenticular bedding: most lithologies are clearly heterolithic in the field. Mud clasts were seen in one specimen.

At Beinn Bhan in central Islay, there is no clear distinction between units 1 and 2. The sediments at this horizon show wave-generated ripples and well-developed desiccation cracks.

#### 4.4.3: Unit 3

Unit 3 is remarkable in that it is a relatively thick deposit of pure dolostone bounded above and below by muddy terrigenous sediments. In Section F however, dolostone appears to be interbedded with terrigenous sediments at the base of unit 4 (fig. 4-47).

The dolomite matrix is homogeneous and non-ferroan, 5-30 $\mu$ m in grain size. In addition there are other features, notably silt and sand sized quartz grains and diffuse quartz-calcite-albite nodules and veins, some of which mark the bedding (fig. 4-51). However the latter appear to be secondary in origin.

A sedimentary lamination is defined in a Beinn Bhan sample by variation in the proportion of floating quartz sand grains. In other samples too, quartz sand does appear to be original detritus. The purity, fine grain size and chemistry of the dolomite are probably also original.

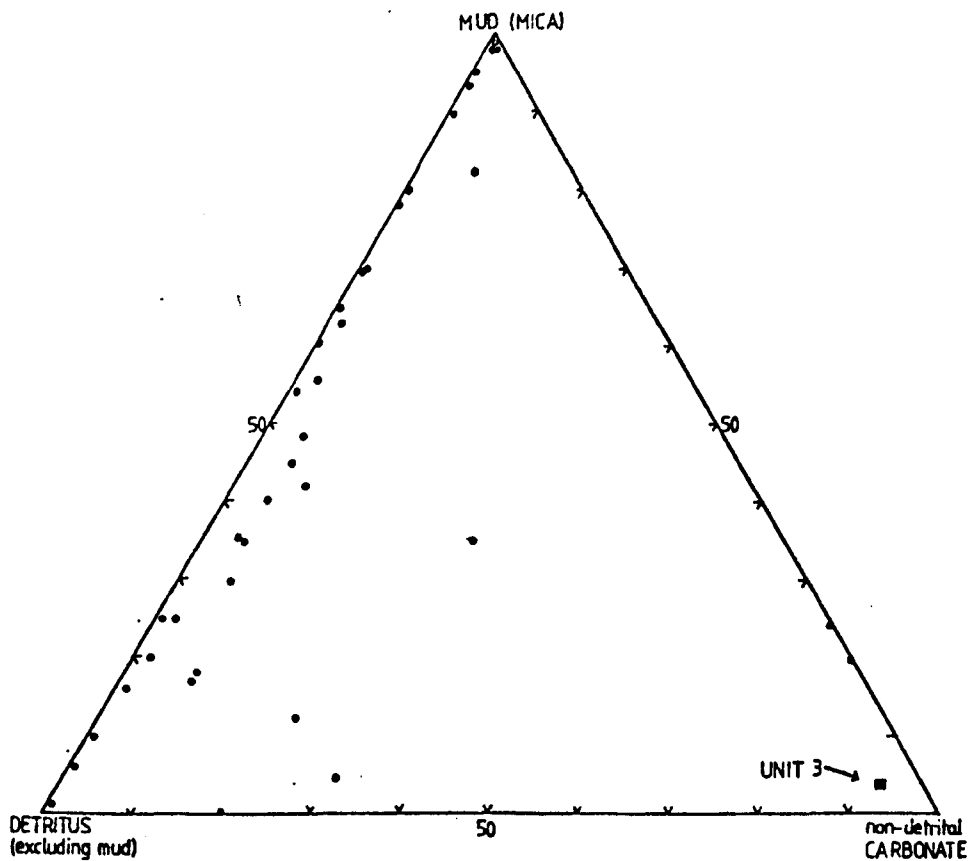


Figure 4-48: Mineralogical composition of individual laminae within samples from member 4 (most points are from visual estimates of abundance in thin section).

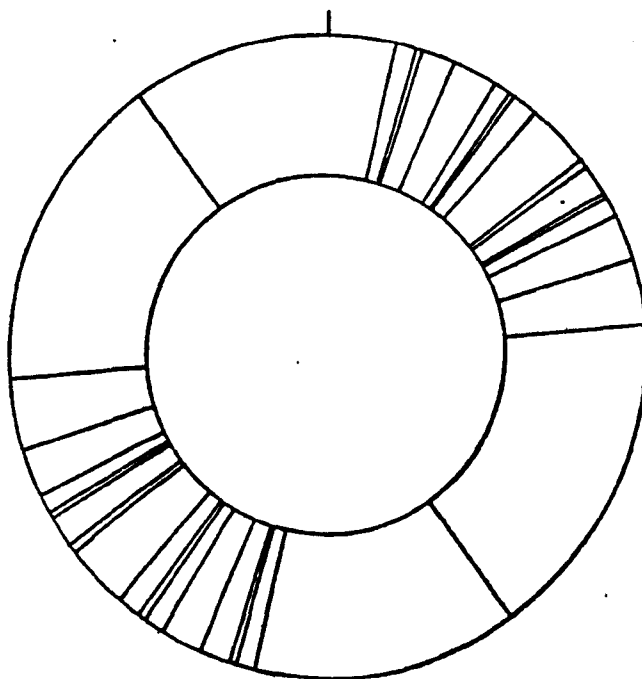


Figure 4-49: Crestline orientations of wave-generated ripples, member 4.

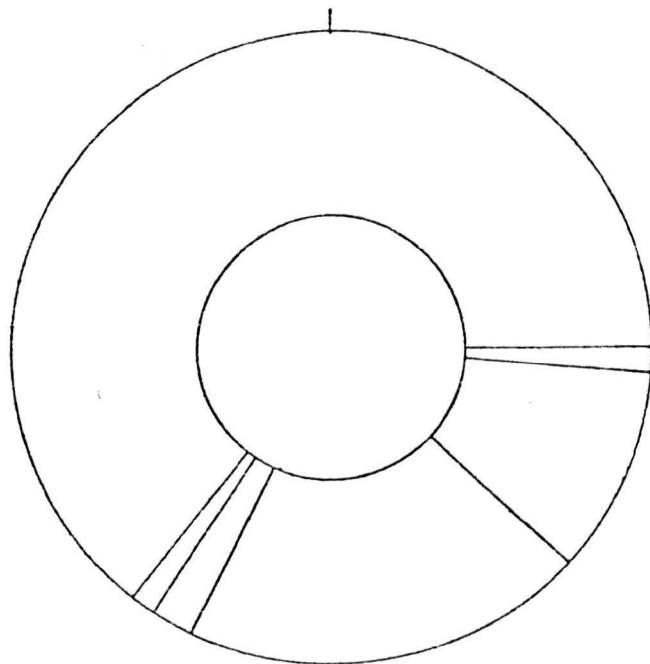


Figure 4-50: Palaeocurrents from cross-strata, unit 1, member 4.



Figure 4-51: Dolostone, unit 3, member 4 from Beinn Ehan. The most obvious structures are secondary veins, many of which are parallel to bedding. Lamination by variation in the concentration of scattered (aeolian) quartz can be seen in thin section.

#### 4.4.4: Unit 4

Unit 4 shows quite strong metamorphic alteration and is characterized by laminated mica-rich and mica-poor domains (fig. 4-52) which were probably inherited from a heterolithic sediment showing sand-mud alternations.

#### 4.4.5: Unit 5

Unit 5 is dominantly mudstone with thin sand beds (fig. 4-53) the latter showing some internal structure in places (fig. 4-47). Contraction cracks were seen in profile, but without any mud clasts.

#### 4.4.6: Interpretation

The flaser bedding and cross-stratification by tidal currents in unit 1 suggests a very shallow tidal environment with fine sediment being deposited in slack-water periods. In addition, abundant wave action is indicated by the preserved ripple form-sets. Emergence at one level is demonstrated by the fragmented mudcracked muddy dolostone lamina. The change from member 3-type sedimentation could be related to the development of a freer circulation (hence the scarcity of dolomite formation) caused by the breakdown of the barrier system.

The finer, heterolithic nature of unit 2, coupled with the presence of mud clasts suggests a mid-tidal flat situation (Klein, 1971). The other possibility of an off-shore situation with storm-deposited sand layers (Reineck & Singh, 1972) seems unlikely because of the absence of graded bedding like that of member 3. Unit 4 is probably similarly a tidal flat deposit.

Unit 5 could be regarded as high-tidal flat on the model of Klein (1971), but current ripples and mud clasts are absent. There seems more to commend a sub-tidal origin



Figure 4-52: Heterolithic phyllitic strata showing S2 microfolds, unit 4, member 4, Section F.

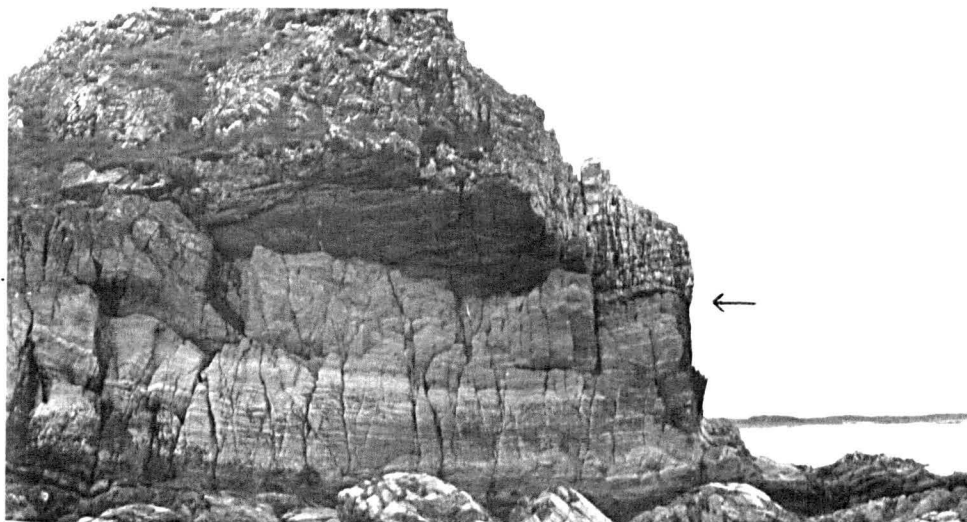


Figure 4-53: Section F; unit 5, member 4 forms the lower part of the sea stack and is sharply bounded above at the arrow by the Jura Quartzite.

similar to that of the fine facies in the overlying Jura Quartzite, described by Anderton (1976). The sand layers would represent distal storm surge deposits. The occurrence within the sands of parallel lamination, wave-generated ripple lamination, graded bedding and a set of cross-stratification (fig. 4-47) is entirely consistent with this view. The contraction cracks could be due to synaeresis because of the lack of associated breccias. Synaeresis cracks are common in the fine facies of the Jura Quartzite (Anderton, 1974, 1976).

The evidence from units 1, 2, 4 and 5 therefore suggests that member 4 represents a regressive-transgressive cycle, with the peak of the regression represented by unit 3. This is also suggested by the apparent restriction of unit 3 to the westward (originally landward) part of the area of outcrop of the Bonahaven Formation (see Chapter 2).

Stratigraphically then, the unit 3 dolostone could be regarded as broadly supra-tidal in origin. This is supported by its pure carbonate nature i.e. it is a chemical deposit. The only terrigenous material appears to be scattered sand grains which could well have been derived by deflation of a nearby aeolian terrain. The absence of other positive indicators of a supra-tidal origin such as evaporites and fenestrae is attributed to the deformation and metamorphism (see also Chapter 6).

The upper boundary of the Bonahaven Formation records a transition from the fine to the coarse facies of Anderton (1976), representing a down-current transgression of the sandier high current velocity areas of a tidal sea. Fine facies sedimentation briefly resumed a couple of metres above the base of the Jura Quartzite before the coarse facies become the dominant mode of sedimentation in northern Islay.

#### 4.5: Detritus

Characterization of the detrital matter is complicated by diagenesis and metamorphism: many of the finer lithologies have lost their detrital textures and contain abundant secondary albite. In member 1, the original detrital grains, especially in units 3 and 4 are readily determinable, but above this level fairly pure (quartzitic) lithologies are the only ones in which the nature of original detritus, particularly feldspar, can be accurately assessed. This has been done by point-counting thin sections stained for feldspar which allows the ready distinction of potassium feldspars (stained yellow), plagioclase feldspars (etched) and quartz (unetched). The results are shown in figures 4-54 and 4-55.

##### 4.5.1: Provenance

The detrital material in the Bonahaven Formation originates from three sources.

Firstly, clasts of mudstone and dolostone clearly are intraformational and very local in origin. Oöids too were formed in the contemporary sedimentary environment, although in an area where quartz sand was absent (the postulated oöid shoal) as in the example of Beukes (1977).

Considering the terrigenous material: chess-board albite, magnetite and apatite are characteristic of the tillites and most of the interbeds in the Port Askaig Tillite (Spencer, 1971a); microcline and green tourmaline are a feature of the Jura Quartzite (Anderton, 1974); and quartz, albite-oligoclase, zircon and brown tourmaline occur in both Formations.

Chess-board albite is the chief feldspar of the 'nord-markite' pebbles which are the dominant extra-basinal clasts



in the Port Askaig Tillite and is the dominant plagioclase feldspar in the Bonahaven Formation. Figure 4-54 shows that above member 1 of the Formation plagioclase never constitutes more than 3% of the detritus in sandstones, and is usually absent. Chess-board albite is conspicuous in the granite pebbles of unit 3 of member 1 in Caol Ila and of course in the underlying Tillite. Magnetite, besides occurring in the Tillite is conspicuous in heavy mineral laminations of unit 4, member 1, but is not common above member 1. The source of this material, which is common to many tillite occurrences in the Caledonides was tentatively suggested to be in north-central Europe by Spencer (1975) in "a southern extension of the Gothide plain". Likewise, Kilburn et al. (1965) regarded the absence of Lewisian-type pebbles in the Tillite as evidence for derivation from the SE rather than the NW. In the non-glaciogenic sediments, the presence of chess-board albite and magnetite is due to reworking of glacial deposits exposed on the sea floor.

Microcline was reported by Spencer (1971a) in the interbeds within Member 3 of the Tillite, but does not occur in any of the other interbeds, nor in any of the tillites. At the top of Member 5 of the Tillite, microcline is sub-equal in proportion to chess-board albite and becomes the dominant feldspar above member 1 of the Bonahaven Formation (fig. 4-54). The source terrain for this material seems to have been a terrain of high-grade igneous and metamorphic rocks to the NW of the depositional area (Anderton, 1974, 1976). Uplift of a NW block periodically from Port Askaig times onwards resulted in erosion of microcline-bearing sand from a fault scarp.

There remains the question of the manner in which the sediment entered the depositional area. Evidence (4.4)

from the dolostone, unit 3, member 4, suggests that some sand at least derived from a nearby aeolian terrain. In member 3 also, the near absence of silt and clay-sized siliciclastic debris in the sandstone facies could be explained if the terrigenous sand was derived from nearby aeolian dunes, mixing with precipitated carbonate (Kendall, 1969; Loreau & Purser, 1973) as has been postulated in other ancient sequences (Beukes, 1977; Tucker, 1977).

The silt and clay in member 1 and the member 3 layered facies would ultimately have had a fluvial source, but the present outcrops do not allow us to say whether or not there was a major river draining into the north Islay area. Much mud may well have been transported out into the shelf, then brought back inshore by storm action. The absence of mud in the marginal sub-facies and the sandstone facies could be due to a situation most remote from the fluvial (or storm) sediment input. More coarse sediment was available than in the lenticular-graded sub-facies because of supply of sand from nearby aeolian dunes, presumably not available during deposition of the latter sub-facies.

#### 4.5.2: Feldspar abundance

Figure 4-54 shows considerable variation in feldspar content in various 'quartzites' in northern Islay. The original sediments ranged from very pure quartz arenites to sub-arkoses and rare arkoses (using the classification of Pettijohn et al., 1973, p158).

Two factors are believed to account for this variation. Firstly, whenever plagioclase is dominant over microcline, that is whenever there is a substantial contribution of glacial detritus to the sandstone, feldspar is abundant, presumably reflecting a lack of chemical weathering of this material.

Secondly there is a grain size control. Figure 4-55 shows that the finer sandstones invariably have much feldspar, whereas the coarser sandstones usually have relatively little feldspar (particularly when the samples in which glacial debris makes a substantial contribution are disregarded). This is due to the relative ease with which feldspar is abraded relative to quartz, and has been recognized elsewhere on a large scale (Odom et al., 1976).

CHAPTER 5: PHENGITE SPHERULES FROM MEMBER 1:

GLAUCONITIZED MICROFOSSILS?

## CHAPTER 6: DOLOMITIZATION

The dolomitic nature of most of the strata in the Bonahaven Formation is so distinctive a feature, having led to the use of stratigraphic names such as Dolomitic Group (Bailey, 1917) and Bonahaven Dolomite (Spencer & Spencer, 1972) that it demands an explanation. The subject is therefore dealt with here in some detail, bringing in stratigraphic, petrographic and chemical arguments. The conclusions bear not only on the local problem, but to some extent on Precambrian dolomite in general.

### 6.1: Outline of dolomitization mechanisms

Partial summaries of the voluminous literature on dolomite and dolostones were provided by Friedman & Sanders (1967), Zenger (1972), Bathurst (1971), Füchtbauer (1974), Folk & Land (1975) and Wilson (1975). No attempt is made to emulate these authors here, but some discussion of our present state of knowledge is required.

Dolomitization can occur at various stages in the history of a sediment. Although these stages may have rather arbitrary limits, it is useful to distinguish four general categories:

1. Dolomite forming as a primary precipitate in a sedimentary environment (primary dolomite) e.g. Behrens & Land (1972), Borch & Jones (1976). It is very difficult to demonstrate primary precipitation of dolomite in Recent sediments and no proof of an ancient dolostone formed by this process has been made. Folk & Siedlecka (1974) regarded certain dolomite rhombs in cavities within Upper Paleozoic dolostones as being formed due to salinity changes in the depositional

waters; these could be regarded as primary, although not all authors would agree with this usage.

2. Penecontemporaneous dolomite, formed by replacement of  $\text{CaCO}_3$ , more or less at the sediment-water interface (e.g. Müller et al., 1972; Illing et al., 1965). Here belong the modern supra-tidal and lacustrine dolomite occurrences. The dolomite is very fine-grained and the boundary of dolomitization lies parallel to bedding.

3. Early diagenetic dolomite (pre-lithification), formed by downward percolation of a dolomitizing brine (Deffeyes et al., 1965; Müller & Tietz, 1966) or by mixing of solutions of high and low salinity (Hanshaw et al., 1971; Badiozami, 1973; Folk & Land, 1975). The boundary of dolomitization may or may not cross-cut bedding and the dolomite may be fine-grained, or somewhat coarser in for example cavity fillings.

4. Late diagenetic dolomite (post-lithification), e.g. Lovering (1969). There is no relationship between the boundary of dolomitization of dolomite and the bedding; the dolomite is coarse-grained.

The formation of dolomite in general is a complex process because there are a number of physical, chemical and mineralogical considerations involved. Although sea water is approximately saturated with respect to dolomite (Blatt et al., 1972), this mineral apparently does not form under normal open marine conditions. This is because the hydration of Mg ions in solution (Lippman, 1973) and the alternating, energetically similar layers of different cations in the dolomite lattice (Goldsmith, 1953) render dolomite formation a very slow process. The precipitation of aragonite or Mg-calcite is favoured instead. This applies even in waters of higher salinity where the condition of super-saturation

makes more rapid nucleation likely, unless the Mg/Ca ratio of the solution is also raised (Folk & Land, 1975). This latter condition is realized if calcium carbonate or gypsum are first precipitated (Illing et al., 1965; Müller et al., 1972) in a hyper-saline lagoon, supra-tidal flat, lake, or in the sediments beneath a downward percolating brine. The 'dolomite' precipitated is generally non-stoichiometric (Ca is present in excess), with poor ordering of the lattice, and is termed protodolomite (Goldsmith & Graf, 1958). With time and increased temperature the Ca-excess decreases and ordering increases; nevertheless non-stoichiometric dolomite is common in the geological record (Goldsmith & Graf, 1958; Badiozami<sup>sm</sup>, 1973; Young, 1973).

It was formerly maintained that all sedimentary dolomite formed from brines (Friedman & Sanders, 1967), but it is now clear that dolomite can form in dilute solutions. It is favoured by higher temperatures (Lovering, 1969) and a high Mg/Ca ratio of the solution (Müller et al., 1972). It seems that dolomite can form with molar Mg/Ca ratios as low as 1:1 at earth surface temperatures provided that the crystallization rate is slow enough (Folk & Land, 1975; Boer, 1977), but a dynamic fluid with a large supply of Mg ions is needed (Hanshaw et al., 1971). Geological evidence in favour of dolomitization by relatively dilute solutions is provided by Badiozami<sup>sm</sup> (1973), Land (1973) and Folk & Siedlecka (1974).

Although a high Mg/Ca ratio will facilitate dolomite formation, it will not be over-ridingly important unless the dolomite forms by replacement of  $\text{CaCO}_3$  by solid-state ion exchange, which seems unlikely (Bathurst, 1971; Badiozami<sup>sm</sup>, 1973). A high alkalinity, which is favoured by local

CO<sub>2</sub> withdrawal by photosynthesis may be of considerable importance (Bathurst, 1971; Davies et al., 1975). If Mg-calcite is present, it will be highly susceptible to dolomitization (Müller et al., 1972; Gebelein & Hoffman, 1973).

As the mere presence of dolomite does not demonstrate high salinities, or any particular environment of formation, are there any petrographic criteria which are diagnostic in this respect? Folk & Siedlecka (1974) and Folk & Land (1975) stressed that clear ('limpid') dolomite rhombs in cavities indicate slow crystallization in dilute solutions. Similarly coarse-grained cavity-fillings were a feature of the meteoric water dolomitization described by Land (1973). Conversely, it has been claimed that an association of fine-grained dolomite with nodular evaporites indicates supra-tidal dolomitization (Folk & Siedlecka, 1974). However, evaporitive-type dolomite can form sub-aqueously (Müller et al., 1972; Füchtbauer, 1974). Fine-grained dolomite was thought by Folk & Land (1975) to indicate a rapid crystallization rate (promoted by high salinities, or photosynthetic CO<sub>2</sub> withdrawal). However the grain size of the dolomite may be controlled by the nature of the material it is replacing, as examples are known where dilute inorganic dolomitization leads to the pseudomorphing of acicular aragonite (Thraillkill, 1968) or to the formation of dolomicrite after micrite (Asquith, 1967, cf. Badiozama<sup>m</sup>, 1973; Land, 1973; Fischbeck & Müller, 1971; Müller et al., 1972). It may therefore be very difficult to deduce the environment or mechanism of dolomitization by petrographic means alone. Consequently it is vital to assemble as much information as possible regarding the sedimentary environment and burial

history of the sediment to deduce the mechanism of dolomitization.

## 6.2: General features of dolomite in the Bonahaven Formation

In the Bonahaven Formation there are three separate important developments of dolomite (in members 1, 3 and 4) which are shown here to have different origins. However there are two features which are common to each of these occurrences.

Firstly the dolomite is stratigraphically restricted (as was shown in Chapter 4) which indicates an early diagenetic origin at latest. In contrast, some dolostone in the Islay Limestone is associated with post-tectonic faulting and so is clearly late diagenetic in origin.

Secondly, the dolomite is non-stoichiometric in the sense that it contains excess calcium (fig. 6-1). (It is also non-stoichiometric in the sense that there is Fe and Mn substitution for Mg). Figure 6-1 shows that the average of the Ca analyses of member 3 dolomite (54.6 mole. %  $\text{CaCO}_3$ ) and member 1 dolomite (53.7%) are both rather higher than the average of the two analyses of member 4 dolomite (51.2%). The dolomite appears to be fairly well ordered (01.5 peak is nearly as high as the 11.0 peak; Badiozami<sup>et al.</sup>, 1973). They are protodolomites, but unlike many modern protodolomites there is apparently no disordering beyond that required by the excess Ca in the structure. Although common in the geological record, it is worthy of note that, in the Bonahaven Formation, calcium-rich dolomite has survived chlorite grade regional metamorphism.

A description of the individual dolomite occurrences now follows in order of increasing complexity, which happens to be the reverse stratigraphic order. Aspects of diagenesis

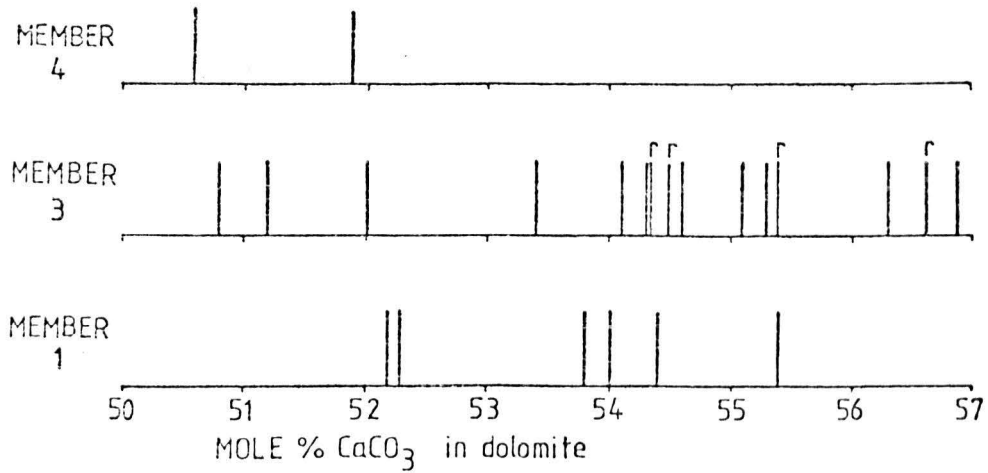


Figure 6-1: Microprobe analyses of calcium in dolomites in the Bonahaven Formation. Each bar represents one analysis. For member 3 dolomite, r= rhombic dolomite, the rest being fine-grained dolomite.

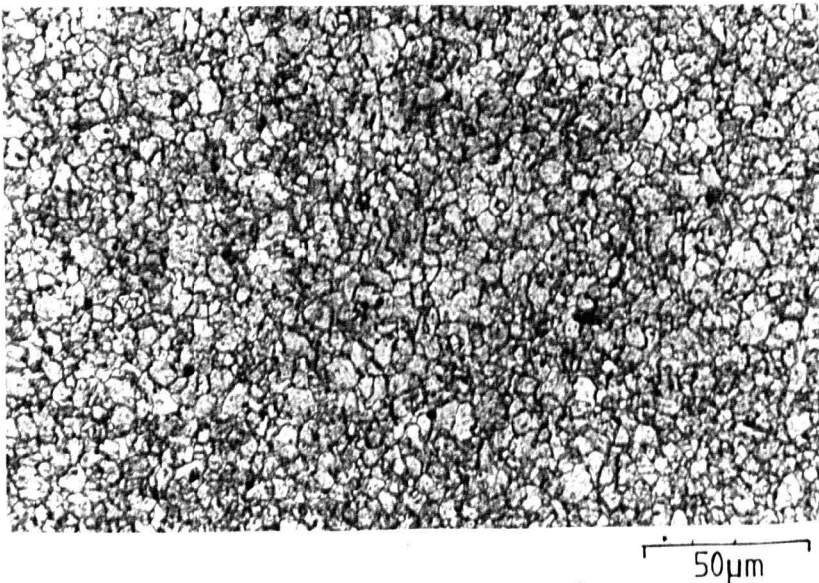


Figure 6-2: Photomicrograph, plane polarized light. Dolomite mosaic, unit 3, member 4.

subsequent to dolomitization in each case are dealt with in Chapter 7, unless important in reconstructing the original form of the dolomite. Accordingly, rhombic dolomite in member 3 is described there as its formation does not involve a pervasive dolomitization, whereas all dolomite in member 1 is treated in this chapter because it involves considerable chemical changes.

### 6.3: Member 4

The characteristic development of dolomite in member 4 is unit 3, which is an interval up to 10m thick composed entirely of cream-weathering dolostone. Some thin dolostones and dolomitic lithologies occur in units 1, 2 and 4, but these resemble those of member 3 and are not discussed further.

#### 6.3.1: Petrography

The unit 3 dolostone consists of a mosaic of dolomite which is xenotopic and 5-30 $\mu$ m in grain size (fig. 6-2). Large and small crystals are juxtaposed throughout, suggesting that there has been aggrading recrystallization of an originally finer mosaic. Samples variously exhibit combinations of the following: scattered silt-sized subhedral albite and silt and sand-sized quartz; groups of crystals of quartz, calcite and albite, occasionally merging to form irregular nodules or veins parallel to bedding (some of which may be syn-tectonic) and stringers of phlogopite. That some of the quartz sand was originally detritus was deduced in section 4.4.3. There is also incipient calcite replacement associated with calcite veins and vug-linings: these are post-tectonic (7.8). Before this calcitization, dolomite was the only mosaic-forming carbonate present. However lamination is never defined by variations in the grain size

of the dolomite mosaic.

There is no doubt that this unit has, like the rest of member 4 suffered considerable metamorphic alteration: a good deal of silt and possibly sand-sized detritus, as well as other penecontemporaneous structures may well have been obliterated. The nodules are too diffuse to be straightforward pseudomorphs of evaporites, but so much alteration has occurred that the original presence of evaporites cannot be ruled out.

### 6.3.2: Chemistry

No chemical zoning was detected in the dolomite mosaic; the uniform dull red luminescence is consistent with this. The Mn and Fe contents (fig. 6-6) are distinctly lower than those of member 3 dolomite, explaining the cream-coloured weathering compared with the deep yellow-orange of member 3 dolostones. Atomic Absorption analysis of one sample showed 134 ppm Sr and 630ppm Na. (A discussion of the significance of minor elements in carbonates is given in section 6.4.2).

### 6.3.3: Discussion

The unique stratigraphic occurrence of this dolostone, its inferred originally very fine crystal size, and, before late calcitization, its totally dolomitic nature throughout the thickness and areal extent of unit 3 (see Chapter 2), suggests a very early stage of dolomitization. Further, it was suggested in section 4.4.6 that unit 3 was supra-tidal so a penecontemporaneous evaporitic origin should therefore be considered.

Supra-tidal dolostones are well documented in the stratigraphic record (e.g. Laporte, 1967; Braun & Friedman, 1969), but their importance may well have been over-estimated.

(Zenger, 1972). The presence of sulphate evaporites or absence of fossils would be evidence in favour of a supratidal origin, although the converse is not true. The absence of a fauna cannot, of course, be used as evidence in these Precambrian rocks, but it may be significant that Downie et al. (1971) recovered no microflora from this dolostone, although acritarchs were found in member 3 dolostones. Evaporite pseudomorphs have been recognized in the Dalradian (Anderton, 1975; Llewellyn, in Spencer, 1969), but their comparative rarity could be used as evidence for a humid climate there as in the present-day Bahamas (Illing et al. 1965; Beukes, 1977) which could explain the absence of evaporites in member 4. On the other hand, the fact that the dolomite is much more nearly stoichiometric with respect to Ca than the member 1 or member 3 dolomite is evidence in favour of an evaporitic origin for the member 4 dolomite (Goldsmith & Graf, 1958; Marschner, 1968, Lippman 1973). A high Na value, as analysed, would also be expected in evaporitic dolomite (Veizer et al., 1977), but many more careful analyses would be needed to confirm this. If an evaporitic origin is acceptable, then the absence of evaporites needs to be explained: remobilization of evaporites, or their pseudomorphs by the metamorphism could well have occurred.

The low content of Fe and Mn and coarser grain size of member 4 dolostones compared with member 3 could be regarded as evidence for alteration by meteoric water after burial (Folk & Siedlecka, 1974) for member 4 dolostone. However, member 4 is more altered metamorphically than member 3 and so would be expected to be coarser-grained (Brown, 1972). Also the chemical differences between the dolomite of the two members can be explained in primary terms: see section 6.4.3.

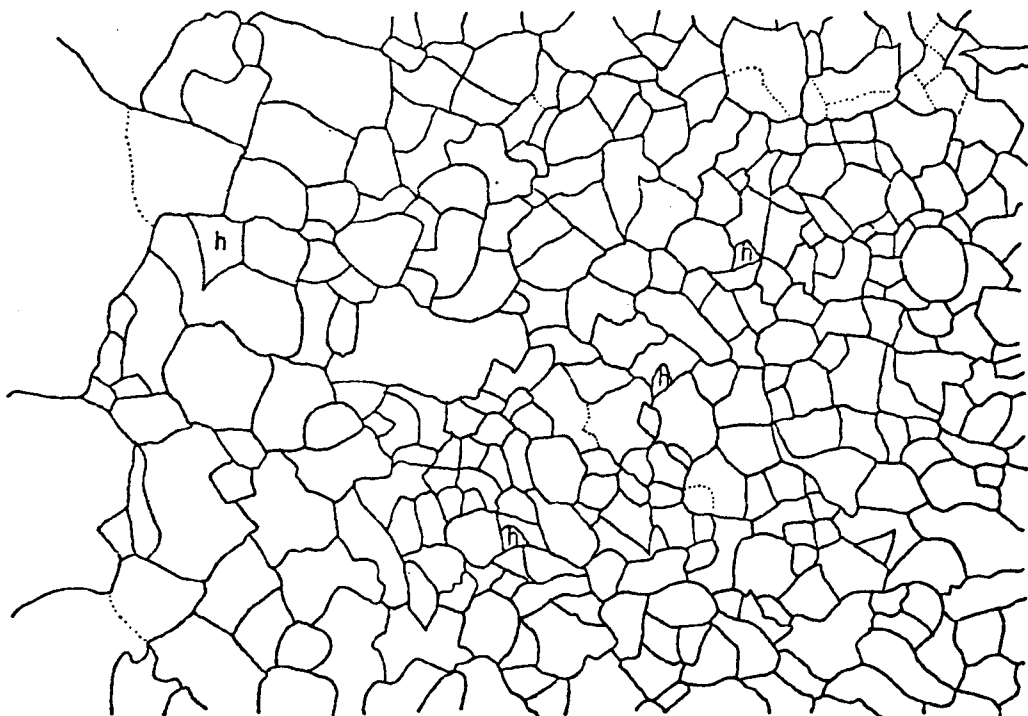
## 6.4: Member 3

### 6.4.1: Petrography

Most dolostones, stromatolites and ooids consist of a fine-grained mosaic of dolomite. Stromatolites may contain detrital mud, silt and sand impurities and there are continuous transitions from non-stromatolitic dolostones to dolomitic mudstones and dolomitic siltstones. The textures of dolomite in dolomitic siltstones and sandstones are described in section 7.2.4.

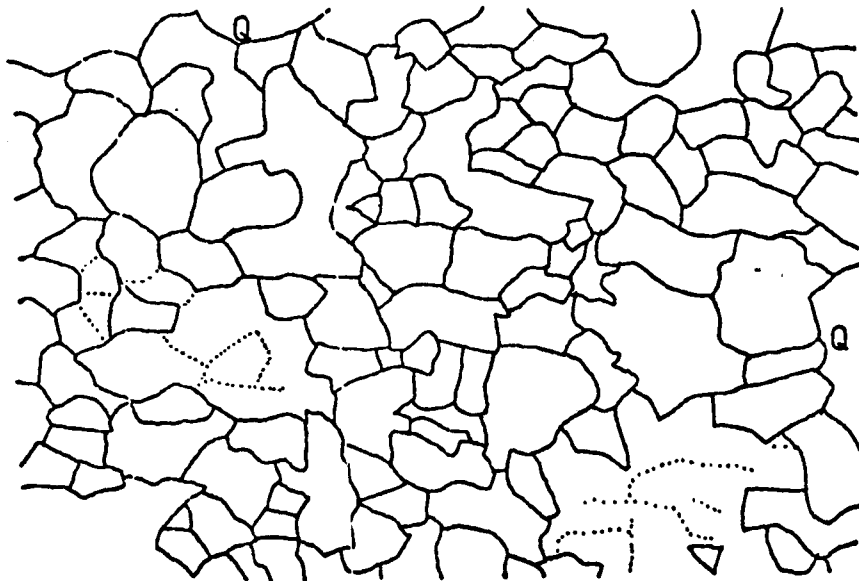
The texture of some pure dolostone mosaics was investigated by microscopic study of ultra-thin sections (5 $\mu$ m thick, see Appendix B3). Figure 6-3 shows the boundary between fine and coarse laminae of a stromatolite (BVI) with well-developed microstructure. The grain size of the fine layer is fairly constant, averaging 3.1 $\mu$ m; it grades to the coarser lamina with grain size 20 $\mu$ m or more. The fine layer is thus a true micrite (Bathurst, 1971). It was not possible to draw the grain boundary junctions accurately, but the shapes of the grains, particularly the smaller ones, are clearly seen to be fairly simple, commonly polygonal.

Figure 6-4 shows a dolostone (bed 69E) thought to be fairly typical of the apparently non-stromatolitic dolostones. The mean grain size here is rather coarser (10.4 $\mu$ m) than in the stromatolite of figure 6-3. However the fabric has been tectonically affected: an analysis of long axes of crystals in this figure shows that there is a preferred orientation (parallel to elongate quartz elsewhere in the section), which is statistically significant up to the 99.9% level by the Rayleigh Test (Mardia, 1972). It thus seems likely that diagenetic and metamorphic processes have led to an enlargement of crystal size: the original dolostones



10  $\mu$ m

Figure 6-3: Dolomite mosaic in stromatolite (BVI), showing junction of coarse and fine layers. Dotted lines are sub-grain boundaries; h= hole in thin section. The drawing was made by simultaneously observing the area under a microscope and tracing the grain outlines onto transparent film placed over a photograph of the area.



10  $\mu$ m

Orientation of elongate quartz elsewhere in thin section

Figure 6-4: Dolomite mosaic in dolostone, bed 69E. Q= quartz grain; dotted lines are sub-grain boundaries. The drawing was made in the same way as figure 6-3.

were thus probably originally true dolomicrites. Muddy dolostones are no finer than pure dolostones; this contradicts the findings of Bausch (1968) on pure and impure limestones.

The only other form of dolomite which probably relates to the original dolomitization process is 20-50 $\mu$ m dolomite with crystal faces projecting into former cavities in some fenestral stromatolites, and flake and grainstones of dolomicrite fragments (see 7.1.1).

Concerning the timing of dolomitization, evidence from dolomicrite ooids suggests that dolomite was not their original mineralogy. Although they exhibit a pseudo-uniaxial cross under crossed polars (fig. 6-5), the individual crystals which make up the ooid have no shape orientation. Therefore the crystallographic orientation must have been inherited, presumably from an earlier carbonate which grew in such a way as to have a radial or concentric dimensional, and hence crystallographic preferred orientation as in Recent ooids (Bathurst, 1971). By analogy dolomite in dolostones and stromatolites is probably replacive too. There is no doubt that the dolomite precursor was primary because there are primary pure carbonate beds from which intraformational pebbles have been derived. The carbonate (dolomite as now seen) was strictly stratigraphically controlled. The original carbonate must have been fine-grained because:

1. the finer the size of terrigenous material present, the more carbonate occurs.

2. carbonate laminae drape over, and thus preserve, bedforms (figures 4-34 and 4-35) and so must have formed when the depositional water was still.

There is no evidence as to whether the original carbonate

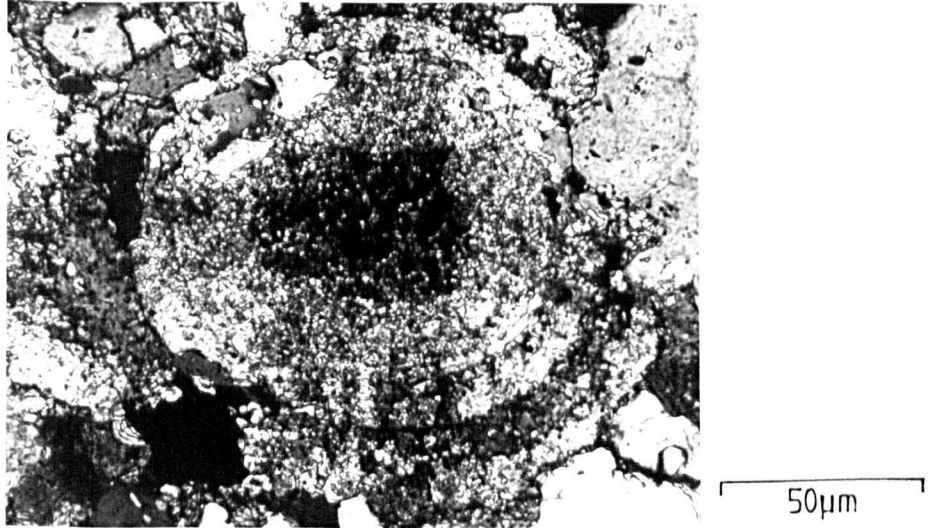


Figure 6-5: Photomicrograph, crossed polars. Dolomierite ooid (partly replaced by quartz near its margins) showing pseudo-uniaxial cross.

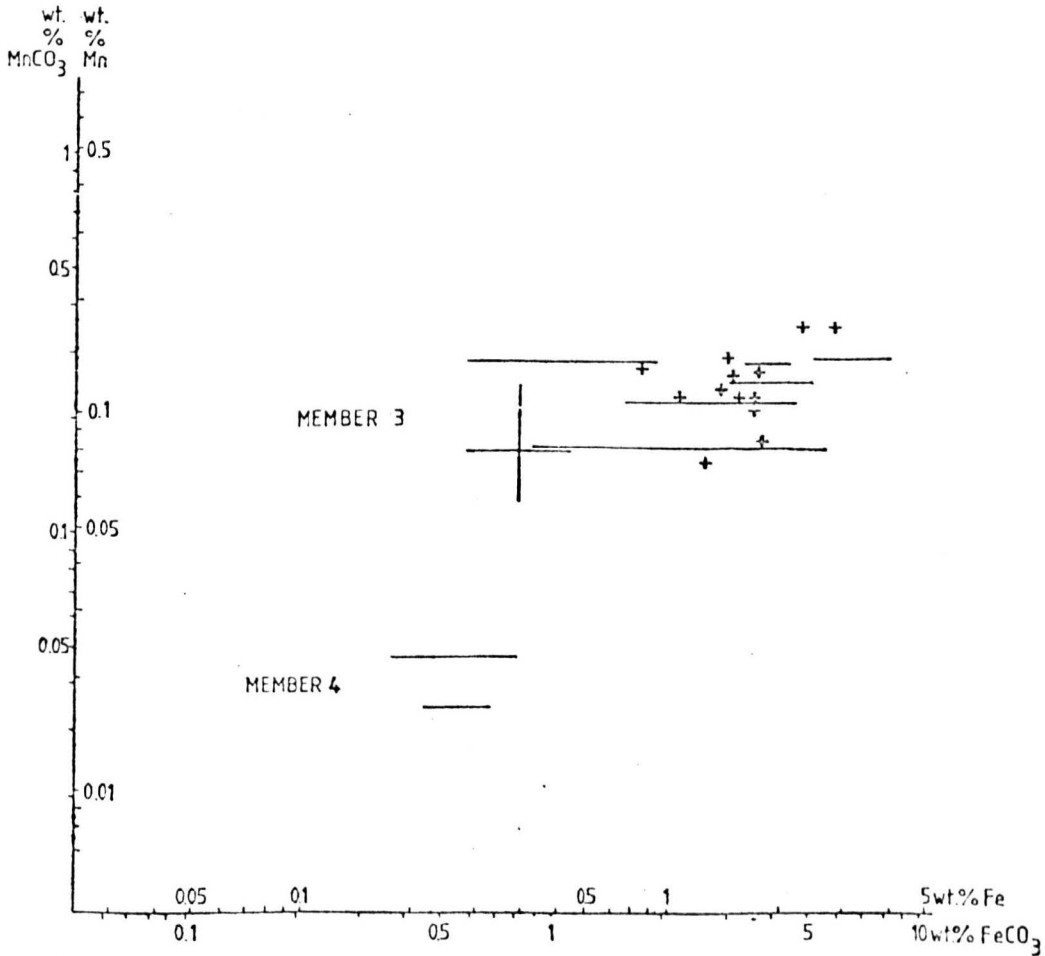


Figure 6-6: Fe and Mn content of member 3 and member 4 fine-grained dolomite. Each line or cross represents the chemistry of one sample.

precipitated on the sediment surface or within the overlying water column.

Dolomitization is complete and therefore no later than early diagenetic. This is not contradicted by the likelihood of some extant calcite in bed 25B pre-dating the dolomitization as this forms discrete laminations in a single bed (4.3.4.2). There is a clear contrast with the variable degree of dolomitization found in diagenetic dolostones within single beds, even when the distribution of dolostone is related to former basin margins (e.g. Schwarz, 1975).

#### 6.4.2: Chemistry

The Fe and Mn content of fine-grained dolomite in member 3 lie within extended, but coherent limits (fig. 6-6). Some specimens showed considerable variation in composition within a few tens of microns, whilst others showed a very constant composition. There is much more variation in iron than manganese content. There seems no correlation between chemical variability and stratigraphic position or geographic location. Sr and Na were near the detection limit on the probe. Using Atomic Absorption, one sample had 177ppm Sr and 310ppm Na.

The incorporation of trace elements into solids is governed by partition co-efficient theory (McIntyre, 1963). If a very small amount of solid, in which a trace element substitutes for a carrier major element, precipitates under equilibrium conditions from a relatively large solution reservoir in which the concentration of the trace element is low in proportion to the carrier element then:

$$m_{Tr}/m_{Cr} (\text{solid}) = K. m_{Tr}/m_{Cr} (\text{solution})$$

where  $m_{Tr}$  and  $m_{Cr}$  are the molar concentrations of the trace and carrier elements and  $K$  is a temperature-dependent constant, the partition co-efficient. Known values of  $K$

with respect to common minor elements are shown in figure 6-7.

The value of K for Sr in dolomite indicates that at 250°C dolomite precipitated in equilibrium with sea water should have 600ppm Sr, which may also be valid at earth surface temperatures as the Sr partition co-efficient with respect to dolomite is not strongly temperature dependent. The values for dolomite in members 3 and 4, although only a quarter of this value, are very similar to other ancient dolomites and dolostones (Graf, 1960; Weber, 1964). The fact that primary textures are still often preserved in such dolostones indicates that Sr is rather mobile during diagenesis as is clear from the work of Al-Hashimi (1976).

Only divalent Mn and Fe can be incorporated into carbonates by solid solution; therefore the partition co-efficient refers to the amount of reduced Mn and Fe in the formation waters. Thus ferroan calcite was considered to form from reducing solutions (Evamy, 1969). However, the concentration of cations in the reduced state need not be very high, as is shown below.

No partition co-efficients are available for Mn and Fe in dolomite. However, calcite considerably concentrates these elements (fig. 6-7) and there are grounds (see below) for supposing that dolomite will concentrate Mn and Fe to a much greater extent. However, the exact value of K will depend on the process of crystallization (that is whether dolomite is simply precipitating from solution, or simultaneously precipitating and replacing say quartz or calcite) and the temperature.

The ionic radii of Fe (0.74Å) and Mn (0.80Å) in

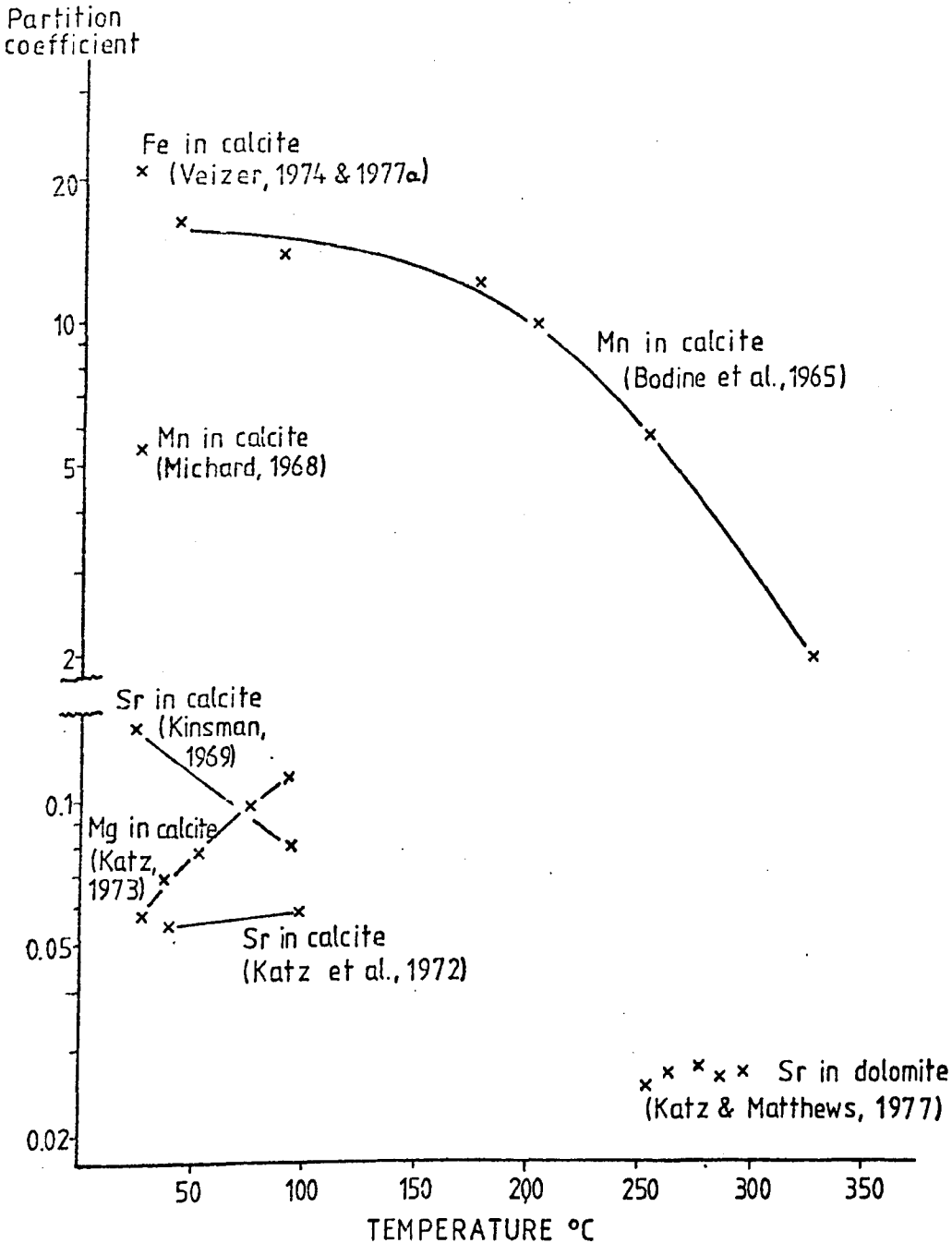


Figure 6-7: Partition co-efficients for calcite and dolomite. All are experimentally determined and refer to molar proportions except the value for Fe in calcite which was deduced by Veizer (1974) and defined by weight (Veizer, 1977a). Once the composition of the solution changes, an assumption has to be made as to whether the crystals precipitated from the solution become zoned (Doerner-Hoskins distribution) or unzoned, but continually adjusting their composition by diffusion (Nernst distribution). The latter seems appropriate when slow relief of supersaturation of a non-agitated solution occurs (McIntyre, 1963) but the Doerner-Hoskins distribution seems more generally appropriate (Bodine et al., 1965; Katz et al., 1972).

rhombahedral carbonates are closer to that of Mg (0.66Å) than Ca (0.99Å) and so Fe and Mn will substitute more easily in the Mg layers of dolomite, than in calcite. Iron partitions between co-existing metamorphic calcite and dolomite by a factor of 5 in favour of dolomite at 557°C, increasing to 8.5 at 400°C (calculated from equation 5 of Bickle & Powell, 1977) and much higher values at lower temperatures. Although these arguments are indirect, the implication is that dolomite has the capacity to scavenge iron from its formation waters to a much greater extent than calcite.

A typical composition of member 3 dolomite is 1.5% Fe and 0.15% Mn. Calcite with this composition would precipitate from a solution (with the Ca<sup>++</sup> composition of sea water) having 0.75ppm Fe<sup>++</sup> and 0.1ppm Mn<sup>++</sup> (after Veizer, 1977a). Therefore a solution with similar Ca<sup>++</sup> concentration would require concentrations of iron and manganese considerably lower than 0.75ppm Fe<sup>++</sup> and 0.15ppm Mn<sup>++</sup> to be in equilibrium with member 3 dolomite. For comparison, present day sea water has 1.9ppb Mn and 3.4ppb Fe (Turekian, 1968) or 2ppb Mn, as Mn<sup>++</sup> or MnSO<sub>4</sub>, and 10ppb Fe as suspended Fe(OH)<sub>3</sub> (Goldberg, 1963).

#### 6.4.3: Discussion

The previous description indicates that member 3 dolomite is replacive: it now remains to be shown whether this replacement was penecontemporaneous or diagenetic.

Penecontemporaneous formation by evaporitive capillary precipitation is ruled out by the evidence from sedimentary structures that there was only intermittent sub-aerial exposure.

Penecontemporaneous formation under a standing water body is a major possibility, either close to the sediment-water

interface (Müller et al., 1972; Folk & Land, 1975), or beneath the sediment, under the influence of refluxing brines (Müller & Tietz, 1966). The latter seems unlikely because of the lack of preserved evaporites needed to raise the Mg/Ca ratio and density of the brine (Deffeyes et al., 1965; Bathurst, 1971) and the low permeability of many of the layered facies sediments.

Synaeresis cracks in the layered facies indicate that the environment was subject to fluctuating salinities. Environments suffering extreme variations of this sort were termed schizohaline by Folk & Siedlecka (1974) and thought to be an ideal place to form dolomite by Folk & Land (1975). Dilution of marine water with 70-95% of fresh water may produce a situation where the solution is undersaturated with respect to calcite, but still supersaturated with respect to dolomite (Badiozami, 1973). Alternatively some, or all of the dolomitization could have been at higher salinities than this (Behrens & Land, 1972), but with a solution with high Mg/Ca ratio (Müller et al., 1972; Folk & Land, 1975). However, the absence of evaporites suggests that the salinities were never very high, although they could have been precipitated, then dissolved when the solution became diluted.

An additional factor may be the presence of algae in the depositional waters. Not only can carbonate precipitation be promoted by extraction of CO<sub>2</sub> from the water by their photosynthetic action or by bacterial decomposition of their organic matter (Lippman, 1973), but the algae have the ability to preferentially concentrate Mg<sup>++</sup> in their sheaths which makes the precipitation of Mg-calcite and ultimately dolomite likely (Gebelein & Hoffman, 1973; Davies et al., 1975). The possibility then arises that the dolostones

could in fact be cryptalgal. There is no pronounced clotted texture, thought to be characteristic of non-laminated cryptalgal structures by Aitken (1967), but the possibility remains that a coccooid-dominated algal community played more than an indirect role in the formation of the apparently non-stromatolitic dolostones.

The possibility that the dolomite formed diagenetically should also be considered. The lack of evaporites again precludes a circulating brine. However the formation of dolomite in the zone of mixing of meteoric and marine waters has been shown to be important by Badiozami<sup>AM</sup> (1973) and Land (1973). However in both these cases there is a period of uplift and sub-aerial exposure in order that fresh meteoric water can flush through the system. There is no evidence for such an uplift within or following the sedimentation of member 3. Alternatively, it is possible that a lens of fresh water at shallow depth extended some distance seaward as is found off the present east coast of Florida (Manheim, 1967). Dolomite could be formed as the sediment passed, on burial, through the brackish layer overlying the fresh-water lens. However the fresh water would need to be capped by an aquiclude to enable the seaward extension of the lens to take place (Manheim, 1967). In the case of the Bonahaven Formation, the only likely system would be an aquifer represented by member 2 sands, possibly extending down to the Port Askaig Tillite, capped by an aquiclude of layered facies member 3 sediments. However this system seems unlikely to produce such stratigraphically restricted developments of pure dolostone, and it does not seem possible for the member 3 sediments to be simultaneously an aquiclude and to be sufficiently permeable to allow

passage of sufficient volumes of water to allow complete dolomitization. Thus an origin of the dolomite essentially before burial is indicated.

There is one remaining difficulty in the penecontemporaneous hypothesis: this is the high Fe and Mn content of the dolomite. This would be readily explicable if the dolomite had formed after burial because, under the water table, reducing conditions would allow the maintenance of Fe and Mn in solution in their reduced states, thus allowing their incorporation in precipitated carbonates (Oldershaw & Scoffin, 1967; Evamy, 1969). The possibility then arises therefore that if the dolomite was originally penecontemporaneous as is concluded above, it may not have been ferroan originally, but iron may have been introduced by a later recrystallization episode. This suggestion is thought highly unlikely because:

1. there is a distinct chemical difference between member 3 and member 4 dolostones.

2. recrystallization on the massive scale required could not have preserved the fine grain size of the dolomite. This is clearly shown in member 1: where later dolomite replaces dolomicrite, the later dolomite is much coarser.

The precipitation of Fe and Mn-bearing carbonates near the sediment surface could occur even under conditions as oxidizing as they are to-day if:

1. the depositional water was stagnant and therefore reducing (Katz, 1971). However, abundant evidence of current activity is apparent in member 3 sediments.

or 2. the activity of bacteria just below the sediment surface created reducing conditions: Fe and Mn would be in their reduced states and could be precipitated in carbonate if sulphate is excluded (Curtis & Spears, 1968). However in a pure carbonate sediment such as the member 3 dolostones

which were analysed, there does not seem to be a source for these elements because clays, which could carry Fe and Mn (Berner, 1971), are absent. Fe and Mn in an oxidized state would travel in suspension rather than solution and so must have been absent, along with the other suspended sediment, from the pure dolostones.

It therefore seems that Fe and Mn must have been taken from solution in the depositional waters in their reduced states, which implies a more reducing atmosphere than at present, although quantification of this is very difficult. In support of this suggestion is the proposal that the oxygen content of the atmosphere in late Precambrian times may have been less than 1% of its present level (Holland, 1972). Also, as previously discussed, dolomite probably has a very high partition co-efficient with respect to Fe and Mn so that, at any one time, the depositional waters need only have had very small quantities of reduced Fe and Mn. These would be replenished by reduction of  $\text{Fe}(\text{OH})_3$  and  $\text{MnO}_2$  to maintain equilibrium, a process called regenerative capture by Altschuler et al. (1958, p84). One contrary factor is the production of oxygen by algal photosynthesis in the depositional environment. The complexity of the chemical system (Sillén, 1965, 1966; Stashchuk, 1972) precludes further evaluation of this problem by the present author at the time of writing.

The higher Fe content of member 3 compared with member 4 dolomite can be explained by the build-up of Fe and Mn in the partially barred 'lagoon' of member 3 times. Rivers draining into the area would have led to concentrations of Fe and Mn relatively higher than in the open sea (Fruth & Scherreicks, 1975). The relatively constant level of Mn compared with Fe in the dolomite suggests a more constant

supply of the former. Member 4 dolomite, on the other hand, would have been deposited adjacent to a more open coast where fluvial influx was not concentrated and so did not incorporate so much Fe and Mn. This idea was put forward by Button (1976) for the Proterozoic Malmani Dolomite of South Africa: dolostones formed in this author's 'barred basin' have similar Fe content to member 3 dolomite, whilst other dolostone in the sequence are intermediate between member 3 and member 4 dolomites.

The idea that the changing oxygen content of the atmosphere might be matched by inverse changes in the Fe and Mn content of carbonates was suggested by A.W.Joliffe (in discussion of Graf, 1962). For dolostones, one would want to be sure that the dolomite formed in equilibrium with sea water and that analyses were made of dolomite without impurities of other minerals. Figure 6-8 illustrates some suitable available data. All are analyses of dolomite except figure 6-8A which represents FeO and MnO analyses of pure dolostones. Although the data suffer markedly from biased sampling, it is clear that there is a tremendous range in composition at any one time. Eriksson et al. (1975) attributed highly variable Mn/Fe ratios in their Proterozoic sequence to primary causes. Considering figure 6-8A and B, part of the variability can indeed be explained (Button, 1976; herein) as being due to precipitation of some of the dolomite within restricted water bodies. The extreme range of values in figure 6-8C-F may indicate secondary alteration of many of these dolomites. However dolomite in figure 6-8A which Eriksson et al. (1975) suggested have been recrystallized have intermediate Fe and Mn contents between the chemistries of the 'open coast' and 'barred basin' dolomites. In the Bonahaven Formation,

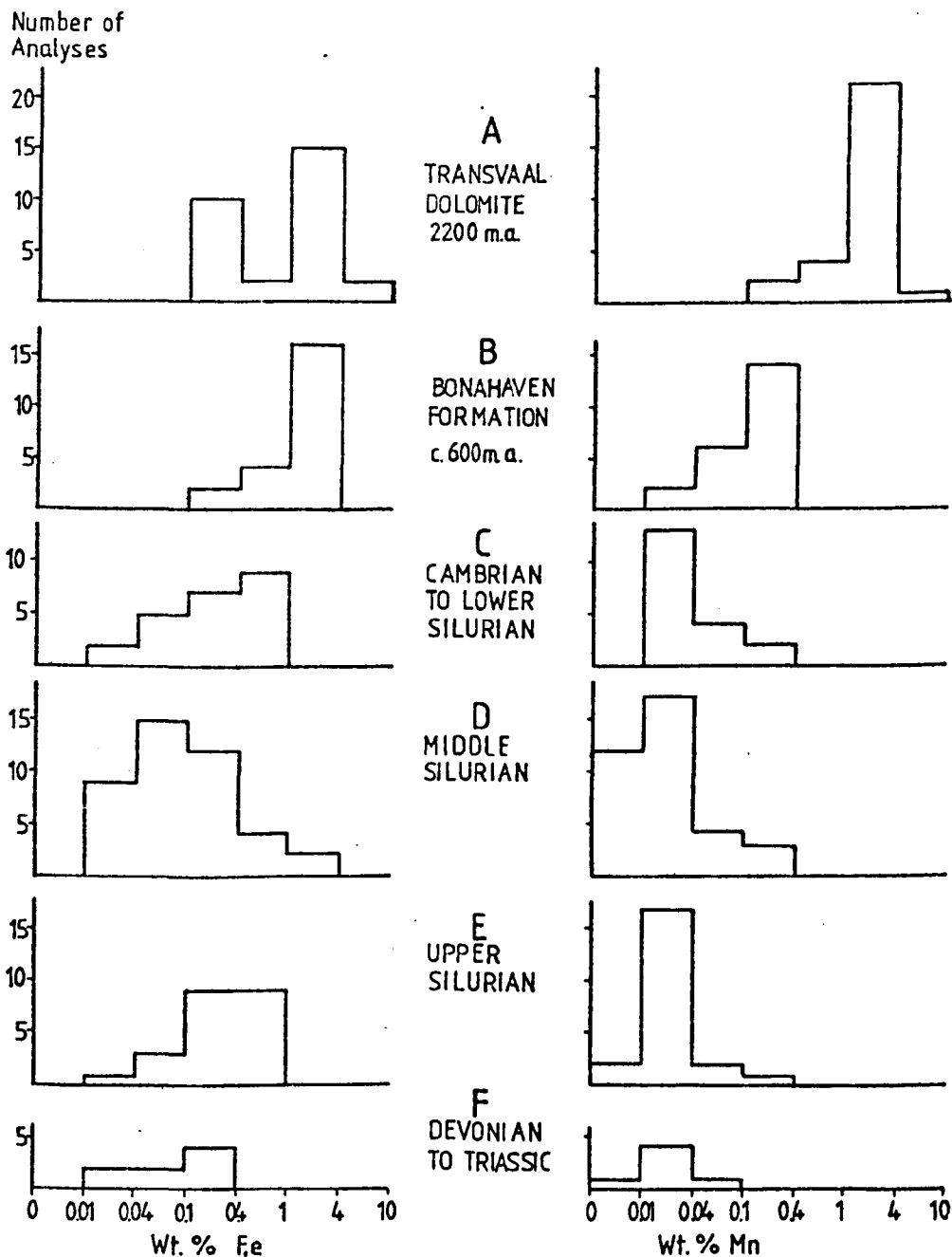


Figure 6-8: Iron and manganese contents of dolomite of various ages. A) Data (Eriksson et al., 1975) are all whole rock analyses, but the dolostones are fairly pure. They include analyses from the stratigraphically equivalent Malmani Dolomite (Button, 1976). In addition, Young (1973) reported 5 microprobe analyses (not plotted above) from the Espanola Formation (2100-2500 m.a.) of Canada which show 6-13 wt.% Fe. B) This study; members 3 and 4. C-F) Dolomites separated from "primary" dolostones. This is a re-ordering of data from Weber (1964) who was concerned only with the differences between primary and secondary dolomite rather than with any differences with age.

the member 3 and 4 dolomite analyses, and their constant difference in weathering colour, seem to be distinct enough to indicate that the difference between them is an original one.

Regarding the general aspects of figure 6-8, a general downward trend of Fe and Mn content with time is hinted at, but no definitive statements can be made until more data is available. Member 3 seems anomalously high in Fe content compared with the Transvaal dolomite considering that the partial pressure of oxygen in the atmosphere should have increased in the meantime. However Young (1973) recorded much higher Fe contents (6-13%) than in the Bonahaven Formation from early Proterozoic dolomite in strata above tillites in Canada. Also values comparable with member 3 occur in younger strata (fig. 6-8F). Manganese in member 3 does seem to be intermediate between the average of early Proterozoic, and the Phanerozoic values, but again there is considerable overlap.

#### 6.5: Member 1

There are three basic petrographic types of dolomite in member 1.

TYPE 1: fine-grained, ferroan ( $>1\%FeCO_3$ ). This is found in some dolostone and sandy dolostone pebbles at the top of unit 5.

TYPE 2: inclusion-bearing, chemically zoned dolomite (fig. 6-9). Zoning may also be defined by variation in the number of inclusions. Early-formed crystals, and cores of larger crystals are non-ferroan, later zones are ferroan ( $>1\%FeCO_3$ ). This type replaces pebbles of various fine-grained lithologies and occurs as intergranular material in sandstones and conglomerates of unit 5. These sandstones

and conglomerates are now so dolomite-rich that they resemble pure dolostones in the field.

TYPE 3: intergranular, ferroan, inclusion-free. This is found in unit 5 sandstones, and unlike the other types, in some sandstones in units 3 and 4.

The different types and the various petrographic forms of type 2 make a complicated story, so Table 6-1 has been compiled to summarize the interpretations of the relative age of the dolomite and to aid the description which follows.

TABLE 6:1 Interpretation of time relations of member 1 dolomite

	refer to section	Type 1 (early)	Type 2		Type 3 (late)
			low Fe/Mn stage	high Fe/Mn stage	
Samples from the top of unit 5:					
2 (equant, m.gr., replaces mudstone)	6.5.2.2.		←————→		
27A (patchy f.gr. & equant m.gr.)	6.5.1.; 6.5.2.2.	←————→	←————→		
27C (equant m.gr. replaces type 1)	6.5.2.2.		←————→		
27E (m.gr. intergranular)	6.5.2.3.		←————→		
27D (c.gr. replaces mudstone)	6.5.2.2.			←-1-3→	
27B (clean intergranular)	6.5.3.				←————→
28A (patchy f.gr. & equant m.gr.)	6.5.1.; 6.5.2.2.	←————→	←————→		
28C (c.gr. intergranular)	6.5.2.3.		←-1-4→		
28B (c.gr. replaces mudstone)	6.5.2.2. 6.5.3.		←---1-2---→	←-3→	←-4-----→
28D (c.gr. intergranular & pseudo-vug fill)	6.5.2.3. 6.5.3.		←-1-4→	←-5-9→	←-10-15-----→
29 (c.gr. intergranular)	6.5.2.3. 6.5.3.		←-1-13→	←-13-18→	←-19-----→
Various samples from units 3 & 4 and the base of unit 5 (clean intergranular)	6.5.3.				←————→

←———— TIME AXIS —————→

Dolomite in each sample can be assigned to one or more of the four stages in the columns above.

Numbers/letters at left are analysis numbers (see Appendix A), used for description in this chapter.

Numbers to right are zone numbers (see Table A5 and various figures in this chapter).

For zoned dolomite, within a single hand specimen zones can be correlated between different petrographic forms of zoned dolomite, but the zoning is different in different specimens.

### 6.5.1: Type 1 dolomite

This consists of a 5-15 $\mu$ m mosaic which makes up the whole or part of pebbles of dolostone and sandy dolostone. It luminesces a uniform very dull red and stains as ferroan dolomite. Mostly it is present only as patches within coarser zoned (type 2) dolomite (figure 6-10). The latter is interpreted to be a replacement of the former simply on the grounds that in general coarser dolomite forms later than finer dolomite. Microprobe scans across material like that of figure 6-10 (analyses 27A, 28A; figure 6-17) show a very inhomogeneous (bi-modal) distribution of Fe and Mn: most of the coarser dolomite is low in Fe and Mn, although there are some areas a few microns across which are high in Fe and Mn; in contrast the fine dolomite is predominantly rich in Fe and Mn, comparable with member 3 dolomite. It is possible that the low-Fe-Mn areas which do occur in the finer dolomite could represent incipient replacement by type 2 dolomite.

Type 1 dolomite thus resembles member 3 dolomite in chemistry and grain size, but in member 1 no undisturbed dolomicrite beds occur, only pebbles. The dolomite (or its precursor) in the sandy dolostone pebbles was probably originally in the form of sand-sized micritic grains or possibly a micritic infiltrated sediment. This is because the dolomite makes up over 50% of the pebbles, too much for it to have been a micritic cement.

### 6.5.2: Type 2 dolomite

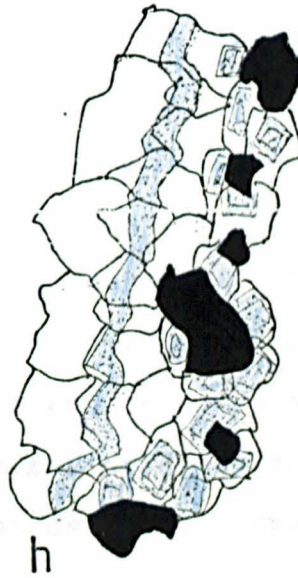
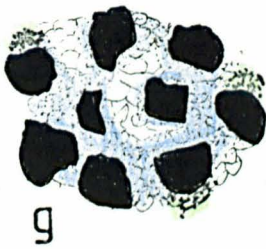
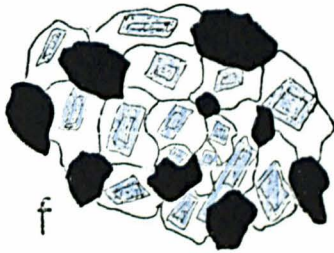
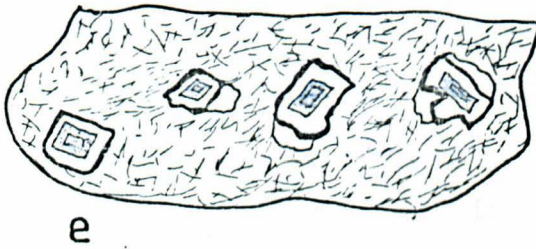
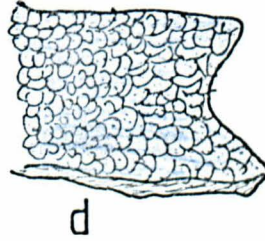
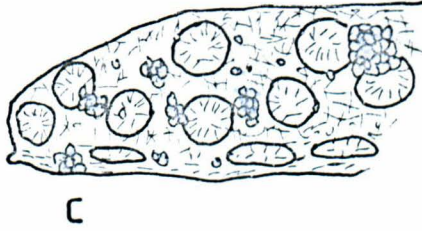
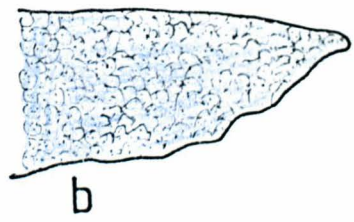
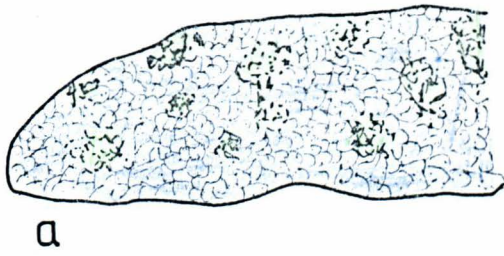
#### 6.5.2.1: General features

Zoned dolomite is characteristic of the uppermost 5m of member 1. It shows a variety of petrographic forms (fig. 6-9): equant, polygonal mosaics, intergranular crystals, and forming zoned fringes that resemble vug-linings. The



Figure 6-9: Petrographic varieties of type 2 dolomite as seen in plane polarized light.

- a) pebble containing patchy fine-grained (type 1) and equant, inclusion-rich medium-grained (type 2) dolomite.
- b) as a), but replacement by type 2 dolomite is complete.
- c) spherule-bearing mudstone clast with patchy replacement by inclusion-rich, equant (type 2) dolomite. Lower margin of clast has elongate spherules (= desiccated margin).
- d) as c), but complete replacement by equant dolomite has occurred, except along the desiccated margin. Grain boundaries are dark because of the presence of impurities.
- e) zoned dolomite replacing mudstone. The early zones are surrounded by a black impurity-rich ring and are thought to be type 2 dolomite, whereas the overgrowth beyond this ring is thought to be type 3 dolomite.
- f) coarse-grained intergranular dolomite (type 2). Later growth is inclusion-free.
- g) medium-grained intergranular dolomite (type 2). Later growth is inclusion-free.
- h) coarse-grained intergranular dolomite passing out into a zoned fringe to the left which resembles the filling of a former cavity (= pseudo-vug-fill).



fluid inclusions  
equant dolomite  
dolomite with  
zones of  
inclusions



mica  
mica spherules  
quartz clast  
fine grained  
dolomite

dolomite is certainly pre-tectonic, because pressure fringes occur around some zoned crystals in mudstone pebbles.

A notable feature is the presence of successive inclusion-rich and inclusion-poor zones, generally rhombic in shape. The inclusions are generally  $\leq 1\mu\text{m}$  in diameter (fig. 6-11) and are known to be fluid-filled because Brownian motion of a gas bubble in a liquid medium is seen at very high magnification within each inclusion. Most inclusions are smoothly rounded, circular or elliptical in section, but some are negative crystals. The significance of the presence of fluid inclusions is not certain, but might relate to the speed of growth of crystals (7.2.4).

Larger crystals display undulose extinction, lattice curvature being up to  $10^0$  in two dimensions. The fact that this undulose extinction is much more abundant than twinning indicates that the undulose extinction arose during crystal growth (as can be inferred from the dolomite cements of Scherer, 1977), rather than being of tectonic origin.

The growth history of this dolomite was deduced by a combination of petrographic means together with cathodoluminescence and microprobe analysis. All the type 2 dolomite shows chemical zoning. The growth zones are different in all but the most major respects between samples, but within samples the different petrographic forms show a zonation which can be correlated.

#### 6.5.2.2: Replacements of mudstone and dolomicrite pebbles

Dolomite replacing mudstone clasts occurs as large optically zoned crystals (fig. 6-9e, fig. 6-12) or an equant polygonal mosaic (fig. 6-9c, d; fig. 6-15). In the samples studied, the latter was only found as replacements of spherule-bearing mudstones (see Chapter 5), whereas the former was restricted to normal mudstones.

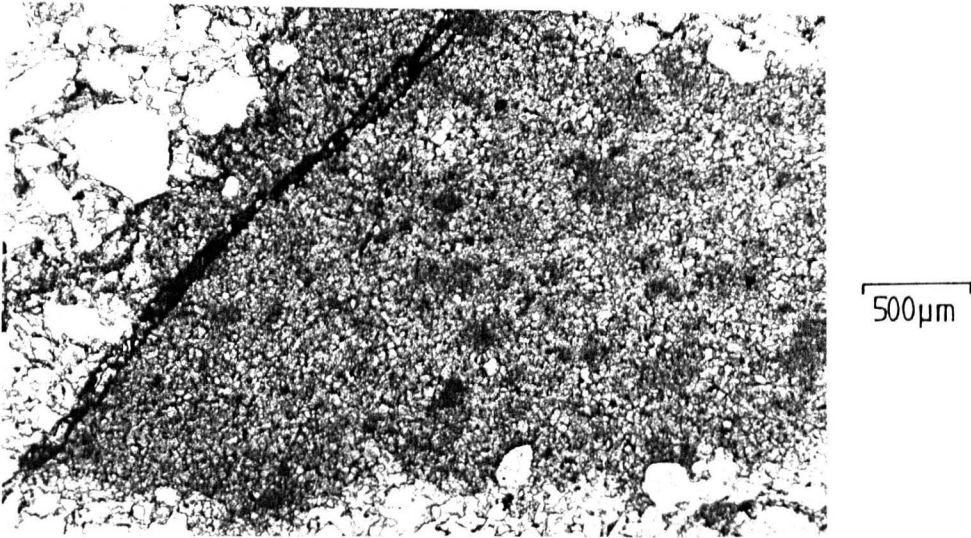


Figure 6-10: Photomicrograph, plane polarized light. Dolostone pebble with patches of type 1 dolomite (dolomicrite) within coarser, type 2 dolomite. Dark vein is post-tectonic.

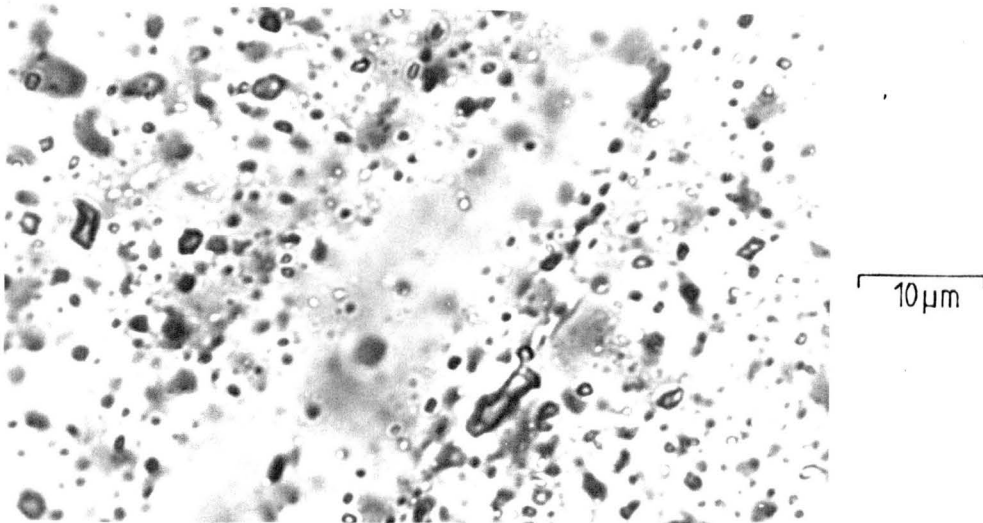


Figure 6-11: Photomicrograph, plane polarized light. Fluid inclusions in type 2 dolomite.

Presumably the number of nucleation sites was greater in the spherule-bearing mudstones.

Zoned rhombs replacing mudstones generally have rather irregular external boundaries compared with the euhedral internal zones. There is generally an approximately rhomb-shaped opaque line near to, or at, their periphery, which seems to represent a concentration of insoluble matter that was not dissolved as the dolomite crystal grew. Some rhombs have an anhedral portion beyond this ring of insolubles which is in optical continuity with the inner part of the crystal. This later growth has no dark rim and seems similar to the dolomite in figure 6-13, which is ferroan and encroaches onto a mudstone clast around its margins. This type of growth is considered to be of type 3 dolomite (6.5.3).

The luminescence and chemistry of zoned rhombs replacing mudstone was found to be different in the two samples analysed (fig. 6-14), although the same within each sample. Analysis 27D shows rhombs constantly higher in Fe and Mn, whereas analysis 28B shows earlier zones poorer in these elements. There is clearly no relation between the presence of inclusions and any particular chemistry.

Where equant polygonal dolomite replaces mudstone it forms a mosaic 30-50 $\mu$ m in size, rich in fluid inclusions and may show a partial or complete replacement (fig. 6-9c, d; fig. 6-15). There is a concentration of insoluble matter (mica and indeterminate material rich in Fe, Si and Ti) along grain boundaries which are dark as a result (fig. 6-15). This is equivalent to the dark rim around the zoned rhombs replacing mudstone (fig. 6-9e; fig. 6-12a). In a conglomerate of spherule-bearing mudstone fragments, one pebble shows

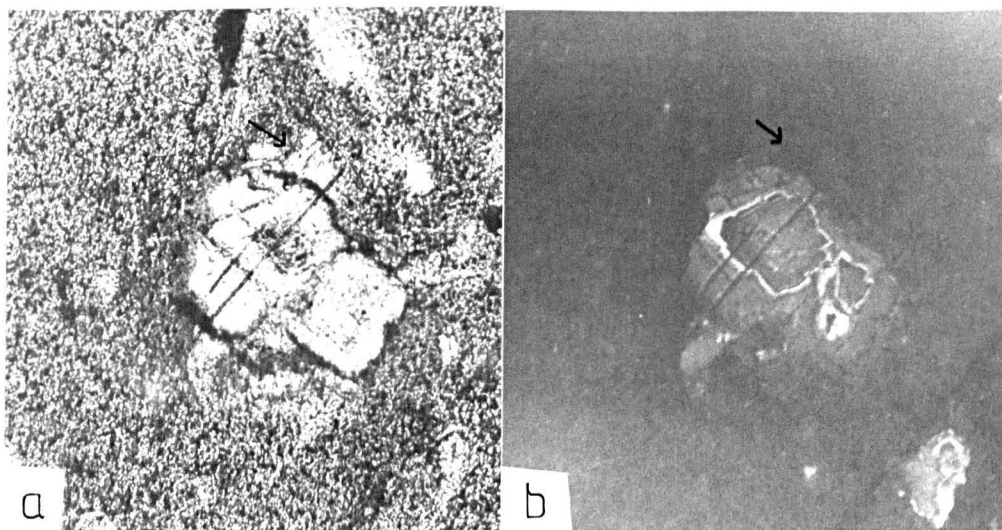


Figure 6-12: Partial replacement of mudstone pebbles by zoned dolomite. a) transmitted light; b) luminescent light. Early rhomb-shaped zones are type 2 dolomite whereas the non-luminescing dolomite (arrowed) beyond the dark line is thought to be type 3. Probe scan lines (analysis 28B) run NE-SW across the rhomb.

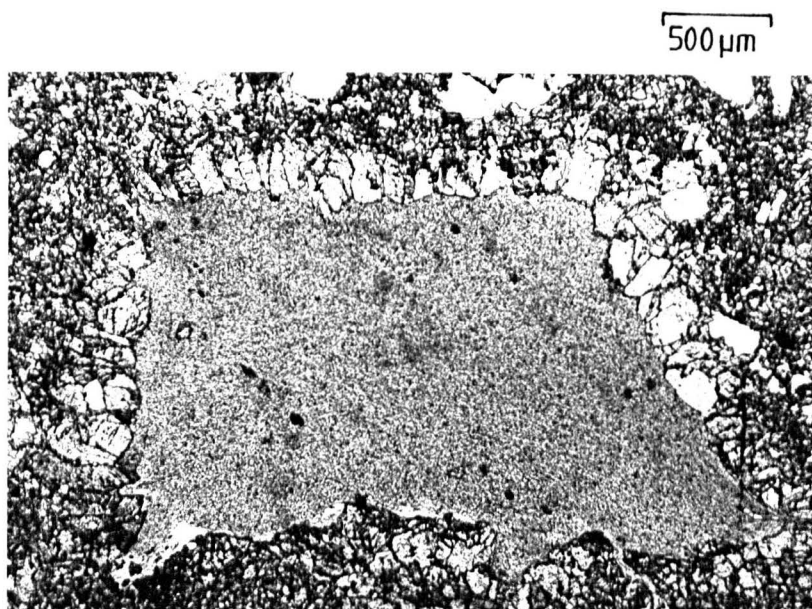


Figure 6-13: Photomicrograph, plane polarized light. Mudstone pebble partly replaced by dolomite around its margins. No dark rim occurs around the dolomite, which is thought to be type 3.

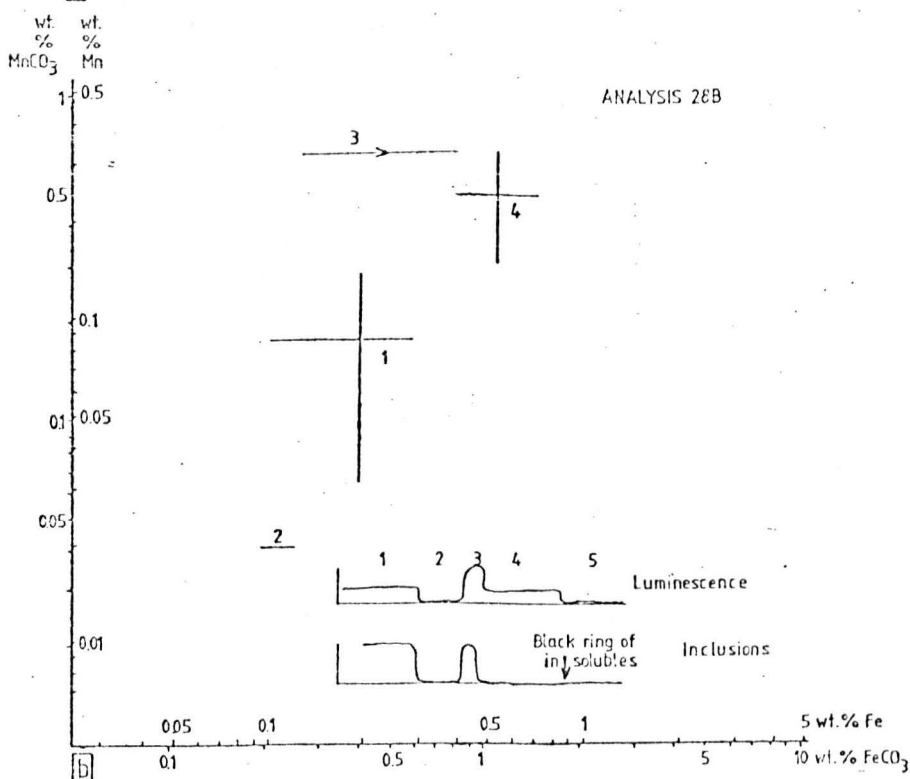
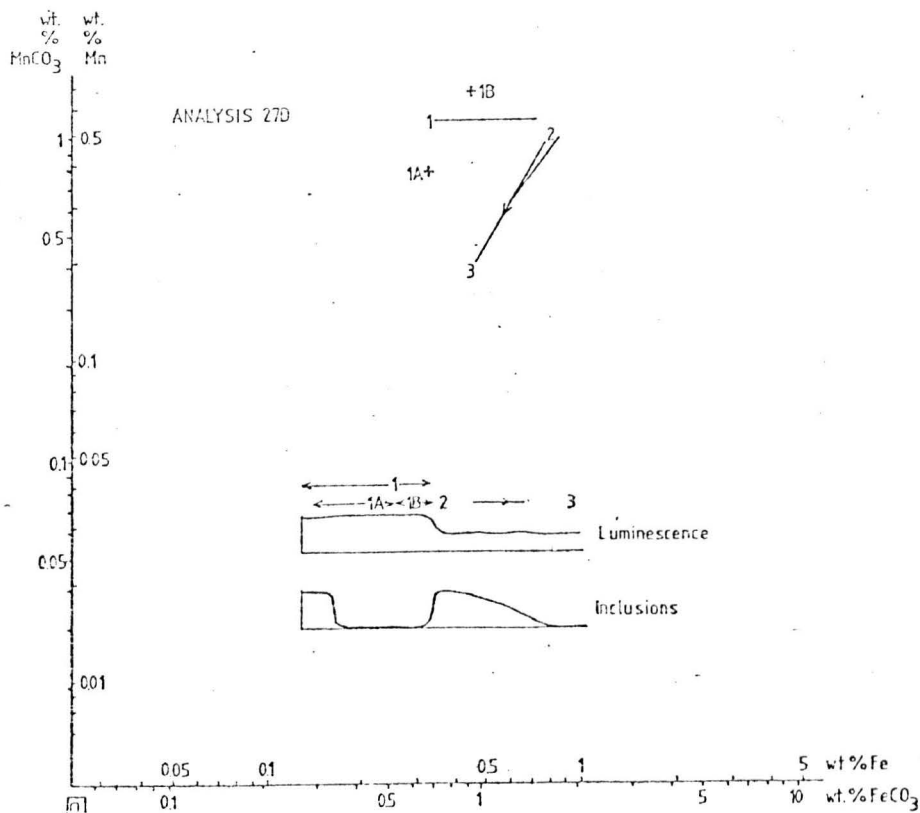


Figure 6-14: Characteristics of zoned dolomite replacing mudstone; a) analysis 27D; b) analysis 28B, scan lines shown on figure 6-12. The graphs of luminescence and inclusions run from the earliest growth zones on the left to the latest zones on the right. A high position on these graphs refers to either bright luminescence or the presence of many inclusions. Growth zones are numbered as shown (see also Table 6-1). The chemical analysis of each zone is shown by a cross where the zone is of fixed composition, a horizontal or vertical line where the composition of one of the elements plotted is variable, a sloping line where both of the elements vary in a correlated way and a large cross where both elements vary without correlating with one another. Where a composition changes smoothly from one zone to the next, an arrow indicating the trend is drawn on the line.

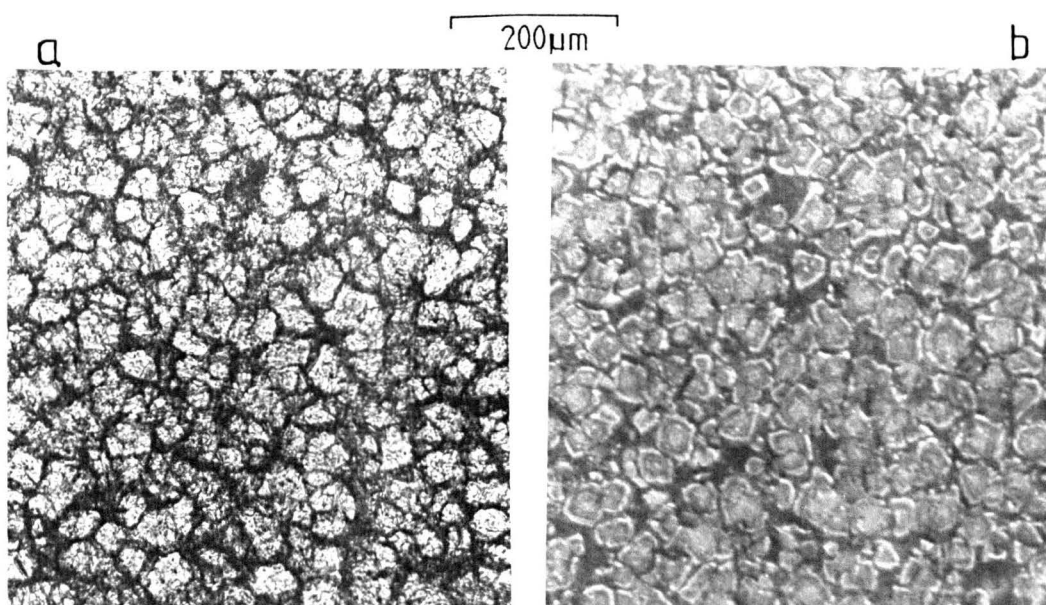


Figure 6-15: Equant polygonal dolomite replacing mudstone, slide 2. a) transmitted light; b) luminescent light. Concentration of insolubles along the (dark) grain boundaries is visible in a). Internal rhombic zones visible in b).

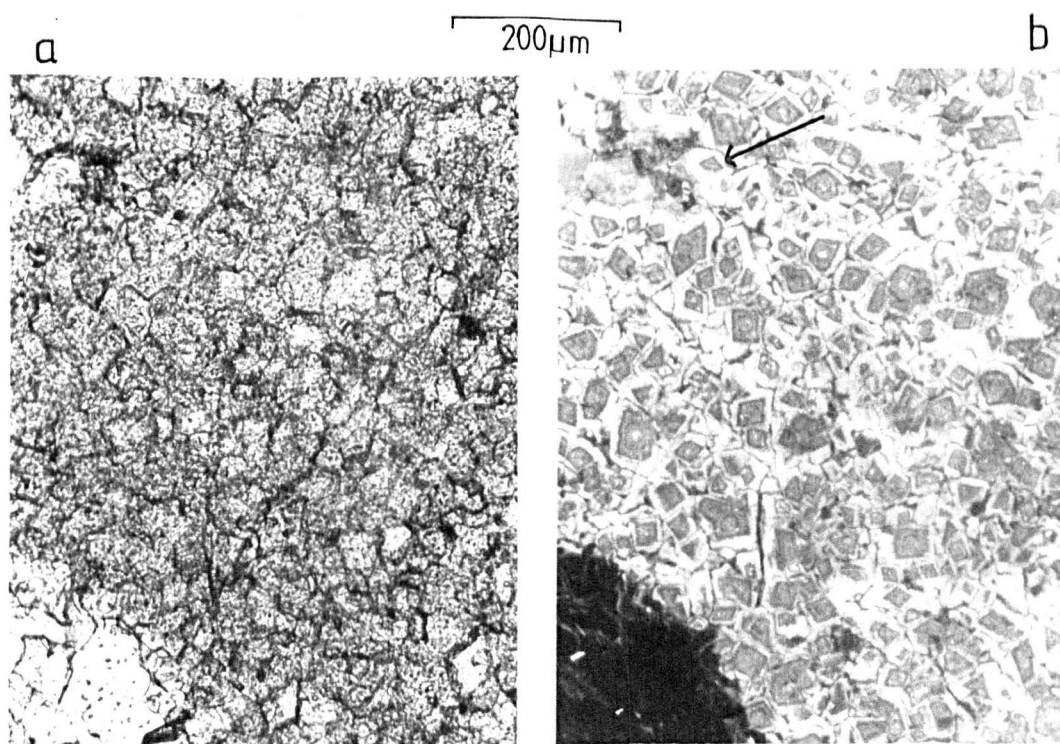


Figure 6-16: Equant polygonal dolomite replacing dolomicrite, slide 27. a) transmitted light; b) luminescent light.

Edge of replaced pebble is lower left. Extensive linking of the rhombic zones is visible in b) with one area (arrowed) containing only very late zones.

complete replacement by dolomite except along one margin which appears identical to presumed desiccated margins in nearby unreplaced mudstone pebbles (fig. 6-9d). Perhaps these margins were not replaced because they were slightly more compact, that is less permeable. However there seems no obvious reason why unreplaced, partly replaced and completely replaced pebbles occur in the same thin section.

Equant, polygonal dolomite similarly partly or completely replaces dolomicrite pebbles (fig. 6-9a, b; fig. 6-10; fig. 6-16). The grain boundaries are clean as there is no insoluble matter. In some cases there is a definite inclusion-rich (rhombic) core, with an inclusion-free rim.

Under luminescence, all examples of equant dolomite show rhomb-shaped zones. In figure 6-15b the nucleation sites seem to have been fairly regularly distributed because many crystals do not meet until a fairly late stage. Crystals were euhedral until they met when compromise boundaries were formed. Zones link from one crystal to another showing that each zone was grown everywhere at the same time. Other equant mosaics with less regular nucleation, show more extensive linking of later zones (fig. 6-16).

Probe analyses of equant dolomite are shown in figure 6-17. All the scans show a lower level composition with little Fe and Mn together with a number of Mn or Fe-Mn peaks a few microns across, which may be similar in composition to the type 1 dolomite. The general Fe-Mn-poor composition can be compared with the inner zones of the rhombs of analysis 28B. Thus one can generalize and say that growth started under conditions where relatively little Fe and Mn could be incorporated into the crystal (except for very brief periods = Fe-Mn peaks). Growth of equant dolomite was completed during this stage, but

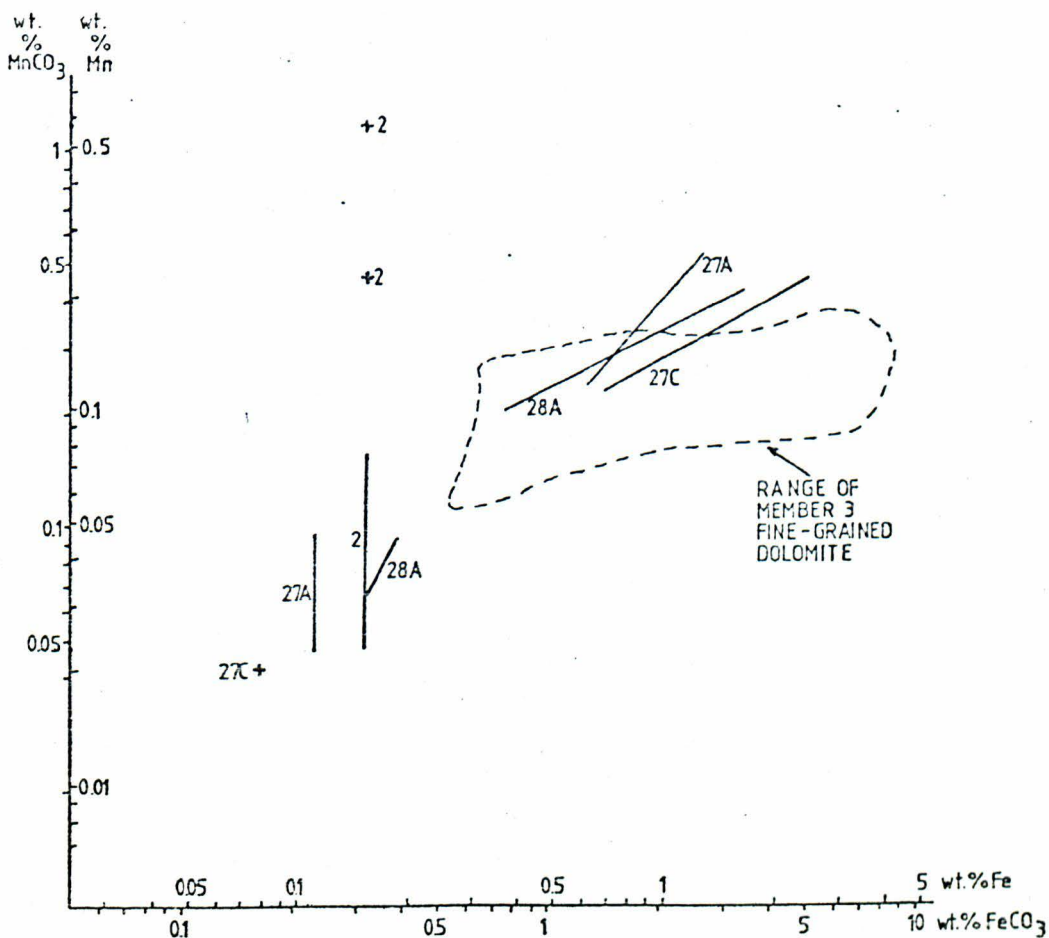
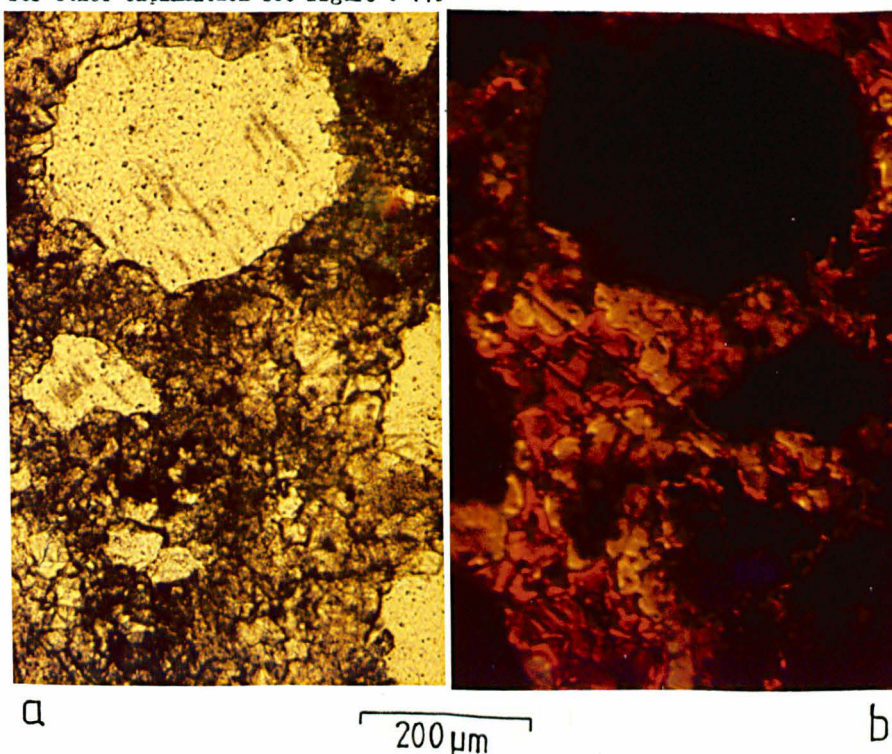


Figure 6-17: Mn and Fe analyses of type 1 (fine-grained) and equant type 2 dolomite from member 1. 27A and 28A are patchy type 1 and type 2 dolomite. The others are type 2 dolomite replacing dolomicrite (27C) or mudstone (2). For other explanation see figure 6-14.



The photographs are mirror-images

Figure 6-18: Medium-grained intergranular dolomite (slide-27); a) transmitted light; b) luminescent light. Initial zones are inclusion-rich, later zones are inclusion-free and define small areas resembling cavity fillings. Remnant dolomicrite shows the intergranular dolomite to be replacive however.

in other cases where there was low nucleation density growth continued into a time when more Fe and Mn could be incorporated (outer zones of analysis 28B, fig. 6-14b) and sometimes growth did not even start until this second stage had been reached (analysis 27D, fig. 6-14a).

### 6.5.2.3. Intergranular dolomite

Type 2 intergranular dolomite is abundant in sandstones; it also occurs in sandy dolostone boulders, apparently replacing dolomicrite (type 1). In places this dolomite occupies larger interstitial areas, resembling vugs, growing into them from the margins.

There are two major points of interest. Firstly, there is the question of whether all this dolomite is replacive like the dolomite described in the last section, or whether some is cavity-filling. Secondly, remarkable truncation textures occur, which demand an explanation.

The intergranular dolomites can be conveniently split up for description into medium-grained types (15-50 $\mu$ m, fig. 6-9g) and coarse-grained types (50-300 $\mu$ m, fig. 6-9f,h).

The medium-grained intergranular dolomite is mostly uniformly inclusion-rich, but some patches of inclusion-free dolomite also occur. The diffuse boundary between inclusion-rich and inclusion-free parts of crystals links from one crystal to another, that is growth was on a continuous front. This feature, with initial growth adjacent to detritus, is what one would expect from a cement. This is seen more clearly under luminescence (figure 6-18), where a zoned sequence from dull orange-red, to yellow, to a brighter red, is seen. However this is a very similar sequence to that seen in equant dolomite replacing dolomicrite in the same slide and indeed a replacive origin for

the medium-grained intergranular dolomite seems appropriate because remnant patches of type 1 dolomicrite occur within it. The intergranular dolomite (analysis 27E, Appendix A) shows a similar sort of chemistry to the equant dolomite as there is a dominant low Fe/Mn level with occasional peaks (representing zones a few microns across), rich in Fe and/or Mn, although the similarity is perhaps clearest under luminescence.

The coarse-grained intergranular dolomite shows a more extensive zonal sequence. That of slide 29, a dolomitic sandstone, shows the same luminescence stratigraphy throughout the two thin sections examined (figs. 6-19, 20, 21). Growth zones link between crystals as was seen in the other petrographic forms. Early zones tend to be low in Fe and Mn and later zones higher in these elements (as was seen in the dolomite replacing mudstone, fig. 6-14), but there is considerable fluctuation and not always a correlation between high Fe and high Mn values.

In slide 28, crystals of coarse intergranular dolomite often form a growth front or fringe. This may be centrifugal in form, growing outwards away from the margins of some pebbles, or centripetal, when it fills areas which resemble vug-fills (pseudo-vugs, fig. 6-22). These are larger, and have a more extensive zonal sequence than the areas of clear dolomite within the medium-grained intergranular dolomite (fig. 6-18). The zonal pattern is the same within pseudo-vugs as in the smaller interstices between sand grains. Analyses of a series of zones in the large pseudo-vug of figures 6-22, 6-24 and 6-25 are shown in figure 6-23. The very early zones of nearby intergranular dolomite are not shown on these traverses, but even so an overall change from Fe-Mn-poor early zones to Fe-Mn-rich later zones is

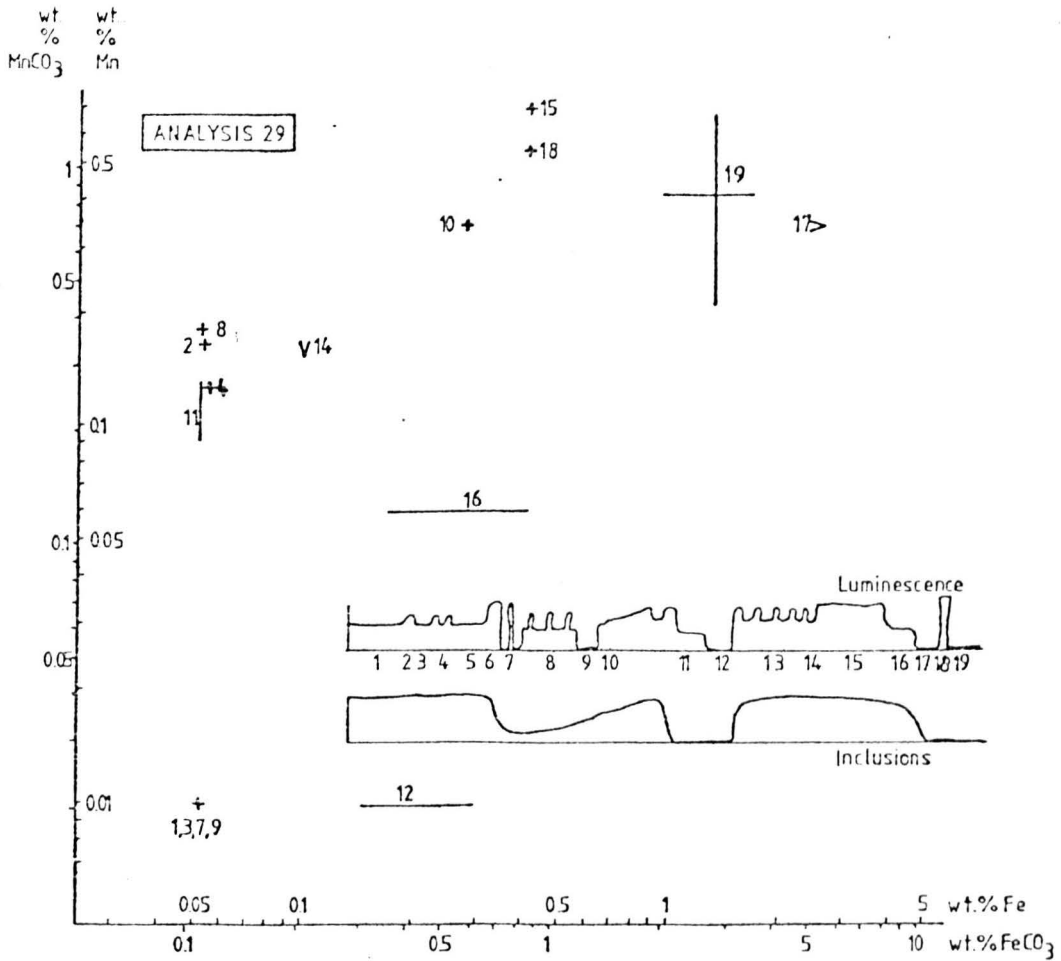


Figure 6-19: Characteristics of coarse-grained intergranular dolomite (type 2) in slide 29, member 1. Explanation as in figure 6-14. The symbol v or > indicates that the zone was too narrow to make an accurate analysis, but that the true analysis lies in the direction of the point of the arrowhead symbol.



Figure 6-20: Photomicrograph of coarse-grained intergranular dolomite (slide 29) under luminescence. Compare with figures 6-19 and 6-21. Arrowed crystal is discussed in section 6.5.4.

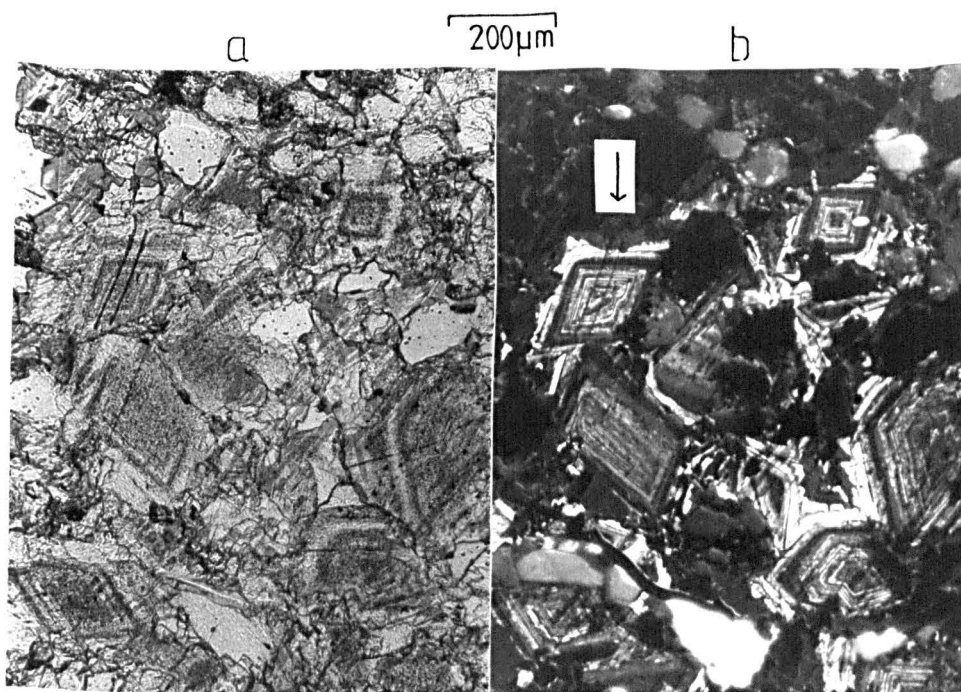


Figure 6-21: Photomicrographs of coarse-grained intergranular dolomite (slide 29) under a) transmitted light and b) luminescent light. Arrowed crystal shows scan lines and truncation of earlier zones by the latest, dull luminescing zone.

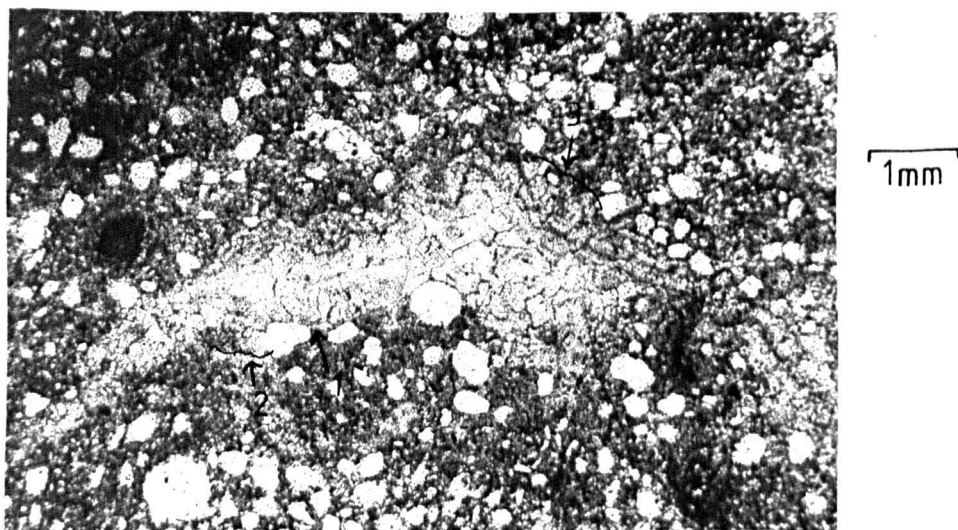


Figure 6-22: Photomicrograph in plane polarized light of dolomite-filled pseudo-vug set in sandstone (slide 28). All intergranular material is coarse-grained intergranular (type 2) dolomite. Arrows indicate locations of subsequent figures: 1. fig. 6-24; 2. fig. 6-25; 3. fig. 6-26.

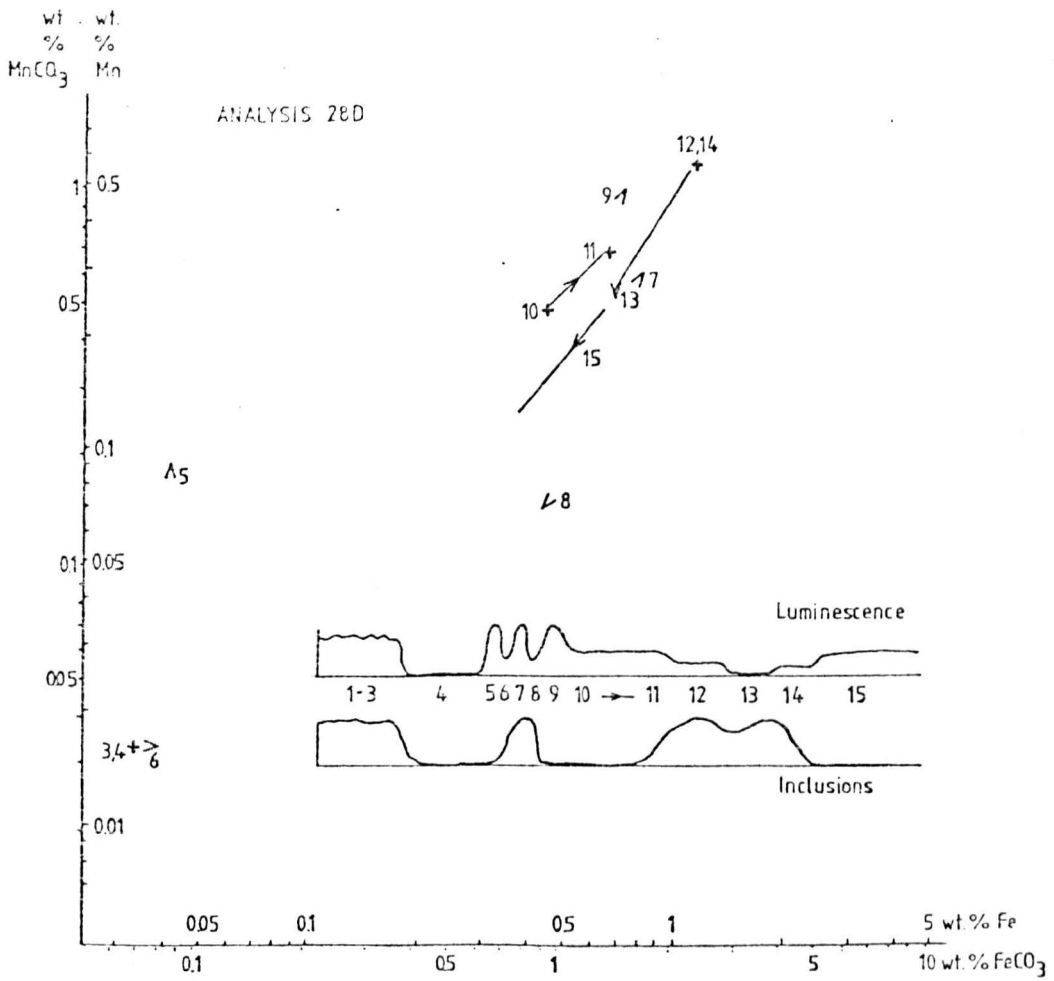


Figure 6-23: Characteristics of pseudo-vug-filling type 2 dolomite (analysis 28D)- see also figures 6-22, 24 and 25. Explanation as on figures 6-14 and 19.

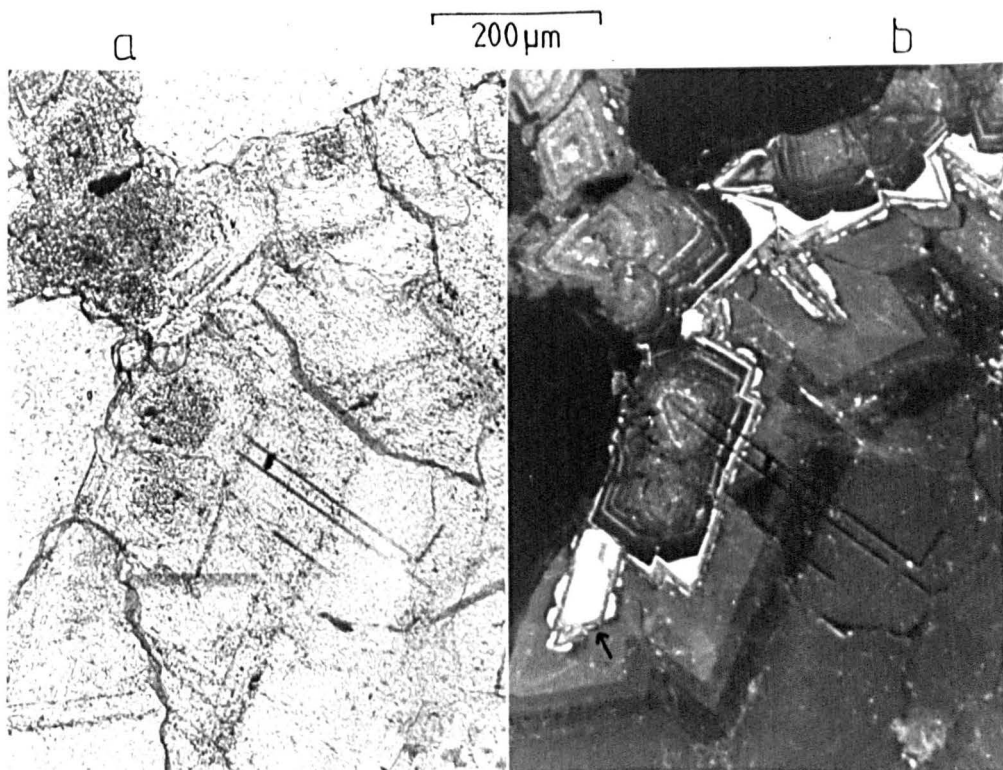


Figure 6-24: Photomicrograph of the edge of the pseudo-vug of figure 6-22, showing zonal sequence; a) transmitted light, b) luminescent light. Microprobe traverse lines (analysis 28D, figure 6-23) run NW-SE in the centre of the photographs. The arrowed area shows truncation of early zones by a later, fully luminescing zone (no. 10 of figure 6-23).

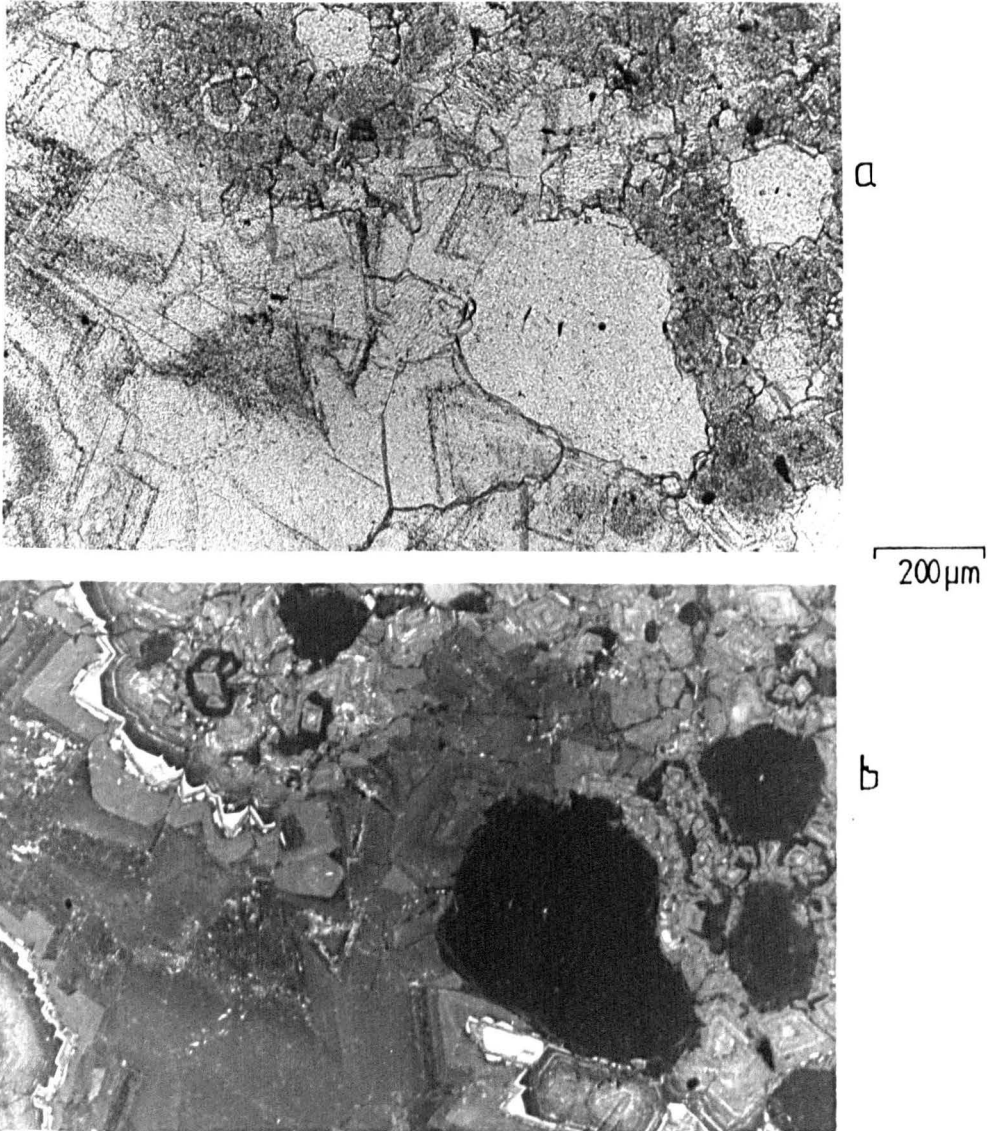


Figure 6-25: Photomicrographs in a) transmitted light and b) luminescent light of part of the pseudo-vug of figure 6-22 whose chemistry is shown in figure 6-23. The prominent brightly luminescing zone is cut out just left of centre by later zones and is absent throughout the central region to the left and above the large, non-luminescing quartz clast.

apparent, albeit with considerable fluctuations between zones. This is the same story as the intergranular dolomite of slide 29 (fig. 6-19), although the zonal sequence is different in detail.

It has been deduced above that not only the pebble replacements, but also the medium-grained intergranular dolomite, are replacive in origin, but what of the coarse-grained intergranular dolomite? One can say immediately that the bulk of this material must be replacive because:

1. Point counting of a dolomitic sandstone shows that dolomite makes up 70% of the rock, much more than original pore space could have been.

2. The points of origin of the crystals are always between sand grains rather than adjacent to them as they would have been if growth was as a cement away from detritus.

3. The dolomite frets detrital grains to some extent.

4. The crystal boundaries are rather irregular, although they do tend towards simpler boundaries (a series of straight and curved segments, rather than a continuously irregular boundary) towards the centre of pseudo-vug-fills. Cements have simple, ideally plane boundaries (Bathurst, 1971). The boundaries cannot have been altered after growth because the original growth zones persist to the grain boundaries.

What then was the dolomite replacing? In the case of the small pseudo-vugs in the medium-grained intergranular dolomite, the local presence of remnant dolomicrite implies that sand-sized grains of micritic carbonate were replaced. In the coarse-grained intergranular dolomite too there is a little dolomicrite, although it is difficult to distinguish it from inclusion-rich type 2 dolomite. It could be argued

that the coarse-grained intergranular dolomite was replacing combinations of squashed sand-sized clasts, infiltrated matrix, or an early cement. In the case of the pseudo-vugs, their shape suggests that they are replacements of intraformational flat pebbles of unknown lithology. They cannot have been primary voids, because they are over an order of magnitude larger than the sand grain-supported interstices (fig. 6-22); reasons 2 and 4 (above) also apply. The weight of evidence thus shows that growth was initially replacive, but it is not possible to prove that no voids developed at any stage. Further evidence is available however in the form of truncation textures, which are now described.

In slide 29 (fig. 6-21b) the latest zone (no.19, fig. 6-19) clearly truncates the earlier zones along a very irregular line, back as far as zone 13 in the arrowed area. Both zone 19 and the earlier zones form part of one crystal. Also in slide 28, within the pseudo-vug, a weakly luminescing zone (no. 10 of fig. 6-23) truncates the earlier zones, for example where arrowed in figure 6-24, yet is in optical continuity with them. A more extreme example is shown in figure 6-25 where just left of centre the bright zone (no. 9) and earlier zones are cut across by later zones. The bright zones are absent throughout the elongate upward-pointing area to the left of the large quartz clast. Similar truncations are present in pseudo-vugs from a sample from an inland locality, several kilometres from the locality (Section B) where the rest of the samples luminesced were collected.

These textures could be interpreted in two ways:

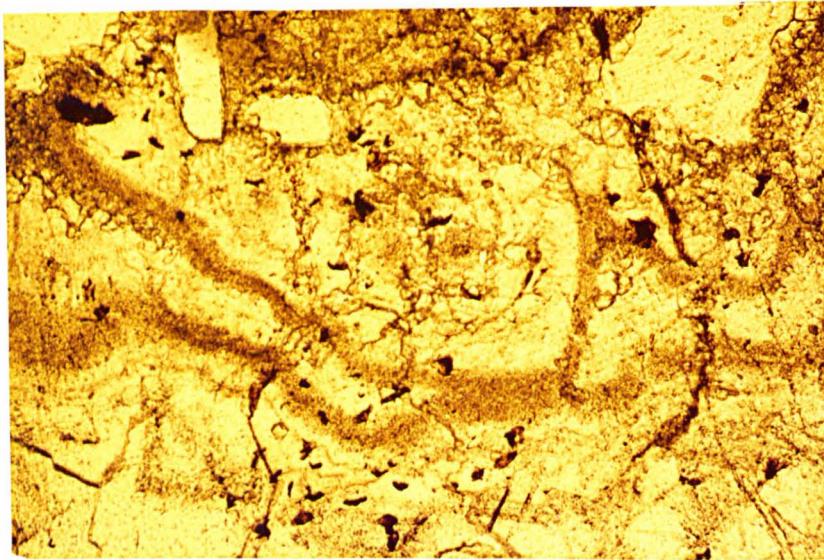
1. Isocrystalline replacement hypothesis. The zone following the line of truncation simultaneously replaces and overgrows early-formed parts of the crystal. The process is called 'isocrystalline replacement' because the original grain boundaries, although not the chemistry of the zoned crystals, are preserved.

2. Solution hypothesis. Following growth of the earlier zones there was an episode of dissolution which corroded the zoned crystals, having dissolved away all the intergranular material that the early zones had not yet replaced. Later, growth resumed, resulting in overgrowth of later, on earlier, zones.

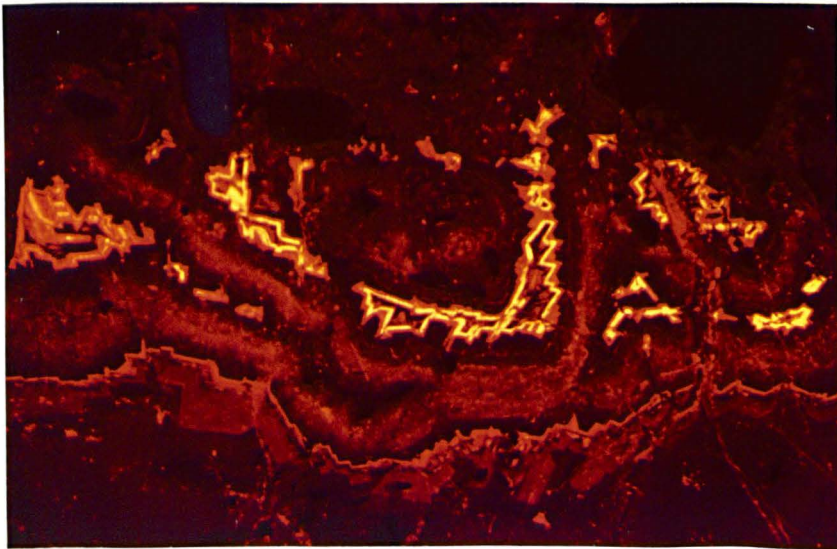
Bearing both these hypotheses in mind, a comparable, but even more intriguing texture is now described.

The texture is displayed along the top of the pseudo-vug of figure 6-22, and elsewhere in the same sample. Photographs of a representative area are shown in figure 6-26 in plane light (a), luminescent light (b), and under crossed polars (c), with an explanatory line diagram (d). The margins of the pseudo-vug run E-W near the top of each illustration. The extraordinary nature of this structure is that, when viewed under luminescence, growth zones of several of the crystals can be seen to indicate growth in several senses of direction, with two different zonal sequences. One zonal sequence contains a bright red zone and is the same as that of figures 6-23, 24 and 25, being the normal sequence around the pseudo-vug and nearby coarse intergranular dolomite. The other zonal sequence has a bright yellow-orange doublet zone (not analysed) and forms small inwardly-growing areas, sometimes within a single crystal. Similar small centripetally-growing areas are seen elsewhere in the sample.

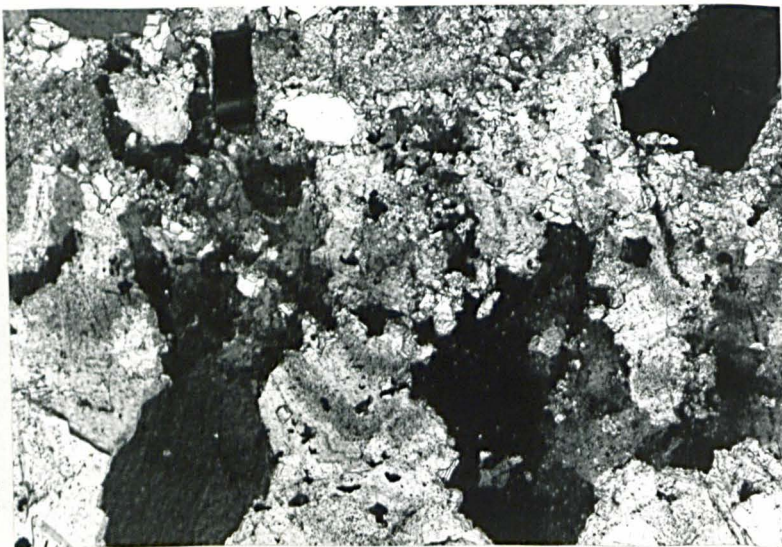




a



b



c

200µm

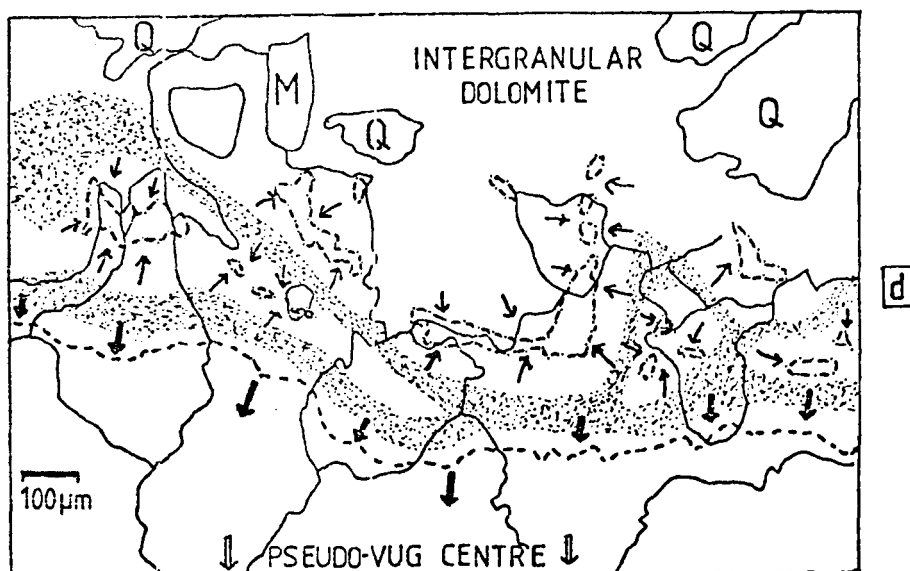
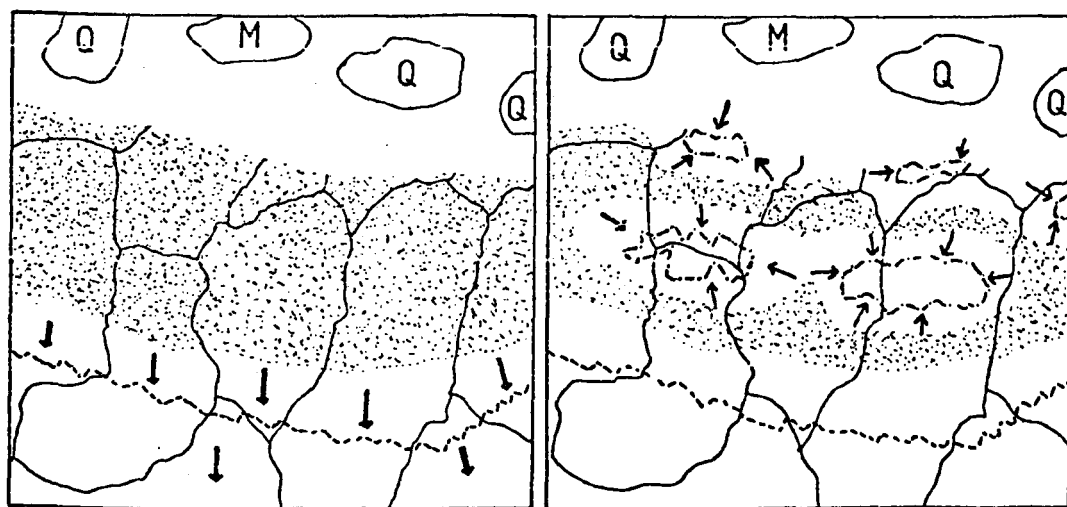


Figure 6-26: Margin of the pseudo-vug of figure 6-22 showing unusual textures which can be interpreted by an isocrystalline replacement hypothesis (see figure 6-27 and text) or by a solution hypothesis (see text). a) plane light ; b) luminescent light; c) crossed polars; d) line diagram, symbols as for figure 6-27.



Y GRAIN BOUNDARIES (NOT SHOWN WITHIN INTERGRANULAR DOLOMITE AT TOP)

Q QUARTZ CLAST

← DIRECTION OF FIRST PHASE OF GROWTH WITH MARKER BRIGHT ZONE

● INCLUSION-RICH DOLOMITE

M MICROCLINE CLAST

← SECOND PHASE GROWTH DIRECTIONS AND MARKER ZONE

Figure 6-27: Interpretation of the textures illustrated in figure 6-26 on an isocrystalline replacement hypothesis. a) Growth of large replacive crystals from the margins towards the centre of the pseudo-vug occurs. The zonal sequence is as seen at a number of places around the pseudo-vug (figures 6-23, 24, 25). b) Later there is a new phase of growth producing a zonal sequence with a bright doublet (yellow-orange) zone. This takes place without the formation of new crystals: the existing crystals are made over on centripetal growth fronts.

Interpretation of this texture in terms of the isocrystalline replacement hypothesis (fig. 6-27) would be as follows:

1. Growth took place into the pseudo-vug by dolomite crystals with the standard zonal sequence (as analysed). Crystals were initially mostly inclusion-rich, later mostly inclusion-free.
2. Many of the crystals were subsequently made over into a new chemically zoned sequence by an inwardly-growing closed growth front. This stage must have happened after growth of the standard zonal sequence because both sides of the centripetal growth front may be within single crystals. As the start of growth in this stage was at many different points, the only way for the end-product to be one optically continuous crystal would be if the crystal was there in the first place, that is before stage 2.

On the solution hypothesis the series of events would be similar to that of figure 6-27 except that following the first stage, solution of dolomite would have occurred leaving a series of thin platelets of dolomite which would be overgrown in the second stage.

Neither hypothesis can be proven because it cannot be seen precisely where the second phase growth started, only the bright zones of the second phase being clearly visible.

The weakness of the isocrystalline replacement hypothesis is that it is difficult to see what the driving force could have been, although it does fit in with the general replacive milieu of the dolomite.

In some ways the solution hypothesis seems most attractive for the small centripetally-growing areas which, as far as it can be discerned, represent growth from fairly smooth surfaces consistent with being the walls of solution

cavities (e.g. as described by Graf & Lamar, 1950). In contrast, under the solution hypothesis, very irregular solution surfaces, with no hint of exploitation of cleavages, would be required for the straightforward truncation textures of figures 6-21, 6-24 and 6-25 and this seems less likely. Scherer (1977) did illustrate very irregular solution textures of dolomite crystals, but attributed this to high Eh conditions under which Fe in the lattice was oxidized which created local weaknesses and hence non-uniform solution. There is no evidence of such oxidizing conditions in the example now being considered. Irregular replacement of for example quartz by dolomite is in contrast quite a common diagenetic feature.

In conclusion, the medium-grained intergranular dolomite is entirely replacive as are the earlier zones of the coarse-grained type. Later zones, particularly in the interior of pseudo-vugs, follow an irregular truncation surface and could be related to overgrowth on a free corroded surface or to isocrystalline replacement. Likewise, small centripetally-growing areas with a distinctive yellow-orange doublet zone could represent isocrystalline replacement or solution of areas of inclusion-rich dolomite leaving a delicate template which was overgrown.

### 6.5.3: Type 3 dolomite

Sandstones in units 3, 4 and 5 of member 1 commonly contain intergranular dolomite, anhedral or rarely subhedral, which lacks inclusions. The crystal size of this type 3 dolomite is generally 20-50µm, although poikilotopes up to 300µm occur. This dolomite is inversely proportional in abundance to the number of mud clasts, although it is not clear whether this is because it has replaced mud or whether it formed preferentially where mud clasts were

absent. It corrodes detritus (fig. 6-28) as can be seen by the fretted grain margins, but crystal faces are not developed in contrast to the intergranular dolomite of member 3 (7.2.4).

Analysis of type 3 dolomite in slide 27 is shown in figure 6-29. A couple of rhombic zones occur in places with an enrichment in Fe in the later growth. Staining shows that type 3 dolomite is always ferroan, bearing out the limited probe work. Zone 19 of slide 29 (figs. 6-19) is chemically (fig. 6-29) and petrographically very similar to the type 3 dolomite just described and may be of the same age. Also zones 10 onwards of the pseudo-vug of slide 28 (fig. 6-23) have similar chemistry and age relations to zone 19 of slide 29, although the former do contain some inclusion-rich zones. A similar age was suggested for the outermost dolomite of figure 6-12 (6.2.2) and the dolomite around the mudstone pebble of figure 6-13. A general relationship of the clean intergranular dolomite being later than the zoned dolomite is established. This is tentatively extended to include clean dolomite in rocks in which no zoned dolomite occurs.

Fretting of quartz and replacements of mud indicate at least a partially replacive origin for type 3 dolomite, but it is difficult to disprove that there was a cementing element, particularly for the dolomite in the centre of the pseudo-vugs. Although marginal encroachment of mudstone pebbles by type 3 dolomite occurs (fig. 6-13), no intermediate cases were seen between this and the pseudo-vug-fills.

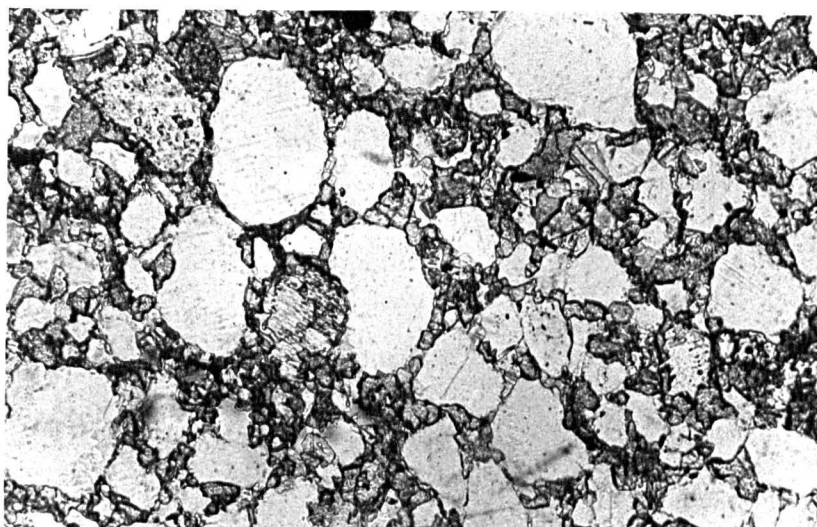


Figure 6-28: Photomicrograph, plane polarized light of clean intergranular dolomite (type 3) in sandstone, unit 5, member 1.

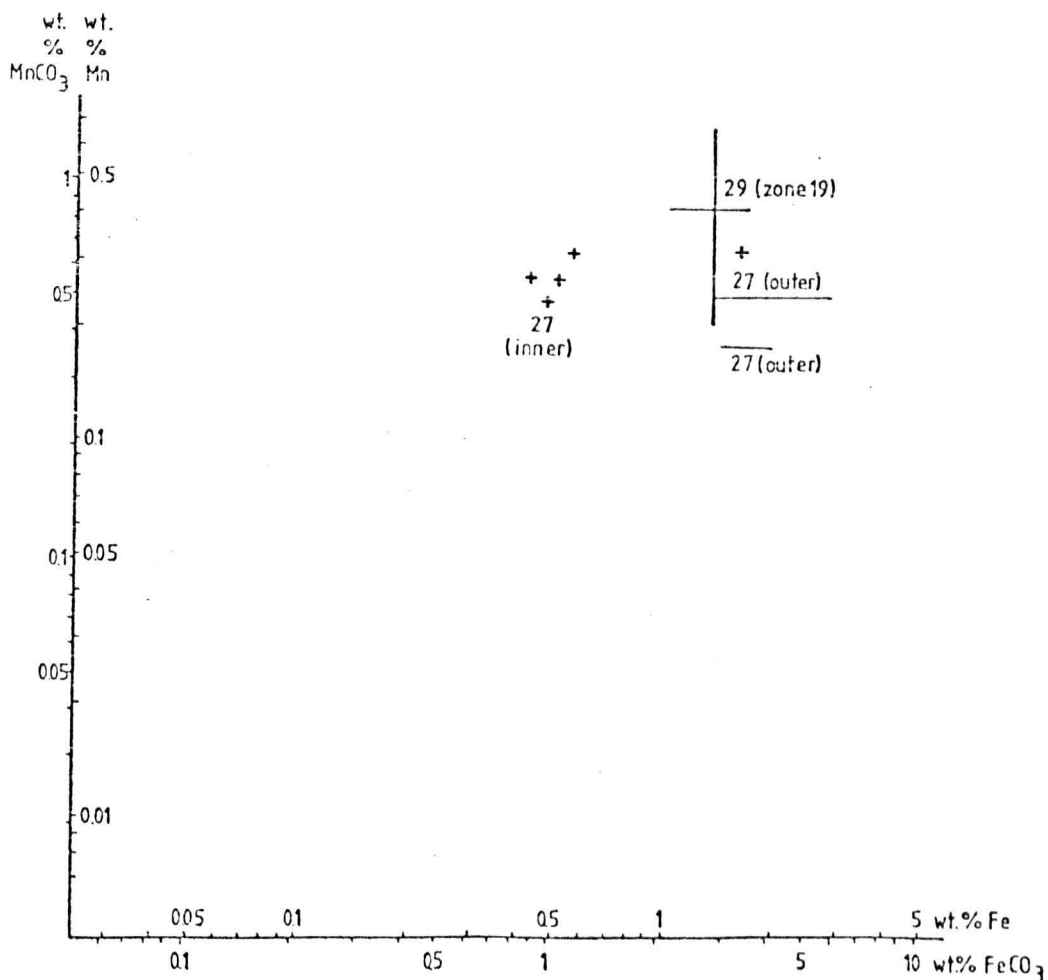


Figure 6-29: Mn and Fe content of type 3 dolomite, member 1. In slide 27 a simple two-fold zoning can occasionally be seen, the inner parts of crystals, or the whole of early-formed crystals being less ferroan than the later growth (outer parts of crystals or the whole of late-formed crystals). Zone 19 of slide 29, which truncates earlier zones (of type 2 dolomite) is petrographically and chemically very similar to type 3 dolomite in slide 27.

#### 6.5.4: Discussion

The remnants of the type 1 dolomite do not allow definite conclusions to be drawn as to its origin. However the fact that the member 1 mudstones contain no carbonate implies that, if formed penecontemporaneously, the dolomite only occurred locally (cf. member 3).

Type 2 dolomite is replacive and often coarse-grained, so presumably formed after some burial. The stratigraphic restriction of its occurrence implies lateral, rather than vertical, movement of dolomitizing fluids, and formation whilst the sediments still had some permeability.

Type 3 dolomite crystallization then followed after type 2 perhaps after a short break during which, under the solution hypothesis, some of the type 2 dolomite and other intergranular material were dissolved. The driving force for type 2 to replace type 1 dolomite could be release of grain boundary energy on increasing the crystal size. Under the isocrystalline replacement hypothesis type 3 partly replaced type 2; if so then perhaps inclusion-free dolomite was more stable than inclusion-rich dolomite.

The extremely complex zoning of much of the dolomite may be typical of cementation (Evamy, 1969; Meyers, 1974) and replacement (Katz, 1971) in the sub-surface and could be related to fluctuating availability of Fe/Mn at source, or fluctuating Eh (Meyers, 1974). Local factors, that is the nature of the material being replaced, do not seem to have affected the zoning as the same zones can be recognized whether the dolomite is intergranular, replacing dolomicrite or replacing mudstone, in any one sample. The between-sample variability probably reflects the isolation of dolomitization channelways between impermeable mud beds.

The replacement fabrics of type 2 dolomite show analogies with cementing fabrics in that there are constant zonal sequences within samples (Katz, 1971) and that growing crystals tend to have crystal faces until they meet others of their kind. However the zoned rhombs in mudstone (fig. 6-12) lose their crystal faces towards their perimeter without meeting any like crystals. In view of the analogies one wonders why it is that the coarser replacements described here should have more complex grain boundaries than cements usually do. Another intriguing point concerns the relative rate of growth of different crystals. Comparison of the arrowed crystals in figures 6-20 and 6-21 shows that the ratio of the thicknesses of the earlier zones to the dull doublet zone (nos. 11/12 of fig. 6-19) is much greater in the former than in the latter, yet the crystal form is the same throughout. Thus the relative rate of growth varied with time. Bathurst (1971) explained enfacial junctions in cements as being due to one crystal actually stopping growing and being engulfed by other crystals. This remains to be tested by detailed examination of zoned crystals. It will be interesting to learn how alike cements and replacement fabrics are in terms of continuity and speed of growth of different crystals.

Some of the examples illustrated of truncation/re-growth textures, whatever the correct interpretation of their origin, are of a type which, to my knowledge, have not been previously described.

## 6.6: Dolomite in the Precambrian

In Precambrian strata, dolostone is dominant over limestone, which is quite the reverse of the situation in younger strata (Ingerson, 1962). There is no generally accepted explanation for this observation. One relevant factor may be the importance of stromatolitic algae. Also, a high proportion of basic igneous material available for weathering may have led to a higher Mg/Ca ratio in the oceans in Precambrian times than at present (Ingerson, 1962). However, Holland (1972) assumed that the oceanic chemistry has not changed since middle Precambrian times. Sandberg (1975) turned the problem on its head by postulating that the Mg/Ca ratio may actually have been much lower before the Jurassic, because Mg could not have built up significantly in the oceans until limestones, rather than dolostones, became the dominant carbonate deposits.

In the Bonahaven Formation, it has been argued that there is supra-tidal dolomitization (member 4), dolomite formed as a penecontemporaneous replacement in waters of fluctuating salinity (member 3) and diagenetic dolomitization (member 1). Here at least there is no one simple cause of dolomitization. Examples of supra-tidal and diagenetic dolomitization are common in the Phanerozoic, so it seems as though the member 3 dolomite is the only form of dolomite in the Bonahaven Formation which may have a direct bearing on the origin of Precambrian dolomite in general.

In member 3 we have penecontemporaneous dolomite associated with stromatolites. The Mg-concentrating ability of algae and hence the likelihood of early dolomitization has been demonstrated by Gebelein & Hoffman (1973). Indeed stromatolites do seem to be generally important in Precambrian

dolostones (e.g. Gutstadt, 1968; Eriksson et al., 1975; Tucker, 1977).

None of the penecontemporaneous dolomite in the Bonahaven Formation has been shown to have formed in an open marine situation: it only occurs in specially restricted environments. Therefore no positive evidence is provided of a higher Mg/Ca ratio in the ocean at that time.

6.7: Palaeotemperatures

The superposition of the dolomitic Bonahaven Formation on the Port Askaig Tillite is but one of many similar dolomite-tillite associations in the Vendian (Roberts, 1976). Because of the usual association of dolomite with warm water this has led to much discussion (Spencer & Spencer, 1972; Schermerhorn, 1974; Williams, 1975). However I feel that too little is known about dolomite formation to set a lower temperature limit to its formation. Certainly it is a mistake to assume that the presence of stromatolites in Precambrian strata indicates warm water (Monty, 1973). In fact the least equivocal warm-water indicator in the Bonahaven Formation seems to be the member 3 oöids. However these occur sufficiently far (over 50m) above the last evidence of supposed glacial activity for a considerable change in temperature to have occurred in the meantime.

## CHAPTER 7: DIAGENESIS AND METAMORPHISM

A comprehensive discussion of the diagenetic and metamorphic textures observed is given in this chapter, excluding dolomitization (Chapter 6) and the specialized topic of stromatolite microstructure (4.3.4.2). A summary of the inferred time relations of these features is given in section 7.10.

### 7.1 Cementation

Cement filling primary porosity occurs in three forms, but is rather uncommon. Firstly there is calcite syntaxial on dolomite in some dolostones (7.1.1), secondly there are some overgrowths on detritus (7.1.2) and thirdly some of the intergranular calcite in sandstones may originally have been a cement (7.1.3). The paucity of cements can partly be explained by the pervasive early dolomitization which eliminated any metastable mineral phases which could have acted as a source of cement. Also diagenetic neomorphism and replacements, and metamorphism have probably obliterated some cementing textures. Cements infilling secondary porosity (post-tectonic vugs and veins) are treated in section 7.9.

#### 7.1.1: Calcite-plugged primary pores

This structure occurs in some oölitic dolostones, dolomitic flakestones and peloid grainstones, and stromatolites (including within breccia flakes). The fabric is distinctive in stained thin sections as the calcite (pink) occurs as discrete patches within near colourless dolomite. In flakestones and grainstones, in areas where the calcite is absent, the allochems are scarcely distinguishable from one another and apparently more closely packed than where the calcite is present, which is consistent with the calcite being an early

cement. The best evidence for this however is in a grainstone (bed 68E; fig. 7-1) where calcite appears to occupy 'shelter' and other intergranular pores. Calcite with identical texture (as described below) occurs in elongate discontinuous areas parallel to lamination in some stromatolites; thus these areas were taken to be fenestrae (4.3.4.2). In one slide, the calcite appears to fill leached allochems with dolomicrite rims, but no such rims are visible elsewhere.

The dolomite lining the former cavities is partly fine-grained ( $<10\mu\text{m}$ ) and partly subhedral ( $10-50\mu\text{m}$ , sometimes  $100\mu\text{m}$  in size) with crystal faces against the calcite. Probe analyses do not show up any chemical differences between the fine-grained and the subhedral dolomite. The crystal faces of the latter suggest that it is a cement, although it is not always possible to distinguish such dolomite from neomorphically enlarged dolomite.

Calcite forms grains  $50-400\mu\text{m}$  in size which completely fill the former cavities (fig. 7-2a). Calcite crystals are commonly seen to be in optical continuity with the subhedral dolomite lining the cavity: three such are seen in figure 7-2b; in three dimensions probably all the calcite is seeded onto dolomite. Sometimes a single crystal of calcite fills the whole of a small vug. Calcite-calcite grain boundaries are straight, curved or irregular: they may well have been adjusted secondarily. Subhedral quartz and albite grains sometimes occur within the calcite and are regarded as a later replacement.

This calcite can be distinguished texturally from later replacive calcite both because it occurs in discrete patches bounded in part by subhedral dolomite and because it lacks

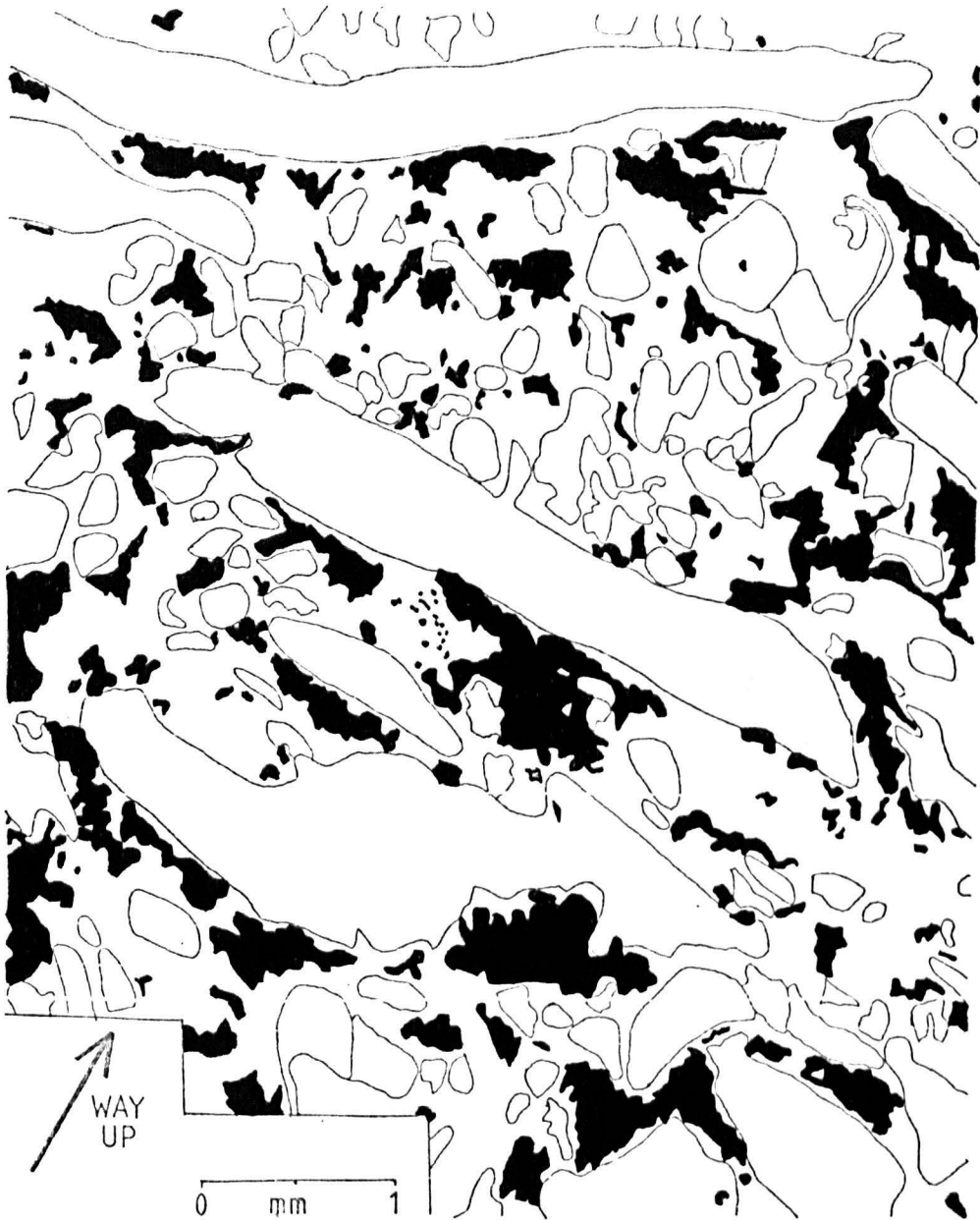


Figure 7-1: Line drawing of a thin section of a breccia of dolomierite flakes from bed 68E. Recognizable clasts are outlined. These are bounded successively by 5-50µm dolomite, most of which represents the initial stages of cavity filling, and by calcite (black). The calcite occurs preferentially under, rather than over long flakes, suggesting that it occupies 'shelter' porosity under the flakes.

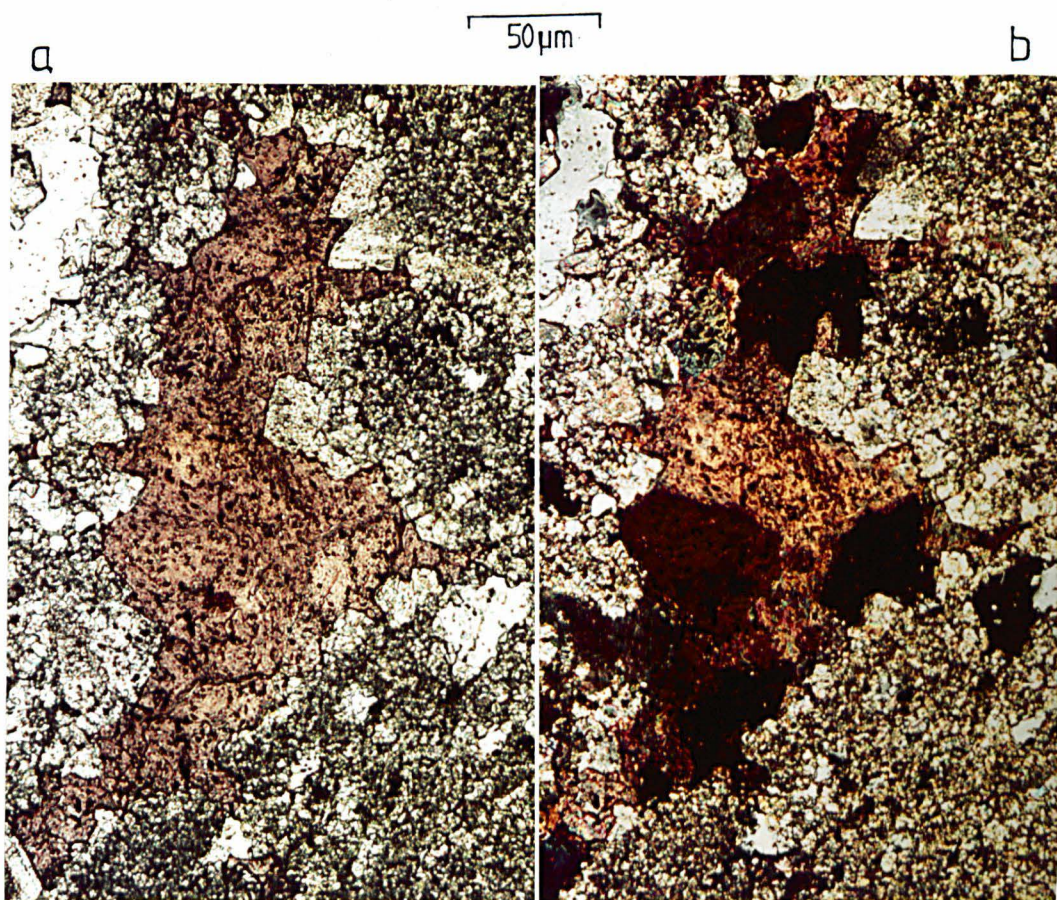


Figure 7-2: Photomicrographs from same thin section as figure 7-1. a) plane polarized light; calcite patch (pink) is partly bounded by subhedral dolomite: this represents a filled intergranular pore. b) crossed polars; several of the subhedral dolomite crystals can be seen to be in optical continuity with adjacent calcite even in this one position. Probably all calcite is syntaxial on dolomite when considered in three dimensions.

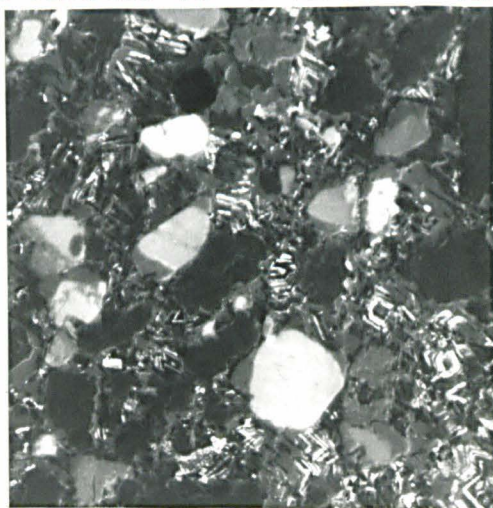


Figure 7-3: Photomicrograph under luminescence of dolomitic sandstone, unit 5, member 1. Quartz shows no luminescence whilst microcline exhibits uniform luminescence of clasts with dullly luminescing overgrowths. Intergranular type 2 dolomite (see Chapter 6) is present.

dolomite inclusions. There is sometimes a clear chemical difference shown by staining and confirmed by probe analysis (see figure 7-13 and compare analyses 7A and 7B, Appendix A). However probe analyses of four occurrences of void-fill calcite fail to show up any common characteristics which distinguish them as a group from other calcites (see 7.9), probably because of later alteration (?metamorphic diffusion). Also diagenetic calcitization commonly masks the distinctive character of this early calcite (7.2.2).

Syntaxial calcite on dolomite has been reported by Zenger (1973), Land (1973) and Borch & Trueman (1974), and related to changes in water chemistry (Mg/Ca ratios). In the Bonahaven Formation, the whole process seems to have been very early diagenetic because primary voids in apparently uncompact sediments are filled. It is possible that the cementation is of a similar age to the dolomitization process as was reported by Land (1973) and Borch & Trueman (1974), although their repeated calcite-dolomite alternations, which are the conclusive evidence, do not occur here. Relatively dilute solutions with Mg/Ca less than 1 (a value of 1/10 is obtained using analysis 7B and the partition co-efficient of figure 6-7) seem most appropriate for the precipitation of equant calcite, enrichment of Ca at the expense of Mg being achieved by dolomite precipitation.

#### 7.1.2: Overgrowths on detritus

Overgrowths on detrital quartz are visible optically in less than 5% of the sandstones examined. Cathodoluminescence gives no further help as no luminescence was detected from quartz detritus. When seen, the overgrowths are marked by a thin line of mica or 'dust' and are small in size compared with the original grain.

Only tourmaline of the accessory minerals shows

overgrowths, and then only occasionally.

Overgrowths on feldspar are visible in 5-10% of sandstones examined and also occur in stromatolites, notably BV. They never constitute more than 20% of feldspar in sandstones and are invariably free of inclusions. The host grains may be cloudy plagioclase with indistinct twinning or more usually clean microcline. The presence of K-feldspar overgrowths on microcline is shown by fourling twinning of the overgrowth (Baskin, 1956) compared with the cross-hatched twinning of the detrital grain and in some cases by the tendency for grains to be approximately rectangular in outline (Kastner, 1971). The overgrowths also luminesce much less brightly than the detrital cores (fig. 7-3). Luminescence study shows that no more overgrowths are present on feldspar than are visible under plane polarized light.

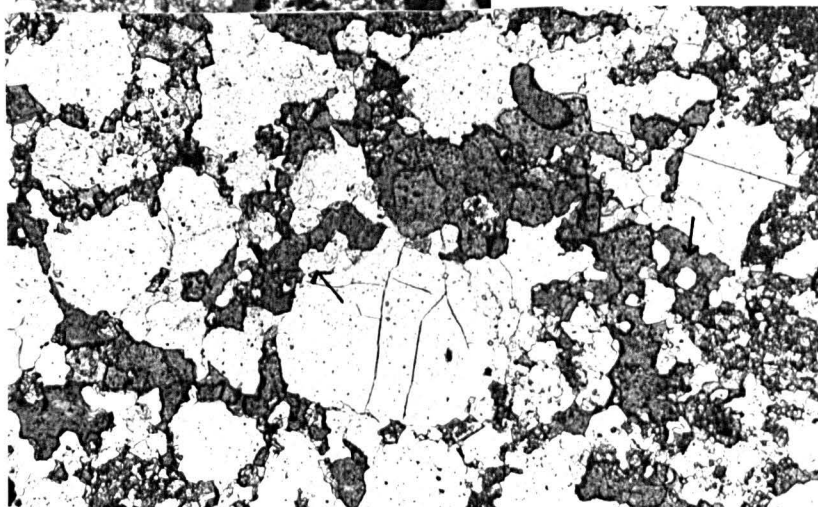
Authigenic K-feldspar is extremely abundant in Cambro-Ordovician strata of the NW margin of the Iapetus ocean. Its derivation has been suggested to be from dolomitized illitic limestones (Swett, 1968), tephra (Buyce & Friedman, 1975) or primary alkaline brines (Mazzullo, 1976). Whatever the mechanism was, in these slightly older rocks, it was not yet important.

Late diagenetic replacements by albite and occasionally quartz, may simulate overgrowths (fig. 7-4). In the figure a rounded core with inclusions, generally of mica, is surrounded by a clear rim. The well-developed albite twinning throughout the grain, and the absence in the core region of the very fine-grained alteration present in genuine plagioclase clasts, shows that it is a replacement. The rounded core was originally a sand-sized clast of mudstone or degraded feldspar.



Figure 7-4: Photomicrograph, crossed polars, bed 66D. Albite crystal, well-twinned throughout with core rich in mica inclusions. this rounded core was originally a mudstone clast or a weathered feldspar clast. The albite is not an overgrowth, but a replacement of the clast and surrounding area.

50 $\mu$ m



500 $\mu$ m

Figure 7-5: Photomicrograph, plane polarized light, bed 66D, a sandstone. Anhedrous intergranular calcite is present. Small polygonal quartz (e.g. arrowed) is metamorphic.



500 $\mu$ m

Figure 7-6: Photomicrograph, plane polarized light, sandy oolitic dolostone, bed 54D. Ooids show concentric structure by variation in grain size (dark = finer mosaics). Some ooids have quartz-replaced cores.

### 7.1.3: Intergranular calcite

Although most sandstones in member 3 contain intergranular dolomite, some are calcitic instead. In such cases the sand grains exhibit an incomplete intergranular border of calcite which makes up 5-20% of the rock and is 20-250 $\mu$ m in grain size (fig. 7-5). The crystals are anhedral, with common re-entrants against quartz. These slightly fretted boundaries between detritus and calcite could be interpreted as being due to some solution of detrital grains when calcite was being precipitated or due to later textural modification. There has also been the growth of small polygonal quartz grains near to grain boundaries of clasts during metamorphism, which obscures the relations. The chemistry of the intergranular calcite (analyses 11, 12, Appendix A) lies within the general field of calcite from the Bonahaven Formation (7.9). Their frequent, sharp Mg-Fe peaks are an unlikely feature for a cement. However, in some cases cross-laminae are defined by variation in the content of calcite which suggests a pre-lithification diagenetic origin, that is before all traces of original variation in grain packing had been destroyed.

It seems that at least some of the intergranular calcite was originally a cement, but has been later modified by grain fretting and growth of polygonal quartz.

### 7.2: Replacement and neomorphism

Diagenetic replacements by dolomite, calcite, quartz, albite and pyrite have occurred, but the rarity of cross-cutting relationships makes it difficult to work out the sequence of events or to distinguish between neomorphic and replacive dolomite.

The range of replacements is well illustrated by ooids

which are therefore described first, followed by examples of calcitization and silicification in other situations. Pyrite and albite are dealt with in section 7.4.

### 7.2.1: Oöids

#### 7.2.1.1: Dolomite

1) Many oöids are composed of a dolomite mosaic (with crystals less than  $10\mu\text{m}$  in size) which displays a pseudo-uniaxial cross under crossed polars (fig. 6-5). This is a replacement texture (6.3.1), but is believed to be the earliest oöid fabric now preserved. In many cases dolomitic oöids have been squashed between detrital quartz grains and it becomes difficult to recognize the origin of the dolomite as primary sand-sized grains.

2) Concentric structure in the oöids is commonly shown by diffuse alternations of finer ( $<10\mu\text{m}$ ) and coarser (mostly  $>10\mu\text{m}$ ) dolomite (fig. 7-6), both showing the pseudo-uniaxial cross.

More complete replacement by coarser dolomite takes one of the four following forms:

3) dolomite showing a very good extinction cross within which crystal boundaries cannot be discerned. Concentric and/or radial structure is marked by tiny dark inclusions (fig. 7-7).

4)  $40\text{--}70\mu\text{m}$  polygonal dolomite exhibiting a very indistinct extinction cross.

5) distinct rings of dolomite, internally divided into segments, each a single crystal.

6) a single large ( $100\text{--}250\mu\text{m}$ ) crystal of dolomite (fig. 7-11) which may show zoning by variation in the number of tiny fluid inclusions. Such dolomite is described further in section 7.2.4.

All the above, except 6 and some examples of 5, exhibit

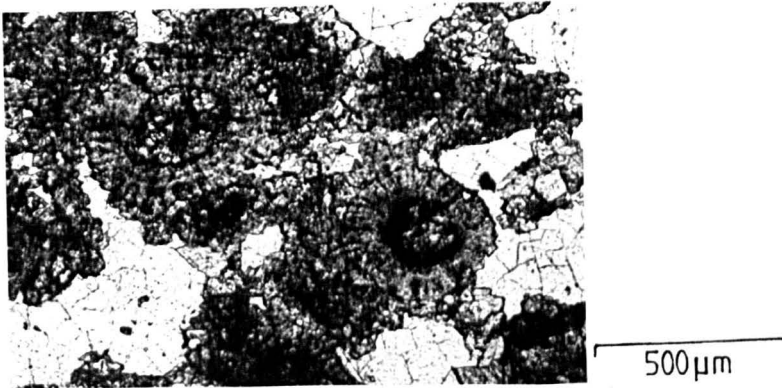


Figure 7-7: Photomicrograph, plane polarized light, sandy oölitic dolostone, bed 42E. Oöids showing radial and concentric structure by tiny dark inclusions.

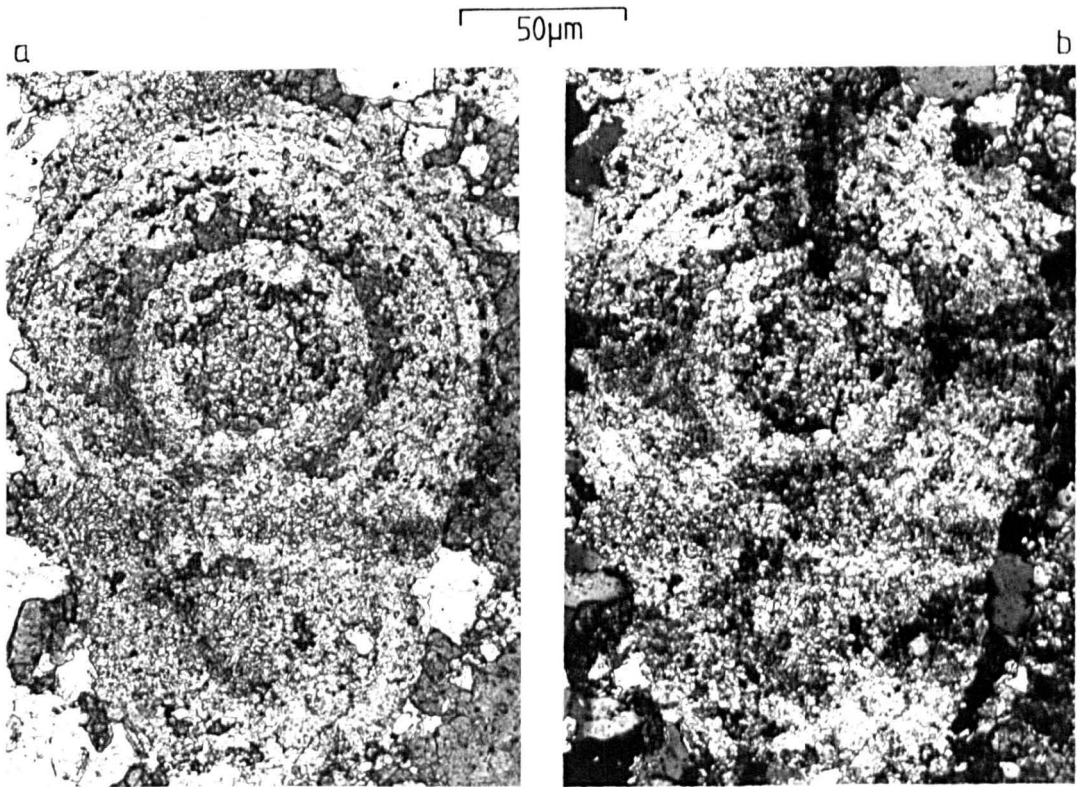


Figure 7-8: Photomicrographs, bed 27B. a) plane polarized light; dolomitic oöids with ring of calcite crystals (dark). b) crossed polars; a clear pseudo-uniaxial cross encompasses both calcite and dolomite.

a more or less well developed radial arrangement of c-axes. There is also no chemical distinction between the coarse and fine dolomite. This suggests that types 2,3,4, and examples of 5 showing the pseudo-uniaxial cross, can be regarded as neomorphic products of type 1. It is not clear why there is so much variability in these neomorphic textures; perhaps the grain size relates to the temperature at which neomorphism occurred.

#### 7.2.1.2: Calcite

About a quarter of the oöid-bearing samples showed partial replacement of oöids by 20-30 $\mu$ m calcite, either isolated, or as a complete ring of crystals (fig. 7-8) generally retaining the optical orientation of the dolomite. Calcite is considered to be later than the dolomicrite because it occurs patchily, is coarser, and shows no internal concentric structure. Occasionally a single anhedral crystal of 100 $\mu$ m calcite may partly replace an oöid.

More extensive calcite replacement occurs in beds 25B and 27B where whole oöids are calcitic with either a coarse radial structure (individual crystals <15 $\mu$ m wide) or occur as 50 $\mu$ m equant grains. Remnant rings, or a core of fine-grained dolomite may occur (fig. 7-9). The calcite may be cross-cut by quartz and albite. Oöid calcite is continuous with intergranular calcite and calcite veins which cut quartz detritus (fig. 7-10). In this case there was evidently an important episode of calcitization.

#### 7.2.1.3: Quartz and albite

Replacement of oöids by 15-30 $\mu$ m polygonal quartz with spokes of 2-5 $\mu$ m pyrite occurs in bed 27E. Also, in bed 27B, there is a little replacement by quartz, in places <10 $\mu$ m in crystal size (fig. 7-10). This resembles the microquartz of diagenetic silicification (Wilson, 1966). It is cut by

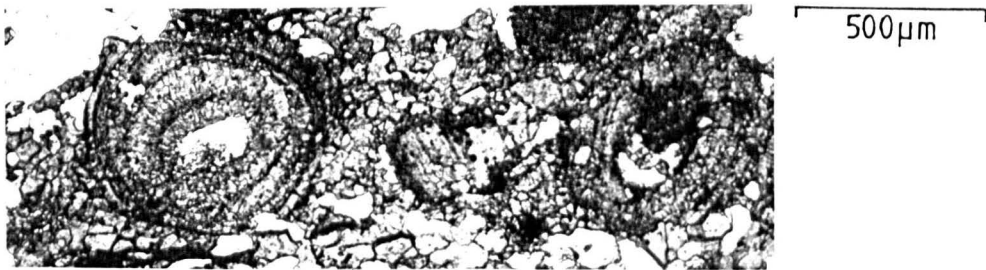


Figure 7-9: Photomicrograph, plane polarized light, bed 25B. Left-hand oöid is mostly of calcite with a radial texture and concentric rings of remnant dolomicrite. The core is partly replaced by subhedral albite. The central (small) oöid exhibits two large calcite crystals surrounded by a dolomicrite rim. The right-hand oöid shows a dolomicrite core surrounded by coarser calcite.

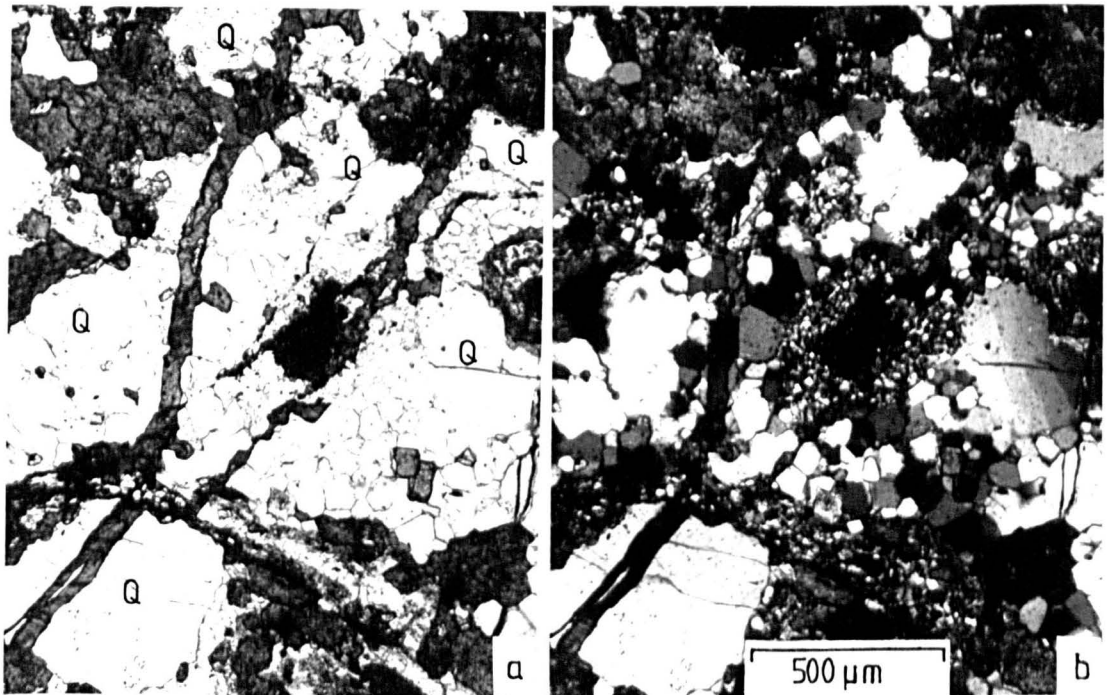


Figure 7-10: Photomicrographs, bed 27B. a) plane polarized light; b) crossed polars. The oöid in the centre has a micritic core surrounded by microquartz in turn surrounded by megaquartz. Q= quartz clasts. Parallel-sided calcite veins cut all the quartz.

calcite continuous with that replacing oöids and so is thought to pre-date calcitization.

In contrast, replacements by coarser quartz, with or without twinned albite, are thought to be more appropriately a result of deep burial (7.4). Commonly there are rings of 30-50 $\mu$ m quartz divided into segments (fig. 7-11), separated by films of calcite or dolomite. Alternatively, replacement may be by a single crystal, or a few crystals of quartz with anhedral inclusions of <10 $\mu$ m dolomite marking the concentric structure of the oöid (fig. 7-12). Intermediate cases are common. Accessory albite, showing well developed twinning is usually associated with this quartz.

#### 7.2.1.4: Pyrite

Pyrite, commonly partly oxidized to goethite, occurs occasionally in oöids as dispersed grains, usually cubes, less than 5 $\mu$ m in size. Pyrite crystals may define a concentric structure, or occur concentrated in the core of an oöid.

#### 7.2.2: Replacive calcite

Calcite mosaics occur in oöids, as have been described, and also in some stromatolite and patchily in other dolostones. Calcite forming metamorphically and post-tectonically is described in sections 7.7 and 7.8.

In stromatolite BIII calcite forms layers which are alternately 5-10 $\mu$ m and 30 $\mu$ m in size; here calcite may be the primary phase. Discrete dolomicrite laminae also occur here. In other stromatolites (BIV, BV, C9), calcitic laminae alternate with dolomitic laminae; the calcite laminae have a mosaic of 30-200 $\mu$ m crystals with included detritus (much altered) and contain no internal lamination save that delineated by dolomite inclusions (fig. 4-45).

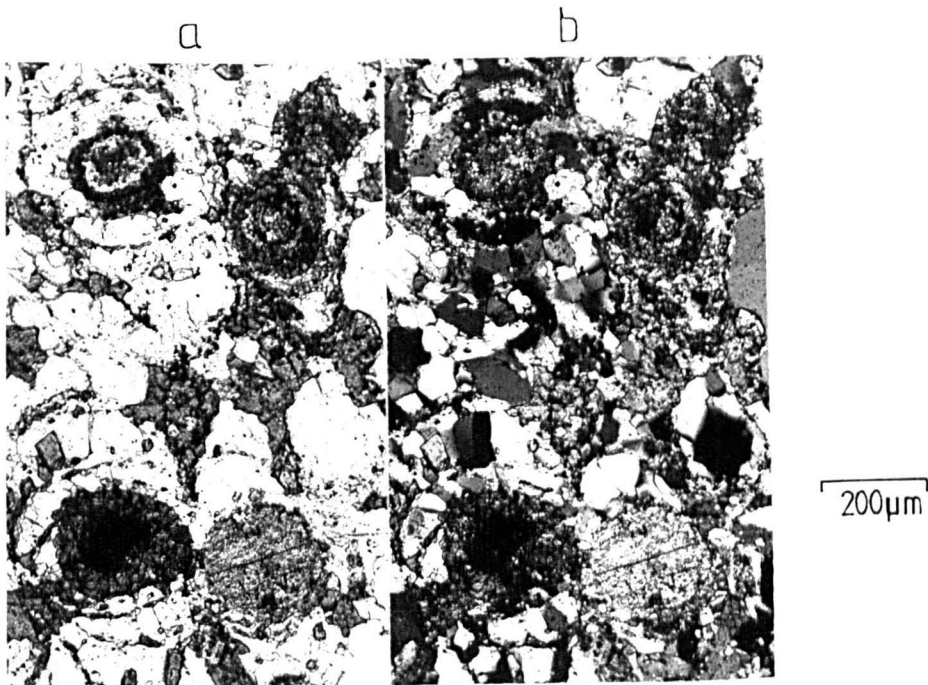


Figure 7-11: Photomicrographs, bed 25B. a) plane polarized light, b) crossed polars. Ooids left exhibit rings of polycrystalline quartz. Ooid lower right is composed of a single dolomite crystal.

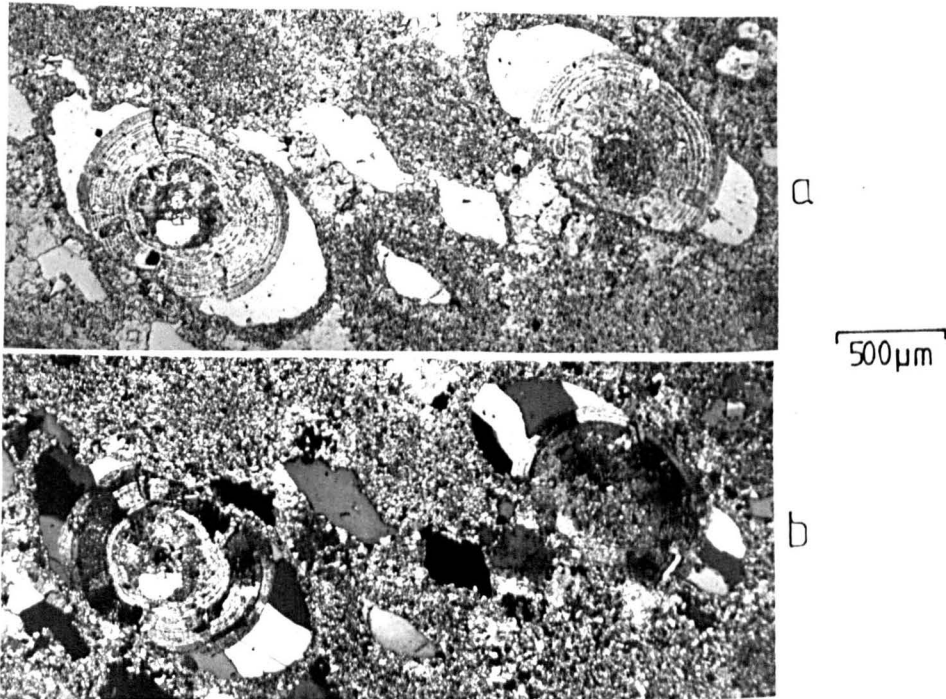


Figure 7-12: Photomicrographs, bed 54D; a) plane polarized light, b) crossed polars. Dolomite ooids showing replacement by quartz leaving myriad tiny dolomite inclusions arranged concentrically. Tectonic solution transfer has subsequently dissolved quartz at points of high stress and re-precipitated it on the lee side of the ooids (= a type of pressure fringe, see 7.5.5).

These calcitic laminae are clearly later than the micritic dolomite laminae which show internal lamination by grain size variations.

Concordant with replacive calcite are calcite veins, both dilational (parallel-sided) and replacive (irregularly-margined). Larger crystals in the veins are heavily twinned consistent with a pre-tectonic age. Likewise the calcite mosaics may show a tectonic fabric in the form of a preferred orientation of grains, or be cut by tectonic quartz-calcite seams or by groups of late diagenetic or metamorphic albite. Zoned dolomite rhombs occur within the calcite mosaic of stromatolite C9 so probably post-date the calcite.

Replacive calcite of ooids and stromatolites has Fe and Mn concentrations proportional to, but substantially lower than, fine-grained dolomite in the same rocks (7.9). A clear chemical distinction from void-fill calcite is seen on staining stromatolites BV and C9. Here the chemistry of the void-fill calcite, but not its texture, can be seen to be in the process of being transformed to that of the replacive calcite (fig. 7-13). More generally where calcitization has affected void-fill calcite, the latter is altered texturally by enlargement of the calcite patches, as well as chemically.

### 7.2.3: Silicification

#### 7.2.3.1: Microquartz

In the field, a 2cm silicified band at the top of bed 16D (a sandstone) can be traced for several hundred metres; also patchy silicification occurs in sandstones 27D and 27E and takes the form of rounded or elliptical bodies up to a few centimetres across. The replacement, by 15-30µm inclusion-free polygonal quartz, is limited to dolomite,



Figure 7-13: Photomicrograph, plane polarized light, stromatolite horizon B $\bar{V}$ ; clastic fill between stromatolite domes. Dolomicrite allochems are partly replaced by calcite (pale pink). Relict patches of void-fill calcite (darker red surrounded by very pale medium-grained dolomite rim) are visible left centre and lower right.

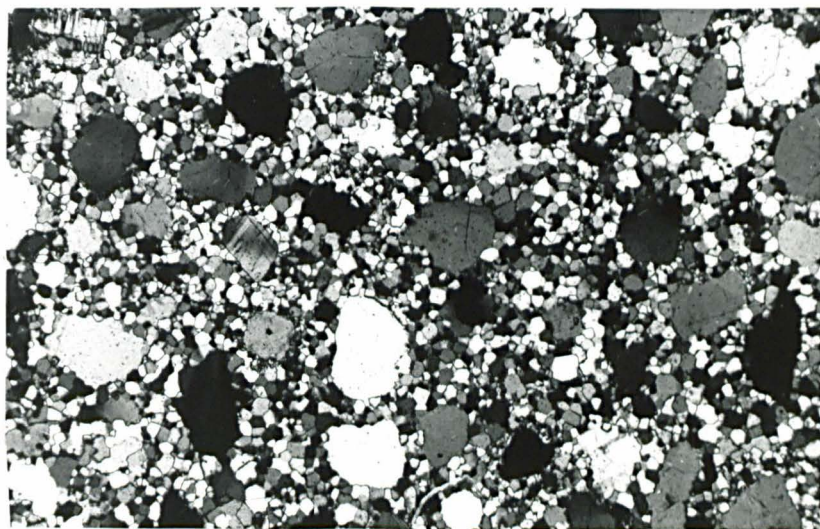


Figure 7-14: Photomicrograph, crossed polars, sandstone, bed 16D. Most of the rock contains intergranular dolomicrite, but in the area in the photograph this has been replaced by equigranular quartz.

both intergranular (fig. 7-14), and in the form of oöids. In bed 27E the clasts are more deformed when set in the dolomitic matrix than in the siliceous matrix indicating that the silicification was pre-tectonic.

#### 7.2.3.2: Glomerulotopes

A contrasting mode of quartz replacement is shown by 7 specimens from various member 3, layered facies sediments where 0.2-1mm quartz forms isolated, widely-spaced nodules (glomerulotopes, by analogy with metamorphic rocks) about 1mm across, replacing silty dolostone. Within the quartz, rings of inclusions of dolomite, mica or iron ore define the shapes of replaced quartz grains (figs. 7-15 & 7-16). Microcline inclusions, representing included detrital grains, also occur within the quartz. The outline of the detritus as shown by the inclusions is smooth, suggesting an origin of the replacing quartz before corrosion of the clasts by intergranular dolomite (7.2.4) took place. Pressure fringe growth around the nodules has occurred later, providing an inclusion-free rim (fig. 7-16).

An alternative to the suggestion made above, that quartz is a direct replacement of silty dolomicrite, is the possibility that the structures represent replacements of gypsum sand crystals. Gypsum crystals incorporating sand grains grow near the sediment surface in the modern Laguna Madre (Masson, 1955) and similar structures have been recognized in the Craignish Phyllites of the Middle Dalradian (Anderton, 1975). Some of the glomerulotopes do have a bi-convex shape reminiscent of some gypsum forms. However, the long axis of described gypsum sand crystals is vertical in sections perpendicular to bedding, whereas none of the glomerulotopes are. Neither is there any positive evid-

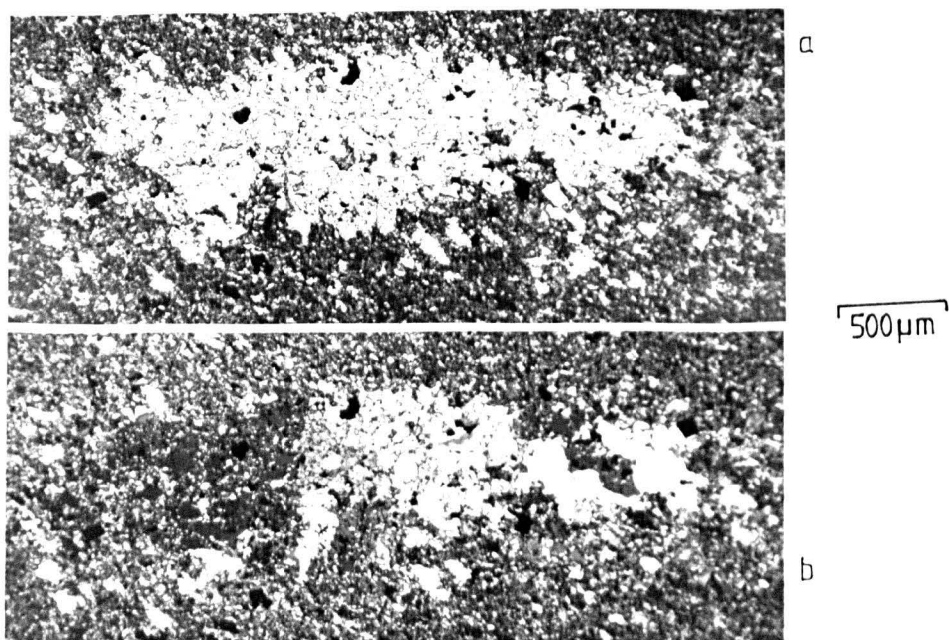


Figure 7-15: Photomicrographs; a) plane polarized light, b) crossed polars, bed 20E. Glomerulotopes of quartz (seen to be composed of 6 or 7 crystals under crossed polars) set in silty dolomicrite. The glomerulotope contains inclusions which delineate replaced quartzose detritus.

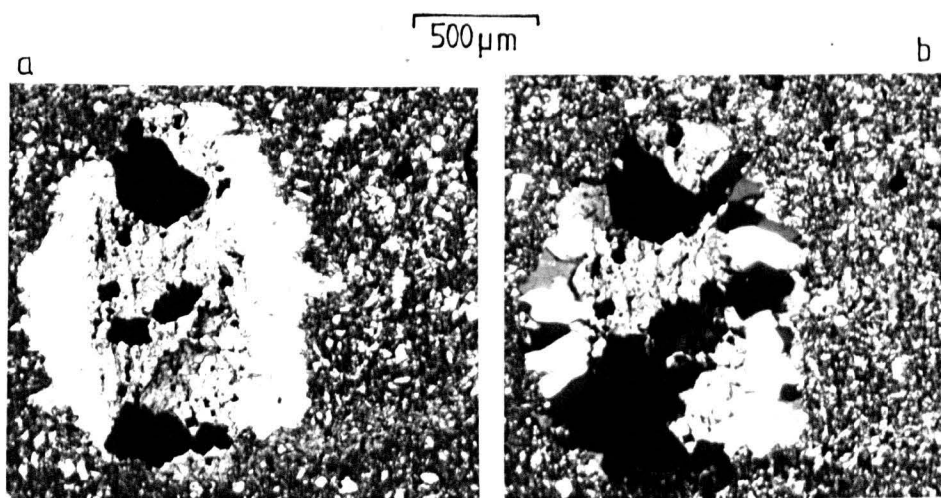


Figure 7-16: Photomicrographs; a) plane polarized light, b) crossed polars, bed 47B. Quartz glomerulotopes with inclusions of pyrite; microcrystalline material outlines replaced detritus. Clean quartz is a tectonic pressure fringe. Running E-W at bottom right-hand side of glomerulotope is an S2 cleavage band composed mainly of chlorite.

ence, such as that found in the Craginsh Phyllites, of rosettes of crystals or a preferred occurrence of the structures at a certain horizon. Also it is only gypsum crystals very much larger than 1mm in size that incorporate detritus in modern sediments (Masson, 1955; Butler, 1970; Miller, 1975).

#### 7.2.4: Zoned dolomite rhombs and intergranular dolomite, member 3

The origin of interstitial dolomite in dolomitic sandstones and siltstones and the formation of zoned dolomite crystals set in dolomicrite are the major topics of this section. For convenience subhedral and euhedral intergranular dolomite crystals are referred to as intergranular rhombs whilst the zoned crystals in dolomicrite are termed matrix rhombs.

##### 7.2.4.1: Petrography

As the rhombs are commonly associated with fine-grained dolomite, some description of the diagenesis of the latter is appropriate.

Sand and granule-sized clasts of dolomicrite are common in member 3. Amongst these clasts are both ooids, and dolomicrite grains abraded from larger flakes and pebbles, although it is not always possible to distinguish between them. On compaction, these allochems are squeezed between adjacent quartz and feldspar grains. This process must start to operate fairly quickly as intraclasts of oolitic sand occur in the sandstone facies, although it is conceivable that undetected early cementation could produce the same result. The effect of compaction in some cases is to provide a discontinuous rim of fine-grained dolomite around the other detritus (fig. 7-17).

As was noted in section 6.4.1, there has been some

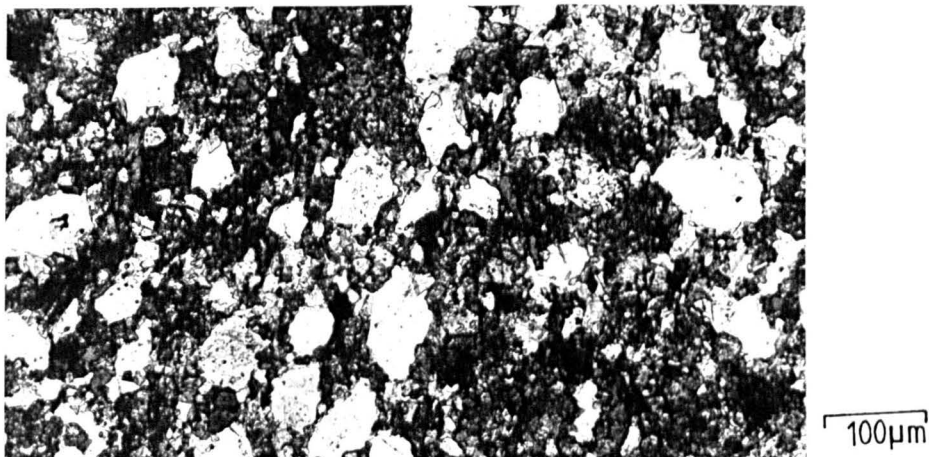


Figure 7-17: Photomicrograph, plane polarized light, bed 37D. Dolomitic sandstone with much dolomicrite, representing squashed sand-sized clasts, between sand grains.

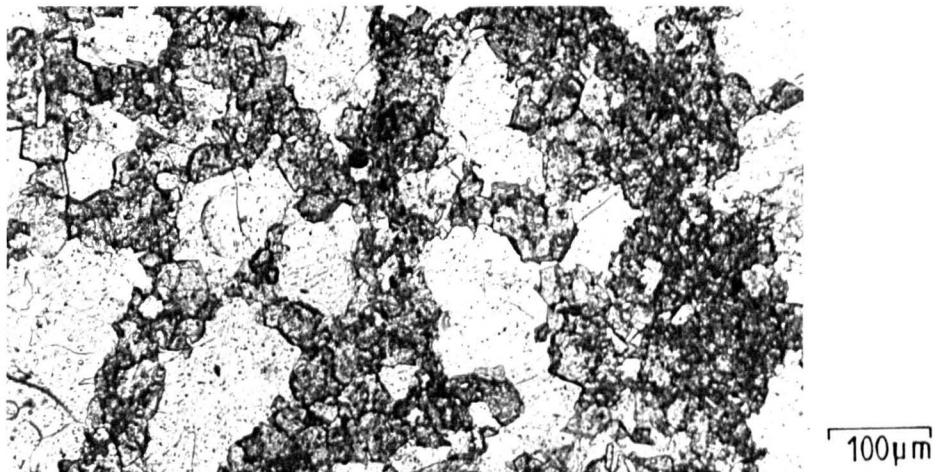


Figure 7-18: Photomicrograph, plane polarized light, bed 15D. Dolomitic sandstone showing interstitial dolomicrite and subhedral dolomite.

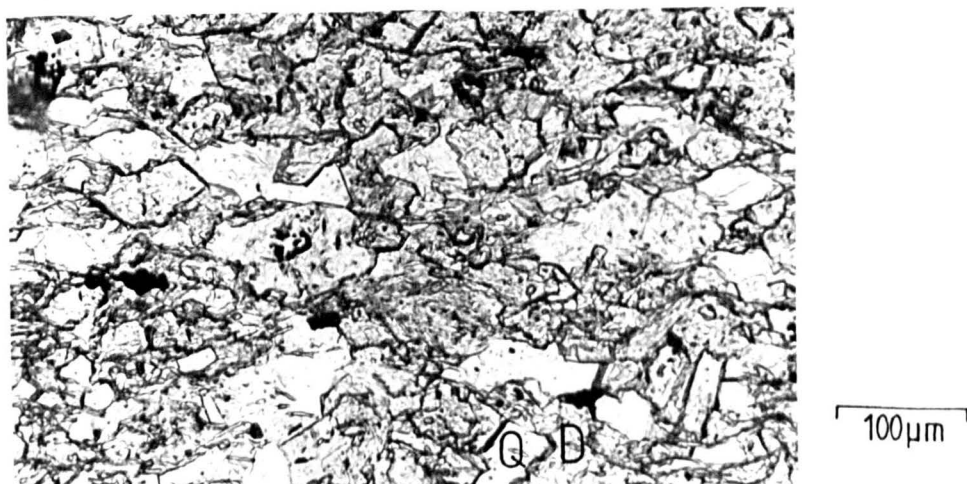


Figure 7-19: Photomicrograph, plane polarized light, bed 22E. Dolomitic muddy siltstone showing subhedral intergranular dolomite with no associated dolomicrite. (Q= quartz clast, D= dolomite.)

coarsening of dolomicrite so that there is now commonly a mosaic of grains 10-20 $\mu$ m in size, or isolated irregularly-shaped grains of this size, set in dolomicrite. These textures almost certainly resulted from the superposition of metamorphic processes on diagenetic neomorphism. Other crystals show zoning in plane polarized light and under luminescence (matrix rhombs) and some exhibit zoning only under luminescence: their origin requires further discussion.

Having considered the unzoned, anhedral dolomite crystals now let us consider subhedral and euhedral intergranular dolomite. Some such was visible in figure 7-17, whilst other sandstones (e.g. fig. 7-18) exhibit proportionally more rhombs compared with the fine-grained intergranular dolomite present. In general, these rhombs range from 20 to 125 $\mu$ m in sandstones and up to 50 $\mu$ m in siltstones. In contrast to the last two figures, other samples exhibit intergranular rhombs without any associated fine-grained dolomite, yet the rhombs may be tightly packed, especially in siltstones (fig. 7-19). In sandstones, the lower the dolomite content, the better formed is the dolomite (fig. 7-20). The intergranular dolomite in these last two figures displays a much less constant and complete intergranular border coupled with a great deal more corrosion of quartz clasts than was the case (figs. 7-17, 7-18) when fine-grained dolomite was present.

Some intergranular rhombs contain fluid inclusions (see description of matrix rhombs below for details), whilst others have a rhomb-shaped core with 1-3 $\mu$ m carbonate and other unidentifiable mineral inclusions. However, most intergranular rhombs lack inclusions.

The simplest explanation for the origin of the intergranular rhombs is that they are a recrystallization product of fine-

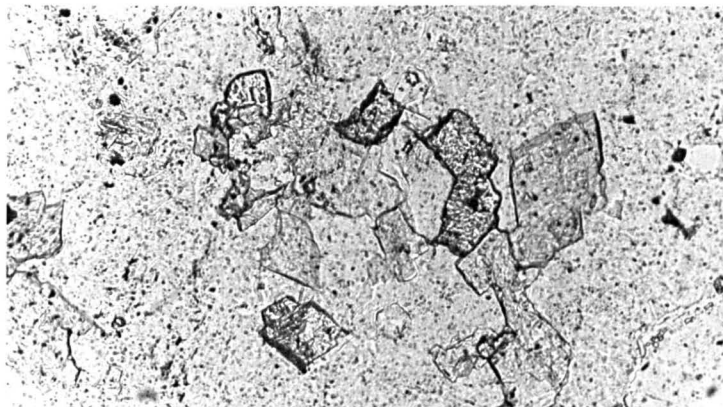


Figure 7-20: Photomicrograph, plane polarized light, bed 6D. Sparsely dolomitic sandstone showing euhedral intergranular dolomite.

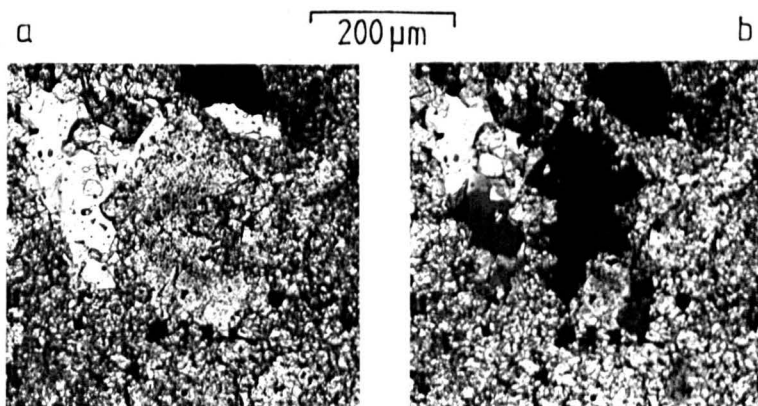


Figure 7-21: Photomicrographs, bed 68E; a) plane polarized light, b) crossed polars. Matrix rhomb with diffuse rhombic ring of inclusions visible in a). In b), the rhomb is shown in the extinction position showing very irregular grain boundaries.

grained dolomite, crystal faces being developed by corrosion of adjacent quartz. However where dolomicrite is absent this explanation is not tenable, but perhaps the rhombs formed as a result of solution of dolomite nearby, perhaps in the same bed. The applicability of these ideas must be viewed in the light of the chemical evidence of the next section.

The most conspicuous form of coarser dolomite set within dolomicrite is that of the matrix rhombs (figs. 7-21, 7-22, 7-63) which are 50-250 $\mu$ m in size. They always show a ring or core (usually rhomb-shaped) rich in inclusions which, like those in member 1 zoned dolomite, appear brownish at low magnification. As for member 1 dolomite, these inclusions are found to be fluid-filled, either spherical (0.5-1 $\mu$ m) or elongate (up to 2 $\mu$ m long). Despite the presence of euhedral internal zones, the grain boundaries of the matrix rhombs are irregular. (fig. 7-21). Their mode of occurrence entirely within fine-grained dolomite suggests on the face of it formation by an isochemical process: crystal enlargement within a closed chemical system. Luminescence and probe work on the matrix rhombs show that the situation is not this simple, however.

#### 7.2.4.2: Luminescence and chemistry

Under luminescence, nearly all the anhedral dolomite which is unzoned in plane polarized light is unzoned here also, but some crystals show one or more bright rhombic rings or a tiny, usually shapeless, bright luminescent speck (fig. 7-22). In one case (slide 5) it was possible to demonstrate that the bright areas are Mn-enriched compared with the rest of the dolomite, but the available data do not allow a conclusion to be drawn as to whether the excess Mn was introduced into the system from outside or whether it had been derived by depletion of the surrounding dolomite of Mn.

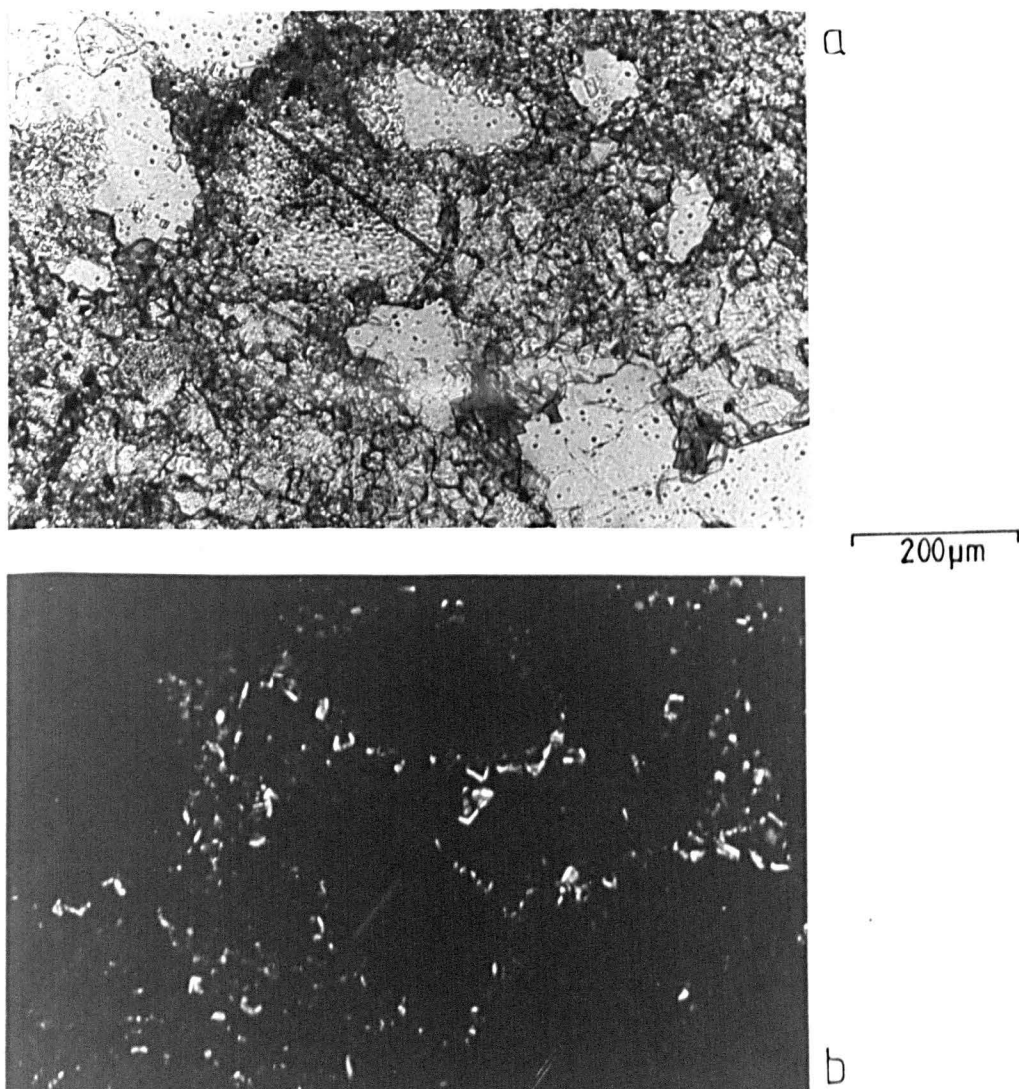


Figure 7-22: Photomicrographs, bed 55D, a sandy oölitic dolostone. a) transmitted light ; a large matrix rhomb with an inclusion-rich core is visible, with a probe scan line (analysis 13B). b) under luminescence the non-luminescing matrix rhomb can be seen to be cross-cut by small anhedral dolomite crystals with a bright rhomb-shaped ring probably indicative of a high Mn concentration.

All matrix rhombs show chemical zoning and many intergranular rhombs do also. In any one slide, the luminescence zones are essentially the same for each rhomb (e.g. fig. 7-63).

Analyses of intergranular dolomite rhombs in five slides are shown in figure 7-23 and a summary of their properties is given in Table 7-1.

TABLE 7-1

	<u>Analysis number</u>				
	11B	12B	14	18	22B
<u>Associated with dolomicrite?</u>	Yes	Yes	No	No	Yes
<u>Iron-poor core and iron-rich rim?</u>	Yes	Yes	Yes	No	No
<u>Homogeneous chemically?</u>	No	No	No	Yes	Yes
<u>Inclusion-rich cores?</u>	No	Yes	Yes	No	No

Thus in both samples with homogeneous rhombs the rhombs lack inclusions, but the converse is not true. Iron-rich rims on intergranular rhombs are very common as is shown in many samples where rhombs luminesce only in their cores (= low iron), or show Fe-rich rims on staining.

Matrix rhombs generally show a more complex chemistry (fig. 7-24). An iron-rich rim is a feature of each, although analysis 13B (fig. 7-24c) also shows an iron-rich core. Analysis 20 (fig. 7-24d) shows a gradual increase in iron outwards from the core, dropping off slightly near the rim. Rhombs from samples 21 and 24 (figs. 7-24a & b), which were sampled 100m apart in the same bed, show broadly similar patterns, at least in the outer zones. It is noticeable for both intergranular rhombs and matrix rhombs that Mn shows much less variation than Fe, although there tends to be more Mn in the rims of some.

When the average composition of rhombs is computed and compared with the composition of dolomicrite in the same

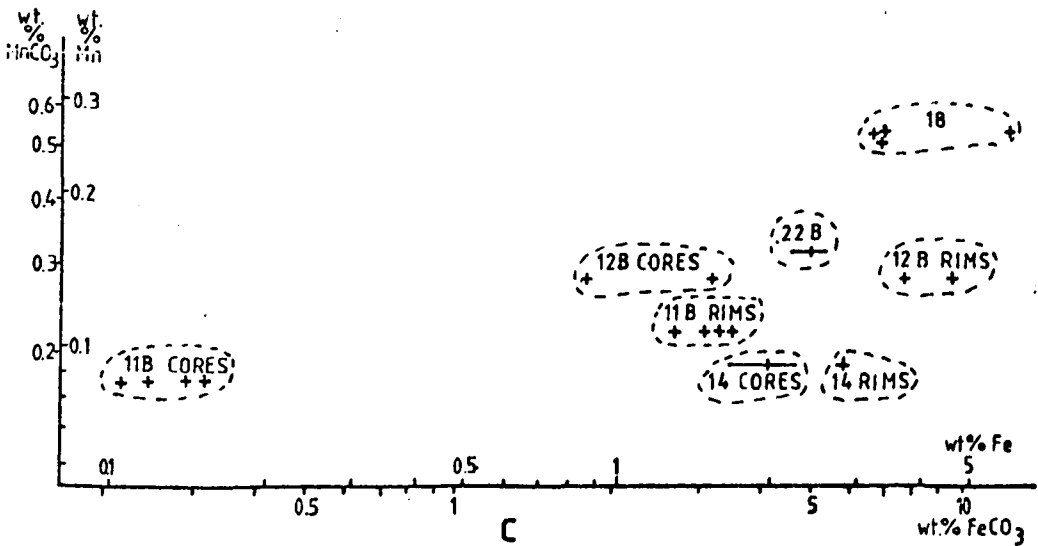
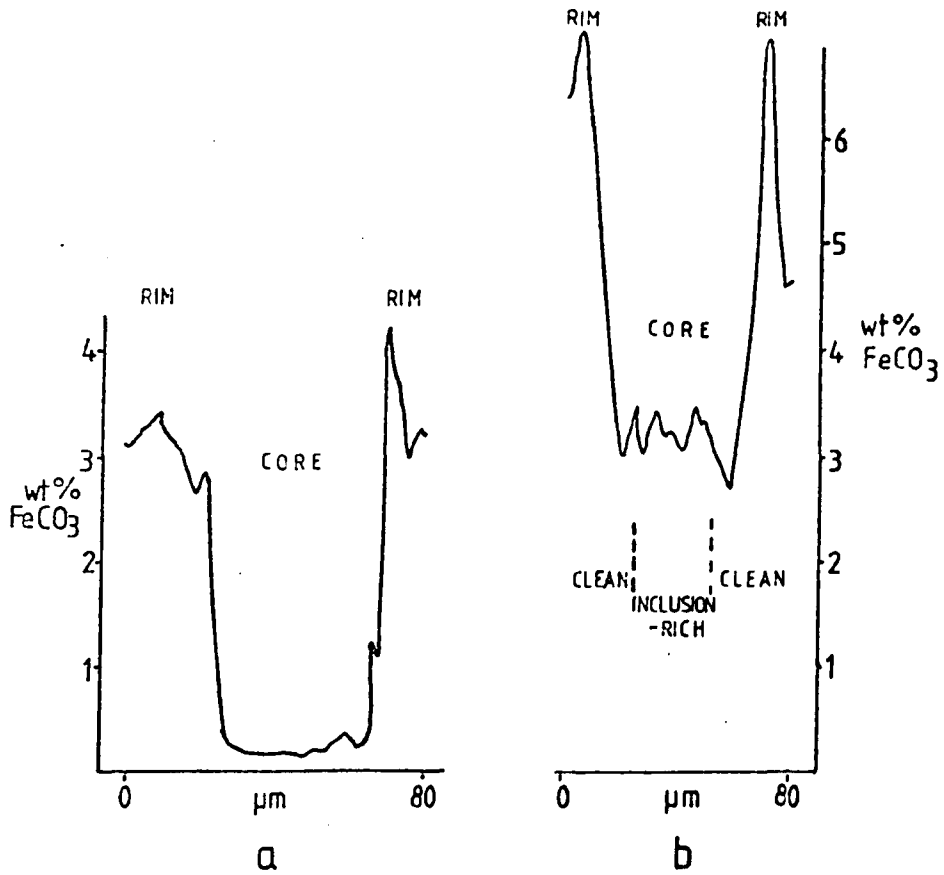


Figure 7-23: Analyses of intergranular rhombs. a, b) Fe analyses (nos. 11B and 12B respectively) plotted as Fe concentration against position in the rhomb. The iron-enriched rims are conspicuous. c) Summary of Fe and Mn analyses.

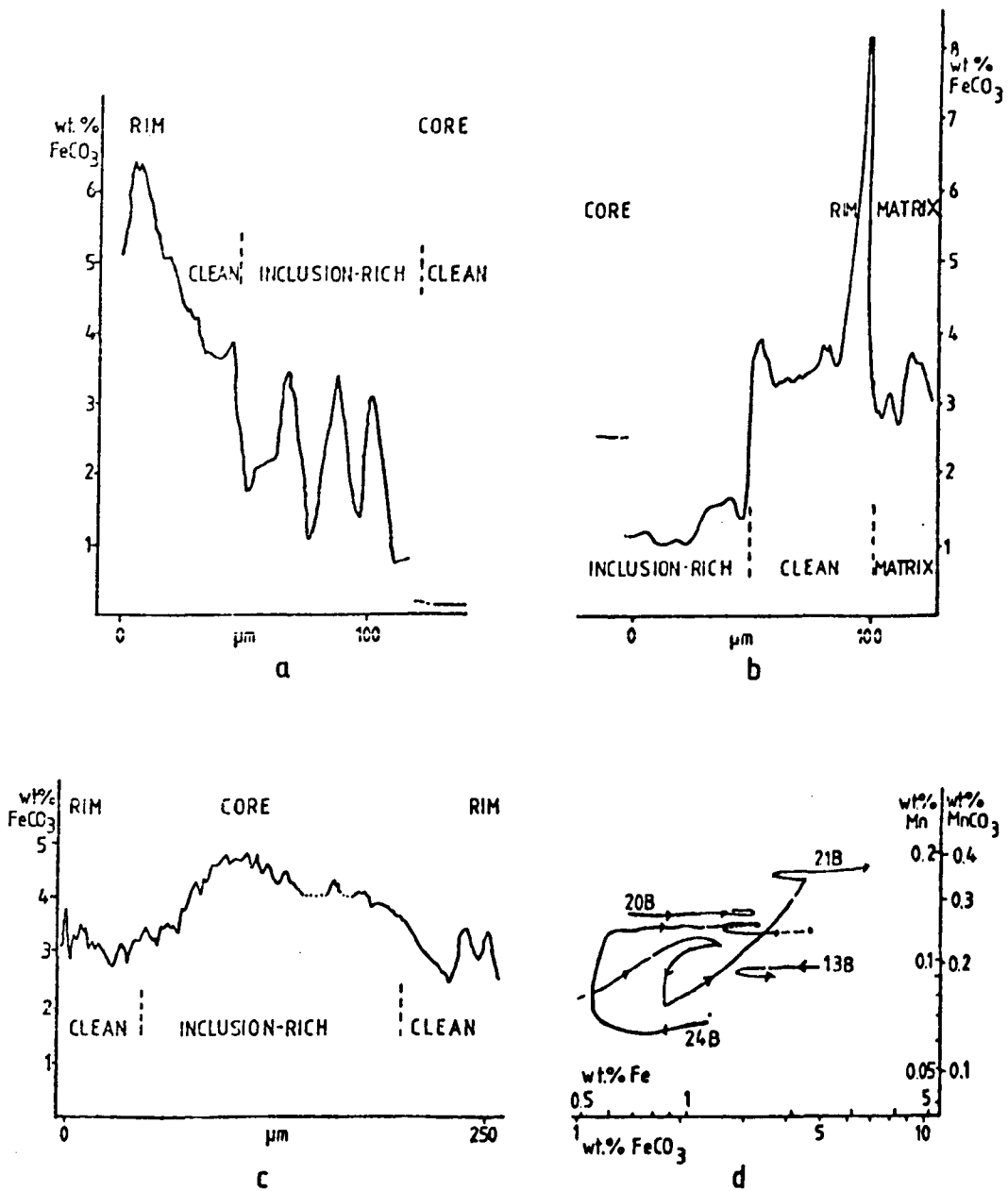


Figure 7-24: Analyses of matrix rhombs. a,b,c) Fe concentrations plotted against position in rhomb for analyses 21B, 24B and 13B respectively. d) Generalized change in Fe/Mn concentrations from core to rim (arrows point to later zones). Heavy line = inclusion-rich; light line = inclusion-free.

slide (where present), the two are very closely similar (fig. 7-25). That is, the overall composition of the rhombs is consistent with dissolution and short distance transport of dolomite. The question of whether the zoning is consistent with this is discussed in later sections.

#### 7.2.4.3: Age of the rhombs

None of the rhombs described in this section are post-tectonic because they are much less ferroan (by staining) than definite post-tectonic dolomite (7.8) and are not associated with fractures as is the latter. An earlier age limit is set by the observation that rhombs with luminescing cores apparently cut replacive calcite. I hope to obtain crystallization temperatures of some rhombs by work on their fluid inclusions. In the absence of such evidence it is not possible to decide on a diagenetic or metamorphic age, bearing in mind the absence of a clear tectonic fabric in the domains in which the rhombs occur. The matrix rhombs are post-dated by brightly luminescing dolomite crystals (fig. 7-22) which are unzoned in plane polarized light: this is some tentative evidence for a pre-metamorphic age for the matrix rhombs. The etching of quartz by dolomite intergranular rhombs could develop during moderate burial (Fuchtbauer, 1974), or at greater depths.

#### 7.2.4.4: Causes of the zoning

Zoned carbonate crystals which form diagenetically, whether by replacement (Katz, 1971) or as cements (Meyers, 1974), unlike most zoned crystals in igneous and metamorphic rocks, are generally attributed to an open system. Complex zonal patterns are a common feature of an open system, although the reasons why this should be so are not well understood (see also 6.5.4).

In the case now being considered, as the rhombs have

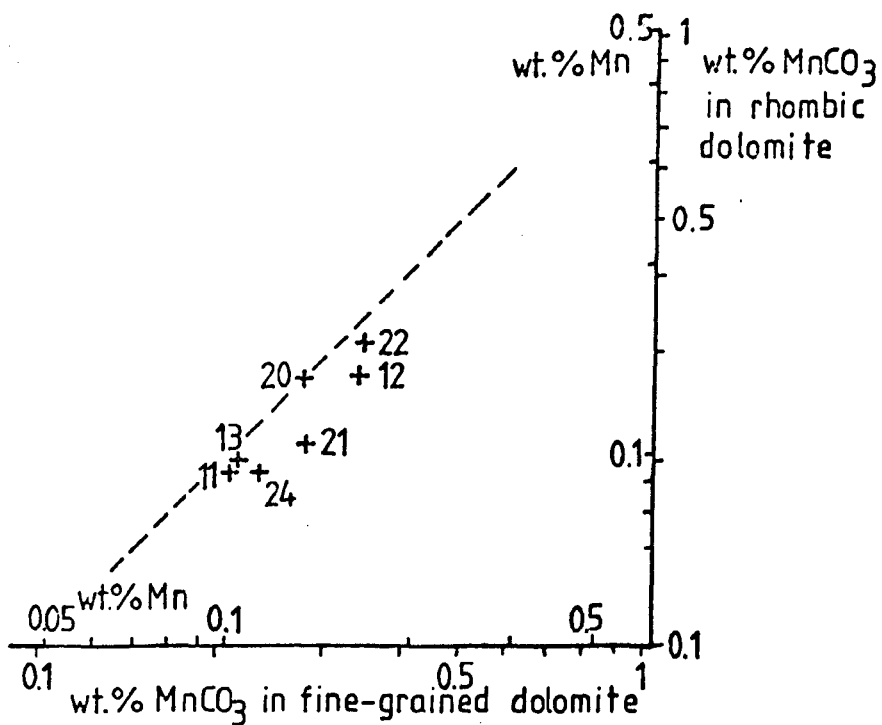
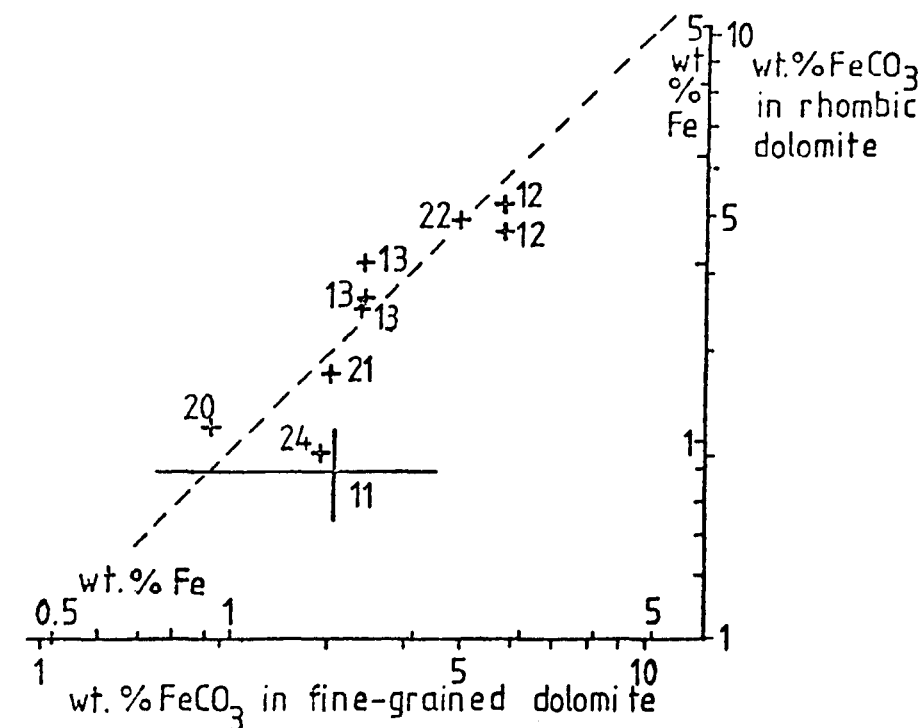


Figure 7-25: Plots of the average composition of dolomite rhombs compared with co-existing dolomicrite. The dashed lines represent equivalence of overall composition of rhombs and co-existing matrix. The data points lie fairly close to these lines.

the same composition as nearby dolomicrite, then the possibility of a local closed system operating should be preferred if it can be shown to be viable.

#### 7.2.4.4.1: Theoretical zonal patterns in a closed system

For the present purposes the closed system is taken to be on a hand specimen or smaller scale. The samples are all fairly pure dolostones or sandy dolostones, so that the only source of Fe and Mn appears to be dolomicrite.

In a closed system, zoning might result from several factors which are now described.

1) Variation in the chemistry of the dolomicrite being dissolved. An inhomogeneous source would give rise to zoned crystals. The zoning would be unpredictable in nature.

2) The value of the relevant partition co-efficient (figs. 7-26a & b) as defined in section 6.4.2. If the partition co-efficient were less than unity (fig. 7-26a) the situation would be analogous to that described by Kinsman (1969) who predicted the Sr content of calcite produced from aragonite by a dissolution-precipitation process in a closed system. A core low in the minor element would gradually pass into an unzoned outer portion where the minor element concentration in the crystal being formed would equal that of the crystals being dissolved. When dissolution of the source ceased, or the supply of source was exhausted, the final increment of the precipitated crystals would be enriched in the minor element, although not necessarily to the degree indicated in figure 7-26a which depicts an overall composition of the precipitate equal to that of the source dolomite.

If the partition co-efficient were greater than one then unzoned crystals would be expected as all of the minor



Figure 7-26: Some theoretical patterns of minor element zoning of dolomite crystals growing in a closed system at the expense of other dolomite crystals.

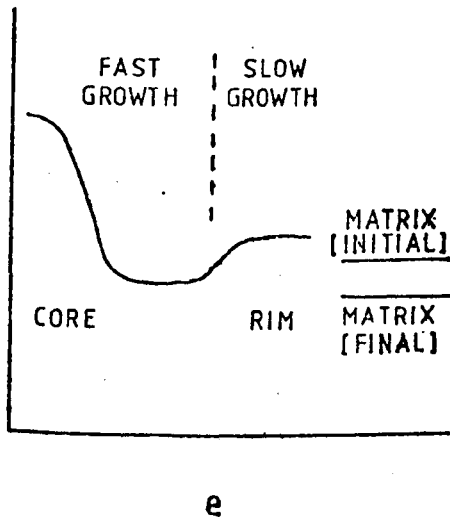
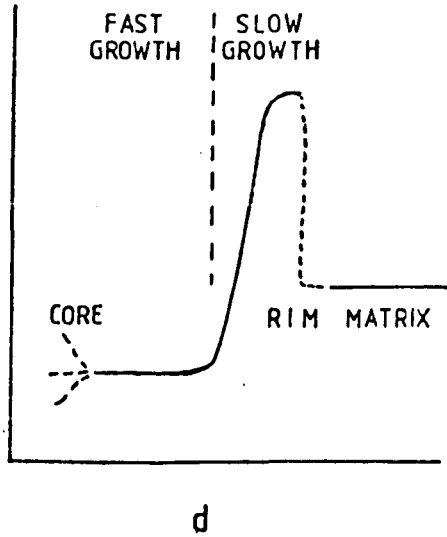
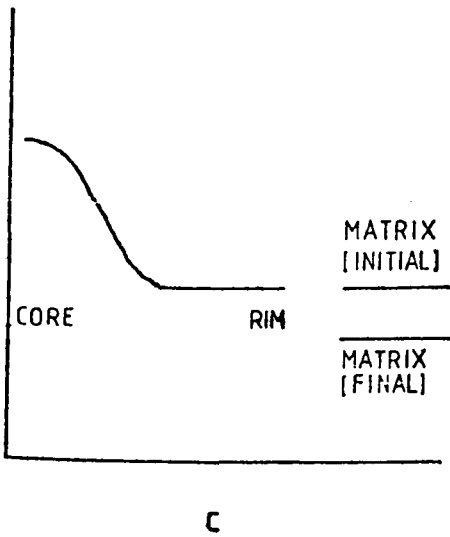
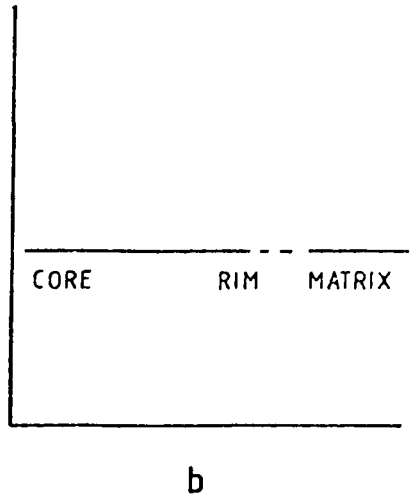
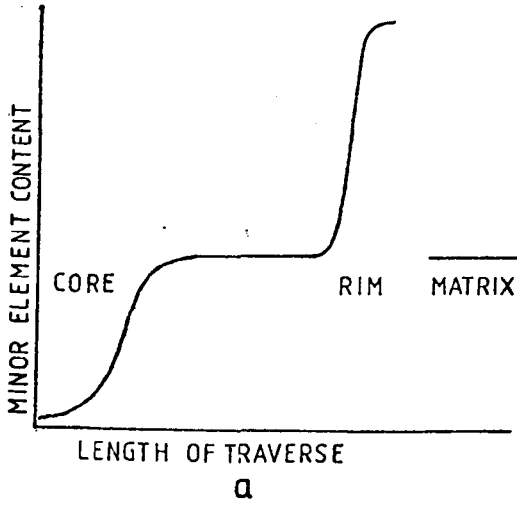
a) Partition co-efficient ( $K$ ) is less than 1; source dissolves congruently. Enrichment of the minor element would only occur in the rim, that is when the source dolomite was exhausted, or ceased to dissolve. The central steady-state stage (horizontal line) could be very long, or entirely absent, depending on the amount of crystallization compared with the size of the solution reservoir.

b)  $K > 1$ ; source dissolves congruently.

c)  $K > 1$ ; source dissolves incongruently, thus releasing the minor element first. The diagram assumes that a steady-state is reached whereby a congruent dissolution front remains a set distance behind an incongruent dissolution front. If incongruent dissolution were to cease and congruent dissolution were to continue the content of the minor element would drop and the average matrix composition revert to its original value.

d)  $K > 1$ ; assumes that the major element cations diffuse faster than the minor element. Growth is initially faster than the minor element can be supplied to its equilibrium concentration by diffusion. Later, growth and the dissolution rate of the source slow and the minor element concentration increases considerably. Further slow growth would incorporate intermediate amounts of the minor element. A model of this type is probably only applicable when the major elements and the minor element are derived from different sources and the minor element is released at a relatively slow rate.

e) as d), but with some incongruent dissolution of source.



element released when the source dolomite dissolved (assuming congruent solution) would be incorporated into the crystallizing dolomite (fig. 7-26b).

3) Incongruent dissolution of the source. The source dolomite could undergo some incongruent dissolution releasing more of the minor element than for the case of congruent dissolution. Later the initial high level of supply of the minor element relative to the major elements may diminish. One variation of this situation is illustrated in figure 7-26c, which assumes that  $K \gg 1$  and that a steady-state is reached whereby a hypothetical front of incongruent dissolution remains a set distance ahead of a front of congruent dissolution of the source. If the congruent dissolution front later caught up with the incongruent front then a rim depleted in the minor element on the precipitating crystal would result. If  $K$  were  $< 1$  then the pattern of fig. 7-26a would be superimposed on that of figure 7-26c thus giving rise to a more complex series of zones.

This model is analogous in a way to the growth of some porphyroblasts where the source of the minor element is to a greater or lesser extent independent of the source of the major elements giving rise to, for example Mn-rich cores in garnets (Hollister, 1966; Atherton, 1976).

4) Variation in the speed of growth of crystals. Edmunds & Atherton (1971) explained Mn-rich rims on metamorphic garnets as being due to variation in the speed of growth of the crystal. The partition co-efficient being greater than one, Mn was incorporated into the garnet as soon as it became available; initially garnet growth was fast and Mn supply by diffusion was not sufficient to maintain the potential Mn content of the garnet. Conversely, later

growth was slower and the Mn content higher.

A variation of this idea is shown in figure 7-26d, although the exact pattern would depend on the relative speed of diffusion of minor and carrier major elements compared with each other, and the actual rate of growth of the crystals and dissolution of the source. Again  $K$  was taken to be  $\geq 1$ ; if  $< 1$  then the pattern of figure 7-26a would be superimposed on that of figure 7-26d in some way.

Figure 7-26e represents a possible zonal sequence, assuming  $K \geq 1$ , if a change of speed of growth were coupled with incongruent dissolution of the source. Again the pattern would be more complex still if  $K < 1$ .

5) Temperature. Some partition co-efficients (see fig. 6-7 and McIntyre, 1963) are strongly temperature-dependent so that temperature changes could affect the zoning. However during the growth of the crystals, the temperature is only likely to change in one sense: the effect would be to tilt and slightly warp the patterns of figure 7-26.

7.2.4.4.2 Application of the closed system to the rhombs

1) Inhomogeneity of source. Comparison of the analyses of member 3 fine-grained dolomite and rhombic dolomite from the same slide (Appendix A) shows that when rhombs show zoning, this is much greater than the variation in chemistry of the dolomicrite. Also local inhomogeneities could not give rise to the observed identical zonal sequences in all the rhombs within any one sample.

2) Partition co-efficient. A partition co-efficient of less than one could explain the Fe-poor cores and Fe-rich rims of many of the rhombs. However the discussion in section 6.4.2 indicates that the partition co-efficients for incorporation of Fe and Mn into dolomite are likely to be

considerably greater than unity, although the effective partition co-efficient in a rock without open pores could conceivably be different.

Closed system precipitation of dolomite with  $K \gg 1$  could give rise to the homogeneous distribution of Fe in the intergranular dolomite of slides 18 and 22, and of Mn in nearly all the intergranular rhombs and two of the four samples containing matrix rhombs.

3) Incongruent dissolution of source. The likelihood of incongruent dissolution occurring is difficult to evaluate, but such a process operating with respect to Fe, coupled with  $K \gg 1$ , could explain the iron-enriched core of figure 7-23c. None of the other zoned crystals can be explained by incongruent dissolution.

4) Speed of growth. In metamorphic rocks, an abundance of mineral inclusions indicates fast growth (Spry, 1969). By analogy, one could say that abundance of fluid inclusions within the cores of many of the dolomite rhombs could indicate fast initial growth, followed by later slower growth. Thus the Fe-enriched rims on many of the rhombs of figures 7-23 and 7-24 could be explained. However, unlike metamorphic rocks, and also perhaps impure (muddy) dolostones, where the various cations may be derived from different sources, zones as observed in the pure dolostones, if resulting from the variation in speed of growth of dolomite crystals, would depend solely on the various cations showing different diffusive behaviour, with  $\text{Fe}^{2+}$  being the slowest ion. This seems unlikely because, in aqueous solutions at least, variations in the speed of diffusions of chemical species are small (Berner, 1971, p95), especially for similarly-sized cations of the same valence (McIntyre, 1963, p1240).

5) Temperature. It seems unlikely that a significant change in temperature would have occurred during formation of the rhombs.

#### 7.2.4.5: Conclusions

Intergranular dolomite rhombs (20-150 $\mu$ m), and anhedral crystals larger than 5 $\mu$ m which are homogeneous chemically, lack inclusions: they were derived by dissolution-reprecipitation (whether diagenetic or metamorphic) of the nearest dolomite source.

Most intergranular rhombs and all matrix rhombs possess a zoning which can be explained by a closed chemical system (on hand specimen or smaller scale) only if:

- 1) the effective partition co-efficient (for Fe in dolomite) is less than unity.
- 2) the effective partition co-efficient (for Fe and Mn in dolomite) is greater than unity, but the incorporation of Fe and Mn in the dolomite was from time to time controlled by the rate of diffusion of these elements to the site of precipitation.

As neither of these conditions is thought to be appropriate, it is concluded that the system was partly an open one and that external factors controlled the zoning, although, where rhombs are partly or wholly encased in dolomicrite, no overall chemical change took place.

### 7.3: Diagenetic solution

#### 7.3.1: Intergranular solution

Solution at grain contacts (pressure solution) is an important process in the lithification of sediments at depth. Although important in the Bonahaven Formation, its effects have been partly obscured by tectonic pressure solution, the latter being recognized by the constant orien-

tation of solution planes parallel to rock cleavage. Two examples of diagenetic solution are drawn from samples showing little tectonic influence:

1) Interlocking quartz and feldspar clasts occur in some member 1 sandstones, although only in areas where mud clasts, rather than dolomite (type 3, Chapter 6) are the intergranular material. Solution of feldspar here probably provides material for K-feldspar overgrowths nearby (fig. 7-3).

2) As dolomicrite clasts are much softer than siliciclastic grains, it is difficult to distinguish squashing at grain contacts from solution. Occasionally ooids demonstrate that a good deal of solution has occurred (fig. 7-27). This supplies material for some of the intergranular dolomite described in the last section.

In quartzites, growth of new crystals at grain boundaries tectonically has obscured the pre-tectonic situation, but some diagenetic solution and overgrowth can sometimes be recognized. Even so the amount of overgrowth visible is less than the amount of solution which has apparently occurred: the inference is that many non-luminescing, optically-continuous overgrowths on clean, non-luminescing clasts have escaped detection.

### 7.3.2: Stylolites

Stylolites occur in about one tenth of the slides examined, particularly in stromatolites, carbonaceous mudstones and at sand-mud interfaces. They are marked by a concentration of opaque grains and occasionally micas, along an undulating surface. They are thus simple stylolites in the classification of Park & Schot (1968) with no marked relief. This fact, coupled with their relatively uncommon

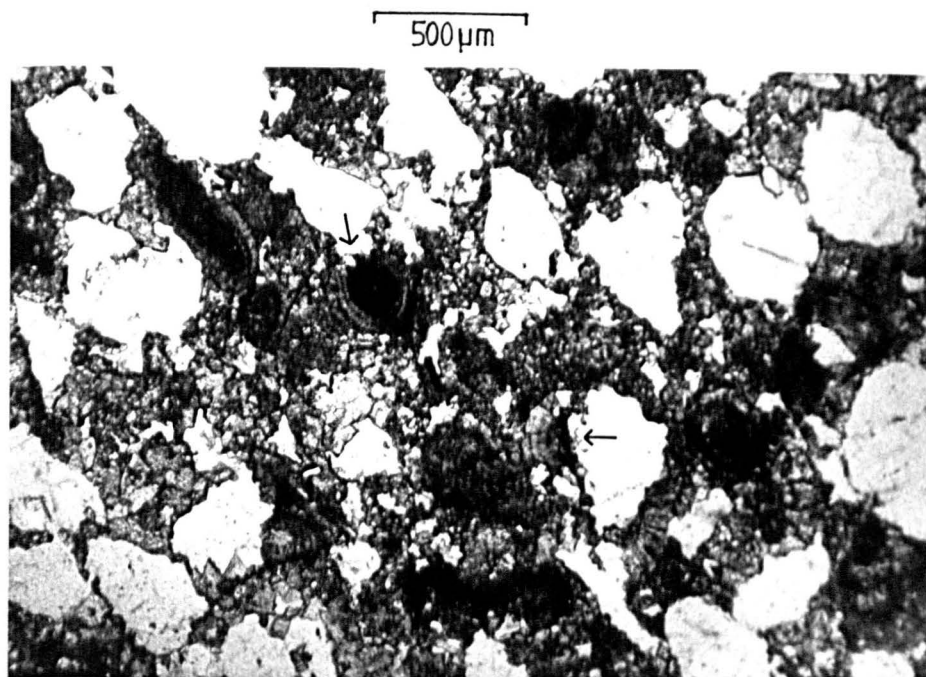


Figure 7-27: Photomicrograph, bed 49E, sandy oölitic dolostone. Dissolution of oöids adjacent to quartzose detritus (e.g. where indicated by the arrows) is clearly important.

occurrence, shows that the amount of solution is volumetrically unimportant compare with, for example, British Carboniferous or Jurassic limestones.

They would post-date lithification (Bathurst, 1971) and are taken to be pre-tectonic because they are almost invariably parallel to bedding, and sometimes serve as central partings in tectonic quartz seams (7.5.5.3), that is they have acted as lines of weakness allowing these dilational structures to develop.

#### 7.4: Deep burial: the diagenetic-metamorphic transition

##### 7.4.1: Introduction

Dalradian sedimentation was fairly continuous following deposition of the Bonahaven Formation with over 10km of sediments being laid down (Harris & Pitcher, 1975). Thus the Bonahaven Formation was steadily buried, following the time of sedimentation, to great depths. Eventually one would expect new minerals to have appeared whose formation depended on the elevated temperatures and pressures consequent upon burial. In other words, metamorphism would have begun.

In volcanic rocks and some greywackes characteristic metamorphic products (zeolites) appear at rather low temperatures (150-200°C) and a whole series of reactions occurs within the zone of very low-grade metamorphism (200-350°C, Winkler, 1976). Most other rocks do not show characteristic metamorphic mineral assemblages until temperatures characteristic of low-grade metamorphism (>350°C, Winkler, 1976) are reached, although predictable increases in coal rank (Teichmuller & Teichmuller, 1968) and the crystallinity of illites (Dunoyer de Segonzac, 1970) do allow comparison with

the zeolitic rocks.

The composition of the Bonahaven Formation is such that none of the diagnostic zeolites of very low-grade metamorphism are recognized or would be expected to have formed. Because of this, the term "deep burial" is preferred to "very low-grade metamorphism". The zone of deep burial (approximately 5-10km depth) has also been referred to as the "anchizone" (Dunoyer de Segonzac, 1970), the "zone of early metagenesis" (Füchtbauer, 1974), and various other names (Gill et al., 1977) reflecting its transitional nature between diagenesis and metamorphism.

Below it is first shown that the Bonahaven Formation has gone beyond this zone of deep burial, then an attempt is made to determine what effects of deep burial can still be recognized in the rocks.

In a progressive metamorphism, apart from porphyroblasts (Atherton, 1976), one would expect to see only the metamorphic minerals representing the highest grade of metamorphism obtained. Measurement of the crystallinity of illitic micas (phengites) in 13 X-ray diffraction analyses was made using the sharpness ratio of Weaver (1960), which is equal to the peak height at  $10\text{\AA}$  divided by the peak height at  $10.5\text{\AA}$ . The result is an average value of 9.7. Using data of Weber (1972), this was found to be equivalent to a Kubler index of crystallinity of  $<4$  which Winkler (1976) indicates is characteristic of micas of low-grade, rather than very low-grade, metamorphism. The presence of phlogopite confirms that maximum temperatures exceeded  $350^{\circ}\text{C}$ .

Few criteria are available for recognizing the products of deep burial in carbonate and mature siliciclastic rocks. However, Füchtbauer (1974) regarded processes producing

large pyrite crystals, especially large feldspars and reactions involving the breakdown of K-feldspar, as operating only at great depths. These criteria are used below.

It should be noted at the outset that the mineralogical and textural changes which occur at a particular depth of burial of a sediment are determined not only by its composition, but also by the burial history. A particular process may for example happen at moderate depths in a slowly buried sediment, but only following deep burial of a rapidly buried sediment. Therefore processes thought to have occurred during deep burial of the Bonahaven Formation should not be taken as diagnostic of processes operating only at 5-10km depth.

#### 7.4.2: Pyrite

Pyrite is common in members 3 and 4, especially in dolomitic and calcitic sandstones, dolomitic silt and mudstones, and in some quartz-calcite nodules. It forms single cubes, or interpenetrating clusters of cubes, some of which are less than 10 $\mu$ m across. The largest crystals, up to 2cm across, are a feature of the sediments around the member 3-member 4 boundary.

It is likely that the pyrite has been remobilized from an original early diagenetic precipitate. This material would have formed close below the sediment-water interface under reducing conditions (Curtis & Spears, 1968), probably as framboids (Sweeney & Kaplan, 1973). Although the smallest crystal clusters are within the size range of framboids, no spherical aggregates were seen.

The constant occurrence of pressure fringes around pyrite cubes indicates a pre-tectonic origin for the pyrite.

Following Füchtbauer (1974), the larger crystals, at least, can be regarded as having formed during deep burial.

#### 7.4.3: Albite

Detrital sodic plagioclase is recognized by its ubiquitous fine-grained, or sericitic alteration. Its distribution within the Bonahaven Formation is summarized in section 4.5 and is not discussed further in this section.

Most albite is fresh and regarded as secondary because of its absence in sandstones which are sufficiently unaltered that all detrital grains can be determined.

Albite occurs, together with quartz, as scattered silt-sized grains in stromatolites; as a component of inclusion-rich mosaics of quartz and albite (7.4.4); and, interlocking with quartz, in the more altered siltstones and very fine-grained sandstones. Also it forms isolated subhedral crystals up to 100-150 $\mu$ m across (fig. 7-28) and anhedral replacements of detritus (fig. 7-4).

The albite is very pure chemically, a semi-quantitative determination of Ca (uncorrected comparison with a dolomite standard) giving a result of 0.1%, yet it always shows well-developed polysynthetic twinning (fig. 7-33).

All this polysynthetically-twinned albite represents replacements, rather than overgrowths on detritus. The size of the albite, and the absence of detrital cores can be matched by diagenetic albite elsewhere (Dickson & Barber, 1976; Baskin, 1956), but the presence of polysynthetic twinning cannot (Engelhardt, 1977, p251). Although twinning is not common in low-grade metamorphic albite either, the presence of the twinning seems to indicate that the albite formed during deep burial or low-grade metamorphism.

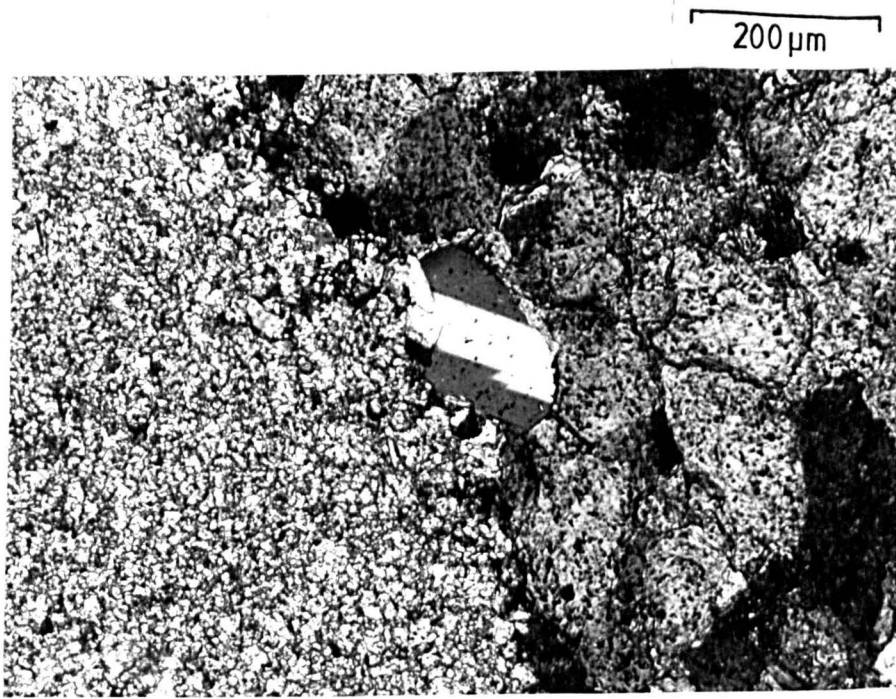


Figure 7-28: Photomicrograph, crossed polars, bed 68E. Subhedral secondary albite at incipiently stylolitized contact between dolomitic micrite (left) and calcite cement (right).

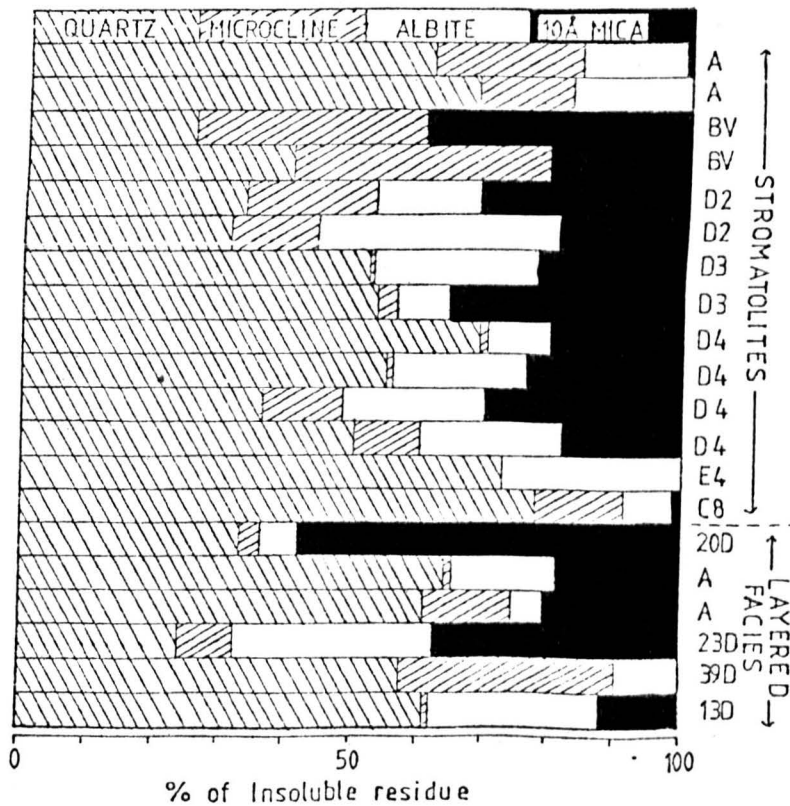


Figure 7-29: Results of X-ray diffraction analysis of some insoluble residues of stromatolites (horizon indicated) and layered facies sediments (bed number indicated). See Appendix B3 for method.

Formation of the bulk of the albite before the peak of the metamorphism may be indicated by the fact that the albite does not form porphyroblasts (cf. Kennedy, 1969).

The main problem for the formation of the albite is the source of the Na. Given that no analcite is likely to have been present, there seem to be two possibilities: 1) mica, and 2) intergranular fluid. An essentially internal origin for the Na seems appropriate as the soda content of the rocks which have been analysed (Table 7-2, p182A) are not unusually high compared with rocks elsewhere (Pettijohn, 1975). Also the albite is quite unlike the large post-tectonic grains which characterize areas elsewhere in the Dalradian which have suffered Na metasomatism (Jones, 1961).

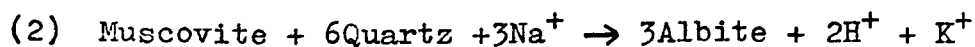
If the Na originated from mica, then this reaction (after Winkler, 1976) seems appropriate:

(1) K-feldspar + Paragonite or phengite with paragonite component  $\rightarrow$  Albite + Phengite.

Reaction (1) would require an inverse abundance of K-feldspar and albite in the resulting rocks. Results of X-ray diffraction analysis of some HCl-insoluble residues are shown in figure 7-29. They show that although the relative abundance of microcline and albite is indeed very variable, so is the total feldspar content. This applies even where there is little albite and so makes an inverse relationship impossible to prove. One point that can be made, however, is that several samples bear albite, but not mica: here reaction (1) does not seem feasible.

This objection does not apply to the second alternative for the source of the Na, that is intergranular fluid. During burial, intergranular fluids become alkaline brines

with a high Na content (Engelhardt, 1977). Such a fluid is capable of forming albite from K-feldspar by ion-exchange (Orville, 1962) or altering clay minerals to albite (Hemley et al., 1961) at temperatures found during deep burial. In-situ albitization of K-feldspar seems a likely process in the clastic lithologies, but not where albite replaces carbonate. The reaction



(Orville, 1962) may also occur, although experimental data is needed.

It seems from the data of Coombs et al. (1959) that albite in deeply buried zeolitic rocks is rather more abundant than would be expected from the quantities of soda-bearing minerals in the equivalents of these rocks at shallower depths. This suggests that the Na for at least some of this albite was derived from intergranular fluid (cf. Engelhardt, 1977, p256). If so, then not only greywackes, but more mature detrital sequences such as the Bonahaven Formation could show the development of albite during deep burial, although with the increased temperatures of low-grade metamorphism, further albite would probably have been produced.

In conclusion, it is considered that the good twinning rules out a diagenetic origin for the albite; much albite probably formed during deep burial, and the rest during low-grade metamorphism. The source of the Na only seems clear where modal phengite is not present: here Na would have been derived from intergranular fluid.

#### 7.4.4: Inclusion-ridden mosaics of quartz and albite

The mosaics are found as bands parallel to bedding in

stromatolites (4.3.4.2, fig. 7-30), forming the margins, or part of dolomicrite pebbles (fig. 7-31) or the whole of some pebbles (fig. 7-32).

The mosaics consist of equigranular quartz together with albite, the latter being 1-50% as abundant as the quartz. Grain size is generally 30-50 $\mu$ m (fig. 7-33), although can be as fine as 10-20 $\mu$ m or as coarse as 100-200 $\mu$ m. The smallest grains are polygonal; larger grains have curved or slightly irregular boundaries, although some albite boundaries are rational. Inclusions, overwhelmingly of very fine-grained dolomite, and occasionally of mica, occupy 5-60% of the mosaics. Larger dolomite inclusions are sometimes euhedral. Some mosaics also bear some phlogopite and/or calcite.

Although having some resemblances to the more altered siltstones, the mosaics are regarded as the result of replacement, generally of dolomite. All transitions are seen, from unreplaced to completely replaced pebbles, the latter resembling siltstone clasts in the field. The quartz-albite replacement of oöids (7.2.1.3, fig. 7-12) probably represents the same phenomenon. The inclusions correspond to the composition of nearby unreplaced material, e.g. replaced muddy dolostone would have common inclusions of mica as well as dolomite. In stromatolites, an origin by replacement of dolomite, rather than transformation of detritus, is less easy to prove, but the mosaics are commonly quite distinct from detrital laminae. As was discussed in the last section, albite is present in quartz-albite mosaics in many specimens where phengite is practically absent, so an origin of the Na from intergranular fluid seems appropriate. Certainly the material is pre-tectonic

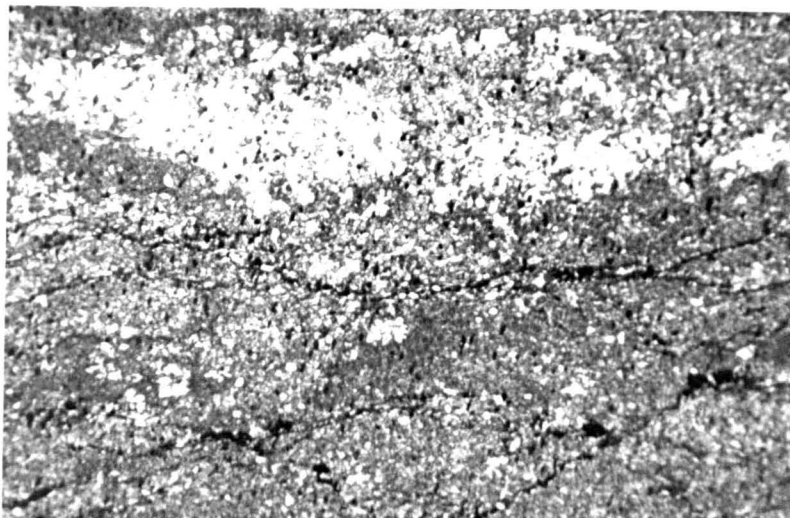
500 $\mu$ m

Figure 7-30: Photomicrograph, plane polarized light, bed 45/6B, stromatolite horizon BVI. Stromatolitic lamination running E-W is paralleled by a band of inclusion-rich quartz and albite (top) and stylolites (black; centre and near bottom). In most stromatolites in the Bonahaven Formation such discontinuities parallel to bedding have served as lines of weakness during deformation, becoming the central partings of dilational 'quartz seams'.

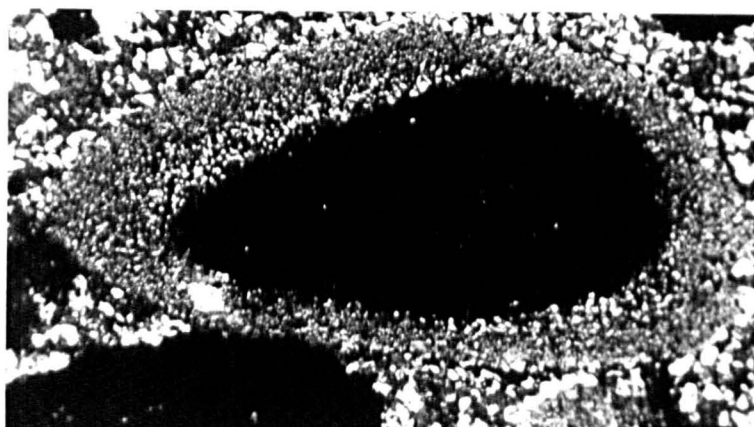
500  $\mu$ m

Figure 7-31: Photomicrograph, plane polarized light, bed 38D. Dolomicrite clast is replaced around its margins by quartz and albite. Many inclusions of dolomite remain within the quartz and albite.

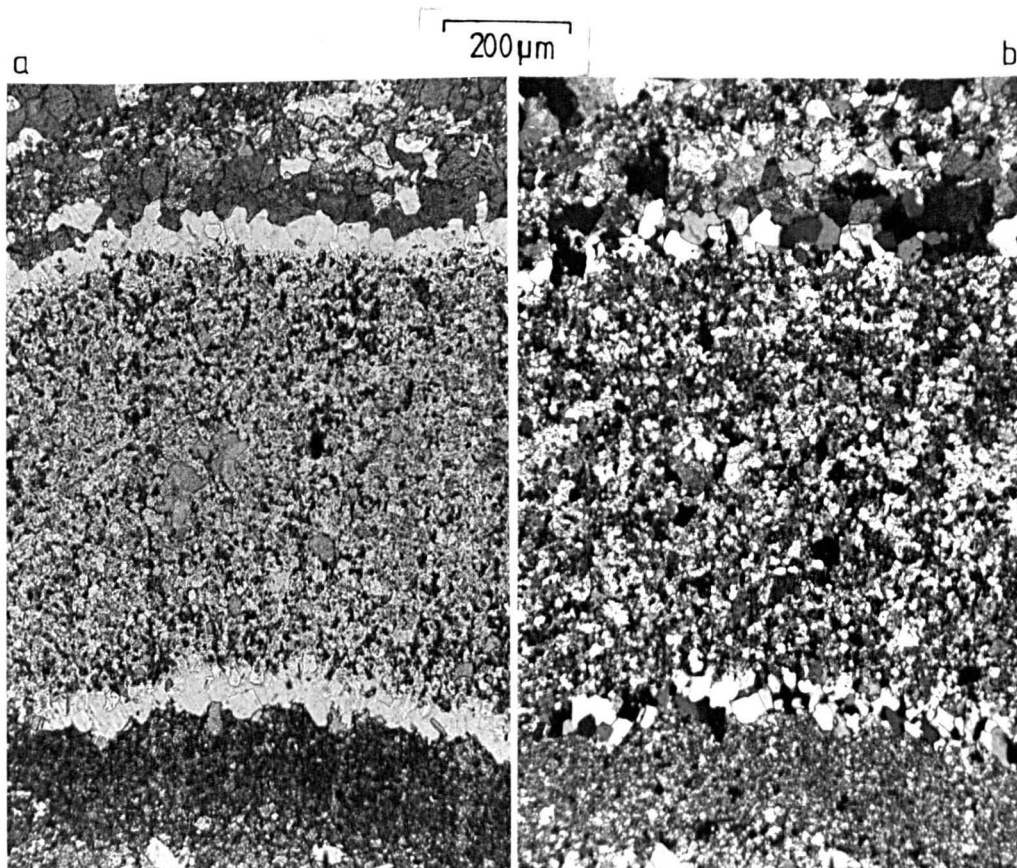


Figure 7-32: Photomicrographs, bed 13D. a) plane polarized light. Running E-W in the centre of the photograph is part of a dolomicrite pebble replaced by quartz and albite (with remnant dolomite inclusions). Flanking the replaced pebble at top and bottom of the photograph is a thin pressure fringe of quartz (white) with some calcite. b) crossed polars. The pressure fringe is seen to have an unelongate texture.

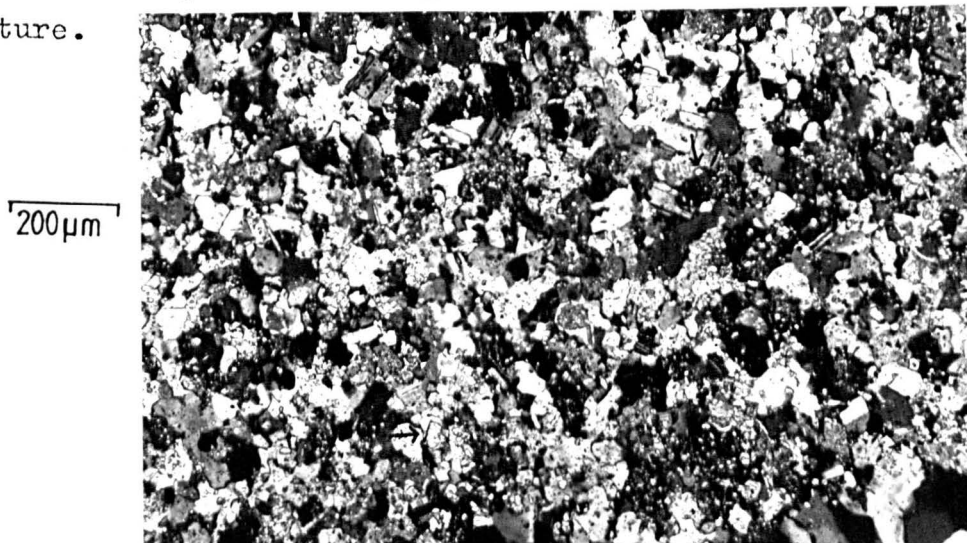


Figure 7-33: Photomicrograph, crossed polars, bed 13D. Interlocking quartz (grey-white) and albite (twinned) replace dolomicrite. Many inclusions of dolomite (tiny bright areas) are present; some of these have crystal faces (e.g. where arrowed).

because it has been the site of pressure fringe-type growth of quartz (fig. 7-32), and in stromatolites it becomes the central partings of quartz seams (fig. 7-53). The occasional subhedral or euhedral dolomite inclusions crystallized later than the quartz and albite because only anhedral dolomite occurs in the dolostone unreplaced by quartz and albite. The phlogopite and calcite are also thought to be later replacements.

It remains to be seen whether these distinctive mosaics are a feature of other deeply buried mixed carbonate-siliciclastic sequences.

#### 7.4.5: Nodules

The nodules described here probably relate to diagenesis, deep burial, and metamorphism, but these various aspects are brought together here for convenience (see also section 4.3.2.11). This discussion excludes quartz glomerulotopes (7.2.3) and nodules developed entirely by pressure fringe growth around groups of pyrite crystals (7.5.5.2).

##### 7.4.5.1: Form

Nodules occur commonly in members 3 and 4 and range in diameter from a few hundred microns up to 10-20cm. They are usually equant with smooth (fig. 7-34b, c), cauliflower-like (fig. 7-34a) or irregular (fig. 7-34d) margins; or in some cases are smooth-margined and elongate, defining a lamination. The margins of the nodules may be diffuse on a sub-millimetre scale (fig. 7-35) or perfectly sharp (fig. 7-37). Others are extremely diffuse and grade to scattered, isolated crystals. The size, shape and mineralogy of the nodules is very similar at any one horizon,

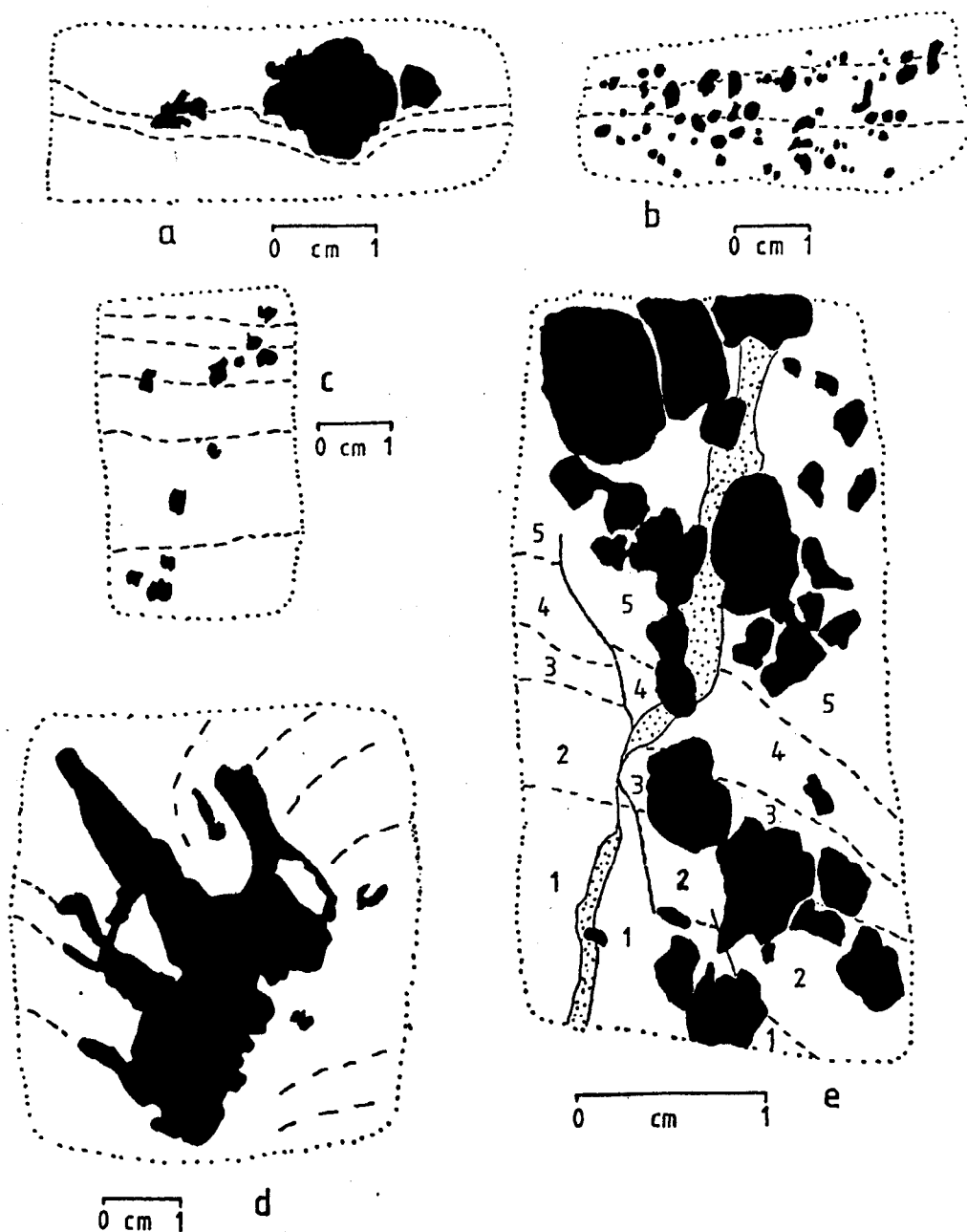


Figure 7-34: Tracings of thin sections or peels of nodule-bearing lithologies; nodules in black. a) bed 33B; some deflection of bedding about the nodule occurs. This is interpreted as being due to diagenetic/metamorphic compaction. b,c) beds 66E, 39D; no deflection of lamination about nodules occurs. d) bed 45/6B, irregular nodule between two stromatolite domes. e) bed 26D, nodules associated with sandstone dyke (stippled). Numbers identify sedimentary laminae. See also figure 7-41.

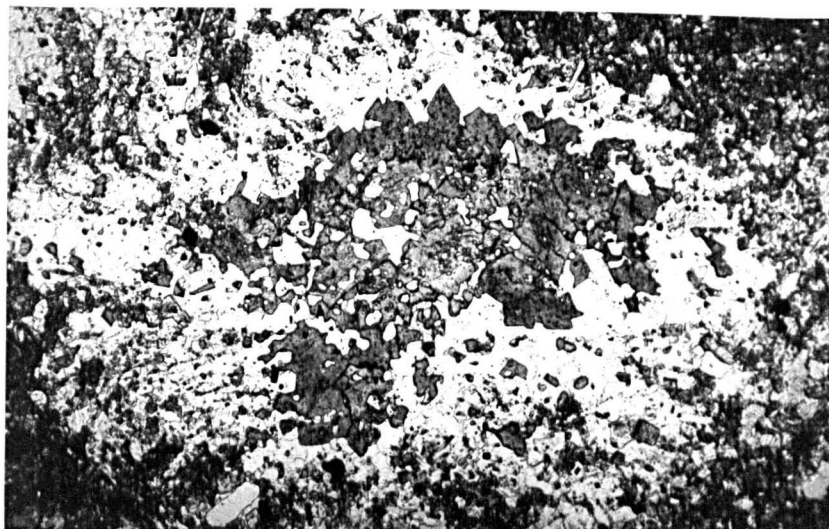


Figure 7-35: Photomicrograph, plane polarized light, bed 39D, showing a nodule of quartz (white) and calcite (grey). Note the variable quartz-calcite grain boundaries which allow no definite conclusions as to the relative age of these minerals. Radial inclusion trains of (dolomitic) matrix are present near the margins, especially on the left hand side.

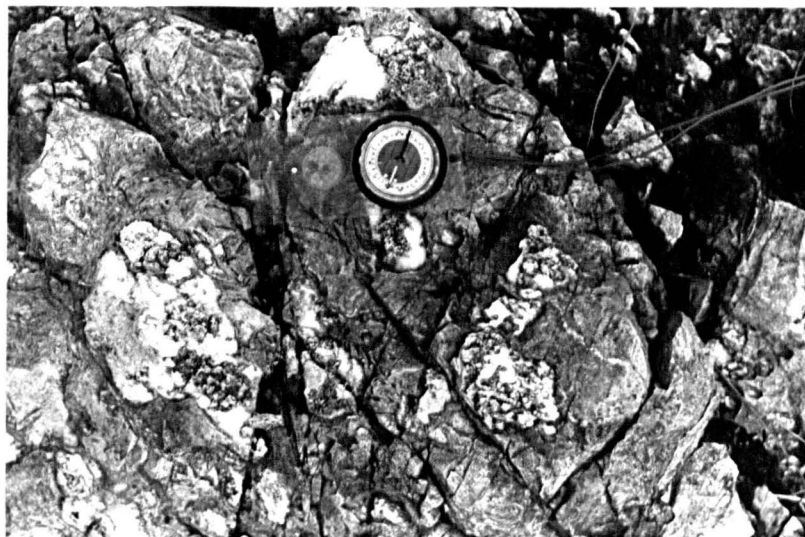


Figure 7-36: Bed 45/6B. A stromatolite (BVI), showing large quartz-calcite nodules (quartz is grey and calcite, white). Host stromatolite is entirely dolomitic (i.e. no calcite occurs).

but differs between localities. The largest nodules occur in stromatolites of various localities, but are particularly well displayed in stromatolites and layered-facies sediments near the top of Section B (fig. 7-36).

When the nodules occur in dolostone containing a fair proportion of mud, the sedimentary lamination may be deflected around them (fig. 7-34a). In pure dolostones, no deflection of sedimentary lamination is noticeable.

Commonly, nodules with sharp margins in muddy lithologies display sweeping and concentration of micas around them due to tectonic solution of quartz and dolomite next to the nodules during the main deformational phase.

#### 7.4.5.2: Mineralogy and texture

Fifty-seven nodule-bearing samples were thin-sectioned. Fifty-six of the samples had nodules containing quartz; 45, calcite; 21, albite; 20, pyrite; 11, dolomite as inclusions of the host rock, and occasionally as coarser crystals; 10, phlogopite; 7, barytes and 3, chlorite. Mineral grains are generally equigranular except for some poikilotopic/blastitic calcite, and rarely quartz. No morphological or optical preferred orientation of grains was detected except for some phlogopite orientated parallel to S1 and some pressure fringe-type dimensionally orientated quartz (fig. 7-37) and calcite.

Quartz is 50-1000 $\mu$ m, sometimes more fine-grained near nodule margins than in the interior, and is usually slightly to moderately strained and therefore probably pre-tectonic in general. Nucleation and growth of new crystals as a result of stress has occurred; in some elongate nodules a completely annealed texture is present (fig. 7-37). Microcrystalline quartz occurs very rarely (fig. 7-38).

Calcite shows a similar range in grain size to quartz.

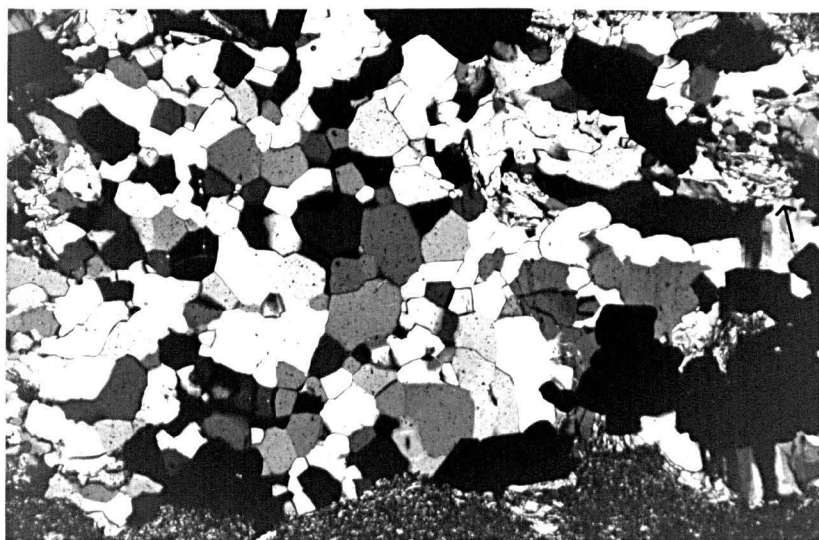


Figure 7-37: Photomicrograph, crossed polars, bed 55D. Part of an elongate nodule (elongation E-W). In hand specimen the nodules define a lineation whose orientation is difficult to interpret. Note the development of elongate quartz next to pyrite (pressure fringe), the unstrained (annealed) texture of much of the quartz, and the presence of some phlogopite elongated E-W (arrow).

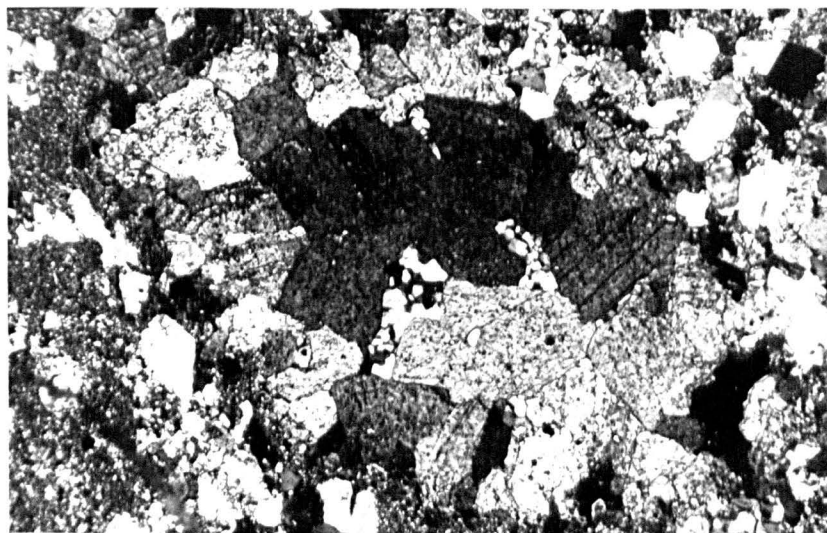


Figure 7-38: Photomicrograph, crossed polars, bed 38D. Quartz-calcite nodular area in sandy flake breccia. Microquartz (centre) is embayed by calcite (cleaved grains) some of which is subhedral.

Many nodules have a marginal zone around their perimeter which is free of calcite and have a calcite-bearing core. Many larger crystals are fairly well twinned: these at least seem to be pre-tectonic. On the other hand, some calcite is continuous with post-tectonic veins. As it is known that calcite and quartz have similar, rather poorly developed, tendencies towards idioblasticity (Vernon, 1968; Spry, 1969) it is not unexpected that quartz-calcite boundaries are extremely variable and difficult to interpret (figs. 7-35, 7-39). The presence of poikiloblastic calcite (Ramdohr, 1969) and/or thin slivers of calcite between quartz grains suggests that the calcite post-dates quartz in some cases. Certainly calcite seems to have crystallized after the microcrystalline quartz of figure 7-38, but in most nodules the relationships are ambiguous.

Pyrite (50-200 $\mu$ m) forms cubes, sometimes concentrated near the nodule margins in a calcite-free area. Pressure fringe growth off pyrite, although present, does not form a major part of the nodules now being described.

Albite (50-200 $\mu$ m) is always subordinate to quartz and calcite, is always well twinned on the Albite Law, possesses some rational boundaries, and may be conspicuous in a marginal calcite-free zone.

Barytes (50-300 $\mu$ m) forms rare, anhedral grains. Phlogopite (50-200 $\mu$ m) never makes up more than 5% of nodules and forms laths, usually randomly orientated, but sometimes paralleling S1. Yellowish-brown chlorite (<50 $\mu$ m) occurs in association with pyrite fringes.

Dolomite (50-300 $\mu$ m) showing crystal size and shape very similar to that normally shown by calcite occurs in some nodules where calcite is absent, or nearly so. Sparse

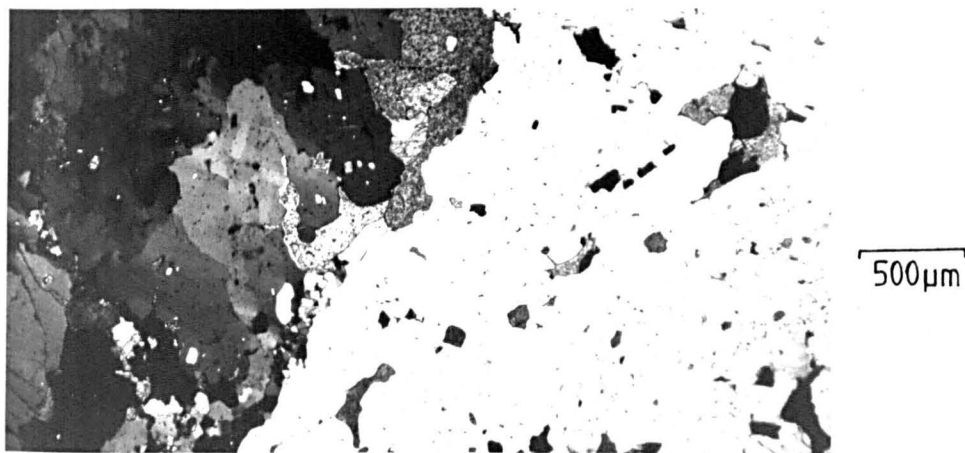


Figure 7-39: Photomicrograph, crossed polars, bed 59E; part of a quartz-calcite nodule. Quartz forms large grains which are strained (left). Calcite (mottled surface, e.g. top centre) has very irregular grain boundaries with quartz.

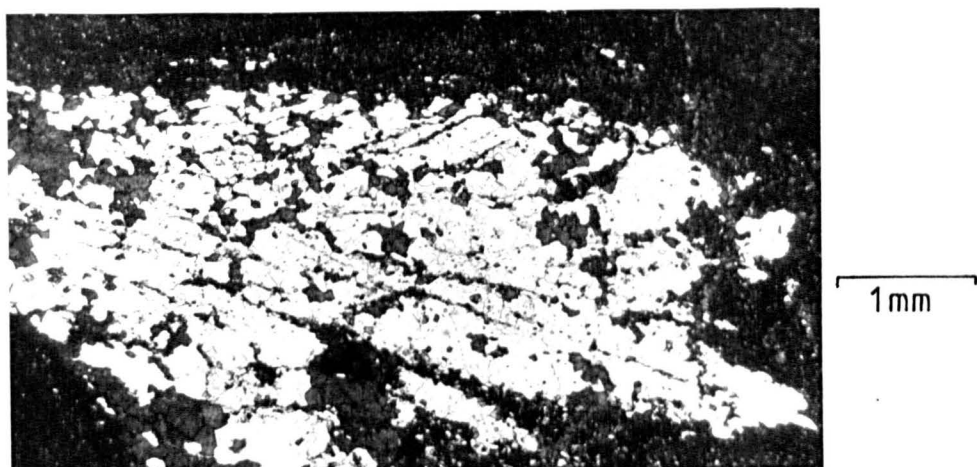


Figure 7-40: Photomicrograph, plane polarized light, stromatolite C8. Nodule of quartz (white) and calcite (dark grey irregular clusters) in stromatolitic dolomicrite. Note inclusion trains of dolomicrite.

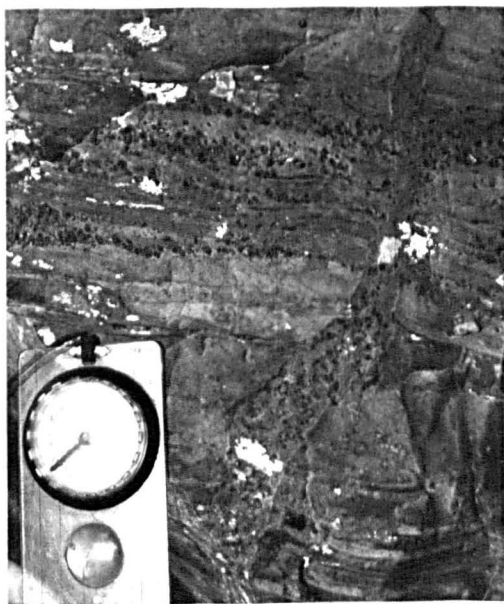


Figure 7-41: Bed 29B, showing sandstone dyke to right of compass. Bedding lamination runs E-W. Small quartz-calcite nodules are concentrated near the dyke, but spread out along the bedding above the compass.

50µm rhombs occur in other cases. A third type is dolomiticrite, similar to the host rock of the nodules. Occasionally this fine-grained dolomite forms radial inclusion trains whose orientation is quite independent of the bedding (figs. 7-35 & 7-40). The nodules containing these trains must have formed by replacement of the dolomite matrix. Growth either parallel or at right-angles to the inclusion trains seems probable, but the former seems more likely because the trains are not equally spaced throughout their length, but convergent. Nodules never contain cores of unreplaced matrix, suggesting that the nodules grew radially outwards rather than inwards. It is thought that this structure of radial inclusion trains passes by transition into the radial slivers of matrix which define the cauliflower-like protrusions in some nodules.

The mineralogy and texture of a number of quartz-calcite veins in member 3 is very similar to that of the nodules. Notably, the presence of highly strained quartz and heavily twinned calcite indicates a pre-tectonic origin.

#### 7.4.5.3: Discussion of origin

The nodules show so much variety that they are almost certainly polygenetic. Firstly, I would like to discuss the common, well-defined equant nodules. Some of these are definitely pre-tectonic because the matrix was deformed around them during D1 as was mentioned earlier. The size and shape of the nodules is consistent with two types of nodules found in sedimentary rocks: anhydrite nodules (as has been proposed for those now being discussed by A. R. MacGregor, see 4.3.2.11) and chert nodules.

The anhydrite nodule theory is supported by these points:

1) The presence of abundant dolomite in member 3 could

indicate an evaporitive regime.

2) The presence of sulphide rims to some of the nodules may indicate the former presence of sulphate.

3) Some evidence of bending of lamination around nodules occurs as would be expected from anhydrite nodules.

4) The common presence of slivers of matrix between nodules resembles incipient chicken-wire texture.

The chert nodule theory is favoured by:

a) The abundant chert in unmetamorphosed Precambrian and Lower Palaeozoic dolomitic sequences including ones of this age (e.g. Tucker, 1977).

b) The presence of some microquartz, embayed by calcite.

Other evidence favouring the chert hypothesis is brought out in the following discussion.

The nodules are associated with dolomitic, rather than wholly siliciclastic, lithologies, but the evidence is against a link with evaporation. Within the layered facies, the nodules are much more abundant in the lenticular-graded than the marginal sub-facies (Table 4-1, p47), yet it is in the latter that the only evidence for desiccation, and hence evaporation, occurs. This contradicts point (1) above.

Regarding point (2), although the pyritic rims to some nodules could indicate the former presence of sulphate, they could also be regarded as evidence of expulsion of iron from the dolomite being replaced by the nodules, as in the chert nodules of Swett (1965). Pyrite rims also occur in the lineation-defining nodules, which are thought to be syn-tectonic.

Point (3) is contradicted by the inclusions of dolomicrite within the nodules as this indicates a replacement origin. Anhydrite nodules grow by displacement, not by replacement

(Shearman, 1966). There is some displacement of sedimentary laminae, but only in muddy rocks where there is likely to have been considerable compaction during burial causing lamination deflection. The observed tectonic solution of quartz and dolomite around the nodules will certainly be important in this respect as Borradaile & Johnson (1973) have shown that considerable volume loss occurred in muddy lithologies during deformation.

At NR 4234 7303 quartz-calcite nodules about 1cm in diameter (figs. 7-34e, 7-41) post-date intrusion of sandstone dykes. At this locality, sandstone dykes strike NE and dip steeply NW, are 1-2cm wide, and penetrate several metres of layered-facies strata to the edge of the outcrop. Similar sandstone dykes in the underlying Port Askaig Tillite were considered by Spencer (1971a) to post-date a period of compaction of the sediments. The nodules occur preferentially along the dyke, also spreading out along the bedding at intervals (fig. 7-41). This clearly demonstrates that these nodules, at least, could not have been anhydrite nodules. Also figure 7-34e shows that thin slivers of matrix are present between some nodules, demonstrating that this structure is not diagnostic of anhydrite nodules as was supposed in point (4) above.

Two final points can be made. Firstly, anhydrite nodules are commonly elongate parallel to bedding (Kerr & Thompson, 1963; Füchtbauer, 1974), which is not the case for any of the Bonahaven Formation nodules. Secondly, if the nodules were originally of anhydrite then one would have expected to have seen associated gypsum pseudomorphs, which elsewhere in the Dalradian are the only evidence of evaporites preserved (Llewellyn in Spencer, 1969; Anderton,

1975). Such gypsum pseudomorphs are not recognized in the Bonahaven Formation. Also, no inclusions of anhydrite or gypsum have been seen within the nodules, yet they are common in replaced sulphate nodules elsewhere (Tucker, 1976). In contrast, some microquartz is present within nodules.

The above evidence shows that the bulk of the nodules are not pseudomorphs of anhydrite nodules, but it is clearly impossible to prove that none of them are. The nodules are pre-tectonic and formed by replacement; the presence of rare microquartz and general geological considerations lead to a tentative conclusion that they were probably chert nodules.

As was mentioned earlier, not all nodules are like those just discussed. For example, in member 4, elongate or equant nodular areas are regarded as metamorphic, as they form ill-defined areas which appear to be the site of first development of a true metamorphic texture. In member 3 dolostones, all transitions are seen from scattered quartz and albite grains to small nodular aggregates presumably formed during deep burial or low-grade metamorphism.

The lineation-defining nodules often show some pressure fringe-type quartz, elongate phlogopite and annealed quartz. As their orientation is distinct, in bed 56D, from that of nearby deformed ooids in bed 54D, they are clearly not simply passively deformed pre-tectonic nodules, but the annealed textures show that they have suffered some strain. They are thus thought to be syn-tectonic, but the mechanism of their formation is uncertain.

The present mineralogy of the pre-tectonic nodules may

have developed to a great extent during deep burial, as albite, pyrite and quartz (recrystallized from chert ?) are suggested elsewhere to have formed then.

Calcite may well have formed at each of the following times:

- 1) during the calcitization episode
  - 2) during deep burial (? formed as Fe/Mg from dolomite enter phengite)
  - 3) during metamorphism as a result of the phlogopite-producing reaction (7.7.2)
- and 4) post-tectonically.

## 7.5: D<sub>1</sub> deformation: mechanisms and textures

### 7.5.1: Appropriate mechanisms

Theoretical and experimental studies of deformation by metallurgist and geologists have enabled predictions to be made concerning the mechanism by which a given mono-minerallic aggregate of a certain grain size will deform at various values of stress, temperature and strain rate. These predictions can be expressed as deformation mechanism maps (fig. 7-42; White, 1976; Rutter, 1976). The assumption is made that the mechanism which yields the fastest strain rate under a given set of conditions will be the one that dominates. It must be emphasized that the experimental studies assume a particular deformation geometry which may not resemble those in nature, and that certain data (e.g. diffusion co-efficients) are not well known for geological materials. Therefore the maps should by no means be taken as definitive.

Considering the Bonahaven Formation, a maximum temperature of about 400°C is indicated by the presence of

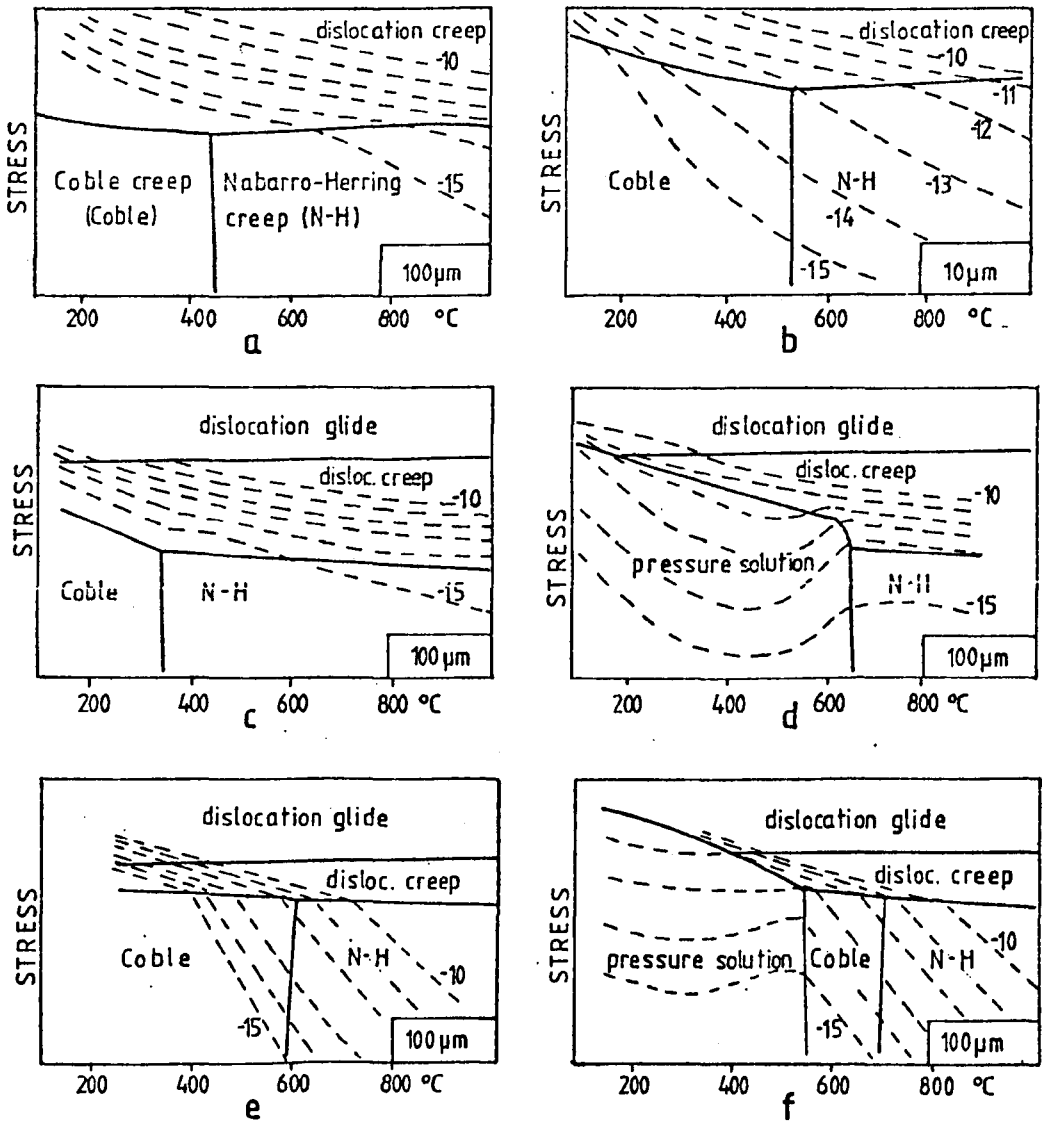


Figure 7-42: Published deformation mechanism maps for quartz and calcite. Geologically important strain rate contours are shown by the dashed lines. (units are  $\log_{10} s^{-1}$ ). Grain size is 100  $\mu m$ , except for b) which is 10  $\mu m$ . a,b) quartz with no pressure solution field (White, 1976). c,d) quartz without, and with, a pressure solution field (Rutter, 1976). e,f) calcite without, and with, a pressure solution field (Rutter, 1976). Note that a) and c) should be the same, but are not. This reflects the uncertainty of the data used to construct the maps.

phlogopite and the absence of talc in dolomitic rocks (Winkler, 1976). Appropriate geological strain rates are in the range  $10^{-10}$  to  $10^{-14}$   $\text{sec}^{-1}$  (Price, 1975; Heard, 1976). Under these conditions, the deformation mechanism maps indicate that:

- 1) Internal diffusion (Nabarro-Herring creep) should not be important for quartz or calcite.
- 2) Faster strain rates and larger grain sizes favour deformation by movement of dislocations, whereas slower strain rates favour grain-boundary-diffusion mechanisms (Coble creep or pressure solution).
- 3) Where pressure solution is an available mechanism, it is likely to be dominant.

Dislocation mechanisms producing the geologically important steady-state flow condition are, firstly, dynamic recovery, by which means grains develop undulose extinction, deformation lamellae and preferred optical and dimensional orientations, and secondly, dynamic recrystallization, when strain-free grains form and the texture tends to be randomized (White, 1973, 1976). The end product depends on the relative importance of these processes, but usually will be distinguishable from those produced by grain-boundary diffusion mechanisms (see below).

Diffusion by migration of lattice defects along grain boundaries (Coble creep) will produce a change in grain shape by loss of material in areas of high stress and addition in areas of low stress. The strain rate is inversely proportional to the cube of grain size, so becomes very important in very fine-grained mosaics. If an intergranular fluid is present then diffusion of material along grain boundaries in solution (pressure solution) will occur because this is

a faster process. This process will be aided in places where the grain boundary region is wider, such as between two grains with mismatched lattices e.g. quartz and mica (Elliott, 1973; Rutter, 1976). Grain boundary diffusion processes are recognizable by solution seams in areas of high stress, by overgrowths in regions of low stress, and by a lack of internal deformation of grains.

As a consequence of grain-boundary-diffusion mechanisms other effects would be expected. Pre-existing grains unaffected by diffusion will be rotated as the rock mass changes shape. Also, a degree of grain boundary sliding will occur so that voids do not open up. When strains are large, grain boundary sliding may become more important (Ashby & Verrall, 1973).

#### 7.5.2: Quartz

Pure quartzites in the area have a characteristic texture (fig. 7-43) of a mosaic of detrital grains which show undulose extinction, deformation lamellae and occasionally sub-grains. Dimensional preferred orientation of grains is weak, or absent, on visual inspection. At the margins of these grains are unstrained polygonal grains up to 50 $\mu$ m in size. This is the core and mantle texture of White (1976), produced by internal deformation by motion of dislocations coupled with rotation of strain-free sub-grains, and perhaps the growth of new grains at the boundaries of the original grains. In this case, the process has only proceeded part-way towards obliterating the sedimentary components.

Where micas are present, quartz-mica boundaries are planar and small mica beards occur suggesting that some

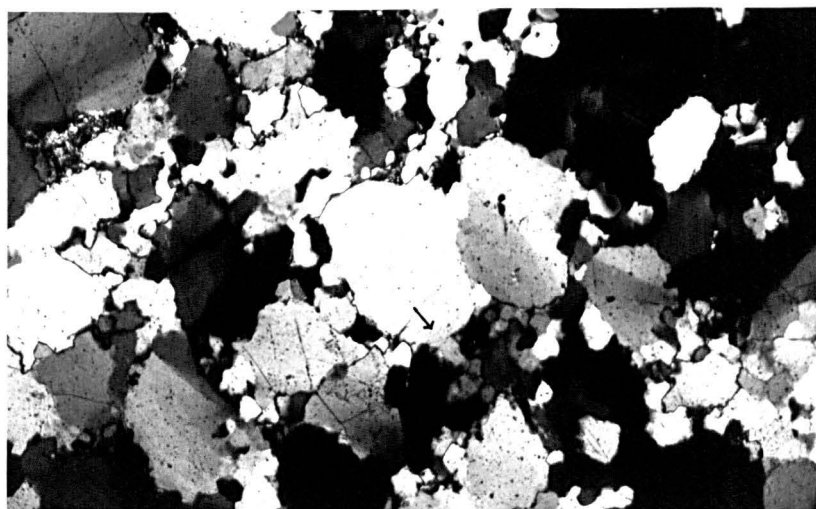


Figure 7-43: Photomicrograph, crossed polars, quartzite, member 2. Large detrital grains are surrounded by small metamorphic polygonal grains. Area shown by arrow is an overgrowth on a clast, separated by a dust line. This could be diagenetic, rather than tectonic as it occurs at a high angle to the (weak) tectonic elongation of the fabric (NE-SW). Some serrated grain boundaries could represent diagenetic solution.

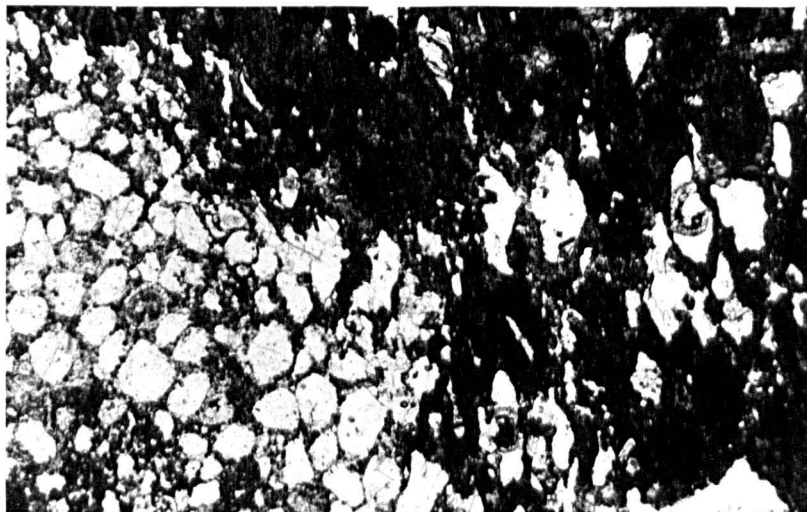


Figure 7-44: Photomicrograph, plane polarized light, bed 54D. Contact between quartzose and oölitic dolostone laminae. Quartz in the oölitic layer has suffered solution transfer and is markedly more elongate than quartz in the quartzose layers.

pressure solution may have taken place (Elliott, 1973), but in the purer rocks this is clearly not the major process.

Clear demonstration of the action of pressure solution on quartz grains encased in dolomicrite is shown (fig. 7-12) by the truncation of circular lines of inclusions (replaced oölitic structure) by the surrounding dolomicrite. Precipitation of quartz has occurred on the lee side of the grains overgrowing the pre-existing quartz. The two effects together (solution transfer, Durney, 1972) have produced a marked dimensional orientation of the former oöids.

In quartzose laminae the shape change is much less pronounced (fig. 7-44); the common development of strong undulose extinction and deformation lamellae suggests that internal deformation was important here. Similarly in dolomitic sandstones where the matrix has been patchily silicified quartz clasts set in microcrystalline quartz show much better developed internal strain features than do clasts in dolomicrite. The strain shown by the latter might well have been present when they were first incorporated in the sediment, as quartz clasts in the Bonahaven Formation are of igneous plutonic, or high-grade metamorphic origin.

In micaceous rocks quartz grains show evidence of pressure solution by their lack of internal deformation and in places very pronounced elongation (fig. 7-45). In sections parallel to cleavage quartz elongation is still present, although much less pronounced (fig. 7-46), and so has a linear, as well as a planar, component.

These observations support a suggestion of A. Morris (pers. comm.) that pressure solution is greatly inhibited

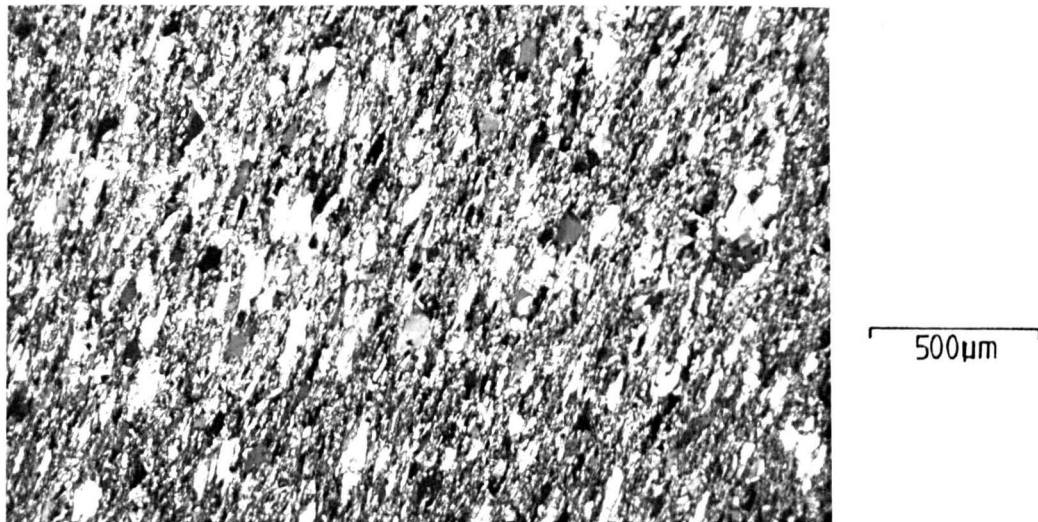


Figure 7-45: Photomicrograph, crossed polars, unit 5, member 4, Section D. Section perpendicular to cleavage in a silty slate showing pronounced elongation of quartz clasts due to metamorphic solution transfer.

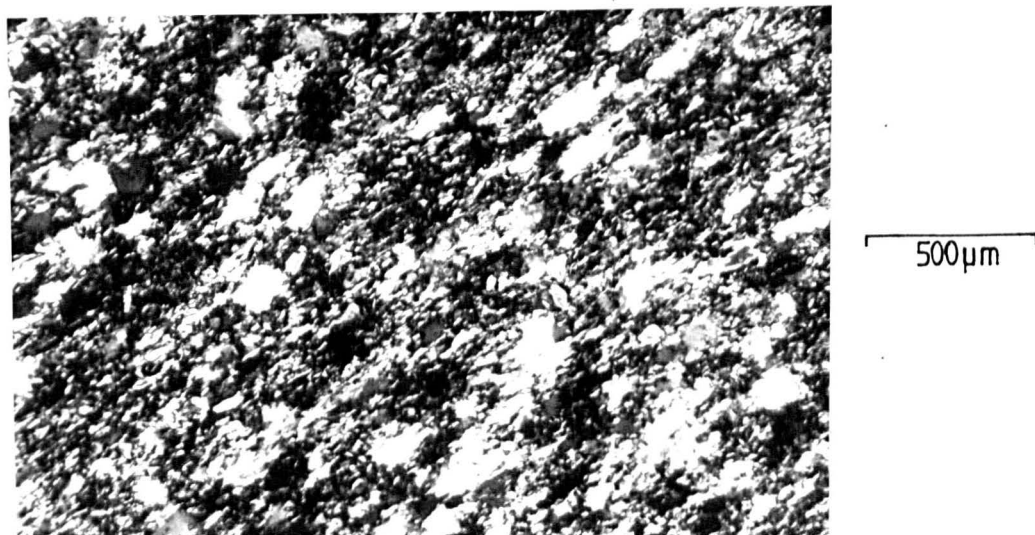


Figure 7-46: Photomicrograph, crossed polars; same specimen as figure 7-45, but in a section cut parallel to cleavage. Weak elongation of quartz clasts NE-SW is present. Most mica shows basal (near isotropic) sections, but the rest has the trace of (001) dominantly orientated parallel to the elongation of quartz clasts.

at quartz-quartz boundaries, because the effective grain boundary width (Elliott, 1973) is too small to allow diffusion of material in diffusion, but occurs readily at quartz-mica (and, one might add, quartz-dolomite) interfaces. Different deformation mechanisms may therefore be acting on different interfaces, which may be only a few microns apart. Such a state of affairs can potentially exist whenever a rock is deformed under conditions where pressure solution, but not Coble creep, can occur.

### 7.5.3: Dolomite and calcite

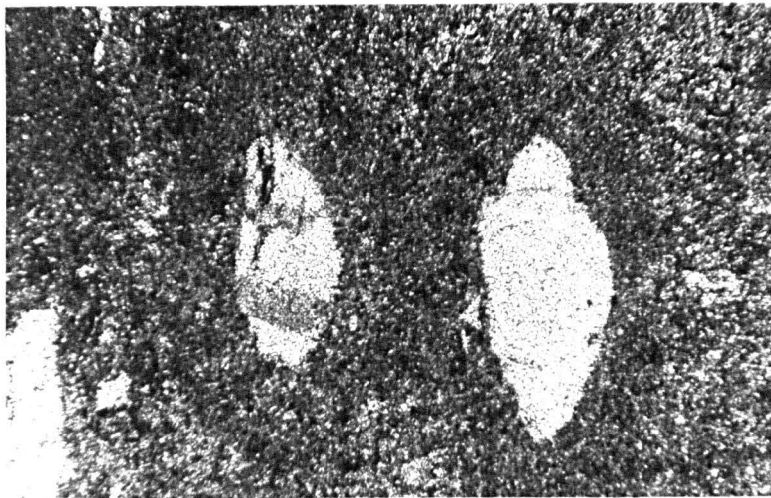
No deformation maps are available for dolomite, so the following discussion is based on the assumption that it behaves similarly to calcite. Extrapolation from the 100 $\mu$ m calcite map (fig. 7-42e) to 10 $\mu$ m calcite by comparison with the quartz maps (figs. 7-42a, b) suggests that conditions will be near the boundary of Coble creep and dislocation mechanisms, although Coble creep will become increasingly important as smaller grain sizes still are considered.

Observations on a 10 $\mu$ m dolomicrite mosaic from member 3 (figure 6-4) showed that a (weak) preferred dimensional orientation is present (p99). The grains do not show marked undulose extinction, although some apparent subgrains are present. These observations are insufficient to decide on the deformation mechanism: the critical information required is data on the presence or absence of a preferred optical orientation of crystals.

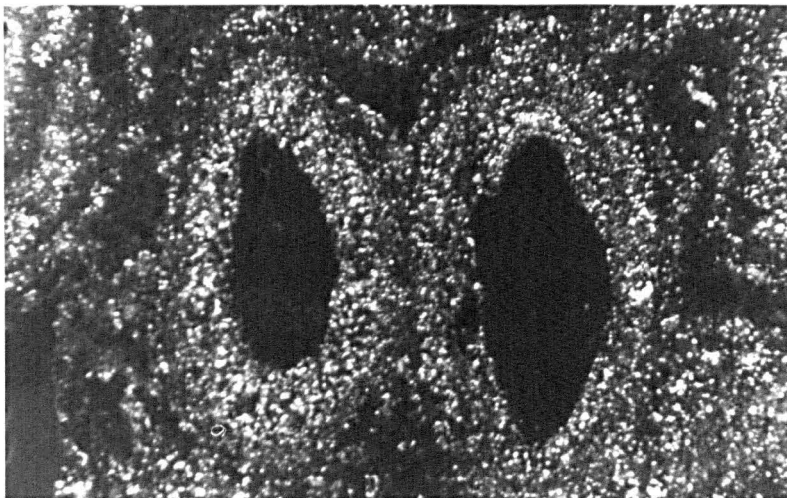
For calcite, a pronounced preferred shape orientation of crystals is present in some mosaics suggesting grain boundary diffusion has occurred as there is no evidence of

internal deformation. Generally calcite grains show little evidence of deformation apart from twinning in larger (100 $\mu$ m) grains, although this is not a constant feature. Grain diminution along twin planes is absent, although important elsewhere (Bathurst, 1971; Tucker & Kendall, 1973).

Special conditions may well have existed within the oölitic dolomicrite envelope around presolved quartz (fig. 7-47). The envelopes have plastically deformed so that their inner margins conforms with the changing shape of the quartz inside. Measurements from bed 54D in sections parallel to the elongation of the oöids shows that the average of the axial ratios of the elliptical quartz cores (approx. 2.3) is consistently higher than the average axial ratio of the outer margin of the envelope (approx. 1.9). Thus the state of strain within the envelope might be expected to have been at its greatest on its inner margin. An illustration of part of a mosaic in this position is shown in figure 7-48. Estimates of the proportion of the grains which, in a particular position, define the pseudo-uniaxial cross of the oöid can be used as an index of how much the optical orientation of the dolomite has been modified by the deformation. None of the dolomite crystals are strained, but many apparent sub-grains are present as can be seen on the diagram. However adjacent crystals must have differed very little in their optical orientation before deformation because of the pseudo-uniaxial cross structure. The apparent sub-grains present thus probably existed as separate crystals before deformation and so are not deformational sub-grains. The strong visual impression, especially in figure 7-48b, is that immediately next to the quartz core there are fewer grains



a

200 $\mu$ m

b

Figure 7-47: Photomicrographs, bed 54D. a) plane polarized light; b) luminescent light. Two ooids are shown; they exhibit a core replaced by quartz within which circular inclusion trails are visible in a). This core has later suffered solution transfer and is now elongate (see also figure 7-12). Around the core is the outer envelope of the ooid (seen most clearly in b)). This envelope has deformed concordantly with the core.

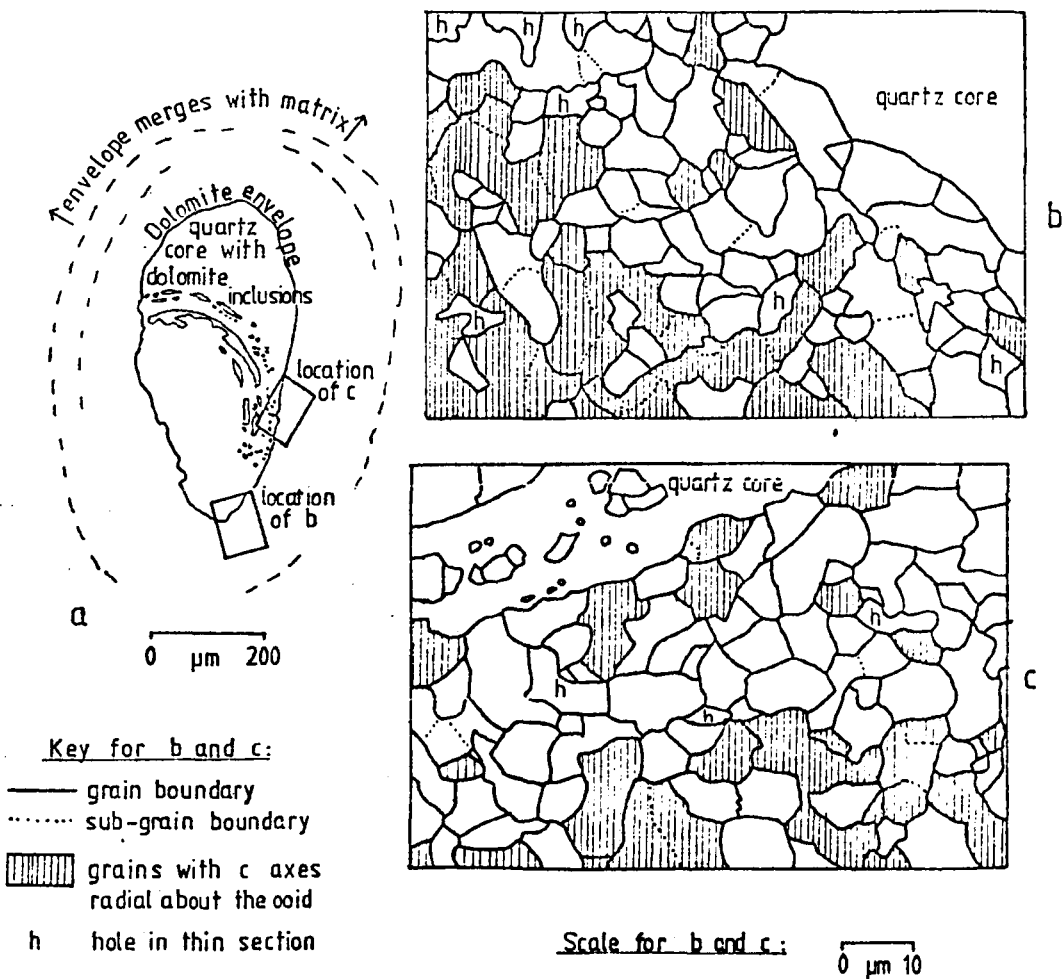


Figure 7-48: Dolomite mosaics on the inner margin of a dolomite envelope around the quartz-replaced core of an ooid which has deformed by pressure solution. a) line sketch of ooid. b,c) drawings of mosaic (see Appendix B2 for methods).

in their pre-tectonic orientation than further from the quartz core. This suggests that more rotation of grains or growth of new grains has occurred next to the core. One interesting possibility is that as the quartz core rapidly changed shape by pressure solution, the dolomite around it was forced to deform quickly, and did so by diffusion-controlled grain boundary sliding which Ashby & Verrall (1973) indicate is faster than creep when strains are large. This would readily explain the loss of the pseudo-uniaxial cross structure next to the core and the apparent lack of internal deformation of the crystals.

#### 7.5.4: Cleavage

Cleavage is defined in the micaceous rocks by a preferred orientation of phengite, and occasionally phlogopite, and varies between localities from weak development to the extremely well-developed fabric of figure 7-45. Disagreement exists in the literature as to whether the degree of preferred orientation of micas relates directly to the amount of strain the rock has suffered (Tullis & Wood, 1975; Siddans, 1976). In the Bonahaven Formation larger sedimentary micas remain nearly parallel to bedding which implies that the cleavage-defining micas grew near to, or within their present orientation, as has been concluded elsewhere (Holeywell & Tullis, 1975; Etheridge & Lee, 1975). A simple relationship between degree of development of cleavage and total strain thus seems unlikely here.

In well cleaved rocks where original detrital grains are difficult to recognize a more or less well developed domainal structure is present. This is composed of micaceous domains separated by polycrystalline lenses of quartz

and albite.

Linear structures within the cleavage plane (pressure fringes, mica beards, presolved detritus, deformed ooids and elongate clusters of pyrite crystals) contribute towards the definition of the cleavage in sections at right-angles to it. The mica fabric too has a linear component. This is seen in sections parallel to the cleavage where, in addition to the abundant basal sections of mica (planar component of cleavage), there are common mica laths with the trace of (001) dominantly parallel to pressure shadows (linear component of cleavage, fig. 7-46)

In the anomalous area at the western end of section D, two stages of deformation have occurred within D1. A slaty cleavage similar to that described above is cut across by foliae composed of mica concentrated by pressure solution (fig. 3-9). Because there is no associated buckling this structure might be called a pressure solution cleavage rather than a crenulation cleavage (Cosgrove, 1976).

#### 7.5.5: Mica beards, pressure fringes and quartz seams

The structures covered in this section are:

- 1) bridges and lenses of quartz and mica occurring between and around detrital grains in muddy sandstones and conglomerates. These structures have been called pressure shadows by Spry (1969) and Powell (1969), and mica beards by Williams (1972a, b) and Means (1975).
- 2) fibrous or equant growths of clean quartz next to pyrite or other grains. These are the pressure fringes of Spry (1969) and Hills (1972), the pressure shadows of many authors (e.g. Pabst, 1931; Durney & Ramsay, 1973) and the strain shadows of Borradaile (1973, 1977).

As this usage is conflicting, I shall use mica beards for (1) and pressure fringes for (2).

3) fibrous or equant growths of quartz, and sometimes calcite, forming veins that parallel bedding. These are here called quartz seams (a convenient field term) and are considered to be equivalent to the fibrous veins of Durney & Ramsay, which are analogous to pressure fringes.

#### 7.5.5.1: Mica beards

Proceeding outward from a quartz clast with a well-developed mica beard (figs. 7-49, 7-52d) there is a distinct line of dust and variably orientated white mica, then an area of quartz and mica where much of the quartz is optically continuous with the detrital grain, and finally a region of intergrown fine-grained quartz and mica. The mica tends to have (001) perpendicular to the margin of the detrital grain, and this preferred orientation improves away from the grain, the structure merging with the matrix distally. On the side of the grain lacking the mica beard, the mica defining the cleavage is relatively concentrated compared with the bulk rock matrix. The beards are lineations because they occur in only one orientation in sections parallel to the cleavage. In such sections, birefringent mica laths with the trace of (001) perpendicular to the grains are seen, as well as basal sections, but such laths seem to be in no greater abundance compared with the basal sections than in the surrounding matrix. The mica fabric in the outer part of the beards thus seems to be closely similar to that of the matrix.

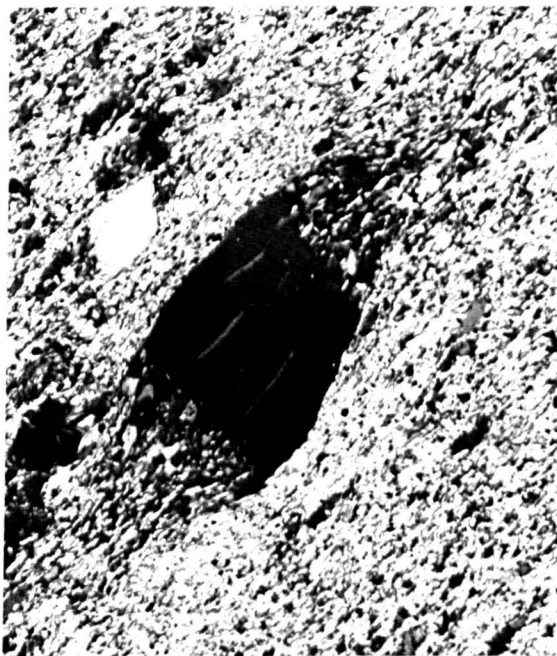
Williams (1972b) could not decide whether the mica beards he described were diagenetic structures (developing initially



Figure 7-49: Photomicrographs, unit 1, member 1, Section B. They show a mica beard around a quartz clast under a) plane polarized light, and b) crossed polars. The section is perpendicular to cleavage. The trace of the cleavage runs NE-SW. The beards are described in the text.

200 $\mu$ m

a



b

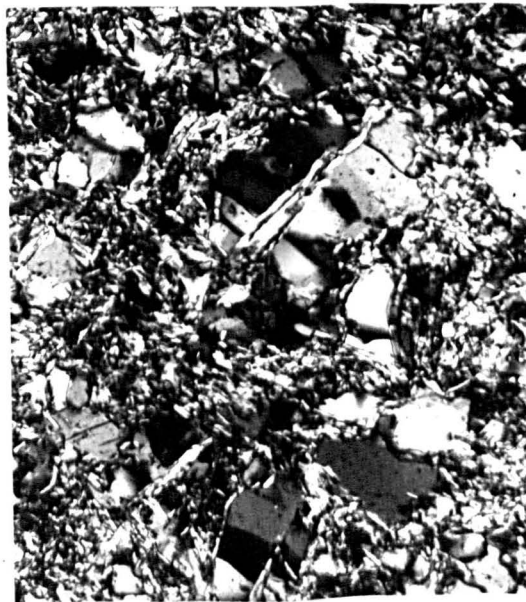


Figure 7-50: Photomicrograph, crossed polars of muddy siltstone, unit 1, member 4, Section E. Bedding-parallel mica flakes (NE-SW) have quartz pressure fringes ('quartz beards'). Cleavage trace runs NW-SE.

200 $\mu$ m

all round the surface of the grains, then later becoming 'wiped off' on the sides parallel to cleavage during deformation), or whether they were syn-tectonic and not subsequently modified. This uncertainty arose because the mica appeared to be equally abundant in all orientations which had (001) perpendicular to the detrital grains, suggesting the absence of a significant stress-field during formation of the beards. Although he cited various occurrences of radially orientated clay cements around detritus to support the idea that mica beards could form diagenetically, it is the intergrowth of mica with quartz that gives the beards their distinctive character. Such a fabric has apparently only been described from the Harlech Dome (Woodland, 1938), where radial chlorite and sericite flakes appear to penetrate detritus, but more work is needed on this occurrence. In the Bonahaven Formation, the presence of a dusty line at the proximal end of the beard is evidence that overgrowth on, rather than corrosion of detrital quartz by mica has occurred. This observation leads to an interpretation of the beards in terms of tectonic solution transfer about the clast:

- 1) Solution of the quartz clast and, to judge from the concentration of mica next to the clast, solution of quartz in the surrounding matrix occurred in regions of high stress.
- 2) This material was re-deposited in a region of extension in the lee of the quartz clast, partly by overgrowth, and partly by growth of new grains. Mica grains which nucleated in this area have a preferred orientation which reflects the stress field at any point; this preferred orientation improves away from the clast, merging with the matrix as the sheltering effect of the clast diminishes.

This interpretation suggests an analogy of these structures with pressure fringes (see next section) which thus implies growth of beards during deformation.

#### 7.5.5.2: Pressure fringes (figs. 3-15, 7-32, 7-37, 7-50 to 7-52)

Pressure fringes form by the same process (solution transfer) that leads to the elongation of quartz grains in dolomitic rocks. Durney & Ramsay (1973) have shown that where the grain on which growth occurs is of the same mineralogy as the fringe, growth is syntaxial; that is, material is added in optical continuity to the grain, at the distal end of the fringe. Examples are calcite fringes on crinoid stems, or, in the Bonahaven Formation, quartz growth on quartz-replaced oöids (fig. 7-12). Conversely, antitaxial growth (crystallization next to the rigid object) occurs where the mineralogy of host and fringe is different. The classic example of this is growth of fringes around pyrite or magnetite porphyroblasts, where antitaxial growth is proved (Pabst, 1931; Fairbairn, 1949; Elliott, 1972) by the correspondence of fringe shape to that of the porphyroblasts, and by details of the internal texture of the fringe.

Some dolomitic rocks in the Bonahaven Formation show fringes about nearly all detrital grains, e.g. K-feldspar and dolostone pebbles (figs. 7-32, 7-52c). Also quartz (occasionally dolomite) overgrowths on elongate, bedding parallel micas (fig. 7-50) are common; features which Means (1975) called 'quartz beards'. The square-ended shape of many of these 'quartz beards' indicates that these are, as expected, antitaxial growths.

Fringes about pyrite often show quartz with the pronounced dimensional orientation perpendicular to pyrite faces

emphasized in the literature (Elliott, 1972; Durney & Ramsay, 1973; fig. 7-52a) although such elongation is lacking in some cases (fig. 7-51). This lack of elongation is thought to be primary, since quartz in fringes never shows signs of strain sufficient to initiate subsequent recrystallization. Quartz shows no sign of a preferred optical preferred orientation. This situation has been well established for fringes in general (e.g. Pabst, 1931; Fairbairn, 1950; Durney & Ramsay, 1973). Calcite and phlogopite also occur in the fringes: where the calcite is elongate perpendicular to the nearest pyrite face, or phlogopite has (001) parallel to the face, as is often the case, then they can be taken to be original fringe minerals (Fairbairn, 1949; Spry, 1969); otherwise a secondary replacement origin cannot be ruled out.

Mica beards and pressure fringes are considered to be genetically related (as suggested previously, but only in passing, by Means, 1975). Both are solution-transfer phenomena: the difference between them is thought to lie in the competence and relative competence of rigid grain and matrix. Fringes have been related to the pulling away of the matrix from a rigid object with crystallization in an incipient void (Spry, 1969; Hills, 1972), whereas no such suggestion has been made for mica beards. However, extension of the matrix in the region of the beard must have occurred during deformation. That this extension did not lead to the formation of an incipient void in the case of the beards seems to be shown by the abundant mica in the beards: beards represent matrix diluted by quartz provided by pressure solution. Why was no incipient void formed? The answer may be that neither the matrix, not the clasts had sufficient rigidity for this to occur. Clasts in dolomicrite matrix

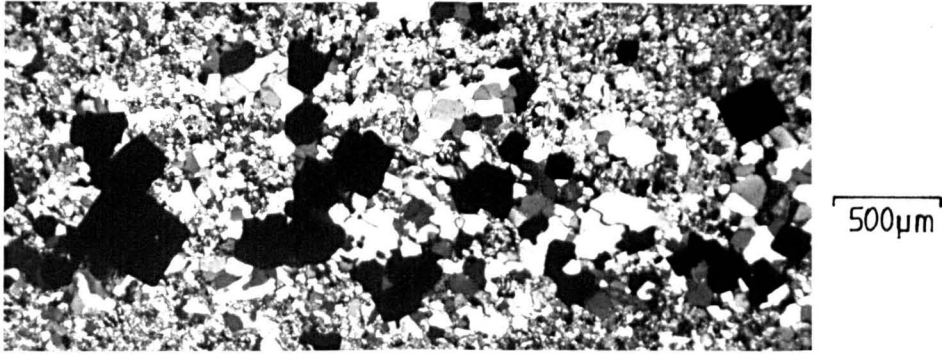


Figure 7-51: Photomicrograph, crossed polars, bed 460. Pyrite (black) shows pressure fringes of unelongate quartz.

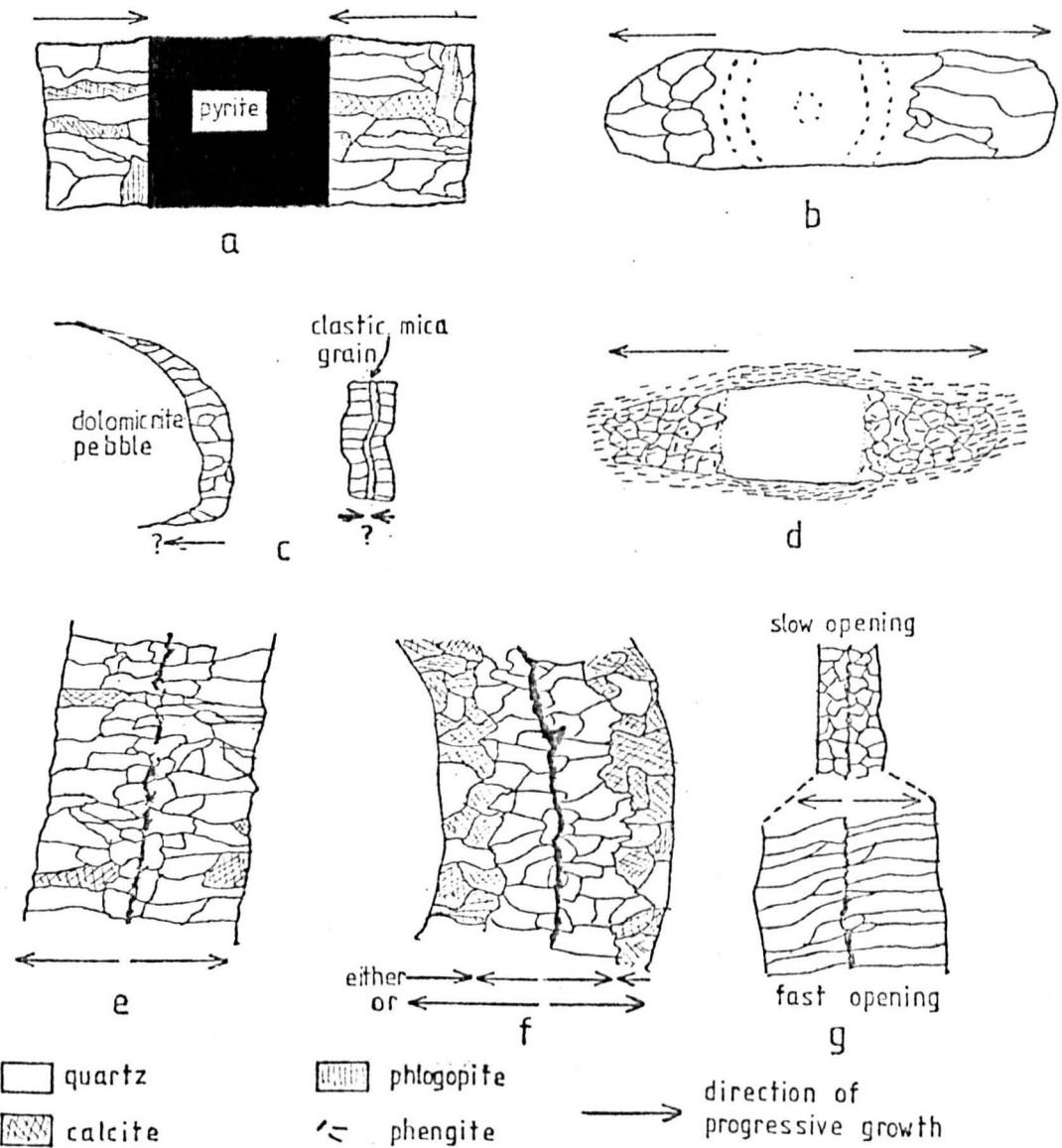


Figure 7-52: Idealized sketches of pressure fringes (a, b, c), mica beards (d) and quartz seams (f, g). The tip of the arrows of progressive growth represent the point at which new growth occurs.

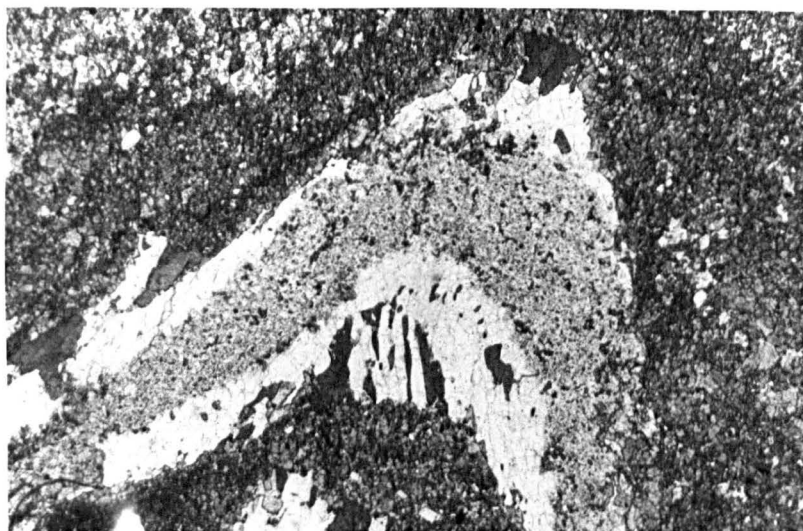
have clean fringes rather than an intergrowth of quartz and dolomite suggesting that a dolomicrite matrix does have sufficient rigidity to pull away from the clasts. Pyrite invariably has fringes rather than beards because of its high rigidity: it does not suffer solution as the quartz clasts do. Structures intermediate between mica beards and fringes may be expected in other lithologies. An example may be provided by Mosher (1976) who described quartzite pebbles on which is grown elongate quartz which contains 5% mica with (001) parallel to the elongation of the quartz.

#### 7.5.5.3: Quartz seams (figs. 3-14 to 3-17; 7-52 to 7-55)

Quartz seams from 90 samples, most of them stromatolites, have been studied. In Chapter 3, their field aspects, their use in determining the tectonic extension direction, and the presence of curved crystals are described.

##### 7.5.5.3.1: Description

The seams invariably contain inclusion-free quartz, and frequently calcite; crystals are usually elongate (fig. 7-53) in a direction which is at a high angle to the seam walls. However whole seams, or areas of equant quartz occur (fig. 7-54). Also where the bedding dips at a high angle, as on the flanks of stromatolite domes, elongation may be nearly parallel to seam walls (fig. 7-55). Two-dimensional studies show no suggestion of a preferred optical orientation of quartz: this is the same situation as exists in pressure fringes. As in fringes, the quartz in the seams is either unstrained, or only very slightly strained. Most seams contain a central parting away from which crystal size tends to increase. The parting is either a zone of inclusion-rich



a

1mm



b

Figure 7-53: Photomicrographs, bed 25E (stromatolite horizon E4). a) plane polarized light; quartz seam at crest of stromatolite dome. There is a wide central parting of inclusion-rich quartz and albite. This is flanked by quartz (white) with some calcite near the margins, some visibly elongate. Matrix is dolomicrite. b) crossed polars. Elongation of crystals is more pronounced when the seam is wider.

quartz and albite (fig. 7-53), or an incipient (fig. 3-12), or well-developed stylolite. The seam walls, and to a lesser extent the central parting, are approximately parallel to one another, although they do not match precisely. In cases where a central parting is absent the seams are thin and most of the crystals extend across the whole width of the seam. This is the usual type of seam developed at lithological boundaries such as between dolomitic sandstone and dolomicrite, or dolomicrite replaced by inclusion-rich quartz and albite (fig. 7-32).

Where calcite is present in a seam it may be restricted to a zone next to the walls, or be scattered throughout. In one sample, which shows seams developed in a calcitic stromatolite (fig. 7-54), calcite forms a continuous zone adjacent to the walls and is seeded onto crystals in the walls. This differs from the usual case in two respects: firstly, the seam walls are generally dolomite, which is so fine-grained that seeding or lack of seeding could not be demonstrated; and secondly, calcite does not usually form a continuous wall zone, but is interleaved with quartz.

Seams are regarded as distinct from the following structures which have some similar characteristics:

- 1) parallel-sided, or irregular veins which occur either oblique to, or parallel to bedding. Their mineralogy is more variable than the seams as quartz, calcite, albite, phlogopite and barytes are common, although the last two do occur very rarely in seams. Abundant irregular areas of included dolomite are present contrasting with the linear central partings of seams. Some of these veins are definitely pre-tectonic because they have highly strained quartz and/or well-twinned calcite.

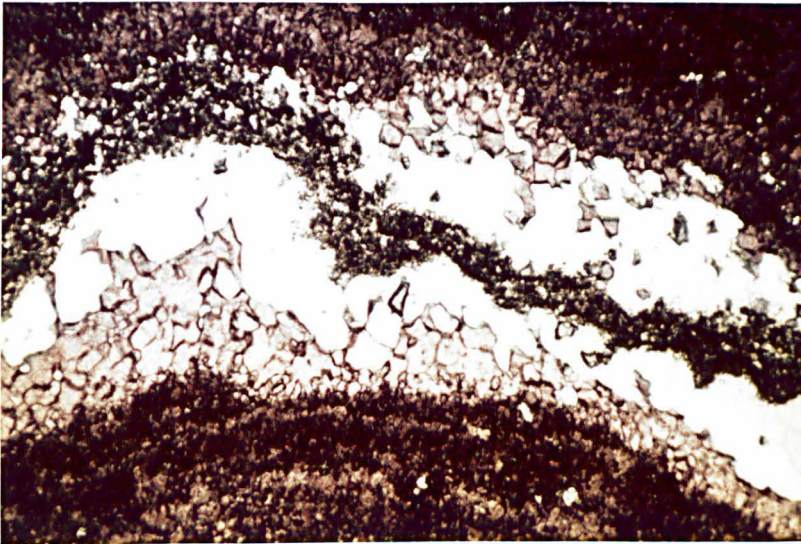


Figure 7-54: Photomicrograph, plane polarized light, bed 25B (stromatolite BIII): Quartz seam in calcitic stromatolite. An obvious central parting of ?solution residue, parallel to the stromatolitic lamination, is visible. Calcite (pink) within the seam only occurs near to the seam wall and is seeded onto calcite of the wall-rock. This is a composite seam (Durney & Ramsay, 1973).

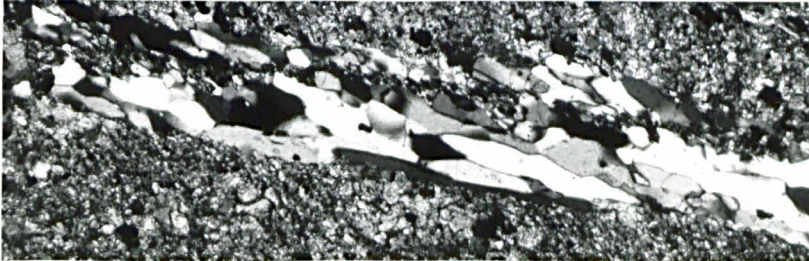


Figure 7-55: Photomicrograph, plane polarized light, bed 25E (stromatolite E4). Quartz seam on flanks of stromatolite dome showing elongation of crystals nearly parallel to the seam walls.



Figure 7-56: Photomicrograph, plane polarized light, unit 1, member 1.  $S_2$  crenulation cleavage bands are visible (N-S). There is some chlorite preferentially associated with the cleavage band.  $S_0$  and  $S_1$  both dip shallowly to the right in the photograph.

2) clusters of elongate calcite grains in some phlogopite-bearing rocks. These do not form distinct or parallel-sided entities.

#### 7.5.5.3.2: Interpretation (fig. 7-52e,f,g)

A comparison is now made between the structures described and the fibrous veins of Durney & Ramsay (1973), which are dilational structures, crystal growth keeping pace with the opening of the vein. Durney & Ramsay distinguish

- 1) syntaxial veins, where growth took place inwards from the walls (see also Raybould, 1975);
- 2) antitaxial veins, where new material is added next to the vein walls, and
- 3) composite veins, where both antitaxial and syntaxial growth has occurred.

Most seams are regarded as antitaxial veins because:

- 1) they are approximately parallel-sided, and contain elongate crystals which are generally free of inclusions, especially at the seam walls.
- 2) they contain central partings which are approximately parallel to seam walls. These central partings represent petrographic entities which exist independently of seams (fig. 7-30), and preceded their formation. The central partings acted as lines of weakness which determined the course, and probably the very existence of the seams.
- 3) crystals increase in size away from the central parting and are of different mineralogy from the seam walls.

Regarding seams containing calcite, the seams in the calcitic stromatolite of figure 7-54 are probably composite because there is a central parting present, away from which quartz grew; and calcite seeded onto, and therefore grew away from the seam walls. Other seams where

calcite is restricted to the wall region, but is intergrown with quartz, may be due to either

- 1) antitaxial growth where first quartz, then calcite and quartz crystallized or
- 2) composite growth with quartz growing outwards and quartz and calcite growing inwards.

In some seams equant calcite is post-tectonic, being related to veining. This is shown by either

- 1) calcite occurring in a seam only near to the region where a post-tectonic calcite vein crosses the seam, or
- 2) by a particular zoning common to both seam calcite and calcite in post-tectonic veins or vugs.

The similarities enumerated above between quartz seams and the fibrous veins of Durney & Ramsay (1973) strongly suggest that they have essentially the same origin.

The differences between them can now be examined in this light.

Firstly, consider seams which lack a central parting or internal discontinuity of any kind. There are all transitions between such seams and pressure fringes, the most common intermediate case being quartz growth off dolostone pebbles. A central parting is lacking because growth was in one direction only.

Secondly, the lack of a perfect fit between seam walls suggests that either some replacement, or some dissolution of the walls has occurred in addition to the dominant dilational factor. Perhaps this may be a feature of veins developing in deep-seated situations.

Thirdly, a dimensional orientation of crystals is not always present. However, this is also a feature of some pyrite fringes. Figures 7-52g and 7-53 suggest a possible

reason for this. Where the seam illustrated is relatively narrow, elongation is poor compared with the wider parts of the seam. This suggests that the rate of opening of the seam may control the elongation of crystals, less nucleation of new crystals occurring when the opening is rapid.

The fact that the orientation of elongate crystals may be at any angle to the seam walls at any stage in their growth reflects the fact that the orientation of the seam was controlled by pre-existing lines of weakness which were parallel to bedding. It is only where dilational veins develop in an isotropic, or practically isotropic medium (e.g. Raybould, 1975 and most of the examples in Durney & Ramsay, 1973) that the length of the vein will be parallel to the compressive stress at the time of fracturing and that the first increment of crystal growth will show crystal elongation at right angle to the seam walls.

A further comparison may be made with fibrous gypsum veins or other veins where a degree of preferred optical orientation of crystals occurs (Shearman et al., 1972; Phillips, 1974). This optical orientation may be due to a rate of opening of the veins sufficiently rapid that only favourably orientated crystals can keep pace with the opening (Pabst, 1931) and/or if tensile strain crystallization (Phillips, 1974) operated. Neither of these conditions were fulfilled in the case of the quartz seams, just as for pressure fringes.

A word of caution concerning the interpretation of elongate crystal fabrics seems appropriate. Even in parallel-sided veins, the development of crystal elongation does not necessarily mean that there was dilation. For example Shearman et al. (1972) described gypsum veins within

anhydrite-rock which have such a texture, but are clearly replacive because they contain abundant inclusions of anhydrite showing unit extinction matching that of the wall-rock. Also, Finlow-Bates (1977) showed how a fibrous texture can develop through strain by movement of a front of dissolution-reprecipitation replacement. The clusters of elongate calcite crystals forming irregular masses that were described earlier may have formed in an analogous way.

#### 7.5.5.3.3: Conclusions

Syn-tectonic veins with a dominant dilational component need not have walls which precisely match, nor need they have a fibrous texture. This extends the guidelines for the recognition of such veins by Durney & Ramsay (1973).

Where there is a fibrous texture in the veins (seams) described here the crystal elongation may be at any angle to the vein walls at any stage in the crystal growth. This rule will apply to all other dilational veins whose orientation is controlled by lines of weakness (in this case parallel to bedding) that are unconnected with the tectonism.

A fibrous texture alone does not demonstrate dilation.

In the Bonahaven Formation replacive veins not only lack a central parting of any kind, but contain irregularly distributed inclusions similar to the wall rock. They also bear albite, which is absent from the quartz seams, apart from some of their central partings.

#### 7.6: D<sub>2</sub> deformation

As was mentioned in Chapter 3, the effects of D<sub>2</sub> are minor. In thin section, crenulation cleavage is developed occasionally in samples where the primary deformation has

produced a good alignment of phyllosilicates. The essential features are a series of microbuckles (Cosgrove, 1976) which usually, but not invariably show metamorphic differentiation. As a result the short limbs of the microfolds, which are the clearest expression of the crenulation cleavage, are often pure mica (fig. 7-56). The buckles develop next to nodules or lithological discontinuities. The micaceous limbs are sometimes the site of concentrations of chlorite. As chlorite would be expected to migrate away from these limbs during the development of a crenulation cleavage (Cosgrove, 1976), the chlorite probably post-dates  $S_2$ . Very occasionally, around pyrite crystals and nodules, are pressure fringes which formed during  $D_2$ , rather than  $D_1$ .

## 7.7: Metamorphic mineralogy

Albite and pyrite are described in section 7.4 together with a brief discussion of phengite. Other minerals which are syn- or post- $D_1$  are described in the present section.

### 7.7.1: Chlorite

Light green chlorite occurs in member 1 as rare laths (some elongate parallel to  $S_1$ ) or shapeless grains, or aggregates of grains up to 100 $\mu$ m in size. As detrital chlorite occurs in the Port Askaig Tillite, a similar origin must be considered in this case. Although some is equivocal, most chlorite is not thought to be detrital because it shows no direct size relationship with clastic quartz (criterion of Williams, 1972a) and is absent in unit 3 of member 1 where pebbles like those in the Port Askaig Tillite are abundant.

Those crystals growing parallel to  $S_1$  could be syn- $D_1$

or post- $D_1$  (growing mimetically); the latter age seems most likely for the anhedral grains. Some chlorite is post- $D_2$  as was demonstrated in the last section.

Yellowish chlorite occurs very rarely in members 1 and 3 as stubby laths, principally in nodules. Age relations are uncertain except where it occurs along crenulation bands as noted in section 7.6.

#### 7.7.2: Phlogopite

Phlogopite has fairly common, but sporadic, occurrence especially in dolomitic rocks of member 3. It occurs extensively in some dolomitic rudites (fig. 7-57) where it directly replaces dolomite and occurs interstitially and within inclusion-rich quartz and albite. Dolomitic sandstones and siltstones, and stromatolites may also bear phlogopite.

Most commonly it forms stubby laths or anhedral grains with no preferred optical orientation. In contrast, it can form sparse trains of elongate grains (along which the rock may split) in the massive dolostone (unit 3) of member 4. Also, in pelitic domains, phlogopite does show a degree of preferred optical and shape orientation parallel to  $S_1$  (figure 7-58), although never to the same degree as phengite. The phlogopite varies in colour in the maximum absorption position from colourless, in iron-poor dolostones, through a light yellow-brown in most dolomitic rocks, to a greenish-yellow in slightly calcareous pelites.

Phlogopite in pressure fringes with (001) parallel to the nearest pyrite face is syn- $D_1$ . The age of other phlogopite is less certain, but both syn- and post- $D_1$  growth may have occurred: this would account for the variability in degree of preferred orientation of crystals. There is no positive

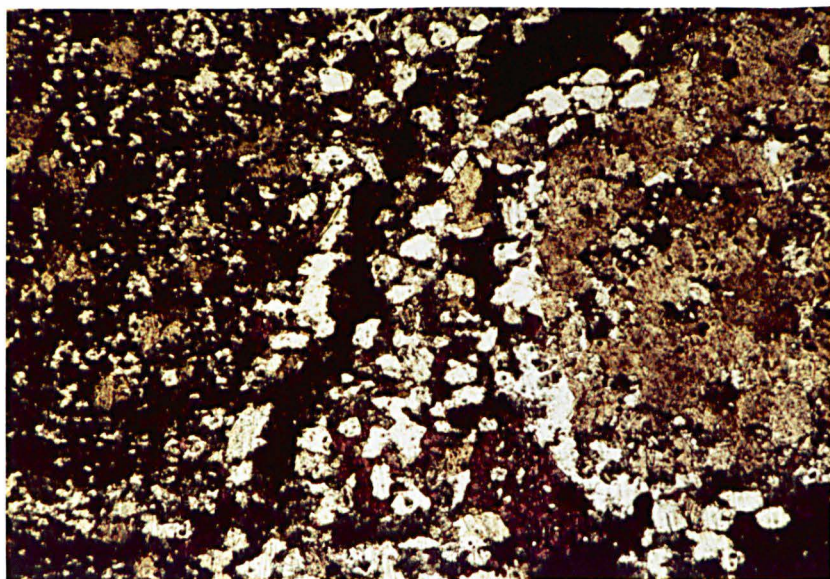


Figure 7-57: Photomicrograph, plane polarized light, bed 38D, a breccia of dolomicrite flakes. To the left, a dolomicrite flake has been partly replaced by phlogopite (yellow); to the right, a clast has been nearly totally replaced by phlogopite. The phlogopite shows no preferred optical orientation, and is anhedral.

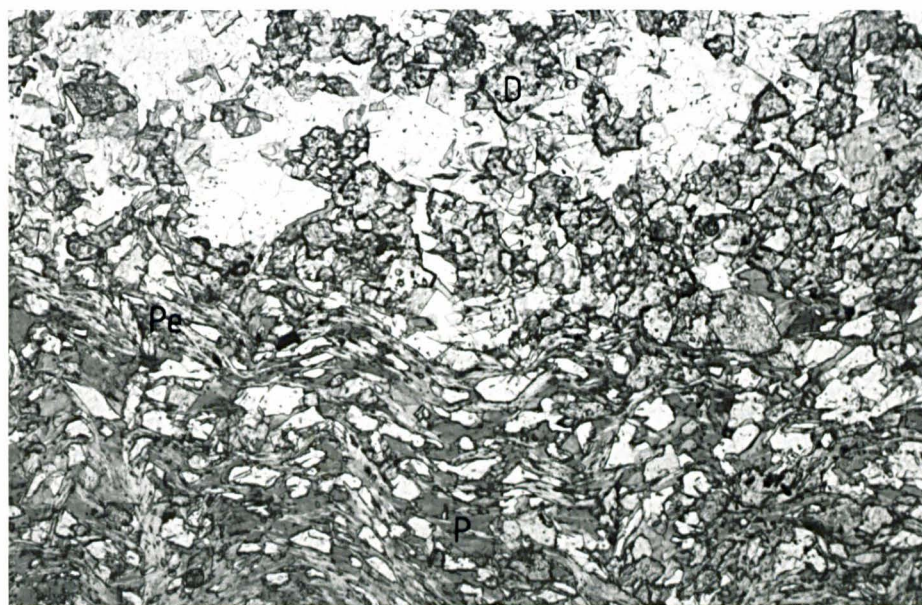
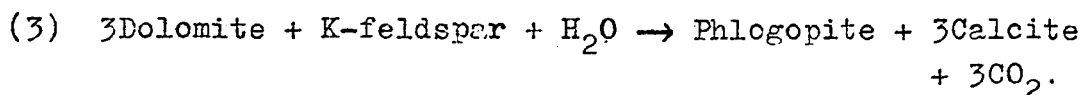


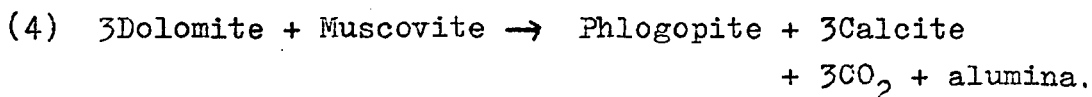
Figure 7-58: Photomicrograph, plane polarized light, unit 2, member 4, Section D. A pelitic lamina (below) shows well-developed  $S_1$  with  $S_2$  crenulations. Both phengite (Pe, light grey) and phlogopite (P, mid-grey) define  $S_1$ , although phengite shows this more clearly. At the top of the photograph is a more dolomitic lamina with subhedral or euhedral domomite (D) whose present texture is probably metamorphic.

evidence (kinking, annealing) that phlogopite was present pre-D<sub>1</sub>.

The usual phlogopite-producing reaction (Winkler, 1976) is:



An alternative (Deer et al., 1962) is:



Reaction (4) is not thought to be appropriate as the expected product, either corundum or spinel, is not seen.

For reaction (3), the higher the partial pressure of CO<sub>2</sub>, the higher will be the temperature necessary to make the reaction go to the right. As CO<sub>2</sub> is then produced, the reaction is clearly self-limiting and will stop unless temperature rises further. The sporadic occurrence of the mineral could be explained by the partial pressure of CO<sub>2</sub> varying from place to place. In some samples, K-feldspar and dolomite are in contact and have not reacted. In other samples, near the base of member 4, phlogopite is associated with calcite, but dolomite is absent. If reaction (3) had operated then it must have gone to completion, in which case some K-feldspar would be expected. This is not seen generally, but could have been albitized subsequently. Modal calcite, which might be expected from reaction (3), is not always present with phlogopite; movement of volatiles out of the rock must be proposed (see also 7.7.3 and 7.7.5).

Although there are some problems with reaction (3), they are not insurmountable. The very simple mineralogy of many phlogopite-bearing rocks seems to leave no alternative to this generally-accepted reaction.

### 7.7.3: Biotite

Biotite occurs in member 1 (units 1 and 2). This is

TABLE 7-2

	1	2	3	4	5	6
Sample number	290021	548097	986863	051897	060897	467370
Member/bed or unit	1/unit1	1/unit2	4/unit1	3/13D	3/13D	3/39B
Lithology	silty slate	sand and mudstone	sand and mudstone	dolomitic sand and muddy dolostone	sandy flake breccia	partly calcitized stromatolite
Mineralogical mode	P,Q,X, C,Ab,O	Q,P,Y, Ab,C,Cc, ?K,O	P,Q,X, Cc,Ab,Py	P,Q,D,Cc, X,K,Py	D,Cc,Q, K,Ab,X, Py	Cc,D,Q, K,X,Py
Phlogopite/biotite						
Colour (with basal cleavage E-W)	dark green	dark green	yellow-green	deep yellow	yellow	colourless
wt.% Fe	16.6	11.5	n.d.	6	0.6	0.4
wt.% Mg	7.7	10.2	n.d.	10.8	16.6	18
Molar ratio Mg/Fe*	1	2	n.d.	4	60	100
Whole rock analysis (wet chemical)						
SiO <sub>2</sub>	64.14	78.22	70.22	55.97	22.42	10.08
Al <sub>2</sub> O <sub>3</sub>	17.69	11.50	13.37	9.74	3.16	2.72
TiO <sub>2</sub>	0.64	0.33	0.42	0.27	0.13	0.06
FeO (total Fe)	3.58	1.76	2.41	2.14	1.54	0.81
MgO	5.18	1.75	3.13	5.30	16.53	6.35
CaO	0.32	0.83	1.11	7.80	26.88	41.65
Na <sub>2</sub> O	2.16	2.63	1.95	0.59	1.12	0.55
K <sub>2</sub> O	6.87	3.31	5.78	4.58	0.94	1.12
MnO	0.03	0.04	0.03	0.06	0.13	0.12
P <sub>2</sub> O <sub>5</sub>	0.28	0.20	0.22	0.23	0.15	0.15
CO <sub>2</sub>	n.d.	n.d.	n.d.	10.2	31.2	36.0
Total**	101.89	100.57	98.64	96.88	104.20	99.61

\*analysis by microprobe (uncorrected comparison with dolomite standard) scrutiny of totals suggests Mg/Fe ratios in phlogopite/biotite are slightly overestimated by this method.

\*\*error in total likely to be SiO<sub>2</sub> determination.

Analyst for whole-rock determinations: I. Beaumont.

Mineral abbreviations: phengite(P), phlogopite/biotite(X), chlorite(C), quartz(Q), albite(Ab), dolomite(D), calcite(Cc), K-feldspar(K), pyrite(Py), ore and heavy minerals(O).

anomalous because the area is generally considered to be within the chlorite grade of regional metamorphism (Johnson, 1963). Indeed, comparison with the phyllites of southern Islay show the latter to be higher-grade texturally, yet biotite-free, the biotite isograd lying SE of southern Islay. Therefore it must be shown that the biotite has been correctly identified, and is not detrital, before its occurrence has to be explained.

The mineral in question shows the normal optical properties of biotite and is pleochroic from light to very dark green. The perfect cleavage and mottled extinction distinguish it from stilpnomelane. It is not an oxidized chlorite (see Chatterjee, 1966; Brown, 1967) because it does not occur interleaved with chlorite and does contain potassium (qualitative microprobe determination).

It is not relict detrital biotite because:

- 1) it shows no relation in size or abundance to detrital quartz and its presence or absence is independent of the distribution of detrital heavy minerals; and
- 2) unkinked elongate biotite occurs parallel to  $S_1$  in some sandy slates (fig. 7-59). In siltstones and sandstones it forms randomly orientated short laths and anhedral grains, for which, like chlorite, it is difficult to rule out a detrital origin. However phlogopite shows exactly the same range of textures elsewhere in the Bonahaven Formation.

Biotite can form during very low-grade metamorphism, but only if phengite is absent (Winkler, 1976), which is not the case here. In low-grade metamorphism biotite can form below the classic biotite isograd (if the rock composition plots below the phengite-chlorite join on an AKF diagram, Mather, 1970) by the reaction:

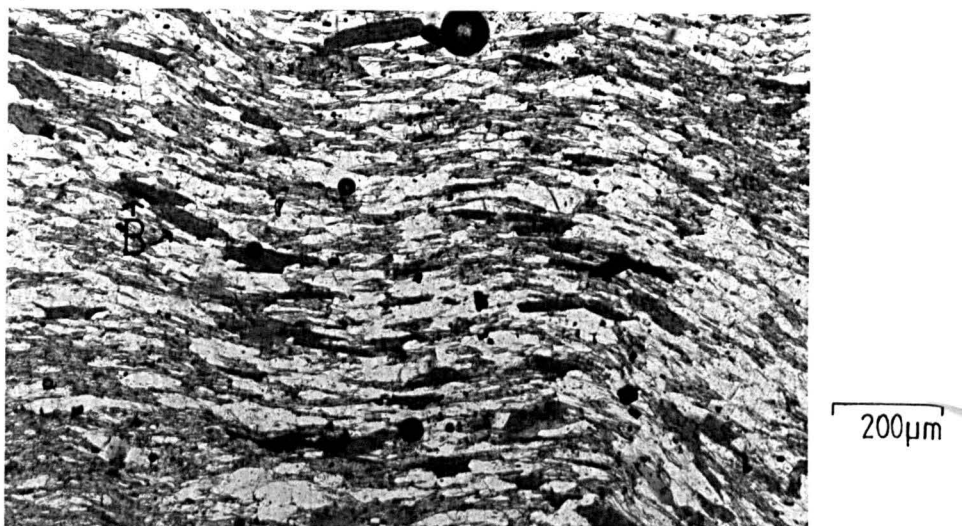


Figure 7-59: Photomicrograph, plane polarized light, unit 1, member 1, Section A. Semi-pelite (originally sandy slate) with well-developed  $S_1$ , which is slightly warped by  $S_2$ . Elongate biotite laths (very dark grey =B) are parallel to  $S_1$  as defined by phengite (fine-grained, mid-grey).

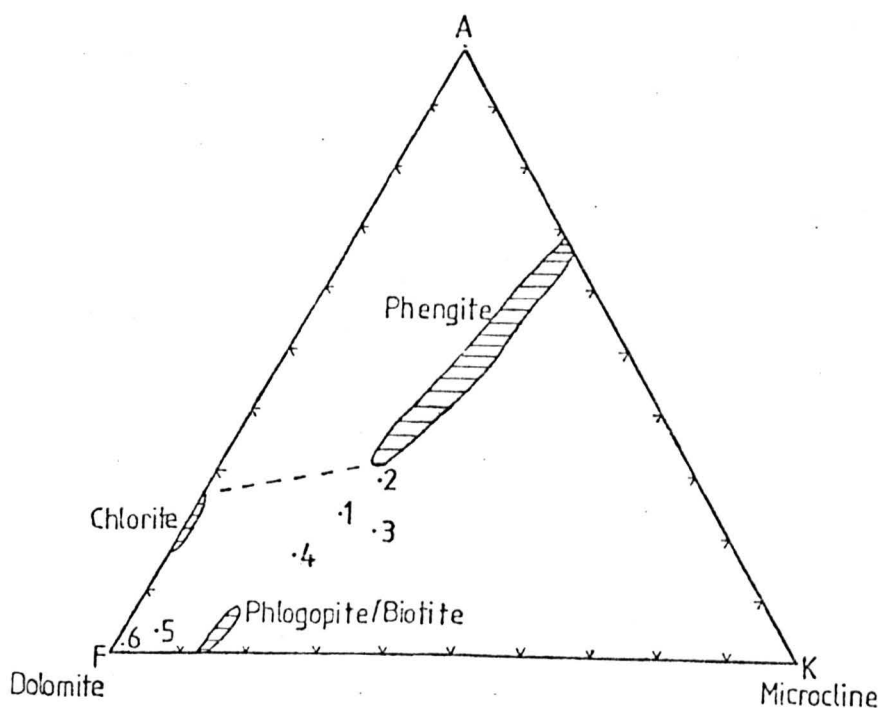


Figure 7-60: AKF diagram of the analysed specimens of Table 7-2. The pre-metamorphic assemblage was dolomite-phengite-microcline. Metamorphic assemblages are dolomite-phlogopite (5,6); dolomite-phlogopite-phengite-microcline (4); biotite-phengite-chlorite(1,2) and biotite-phengite (3). Analysis 3, and possibly no.2 (of Table 7-2) contain more normative K-component than is evident from their mode. The reason for this is not understood.

(5) Microcline + Chlorite + phengitic Muscovite →

Biotite + less phengitic Muscovite + Quartz + H<sub>2</sub>O.

Figure 7-60 shows that the rocks in question do indeed plot in this region. However this reaction only occurs in the upper part of the chlorite zone where clastic textures are completely subordinate (Mather, 1970). Temperatures are not thought to have been high enough in this area for reaction (5) to have occurred because:

- 1) clastic textures are preserved.
- 2) talc is not found in dolomitic rocks, and
- 3) the area is some tens of kilometres away from the steeply dipping biotite isograd.

An alternative is that biotite is being formed by the same reaction that produces phlogopite, that is:

(6) 3Dolomite (Ankerite) + K-feldspar + H<sub>2</sub>O →

Biotite + 3Calcite + 3CO<sub>2</sub>.

This reaction was suggested by Thompson & Norton (1968), although no experimental work has been done to determine the effects of varying Fe/Mg ratio on the course of this reaction: it is not a generally accepted means of producing biotite. However, reaction (6) is offered as the explanation for the occurrence of biotite in these rocks because:

- 1) biotite forms textures congruent with those formed by phlogopite, and
- 2) phlogopite and biotite never occur together. Table 7-2 shows that the composition, and corresponding colour, of biotite/phlogopite in six specimens relates to whole rock composition, particularly Fe content and Mg/Fe ratio.

Two objections to this hypothesis are:

- 1) modal dolomite is not present in the biotite-bearing rocks, and

2) calcite is not always present with biotite as would be expected from the reaction.

However both these points apply equally well to the phlogopite discussed earlier and the same explanation can be produced: dolomite is absent because the reaction has gone to completion (K-feldspar is also generally absent because it is supposed that it was subsequently albitized) and calcite may be absent in some cases because  $\text{CaCO}_3$  or  $\text{CO}_2$  have migrated out of the bed in question.

Clearly this problem is amenable to a more thorough study, but if the preliminary conclusions as stated above are correct, then they have the corollary that biotite should be more commonly developed than presently recognized in slightly calcareous pelites and greywackes in the chlorite zone.

#### 7.7.4: Dolomite

Unzoned subhedral dolomite found occasionally in quartz seams, and subhedral or euhedral dolomite interlocking with secondary albite and quartz in some metamorphosed siltstones of member 4, is presumably metamorphic. Unzoned intergranular dolomite in siltstones and sandstones with detrital textures could be diagenetic or metamorphic.

A general coarsening of limestones with incipient metamorphism was reported by Brown (1972), the first stage of marmorization. Whilst the matrix rhombs could have formed at this time, and some dolostone mosaics enlarged (especially member 4 dolostone), such features could equally be diagenetic. It is only the tectonic elongation of the fabric that can be shown to be post-diagenetic.

#### 7.7.5: Calcite

Grains of metamorphic calcite, anhedral or subhedral,

with many re-entrants against other minerals, are associated with phlogopite. This calcite is 20-100 $\mu$ m in grain size. When especially abundant, the calcite forms polycrystalline aggregates within which the crystals may be elongate. This is the texture referred to at the top of page 176.

Calcite occurs quite commonly in quartz seams (7.5.5.3). Where seam calcite is elongate, it is syn-tectonic. Calcite-bearing quartz seams are very common in stromatolites which contain no other calcite; this also applies to calcite in nodules. As phlogopite is generally absent from these rocks there is a strong implication that calcite has been introduced from outside the bed. The obvious source is the many phlogopite-bearing horizons where calcite is either absent, or else is not present in the quantity required by reaction (3).

## 7.8: Post-tectonic features

### 7.8.1: Dolerite dykes

Two contact metamorphic effects were noted next to these Tertiary (Walker, 1960) intrusions.

- 1) Thermal spotting is present in mud laminae at NR 4111 7883.
- 2) Conversion of member 4 dolostone with quartz bands to a calcite-serpentine marble has taken place at NR 4000 7837. Although the dyke is only 5m wide, the marble is present up to 2m away from the dyke. Probe analysis (No. 11) of fibrous calcite in the marble shows it to have consistently low Fe, Mg and Sr, but Mn values vary from fibre to fibre.

Another phenomenon, present at NR 4019 7895, is that of calcite pseudomorphing phenocrysts in dykelets and fibrous calcite veins occurring in the country rock. Perhaps some of the calcite described in section 7.8.3

may have resulted from hydrothermal solutions associated with dyke intrusion.

### 7.8.2: Dolomite

Rare, thin ferroan dolomite veins, associated with minor scattered 50 $\mu$ m ferroan dolomite in the matrix of the rock, visibly cross-cut the tectonic fabric. The fact that the veins have matching, parallel sides and that the crystals within the vein have straight crystal boundaries suggests that the veins have a largely dilational origin, yet the matrix dolomite must be replacive.

Ferroan dolomite rhombs in stromatolites D2 and E8 and sandstone 16D are found in association with leached vugs (fig. 7-61) and so must be post-tectonic. Leaching probably could not have occurred until the rocks were under the influence of groundwater action after a great deal of uplift. Probe analysis 19B shows that cryptic chemical zoning is present and that different rhombs have different compositions (especially with regard to Mn) suggesting growth at different times from a solution of changing chemistry. They are more ferroan and less manganoan than nearby dolomicrite which contrasts with the preserved pre-tectonic matrix rhombs (7.2.4) of member 3 which have overall chemistry similar to that of associated dolomicrite.

### 7.8.3: Calcite

Post-tectonic calcite occurs as vug-linings associated with veins which may cross-cut, fracture or displace quartz seams and albite and phlogopite grains. Some calcite crystals show a little twinning. In the unit 3 dolostone, member 4, such calcite is abundant. Although it is unzoned optically, it shows superb growth zones under luminescence (fig. 7-62). Incipient calcitization in the surrounding

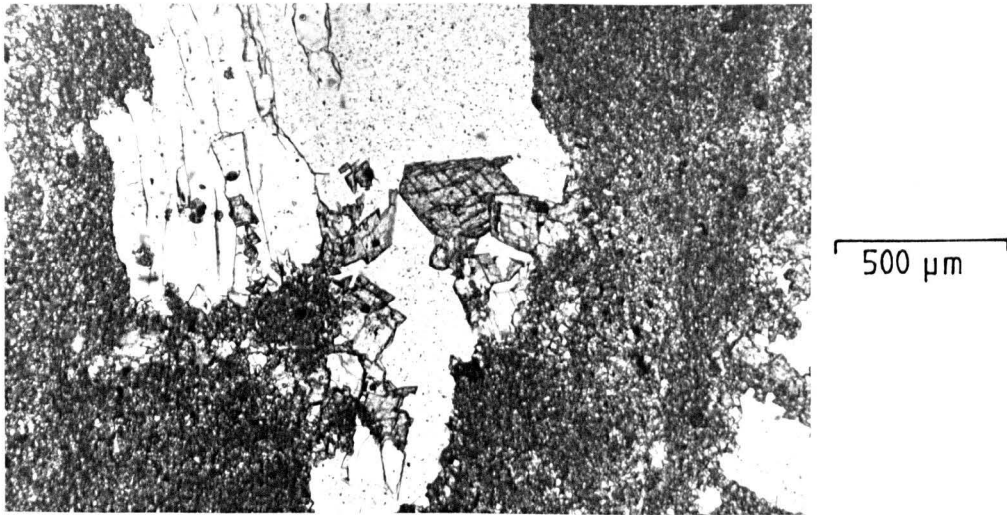


Figure 7-61: Photomicrograph, plane polarized light, bed 66E (stromatolite horizon E8). Post-tectonic dolomite shows well-formed crystals within a cavity.

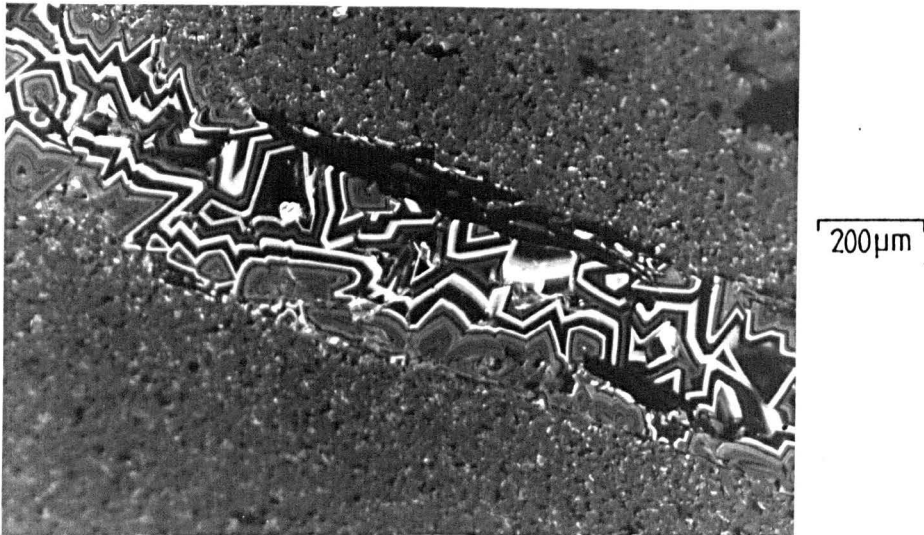


Figure 7-62: Photomicrograph, luminescent light, unit 3 dolostone, member 4. This is slide 1 of the probe work. Top right and bottom left is fine-grained dolomite. Within the vein is post-tectonic calcite with a clear zonal sequence. Elongate phlogopite (black) runs parallel to the vein walls; lines of such phlogopite crystals acted as lines of weakness guiding the course of post-tectonic fracturing and the subsequent calcite cementation.

dolomicrite is associated with the calcite veins.

In member 3, calcite veins are less common, but some calcite in nodules can be proved to be post-tectonic because it has identical zones to calcite in post-tectonic veins. Some veins are extremely irregular in outline with non-matching sides and thus seem to be replacive (fig. 7-63). Incipient calcitization of surrounding matrix commonly takes the form of isolate, embayed grains less than 20 $\mu$ m in size. Other veins are parallel-sided and apparently dilational, but commonly contain crystals which occupy the whole vein width. This structure could have arisen where growth kept pace with the opening of the vein, or where the number of nucleation sites was low. The latter seems most likely as the crystals generally have their long axis parallel to the length of the vein.

#### 7.9: Summary of calcite chemistry

At the start of the work it was hoped that it might be possible to demonstrate some clear chemical distinction between different petrographic varieties of calcite. In general, this has not proved possible: most of the calcite seems to form one suite. Also the degree of inhomogeneity within single crystals in some cases is nearly as much as the total chemical variation of the whole suite.

Four different categories of calcite are distinguished below and coloured in the following diagrams as follows: calcite filling primary pores in dolostones (red); replacive calcite (green); main suite calcite (blue) and post-tectonic calcite (orange).

##### 7.9.1: Calcite filling primary pores in dolostones

The petrography of the calcite was described in section 7.1.1. The analyses (5, 6, 7B and 20B) show no consistent

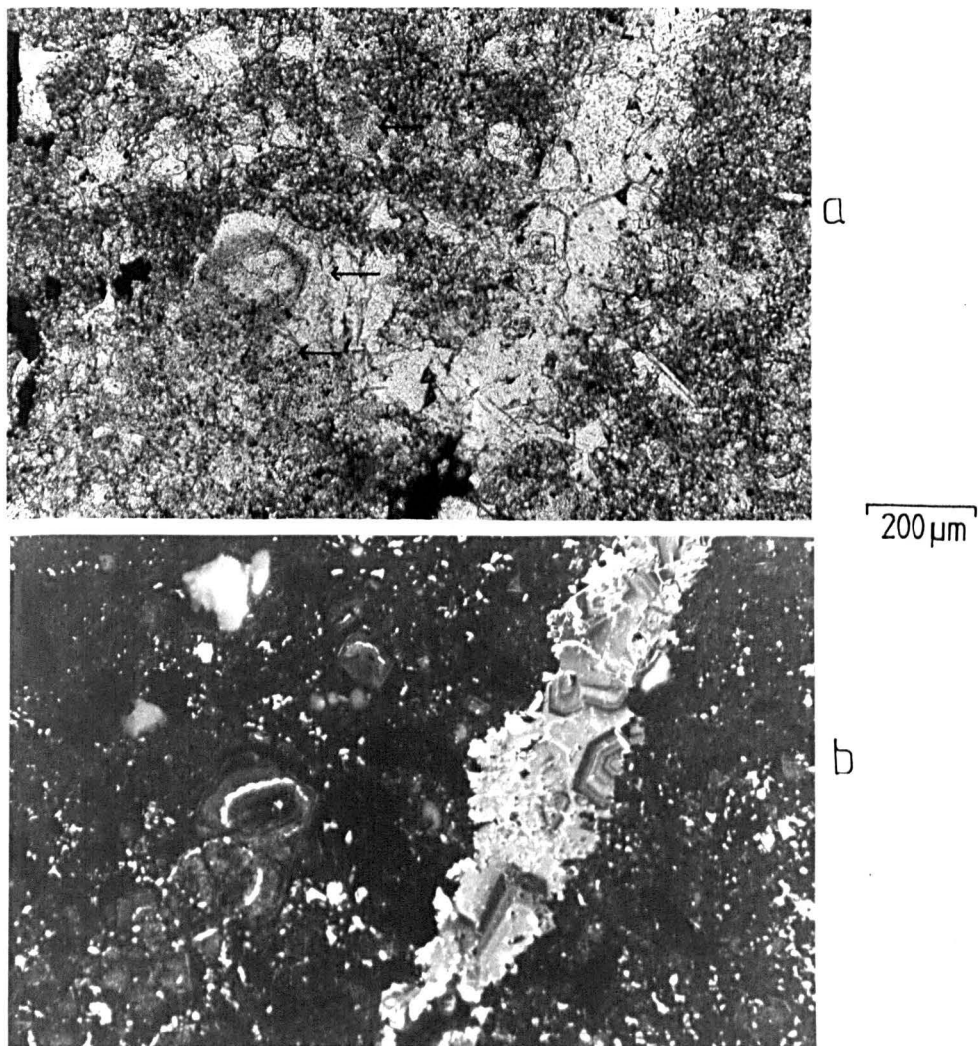


Figure 7-63: Photomicrographs, bed 68E. a) *transmitted light*; b) *luminescent light*. The conspicuous vein of calcite has extremely irregular margins suggesting a replacive origin for it. It is associated with minor replacive calcite in the matrix (small bright patches in b)). Evenly luminescing areas in top left area are detrital microcline. Dolomite matrix rhombs (arrowed) are present left of centre and exhibit an inclusion-rich ring in a) and zonal sequences in b).

chemistry (figs. 7-64 and 7-65) or trends of chemical variation. It is difficult to separate out any primary difference in chemistry between the various occurrences from differences due to later modification of the chemistry during metamorphism.

#### 7.9.2: Replacive calcite

Three analyses (7A, 8 and 15) are available of replacive calcite (7.2.1.2 and 7.2.2). They all show high, albeit variable, Mg content (fig. 7-64) and, as in the main calcite suite (7.9.3), Fe and Mg show sympathetic variation. Unlike these other calcites, analyses 7A and 8 show high Mg even when Fe is low. This suggests that the high Mg content of the replacive calcite was determined by the fact that it was replacing dolomite (Richter, 1974, cited by Füchtbauer, 1974). Also the content of Fe and Mn in the calcite seems to be related to the Fe and Mn content of the dolomite being replaced (fig. 7-66).

#### 7.9.3: Main suite calcite

Belonging to the main suite are all intergranular and nodular calcite, calcite in quartz seams and that of pre-tectonic veins. Fe and Mg contents are positively correlated and highly variable (fig. 7-67), generally showing variation in the form of sharp peaks a few microns across. These peaks have much lower Fe/Mg values than peaks due to inclusions of dolomite which are large enough (2-3 $\mu$ m) to be seen optically after staining. It is not possible to say whether the former peaks simply represent inhomogeneous areas within calcite, or whether they represent sub-micron-sized dolomite inclusions (?in optical continuity with the calcite). The trend of chemical variation within individual crystals and samples is the same as that shown by the suite

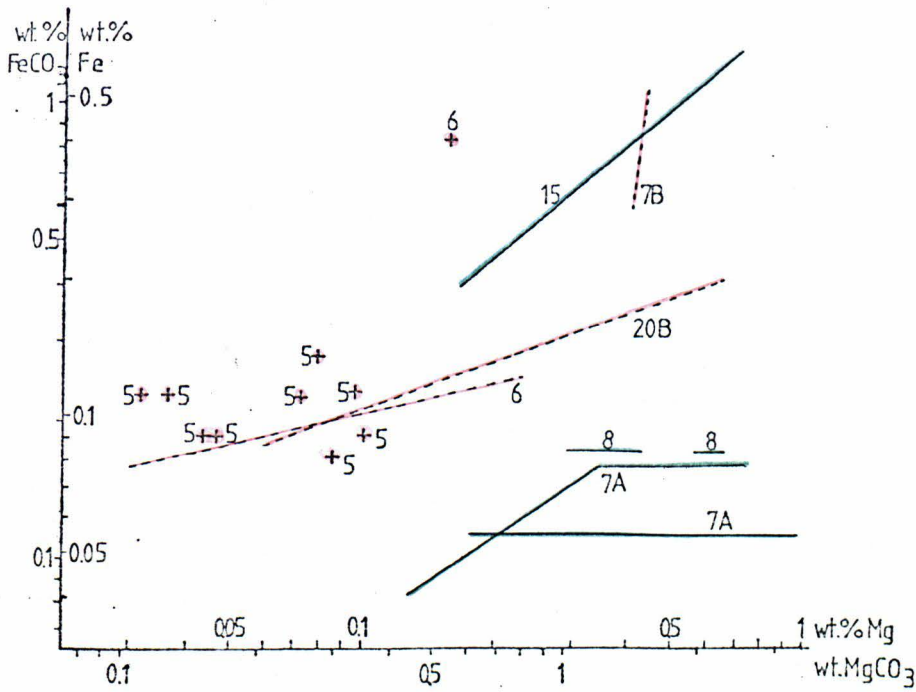


Figure 7-64: Fe and Mg analyses of calcite having textures of early diagenetic cavity-fills (7.1.1; analyses 5, 6, 7B and 20B) and of calcite replacing dolomite pre-tectonically (7.2.2; analyses 7A, 8 and 15). Conventions used in plotting the analyses are explained on figure 6-14.

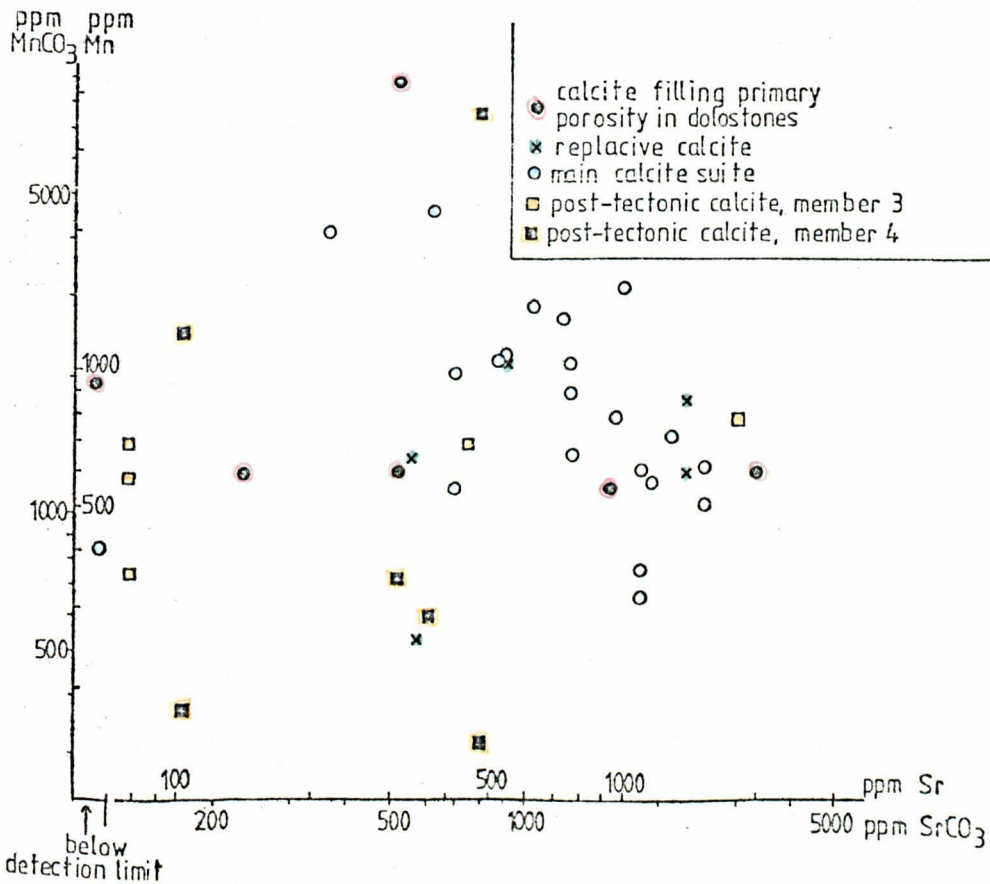


Figure 7-65: Mn and Sr contents of calcite from the Bonahaven Formation. No trends of variation are apparent. Most Sr values lie within the range 300-2000ppm Sr.

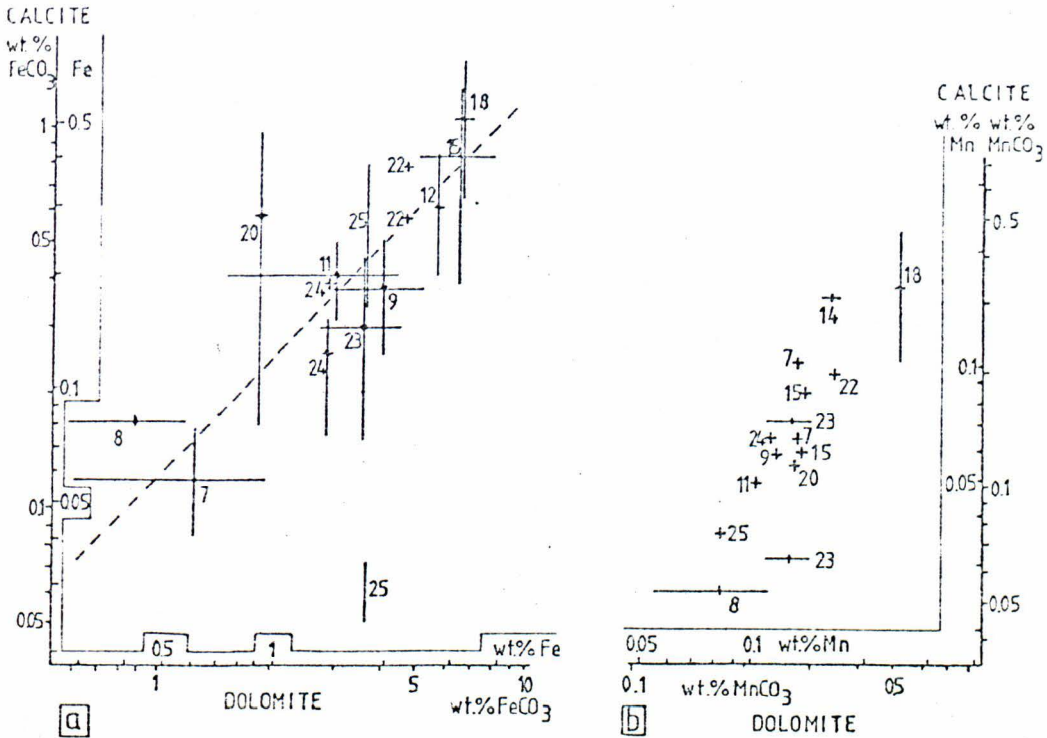


Figure 7-66: Fe (a) and Mn (b) analyses of co-existing, replacive or main suite calcite, and micritic, or unzoned rhombic dolomite. For iron, the data appear to indicate that there is a constant fractionation factor of about 8 in favour of dolomite (shown by dashed line). Manganese fractionates in favour of dolomite too, but by a variable factor.

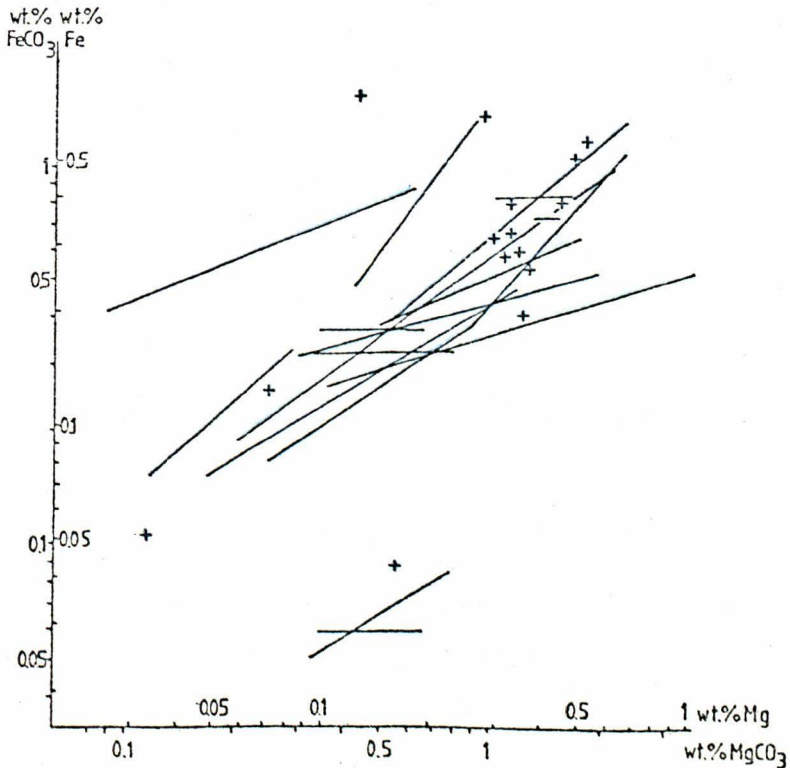


Figure 7-67: Fe and Mg concentrations of the main calcite suite. Most results lie within a field which is parallel to the Fe/Mg variation of individual analyses. Analyses are plotted as diagonal lines because Fe and Mg correlate with one another. Some calcite in slide 25 lies outside the main field (= analyses at the bottom of the diagram).

as a whole (except analysis 25 which has two iron modes, the lower of which lies outside the main area). There is also possibly a positive correlation of Fe with Mn in the suite, although this is not clear (fig. 7-68). Sr values tend to be in the range 500-1500ppm (fig. 7-65) and show no trends of variation with other elements. These Sr values are comparable with that of many limestones of similar age (Veizer, 1977b). There seems to be the same relationship between the Fe and Mn content of calcite and nearby dolomite as was the case for replacive calcite (fig. 7-66).

To summarize, the main suite shows:

- 1) a positive correlation of Fe and Mg within each sample (fig. 7-67),
- 2) a relationship between the Fe and Mn content of calcite and that of nearby dolomite (fig. 7-66),
- 3) overall similarity in the range of composition of the suite (fig. 7-67), and
- 4) an absence of growth zones (cf. post-tectonic calcite).

Replacive calcite also shows characteristics 1, 2 and 4; in addition Mg in replacive calcite seems to be high in each case, irrespective of Fe content.

These characteristics may be due to partial 'inheritance' of the minor element chemistry of nearby dolomite and possibly even inclusion of sub-microscopic dolomite crystals, followed by (inhomogeneous) diffusion during metamorphism. Metamorphic diffusion was apparently inhomogeneous because metamorphic calcite (slide 18), recognized by its association with phlogopite, shows considerable differences in composition between crystals. Nevertheless, it is interesting that the fractionation factor of Fe between co-existing calcite and dolomite (fig. 7-66) has a value of 8 in favour

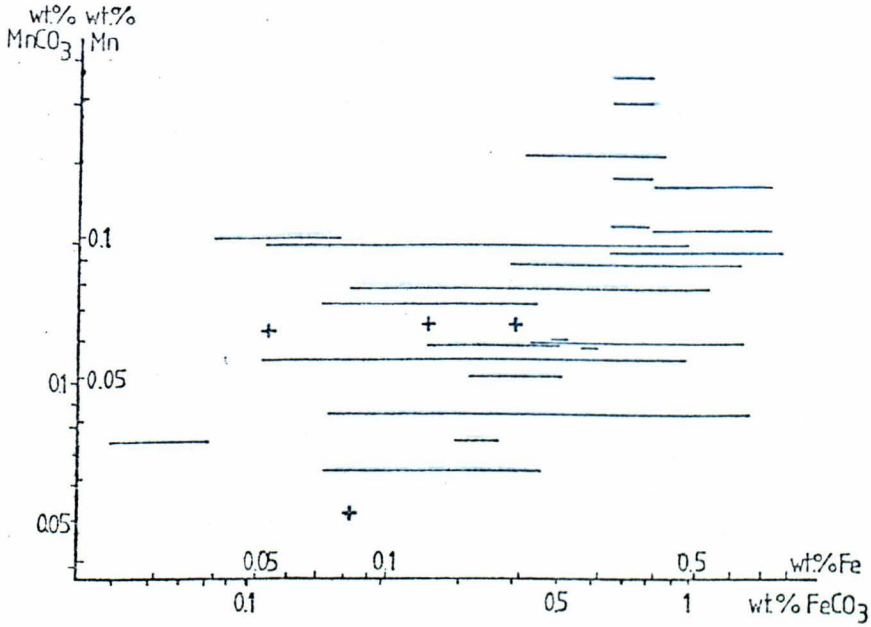


Figure 7-68: Mn and Fe analyses of calcite from the main suite. A weak positive correlation may be present.

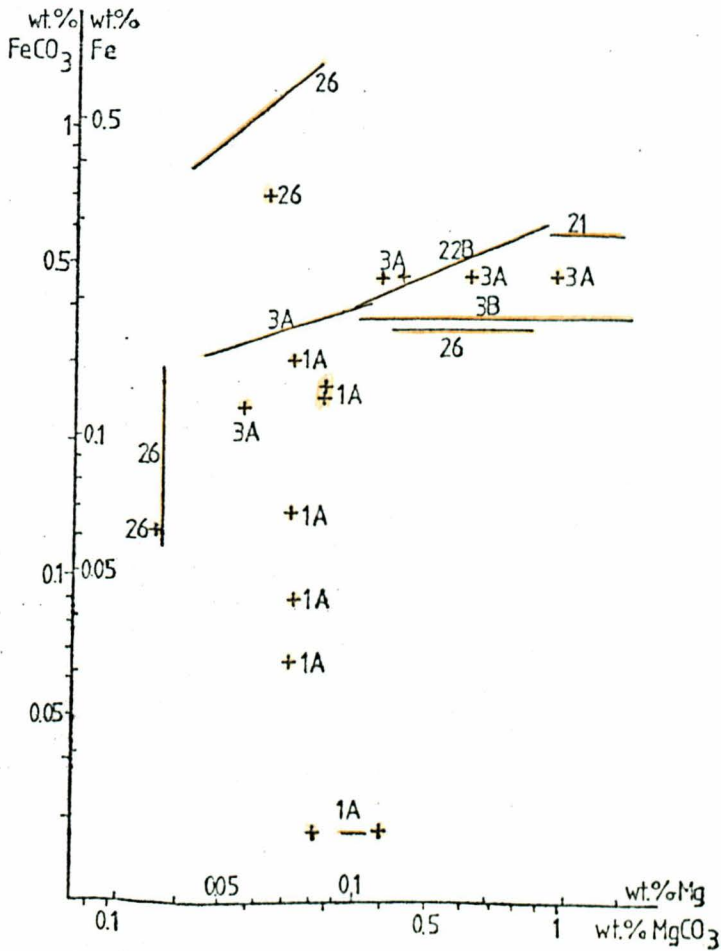


Figure 7-69: Fe and Mg analyses of post-tectonic calcite.

of dolomite. This is almost identical to the theoretical value derived by Bickle & Powell (1977) for metamorphic calcite and dolomite at 400°C, which is an appropriate maximum metamorphic temperature of the Bonahaven Formation. This provides some evidence against the general rule that it is only at rather higher temperatures than those reached here that metamorphic processes lead to a predictable minor element content (Bickle & Powell, 1977).

#### 7.9.4: Post-tectonic calcite

This calcite (figs. 7-65, 7-69) shows growth zones and so retains its original chemistry. Some occurrences are comparable in composition with pre-metamorphic calcite in terms of Fe and Mg content (e.g. analyses 21, 22B) which might suggest a local source, but others show considerable chemical variations (e.g. analyses 1, 3 and 26) indicating an external source, at least of Fe and Mn.

#### 7.10: Summary of post-depositional history

A rationalization of the diagenetic and metamorphic events is shown in figure 7-70. This diagram is bound to be an over-simplification, both because some diagenetic phenomena must have been missed and because others may have occurred more than once, or over a more protracted span than indicated on the diagram. Therefore figure 7-70 simply offers an interpretation with the fewest possible events consistent with the observed textures. The processes involved in producing these textures will now be discussed.

Although the Bonahaven Formation contains much carbonate, it does not exhibit the diagenetic textures of limestones which have been emphasized in the literature (Bathurst, 1971). This is because of the absence of skeletal debris

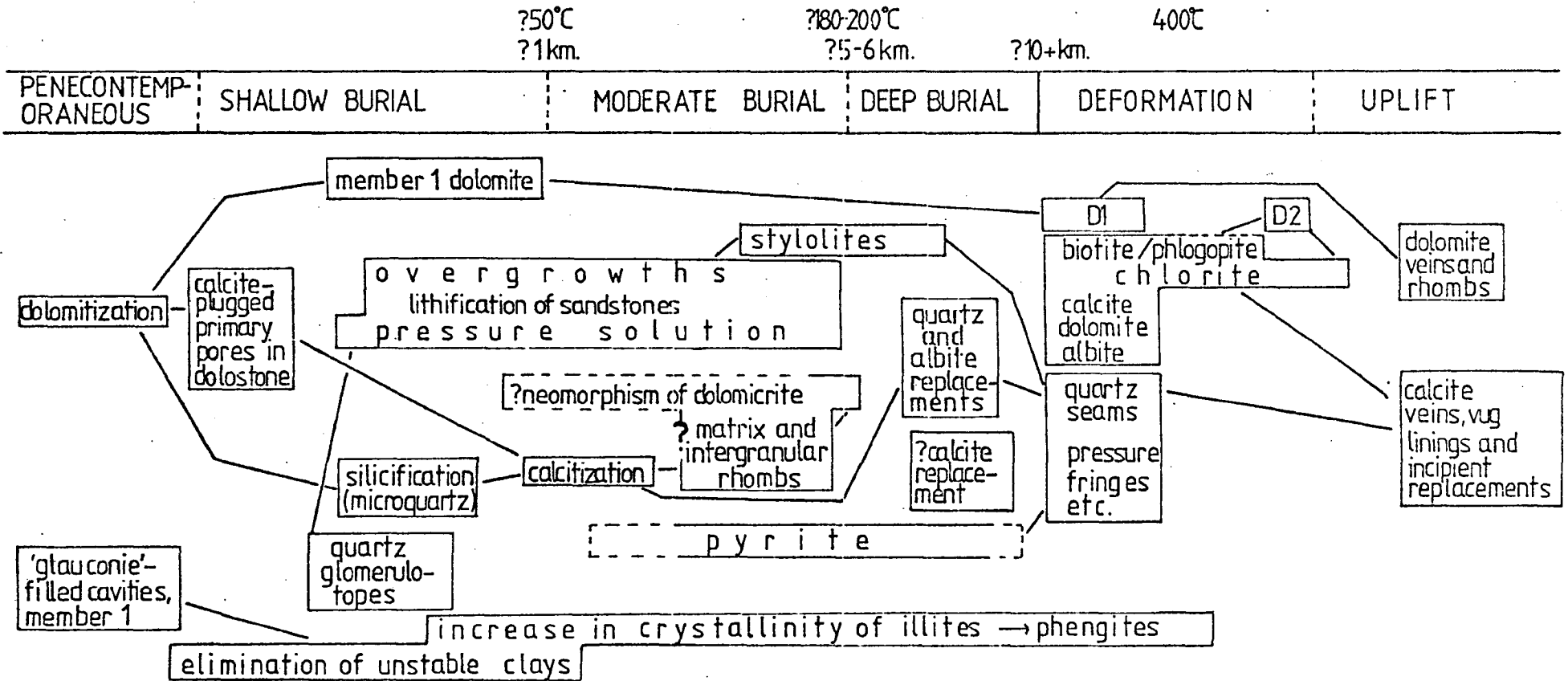


Figure 7-70: Summary of the post-depositional history. Where the relative age of two petrographic forms is directly determinable, they are connected by a solid line. The values of temperature and depth are given as an approximate guide. They were deduced by an examination of data presented by Füchtbauer (1974), except for the maximum temperature which follows from the metamorphic mineralogy.

and because the early and essentially complete dolomitization established a stable carbonate mineralogy from the outset. No recognized unconformities are present within the Bonahaven Formation, or the overlying strata. Thus no early phase of widespread leaching and/or cementation related to meteoric water could have occurred. Rather, the key to the diagenetic sequence should be found by considering a history of continuous, steady burial.

In general, as burial proceeds and pore water is expelled, interstitial solutions become brines, probably because of reverse osmosis (Pettijohn et al., 1972). These solutions are modified by in-situ chemical reactions, dissolution (including pressure solution), and cementation. Lateral migration of solutions may be important, but predictions as to the extent of this movement and the chemistry of the solutions are difficult to make. However, in general, diagenetic solutions are reducing (thus diagenetic carbonates are commonly ferroan) and slightly alkaline. They become more alkaline at depth (Füchtbauer, 1974, p332), possibly because of CO<sub>2</sub> loss (Blatt et al., 1972, p365). The post-depositional history of the Bonahaven Formation will now be interpreted in the light of these comments.

Following dolomitization of an initial carbonate precipitate (Chapter 6) there was the local development, in dolostones, of pore fillings of dolomite with syntaxial calcite. The precipitating solutions would have been only slightly modified from the original pore water. All other events are thought to have post-dated some compaction of the sediments.

Primary porosity was eliminated in sandstones by compaction, squeezing of dolomicrite clasts between sand grains

and pressure solution at grain contacts, together with some cementation. Dissolution of quartz and dolomite provided an internal source for quartz overgrowths and at least some intergranular dolomite in sandstones. Zoned and intergranular dolomite in member 1 has an external source. The presence of calcite which was probably originally a cement in some sandstones indicates a locally high Ca/Mg ratio, either because no dolomite was being dissolved or perhaps because of interactions of the pore solutions with clay minerals.

Silicification occurs as:

- 1) rare glomerulotopes with inclusions delineating replaced detritus. These crystallized before etching of clasts by dolomite occurred.
- 2) microquartz. This was probably originally chert.

A silica source in the late Precambrian is more difficult to find than in older rocks which may have been deposited in silica-saturated water bodies (Eugster & Chou, 1973) or in Phanerozoic strata where opaline skeletal material is to be found. In the Bonahaven Formation only a small amount is needed, even if many of the quartz-calcite nodules were originally chert. This would have been derived in part from the material being replaced, from pressure solution of quartz, and by silica-releasing clay mineral transformations.

More controversial is the calcitization episode placed next in the diagenetic sequence. Evamy (1967) stated that for calcite to replace dolomite, near surface temperatures (<50°C) and a solution of high Ca/Mg ratio would be needed. Thus dedolomitization is generally a feature of sediments being uplifted, rather than being buried. On the other hand,

Swett (1965) and Kepper (1974) recorded calcitization as part of a 'prograde' diagenetic sequence followed later by (further) dolomitization, as is the case in the Bonahaven Formation. Zenger's (1973) dedolomite is also associated with burial rather than emergence. Calcitization is restricted to particular beds in member 3 and so may be due to lateral movement of a Ca-rich fluid. The offshore equivalents of member 3 are not exposed, but an ooid shoal is inferred to be present: this could be the source of the calcite.

Rhombic dolomite in member 3 is at least partly later than calcitization. Mass balance calculations indicate that no material need have been introduced, although the complexity of the zoning seems to require an external source in some cases. Fretting of quartz clasts by dolomite suggests a higher temperature or higher pH, or both, for the fretting than for the silicification episode. This is consistent with the evidence of calcite replacing micro-quartz. Carbonate replacement following silicification is a very common diagenetic phenomenon (Swett, 1965; Gutstadt, 1968; Füchtbauer, 1974).

Changes which might be expected in the zone of deep burial are yet poorly known. Here it is thought that quartz, albite and pyrite crystallized, forming various isolated crystals and nodules and probably replacing previously formed structures such as chert nodules, and perhaps veins.

In contrast the effects of the deformation are more obvious: extensive redistribution of quartz by solution transfer being one prominent example. Low-grade regional metamorphism involved formation of chlorite, phlogopite-

biotite, calcite and probably albite, together with the upgrading of phengite.

Within the wide post-tectonic time span, the observed post-tectonic phenomena were probably fairly late, perhaps within the zone of meteoric water circulation. Calcite veining and incipient calcitization may relate to dyke intrusion, or be a true surficial dedolomitization like that described by Evamy (1967).

## CHAPTER 8: REGIONAL SETTING

### 8.1: Some general palaeogeographic considerations

A landmass lying to the NW of the area studied can reasonably be postulated because of the absence of latest Precambrian sediments in NW Scotland. Anderton (1974, 1976) considered this to be the source area for the Jura Quartzite.

Wave-ripple strikes are consistently orientated NE-SW in the Port Askaig Tillite and Bonahaven Formation suggesting that the shoreline had this approximate trend. In the Bonahaven Formation a shoreline always lay close to or within the depositional area. A landmass to the NW is indicated by three pieces of evidence:

1. The overall thinning of the sequence, particularly members 1 and 3, to the west indicates a positive block in this direction.
2. The inter-tidal and supposed supra-tidal parts of member 4 thin to the east, implying a deepening of water in this direction.
3. Asymmetric wave-generated ripples in member 3 indicate a dominant wave transport direction to the NW.

This contrasts with some statements made in the literature (Klein, 1970a; Harris & Pitcher, 1975; Phillips et al. 1976) and will be discussed later.

Before a narrative of the sedimentation history is given, some problems concerning the time relations of the strata at the base of the sequence need to be discussed.

## 8.2: Sedimentation at the top of the Port Askaig Tillite

The sequence of the Port Askaig Tillite in the eastern coastal tract of Islay was considered in detail by Spencer (1971a), but he did not discuss the poorly exposed ground further inland to the west. The lack of continuous exposure in the latter area precludes a detailed stratigraphic treatment, but the width of outcrop suggests that the Tillite, like the overlying Bonahaven Formation, is thinner in this area (Knill in Spencer, 1969). At the top of the Tillite west of Loch Giur-bheinn (fig. 2-3) is a sparsely pebbly mixtite changing eastward to a pebbly sandstone (rarely mixtite). These variations could be explained either in terms of an original variation in the type of sediment deposited beneath a grounded ice sheet (Dow & Gemuts, 1969, p45) or in terms of a partial reworking of till and concentrating of pebbles subsequent to deposition.

In the exposures on the east coast, pebbly horizons are only met with some tens of metres below the Bonahaven Formation. Which part of this section is equivalent to the glacial deposits at the top of the Tillite in the western area? The most sedimentologically consistent answer would be that the highest (thin) mixtite in the coastal succession (fig. 2-2) of the Port Askaig Tillite is this equivalent horizon. If any higher horizon were to be taken as the equivalent horizon it would be very difficult to explain the contemporaneous presence of an ice sheet depositing till in the western area, whilst a couple of kilometres to the east no trace of glacial activity is visible. The interpretation is thus that partial reworking of the topmost till took place in the western area (to produce the pebbly sandstones) with no net subsidence there, whilst

to the east continuous subsidence with deposition of quartzite occurred.

The palaeogeography of the Tillite was discussed by Spencer (1971a) and by several authors in Spencer (1969). The only evidence for the direction of movement of the ice are overfolds indicating that the last movement was to the NW (Spencer 1971a). This seems to be consistent with the conclusions of section 4.5 that there are two separate sources of sediment (apart from intraclasts) in the lower part of the Middle Dalradian: essentially microcline-bearing and chess-board albite-bearing. The microcline-bearing source lay to the NW (Anderton 1974, 1976), implying that the other lay elsewhere, presumably on the other side of the depositional basin, to the SE. However, during Bonahaven times the margin of the NW landmass lay close to, or within, the NE Islay area, whilst the wavelength of wave-generated ripples implies a width of sea to the SE of at least 100km. If the Port Askaig geography was similar, one would perhaps have expected that the ice sheet would have debouched from the nearest landmass, as in the grounded ice sheet model of Carey & Ahmed (1961) and Reading & Walker (1966), that is from the NW, which apparently was not the case. These interpretations may be reconciled if:

1. The NW landmass was low-lying at this time and hence not able to nurture glaciers. (This is the case in Anderton's (1974) model).

2. The width of the sea separating the landmasses was relatively narrow.

The effect would be similar to the Pleistocene glaciation of eastern Great Britain by movement of ice from Scandinavia (Charlesworth, 1957, p745).

### 8.3: Sedimentation of the member 1 wedge

The wedging out of a sedimentary unit may develop in a number of different ways. The most important factors are the possibility of diachroneity and/or the presence of an hiatus or unconformity at the top or base of the unit. In the case of member 1, sedimentation seems to have been continuous across the member 1/member 2 boundary. When traced westwards the lower units within member 1 disappear first, that is the boundaries between lithological divisions in member 1 intersect its lower boundary surface as it is traced westwards. These observations limit the hypotheses which can be put forward to explain the geometry of member 1; two possibilities are put forward and evaluated below.

Hypothesis 1 (fig. 8-1a). The main feature of this hypothesis is that the subdivisions of member 1, and member 2 are considered facies equivalents of one another so that time lines cut lithological boundaries: Walther's Law applies. Subsidence would have been continuous across the area in Bonahaven times, although a much thicker sequence accumulated in the east. A facies mosaic would have been set up, which migrated eastwards with time.

Hypothesis 2 (fig. 8-1b). The lithological boundaries would not be time-transgressive to any marked degree. The re-working of the top of the Port Askaig Tillite in the western area postulated in the last section would have continued into Bonahaven times, at least until unit 3 was being deposited at Caol Ila. This would explain the presence of the chess-board albite-bearing pebbles at Caol Ila at the base of unit 3. Sedimentation of units 4 and 5 would then have overlapped onto the reworked till, but unmodified (?sub-aerial) till was still the surface sediment further west. A transgression early in member 2 times then affected the whole area.

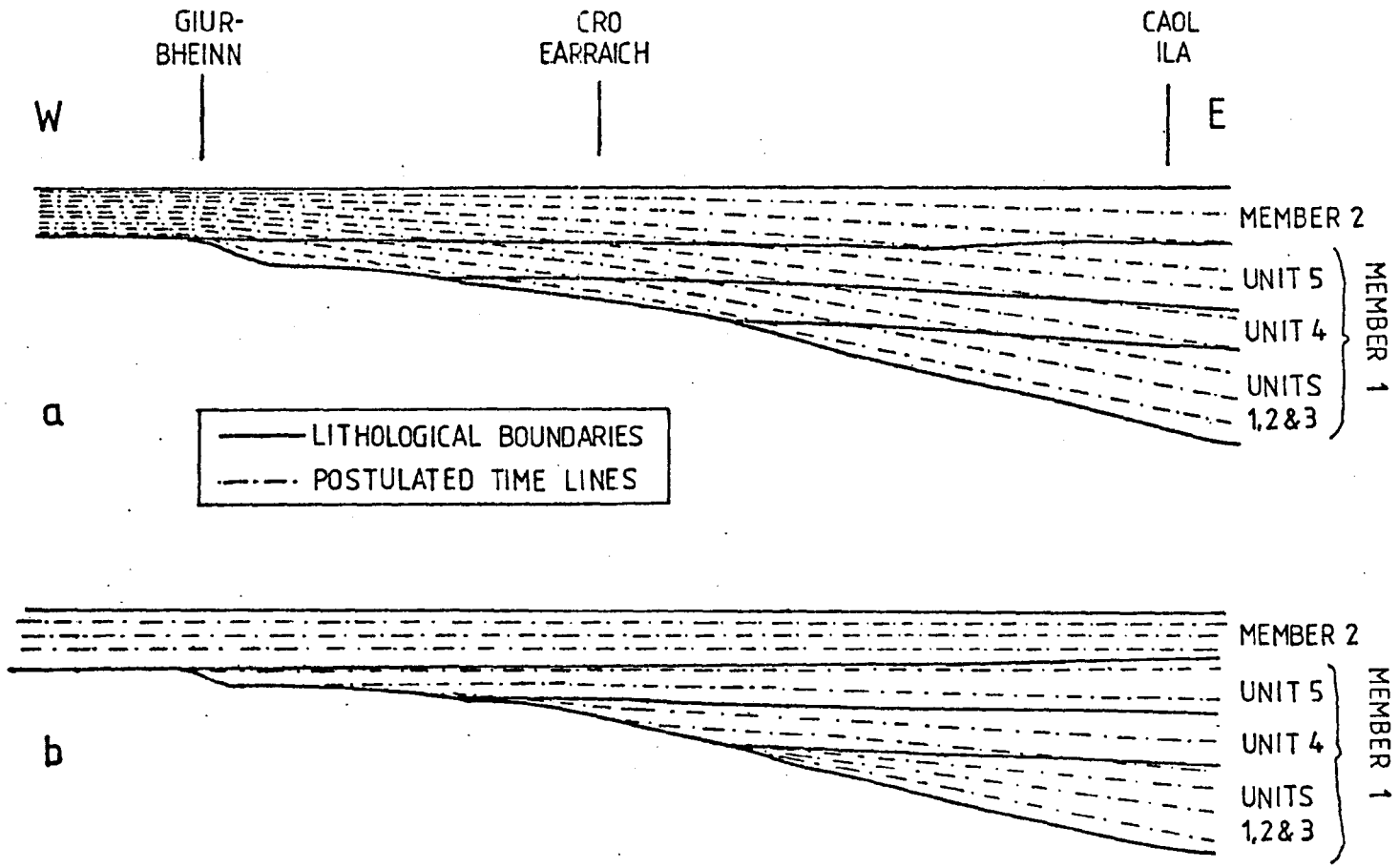


Figure 8-1: Hypotheses for the time relations of member 1 and member 2 sedimentation: see text for discussion. a) Hypothesis 1. b) Hypothesis 2.

Three objections to the first hypothesis are offered below:

1. The hypothesis requires that back-barrier tidal flat deposits (unit 5) would occur offshore of sub-tidal high-energy sands (member 2) which does not seem feasible. Also it does not seem likely that current-rippled sands (unit 2) could occur immediately offshore of barrier/back-barrier deposits (units 3 and 4).

2. There is no obvious source for the chess-board albite-bearing pebbles at the base of unit 3 at Caol Ila.

3. Spherules (Chapter 5) only occur at one horizon in each of the Bonahaven and Caol Ila sections, immediately below member 2, despite potential host lithologies occurring at a number of horizons. The occurrence of spherules is therefore taken to be a time-horizon. Spherules occur near to Loch Giur-bheinn, again immediately below member 2. This suggests that the base of member 2 is a time-line, at least as far west as Loch Giur-bheinn.

In contrast, the second hypothesis fits the available evidence much better. Although marked diachronism seems inappropriate, there may have been limited diachroneity between some of the stratigraphic divisions, but more complete exposure would be needed to develop this idea further.

The second hypothesis is assumed correct in the sedimentation history narrative which follows.

#### 8.4: Sedimentation and palaeogeography during Bonahaven times in NE Islay

Sediment was derived by reworking of glacial deposits and from the shelf by wave transport; there may also have been a direct fluvial input which was trapped in the coastal region of the NW landmass. The rate of subsidence may have been controlled by faulting (Anderton, 1974); no syn-sedimentary

faults have been recognized in the area, but contemporary fault-related earthquake activity is indicated by liquefaction structures in members 1 and 3 and possibly also by the load structures there.

Following the last glacial activity of Port Askaig times a high energy shallow sea covered the eastern area, considerable subsidence occurring there. In the western area, which was probably close to sea level, there was neither erosion nor deposition west of Loch Giur-bheinn, whilst beach reworking took place immediately to the east. The sudden change to quiescent deposition on the east coast at the start of Bonahaven times may be related to the build-up of a barrier off-shore or the landward migration of a pre-existing barrier.

Within member 1 of the Bonahaven Formation, unit 4 provides the best evidence for a barrier having been present, the deposits representing inter-fingering washover and back-barrier mud flat and pond sediments (fig. 8-2a). The washover sediments imply a microtidal environment (tidal range 0-2m, Hayes & Kana 1976), the system being comparable to the Laguna Madre (Rusnak 1960), although hyper-saline conditions do not seem to have developed at Caol Ila. Hurricanes could open temporary tidal inlets in the barrier, which could be represented by unit 3, with NNE-SSW palaeocurrents. On the other hand, the unit 5 tidal sand flat environment may suggest a somewhat higher tidal range; this would also be indicated if unit 3 were a tidal channel, rather than temporary tidal inlet deposit. Thus one may have to postulate variation in the tidal range, perhaps controlled by changes in the configuration of the Dalradian basin. The unit 5 sand flat extended as far west as Loch Giur-bheinn.

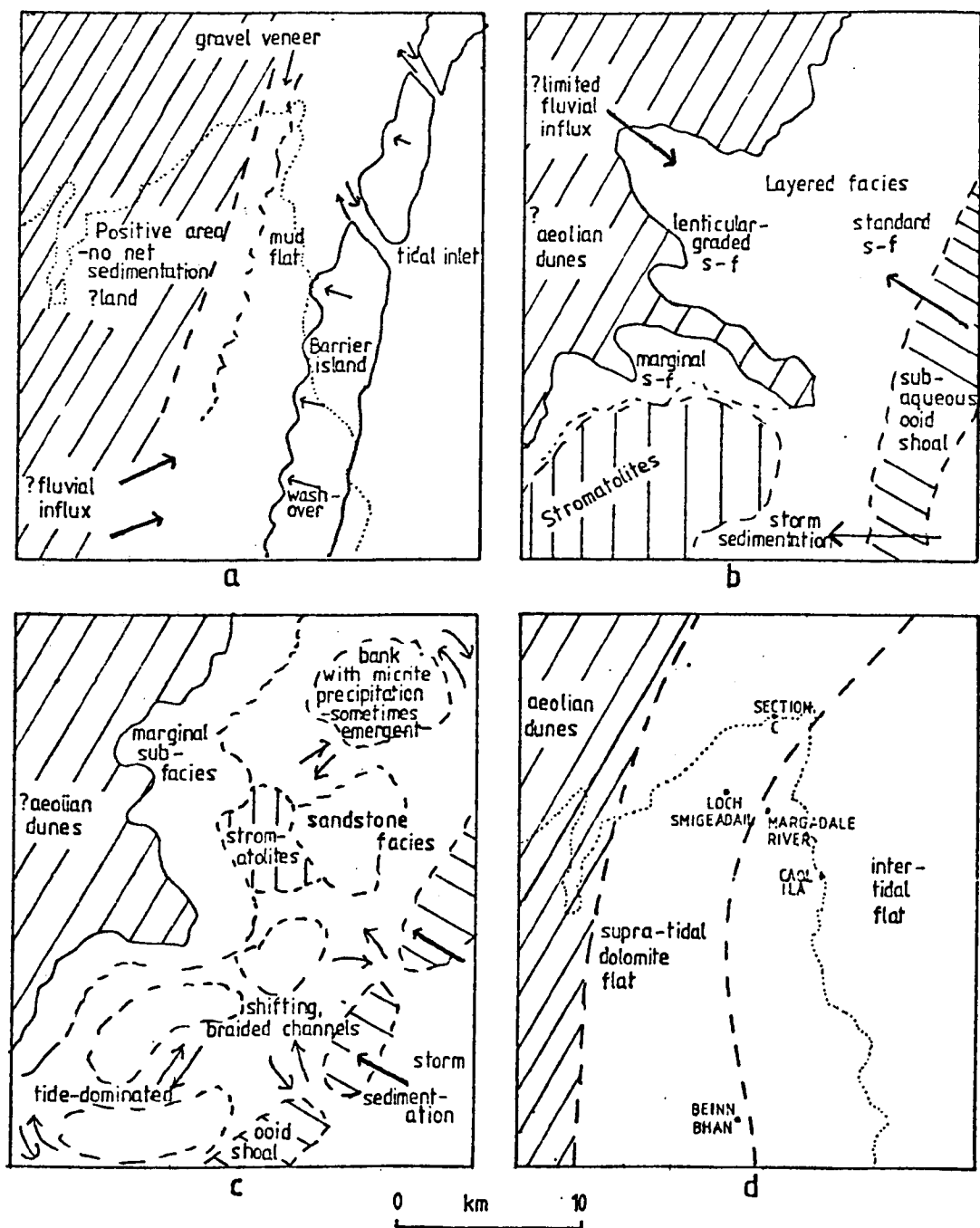


Figure 8-2: Palaeogeographic cartoons; present day outline of the Islay coastline is shown in a) and d) as an approximate guide. a) member 1, during the deposition of unit 4 at Caol Ila. b) member 3; paleogeographic elements contributing to layered facies sedimentation. c) member 3; palaeogeographic elements leading to sandstone facies sedimentation. d) member 4, during the time of maximum regression when unit 3 was being deposited over the widest area.

A general subsidence of the whole area then followed, leading to the deposition of member 2 sediments throughout the area in a renewed high energy shallow marine environment. It is not possible to say whether wave or tidal action was dominant in this environment.

The character of sedimentation changes distinctly at the member 2/member 3 boundary. Deposition was now in one of two situations:

1. a permanently submerged water-body with fluctuating salinity, very little tidal activity, but affected by storms (the layered facies, fig. 8-2b).

2. an inter-tidal/very shallow sub-tidal sand flat, probably suffering salinity fluctuations. Tidal currents and wave activity were important. Ooids found in the area were not actively accreting there; they are postulated to have been derived from an off-shore bank whose existence led to restricted circulation and associated salinity changes (fig. 8-2c).

The occurrence of stromatolites appears to be largely independent of the environmental conditions, although they were more easily established when there was little sediment influx.

The oscillation between the two situations could be related to changes in the configuration of the ooid shoal which reinforced or dampened the action of the tides.

Eventually the carbonate-producing system was brought to an end and siliciclastic low-energy inter-tidal and shallow sub-tidal sedimentation commenced in member 4 times. The existence of tidal flats must have been due to some sheltering from wave action, but it is not clear how this was achieved during the deposition of member 4. A gradual regression later in member 4 times allowed carbonate-producing supra-tidal

flats (unit 3, member 4) to encroach over the whole of the western part of the area of outcrop of the Bonahaven Formation (fig. 8-2d). A transgression then followed and the shoreline was displaced away from NE Islay. Deposition was now in the tide- and storm-swept sea of the Jura Quartzite (Anderton, 1976).

#### 8.5: Stratigraphic equivalents of the Bonahaven Formation

The Dalradian correlation chart in Harris & Pitcher (1975) has made it a straightforward exercise to assess which rock units should be correlated with the Bonahaven Formation. This is made a more fruitful task because of the widespread presence of the Port Askaig Tillite horizon in Scotland and Ireland as this can be used as a reliable time marker. Distinct sequences have been worked out in nine separate areas (fig. 8-3), although little sedimentological work has been done, mostly because of the deformation and medium to high-grade metamorphism of much of the Dalradian outcrop.

In poorly exposed ground in Banffshire, Spencer & Pitcher (1968) recorded that a quartzitic sequence overlay the Tillite, although no complete sections were seen.

In the Central Highlands (Bailey & McCallien, 1937) the top part of the Tillite consists of a quartzite unit capped by conglomerate, similar to the sequence on Islay inland to the east of Loch Giur-bheinn. These lithologies are overlain by a white dolomitic limestone and quartzose flags, then by mica schists below a thick quartzite sequence. The lithologies are reminiscent of at least member 4 of the Bonahaven Formation sequence on Islay.

In the Loch Creran area (Litherland, 1970, cited by Harris & Pitcher, 1975) there are dolomitic beds overlying a thin quartzite capping the Tillite in the Ardmucknish Bay area, but the Tillite was not recognized further east in Glen

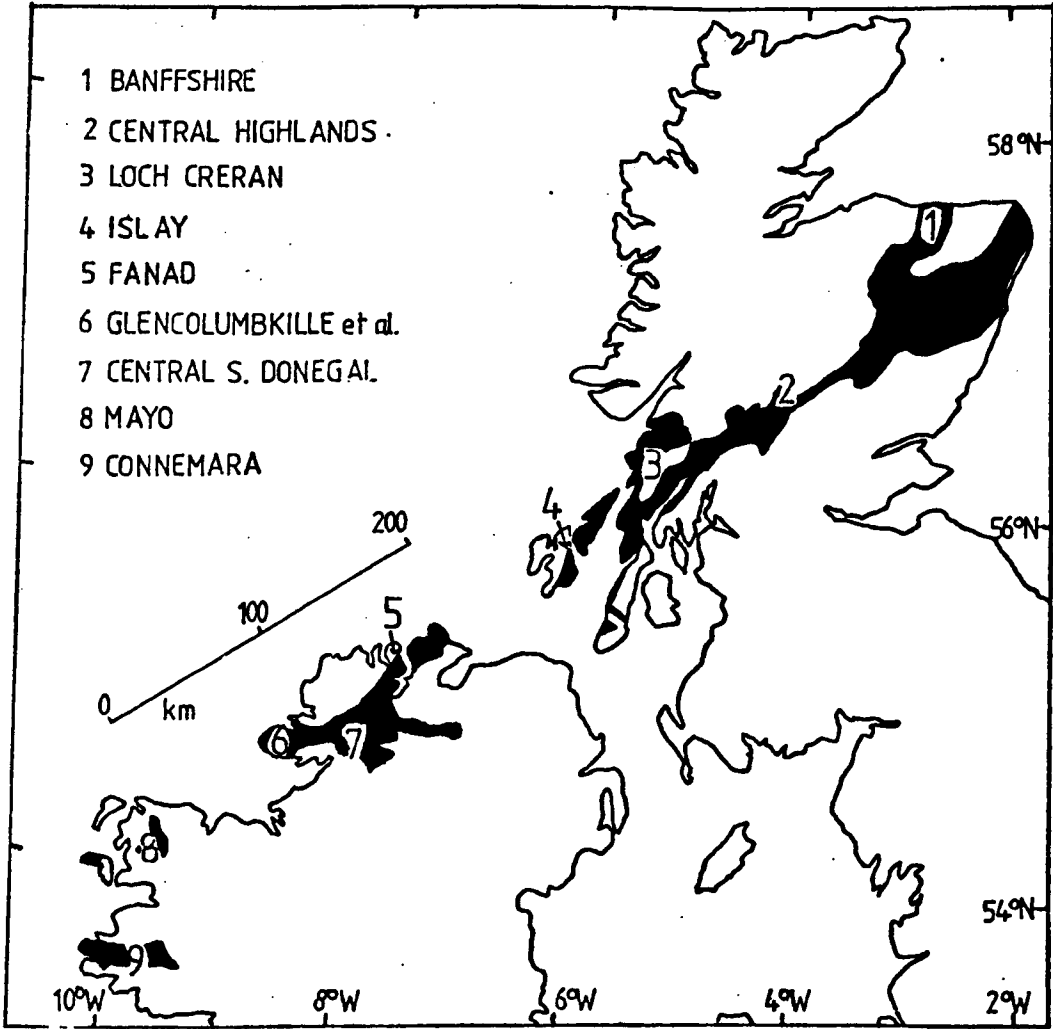


Figure 8-3: Localities of studied stratigraphic equivalents of the Bonahaven Formation. Outcrop of the Middle Dalradian is shown in black.

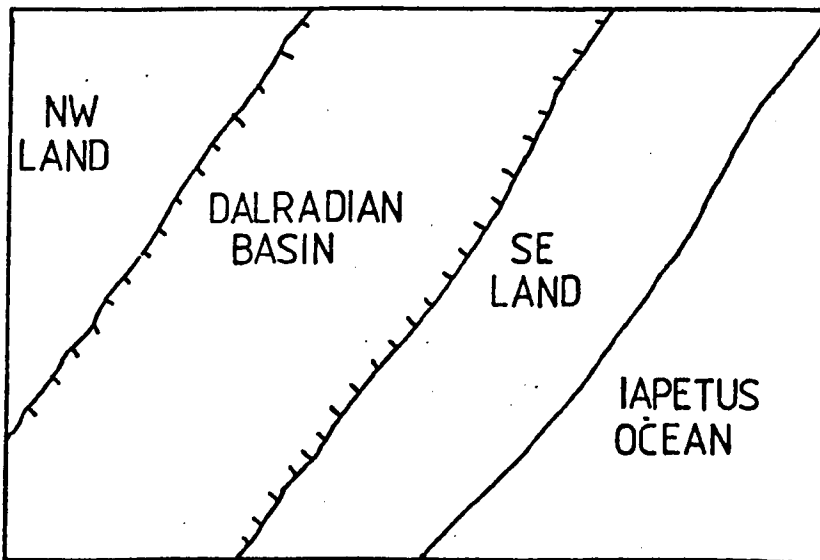


Figure 8-4: The simple man's guide to the Dalradian basin.

Creran, possibly a deeper water area.

The mixed carbonate-clastic sequence overlying the Tillite on Islay as described in this thesis seems to be the most diverse, although not quite the thickest development of its kind in the Dalradian outcrop.

At Fanad, like Islay, the grade of metamorphism is low. Here Spencer (1971a) indicated that Member 5 of the Tillite consists of quartzites with thin tillite horizons as on the east coast of Islay. Then follows (Howarth, 1971) 50-57m of dolomitic strata, mainly dolomitic sandstone which is cross-stratified (sets less than 15cm thick) and ripple-marked, but including up to 20m of dolostones. This sounds very reminiscent of the sandstone facies within member 3 on Islay. Elsewhere on Fanad thin pelites may occur instead of the dolomitic sequence (Howarth, 1971).

Further south in Donegal (e.g. Glencolumbkille) a pelitic, slightly calcareous schist (10-30m thick) is the dominant lithology immediately above the Tillite (Kilburn et al., 1965, Howarth et al., 1966, Howarth, 1971) with some dolomitic beds locally (Slieve League, Pitcher & Berger 1972).

In central southern Donegal a poorly exposed Tillite is overlain by quartzite correlated with the Jura Quartzite by Harris & Pitcher (1975).

In SW Mayo occur 360m of dolomitic schist with dolomite bands overlying successively pelitic schist, sandy limestone and tillite (Kennedy 1969b, Harris & Pitcher 1975). In NW Mayo only quartzite occurs above the Tillite (Crow et al., 1971).

In Connemara the highest boulder-bearing horizon forms a wedge in quartzite and is followed upward by more quartzite which locally contains dolomitic limestones (Edmunds & Thomas, 1966).

The occurrence of dolomitic lithologies, as described above, at intervals along the Dalradian outcrop confirms the supposition that the depositional shoreline roughly paralleled the present outcrop. Further interpretation would require more information than is available from the literature at present to distinguish, for example, member 3-from member 4-type dolomite, a distinction which will lead to a different environmental interpretation in detail.

The presence in some areas of schist or quartzite with little calcareous component does not necessarily imply a different environmental setting as the nature of the sediments deposited in the nearshore region is very dependent on details of coastal configuration and off-shore bathymetry. One should not in any case expect to see the same lithological sequence as recorded on Islay to be present elsewhere as this will depend on local geographic features as well as the amount of subsidence.

### 8.6: The nature of the depositional basin

Anderton (1974) presented a synthesis of Middle Dalradian sedimentation which postulated a down-faulted elongate basin flanked to the NW by a major landmass and to the SE by a relatively positive ridge (not a major landmass). This concurs with Dewey's (1969) model of Dalradian sedimentation on an Atlantic-type margin which later changed to a subducting margin in early Palaeozoic times. The margin would have been bounded to the SE by the proto-Atlantic (Dewey 1969) or Iapetus (Harland & Gayer 1972) ocean.

Alternatively Phillips et al. (1976) regarded the Dalradian as being sedimented in an ensialic basin rather

than on a continental margin. Various lines of evidence were brought forward to support this point of view, but not all are valid. In particular Klein's (1970a) suggestion of a southern derivation of sediment for member 1 of the Bonahaven Formation was based on a failure to realize the existence of the Bonahaven section of this horizon. Also the northward-directed Jura Quartzite palaeocurrents were viewed as indicators of sediment transport from a southern landmass rather than as a dispersal of sediment brought in from a NW landmass by northward-flowing tidal currents (Anderton, 1976). However the discussion in section 8.2 showed that a nearby southern landmass (north of the Iapetus ocean) was needed to supply the glacial detritus for the Port Askaig Tillite (fig. 8-4). Also there is evidence of sediment derivation from the SE in the Upper Dalradian (Phillips et al., 1976; Smith, 1976). The tholeiitic igneous activity in the Upper Dalradian is good evidence for a phase of continental rifting at that time (Graham, 1976), probably behind an island arc (i.e. back-arc spreading, Phillips et al., 1976; Wright, 1976). The Middle Dalradian sedimentation in a fault-bounded basin (Anderton, 1974) would thus represent the first stages of extension of this rift.

This view of the nature of the Dalradian basin is essentially the same as the independent synthesis of Harris et al. (in press), although these authors did not have any evidence for the existence of a SE landmass before Upper Dalradian times.

Dalradian deformation and metamorphism (the Grampian orogeny, Wright, 1976; Lambert & McKerrow, 1976) would relate to subduction of Iapetus crust (Phillips et al., 1976) or more specifically to the subduction of an oceanic

ridge (Lambert & McKerrow, 1976).

Further detailed studies of Dalradian sedimentology are warranted to develop or revise the interpretation of the significance of this celebrated sequence in the geological history of the Caledonides.

APPENDIX AElectron microprobe analysis:methods and tabulated resultsA1: Introduction

The microprobe work was carried out on a Cambridge Microscan mark V in the Wolfson Institute of Interfacial Technology at Nottingham University. The work involved in searching for suitable standards and a satisfactory analytical technique was carried out in conjunction with Dr. J.A.D. Dickson.

Carbonates present difficulties when an accurate analysis of their minor element constituents is required using the microprobe. This is because a high specimen current is needed to obtain adequate count rates for these elements, and under these conditions the minerals decompose. This decomposition ('burning', Moberly 1968) is induced by the high temperature conditions under the electron beam. It is deduced to be a decarbonation reaction because after the focused beam is allowed to impinge on the specimen the apparent concentrations (count rates) of the cations increase with time, whereas those of carbon and oxygen decrease. If there is significant decomposition, the normal microprobe procedure of comparison with inert standards is invalidated.

A variety of approaches to quantitative carbonate microprobe analysis have been taken by different workers. As there is no generally accepted method, the practice of Moore (1973) and Land et al. (1975), who claimed quantitative results, yet gave no explanation of the technique used, is to be deplored. MacQueen & Ghent (1970), MacQueen et al. (1974), Gablina & Tsepina (1975) and Bickle & Powell (1977) used non-carbonate standards and applied a full

correction procedure. This is quite satisfactory provided the specimen current was low enough to avoid specimen damage, but then the statistical errors for the minor elements are relatively large. The same remarks apply to the method of Benson & Matthews (1971) and Benson et al. (1972) of using end-member carbonate standards ( $\text{FeCO}_3$  for Fe analyses etc.), but applying no corrections. However the disparity in composition between their samples and standards is bound to have introduced errors. Loberly (1968, 1970) also used end-member carbonate standards. He used conditions harsh enough to produce specimen damage, but had the advantage of the resulting high count rates. Some of his analytical totals are rather low, which he attributes to differential burning of specimen and standard, and recalculates to 100%.

A common feature of all the published methods is that analysis of spots rather than continuous scanning was employed, although Benson & Matthews (1971) and Benson et al. (1972) did use a step-scanning procedure. As a result it would not have been possible to adequately characterize inhomogeneity on the scale of a few, or a few tens, of microns.

The approach used in the work presented here has been to scan the specimen using rather severe conditions under which visible specimen damage does occur, but by using carbonate standards of similar composition to the specimens, the effects of burning on specimen and standard are equalized. The advantage this brings is that of low detection limits corresponding to high count rates so that changes in elemental abundance are readily seen on scanning.

## A2: Operating conditions and methods

Thin sections and standard blocks were polished, finishing on  $\frac{1}{2}\mu\text{m}$  abrasive. They were given a transparent conducting coat of gold (estimated to be  $350\text{\AA}$  thick) rather than the usual carbon coat. This was because tests on carbonate standards showed that the use of gold makes the decomposition of the material a much more even and predictable process (fig. A1).

The accelerating voltage used was 15-16 kV and the specimen current 380nA: these conditions give a high count rate whilst not inducing the very erratic burning behaviour characteristic of more severe conditions. The electron beam was used focused, with a diameter of 4-4.5 $\mu\text{m}$ . A smaller beam size gives lower count rates as would a defocused beam; the latter would also reduce the possibility of recognizing micro-heterogeneity of the samples. The focus was checked whenever the beam was moved from specimen to standard or vice-versa.

Scanning, rather than spot analyses was thought necessary for this work given the other conditions employed, as scans across a fine-grained dolomite mosaic indicated that the rate of decomposition was variable across the specimen (fig. A2). There is considerable, correlated variation in Ca and Mg which is negatively correlated with that shown by C and O. Thus, if spot counting were to be used, many spots would be needed to average out this effect. Also, it would be very difficult to build up a series of counts on one spot to reduce the statistical error, because the counts rise continuously once the specimen is exposed to the electron beam. Step-scanning also suffers from these disadvantages.

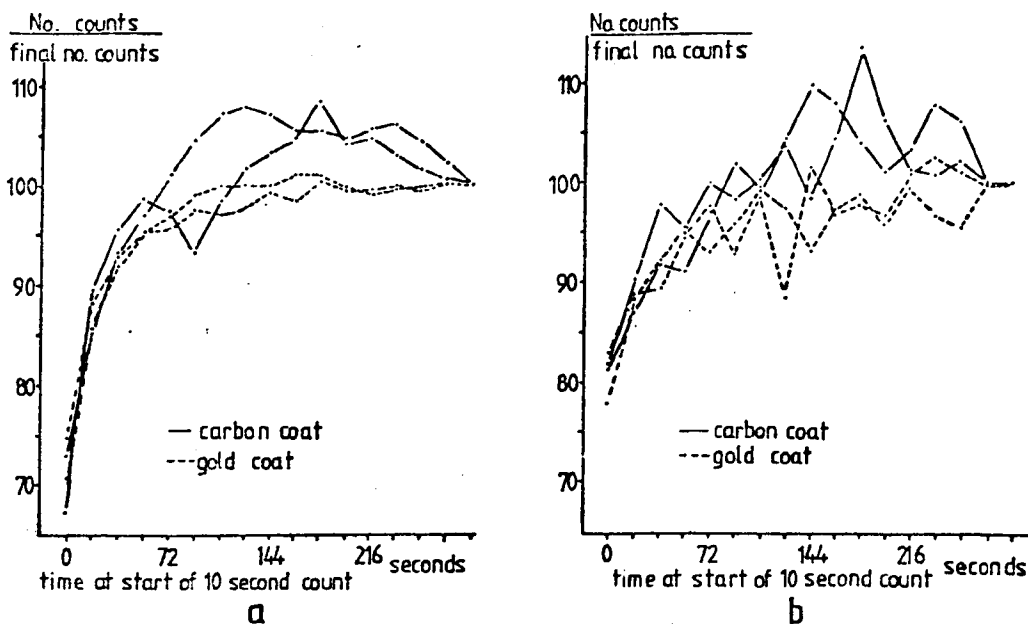


Figure A1: graphs showing the increase in counts with time following exposure of the Amli dolomite standard to a focused electron beam spot (beam size  $3.5\mu\text{m}$ , specimen current  $150\text{nA}$ ). Analysis is for (a) Mg and (b) Mn. Each point represents a 10 second count. The standard was coated successively with carbon and with gold. Gold shows the more reproducible burning behaviour.

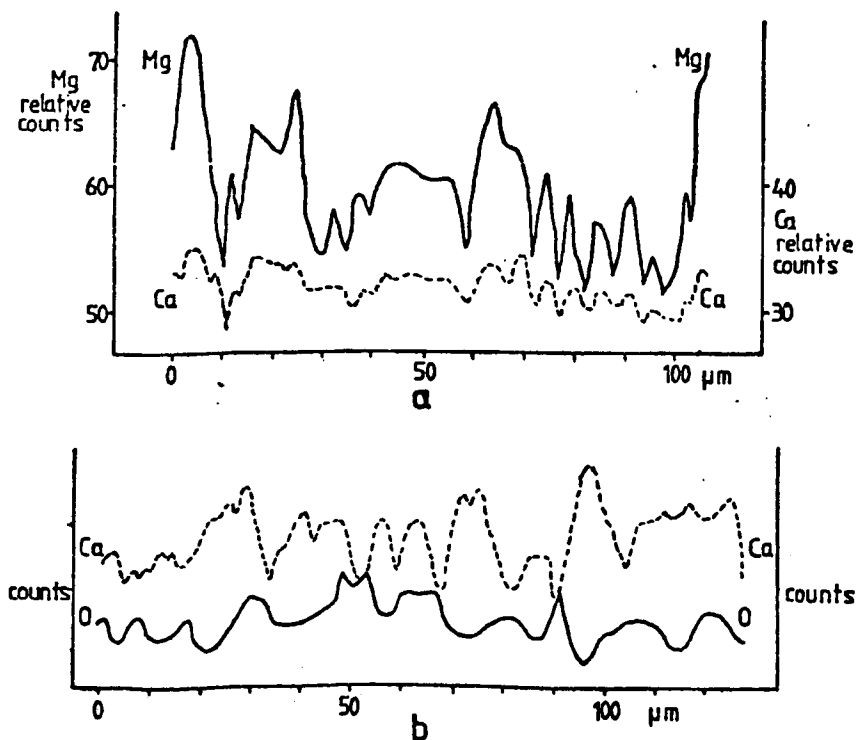


Figure A2: scans across fine grained dolomite (slide 6 of table A4).  
 a) Ca/Mg ( $10\mu\text{m}/\text{minute}$ ,  $4\mu\text{m}$  beam, specimen current  $380\text{nA}$ ). The elements show sympathetic variation. b) Ca/O ( $10\mu\text{m}/\text{minute}$ ,  $4.5\mu\text{m}$  beam, specimen current  $1460\text{nA}$ ). The elements show antipathetic variation.

The scans were run at the same speed for both standard and specimen and were calibrated by repeated 10 second counts. Dolomites were scanned usually at 10 $\mu$ m/minute, although occasionally at 3 or 30 $\mu$ m/minute, whilst calcites were scanned at 10 or 30 $\mu$ m/minute. Variations in decomposition can be recognized by the variation in major element count rates along the scan, and were averaged out. Scans provide a great deal of information about sample heterogeneity which was especially useful in this work where homogeneous samples were the exception, rather than the rule. The specimen stage scanning mechanism (specimen moves) was used in preference to the electronic scan mode (electron beam moves), because the latter involves producing an oscilloscope image which would involve some decomposition of the carbonate before the scan started. The specimen stage scan method is simple to use and scans can be performed in a wide variety of directions.

Various other operating conditions are shown in Table A1. Counter supplies were raised for Mg to assist in 'energy gating' the Mg peak. The combinations of elements analysed simultaneously on channels 1 and 2 were as follows:  
 dolomites: Ca/Mg, Fe/Mg, Mn/Mg, also Ca/Sr;  
 calcites: Fe/Mg, Mn/Sr, occasionally Mn/Mg, Ca/Mg.

### A3: Standards (Table A2)

One standard for each element was available for each of calcite and dolomite. Increased accuracy would have resulted from the use of more standards, but it was found that homogeneous carbonates are uncommon. Samples of the standards were analysed by A.A. several times, and the results averaged.

Dolomite: fragments of a large specimen of ferroan dolomite

TABLE A1: Analytical conditions

Element	Channel	Counter	Line	2θ	Energy gates		Backgrounds	Crystal
					(ε)	(δε)		
Iron	1	sealed	K	57°29'	240	240	±2° 2θ	LiF
Manganese	1	sealed	K	62°56'	220	230	±2° 2θ	LiF
Calcium	1	flow or sealed	K	113°3'	100	220	±2° 2θ	LiF
Magnesium	2	LAND	K	43°33-38'	40	120	±2° 2θ	KAP
Strontium	2	LAND	L	29°50'	30	100	±20' 2θ	KAP

TABLE A2: Composition of standards

(weight %)	CaCO <sub>3</sub>	MgCO <sub>3</sub>	MnCO <sub>3</sub>	FeCO <sub>3</sub>	SrCO <sub>3</sub>
Dolomite, Norway (16654)	54.6(53.2, 53.9,55.8)	34.0(33.7, 33.8,34.0)	0.275(0.258, 0.278,0.297)	11.1(1.05, 1.06,1.10,1.18)	0.017
Calcite, Islay (879828)	97.7	1.5	0.125(0.117, 0.120,0.124, 0.132,0.132)	0.5	0.260(0.226, 0.258,0.309)
Calcite, Lincolnshire	98.4	0.205(0.185, 0.208,0.220)	0.086	1.31(1.24,1.25, 1.34,1.34,1.35)	0.031

Figures used to compute analyses of unknowns are followed by the individual Atomic Absorption analyses in brackets.

TABLE A3: Calculated detection limits, from typical data on standards

Mineral	Element	Content in standard (ppm)	counts/10 seconds		Total counts amassed	Detection limit (ppm)	
			peak	background		element	element carbonate
Calcite	Mn	600	1560	1236	19248	14	29
Calcite	Sr	1550	4689	3744	53361	21	36
Calcite	Fe	6300	6080	1814	57072	31	65
Calcite	Mg <sup>1</sup>	590	2335	1230	26185	8	28
Calcite	Mg <sup>2</sup>	590	1196	665	9836	13	45
Dolomite	Mn	1300	1869	1076	23560	20	42
Dolomite	Fe	53500	33190	1519	228776	22	46

<sup>1</sup>with L.A.N.D. Flow counter

<sup>2</sup>with normal Flow counter

from high grade metamorphic rocks, Amlı, South Norway, collected by C. Peter and housed in the Departmental collection.

Calcites: 1. for Mn and Sr (Fe and Mg inhomogeneous), calcite from a nodule in the study area, North Islay (analysis 30).

2. for Fe and Mg (Mn and Sr homogeneous, but low in concentration), a ferroan calcite from the Jurassic of Lincolnshire.

In most cases the standards were scanned both before and after the specimen and the results averaged.

#### A4: Corrections

Backgrounds: repeated plus and minus background counts were taken at the angles shown in Table A2 and their average subtracted from the peak value.

Decomposition corrections: The fact that the minerals analysed decomposed under the electron beam, and that the extent of this decomposition varied from point to point on the specimens indicates a large source of error in the results. This observation, together with the fact that the samples and standards are similar in composition, removes the necessity for applying the ZAF corrections which are normally performed on microprobe results.

Considering calcites, whenever specimens and standards were analysed successively for Ca very closely comparable results were obtained indicating they decompose to the same extent. The sums of the analyses for dolomites however tend to total more than 100% (extreme range 95-125%) indicating that the specimens tend to decompose to a greater extent than the standard. All the dolomite results have therefore been subject to a correction (indicated in Table A5)

so that the analyses total 100%. As the necessity for this correction was not realised until late in the work, Ca was not determined for all the specimens, in which case a correction was applied assuming a calcium content equal to the average of all the other dolomites in the same suite. Samples re-analysed after luminescence work had slightly increased totals presumably due to heating of the specimens under the broad electron beam of the cathodoluminescence instrument.

#### A5: Errors

There is no objective way of estimating the error in the final tabulated results, but a figure of plus or minus 10% seems likely for average results, perhaps lower than this for major elements and higher for the lowest recorded values. However the concentration of the minor elements in many samples varies so extremely within a short distance that this error is fairly insignificant.

Detection limits have been calculated (Table A3) following the method of Reed (1973). The actual concentrations in the samples are almost all well above these theoretical figures. However in the case of Sr, as the peak position is near the lower limit of the spectrometer drive, the background is high, sloping and somewhat unpredictable. The effective detection limit is therefore probably considerably higher than that calculated; perhaps about 100-150ppm  $\text{SrCO}_3$ .

#### A6: Summary and evaluation of method

The method involves the use of rather severe conditions resulting in visible specimen damage. The standards, however, are of similar composition to the specimens and show burning to roughly the same extent. Fluctuations

in major element concentration attributable to variable burning occurred and the assumption was made that this is the major source of error in the results and that totals deviating from 100% are due to differential burning of specimen and standard. An empirical correction was made on this basis. If this assumption is acceptable then this method scores over the published ones by virtue of the low detection limits and the wealth of information that is provided by using scanning rather than point counts. The conditions were similar for all analyses and the same small area of each standard crystal used, so the results should be precise. The 'burn' lines on the specimens are useful as a marker of the course of the scan (invaluable for zoned crystals) and also for avoiding using the same path twice on the standards.

As only one standard was available for each element for each of calcite and dolomite then any inaccuracy in the A.A. analysis of the standards would be reflected by a proportional error in all the results, but the precision is unaffected. The uncertain magnitude of, and the assumptions made concerning, the decomposition of the samples are definitely the greatest drawbacks to the method.

A description of the analysed samples follows in Table A4 followed by the tabulated results in Table A5.

TABLE A4: Description of specimens analyzed

	Slide reference no.	Locality reference no.		Lithology	Mineral analysis of:	
		Member	Bed/section		Calcite	Dolomite
1	979847	4	D	dolostone	post-tectonic veins and vug linings	fine-grained
2	485332-G	1	B	conglomerate		equant replacive dolomite in pebble
3	861820	4	E	dolostone	A:post-tectonic vug linings and veins B:later veins	fine-grained
4	485332-F	1	B	conglomerate		intergranular (analysis unsatisfactory)
5	46953755-1	3	41B	stromatolite with good microstructure	originally void-infill	fine-grained, and void fringe rhombs
6	846816	3	68E	dolostone and grainstone	originally void-infill	fine-grained, and void-fringe rhombs
7	467370	3	39B	stromatolite, partly calcitised	A:replacive B:originally void-infill	fine-grained
8	105885-1	3	69C	stromatolite, partly calcitised	replacive	fine-grained
9	987870-1	3	62D	stromatolite	quartz-calcite vein (pre-tectonic)	fine-grained
10	009889-1	3	39D	dolomitic silt and dolostone		fine-grained
11	986868	3	62D	flake breccia	intergranular	A: fine-grained B: intergranular rhombs
12	060897	3	13D	flake breccia	intergranular/nodular	A: fine-grained B: intergranular rhombs
13	000864-2	3	54D	sandy oolitic dolostone		A: fine-grained B: matrix rhombs
14	545147	3	A	dolomitic silty mudstone	quartz-albite-calcite vein	intergranular rhombs
15	482349	3	27B	oolitic, partly calcitised dolostone	replacive	fine-grained
16	991873	3	54D	sandy oolitic dolostone		fine-grained
17	002837	4	D	serpentine marble	fibrous	
18	051897	3	9D	dolomitic silt and dolostone	A:quartz-calcite seams B:intergranular	intergranular rhombs
19	904826-1	3	66E	stromatolite		A: fine-grained B: post-tectonic rhombs
20	871824-1	3	69E	stromatolite	A:quartz-calcite vein B:originally void-fill	A: fine-grained B: matrix rhombs
21	869821	3	68E	dolostone and grainstone	calcite vein (post-tectonic)	A: fine-grained B: matrix rhombs
22	887826-2	3	69E	flake breccia	A:quartz-calcite seams B:calcite veins (post-tectonic)	A: fine-grained B: intergranular rhombs
23	477370	3	46B	stromatolite	nodule	fine-grained
24	871825-2	3	68E	stromatolite	A:calcite vein B:quartz-calcite vein (both pre-tectonic)	A: fine-grained B: matrix rhombs
25	17028	3	69C	flake breccia	nodular	fine-grained
26	848827	3	EII	stromatolite	post-tectonic vug-lining	fine-grained
27	233283	1	B	conglomerate		A: patchy fine and medium grained B: intergranular C: equant replacive D: zoned rhombs in mud E: zoned intergranular
28	236284-1	1	B	conglomerate		A: patchy fine and medium-grained B: zoned rhombs in mud C: zoned intergranular D: zoned fringe (pseudo-vug) E: zoned intergranular
29	491332	1	B	dolomitic sandstone		
30	879828	3	69E	stromatolite	nodular	
31	990871	3	62D	stromatolite	nodular	

TABLE A5: Results

Explanation to table:Column 1: Analysis number (see Table A4)Column 2: ++ bright luminescence; + weak luminescence; 0 no luminescence; z series of luminescence zones which were not separately analysed.Column 3: u unzoned; z series of zones not separately analysed; for a zoned crystal c indicates composition of core, or earliest zone analysed and r indicates composition of rim or latest zone analysed.Columns 4-7: chemical composition (in weight % or ppm) e.g.

0.31= very constant composition

0.31= average composition

0.31,0.67= two modal compositions

0.31(0.24-0.36)= average of irregularly fluctuating composition

0.24-0.48= limits of considerable fluctuation

0.24+0.9-2.2= lower level plus sharply defined peaks

0.24 +3.6max=lower level plus series of peaks up to maximum given

0.24/0.36= gradual change in composition from first to second figure

Column 8 (for calcites): in addition to self-explanatory comments, figures in brackets indicate sections of the thesis which discuss the result in question. Where there are compositional peaks, f= frequency (%) of the peaks and p= width of the peaks in microns. dol. indicates dolomite peaks (followed by f=, p=).Column 8 (for dolomites): % correction applied to analyses.Column 9 (for dolomites): as for column 8 for calcites.

## CALCITES

1	2	3	4 % FeCO <sub>3</sub>	5 % MgCO <sub>3</sub>	6 ppm MnCO <sub>3</sub>	7 ppm SrCO <sub>3</sub>	8
<u>Member 3: calcite filling primary porosity in dolostones (7.1.1.;7.9)</u>							
5	++	u	0.22	0.25,0.110	1210	530	f=10,p=<5-10.
	++	u	0.23	0.34,0.127	1340+2300, 3800-8900	530 530	dol.:f=20+,p=2-10. no apparent relation between Mg content and position in void.
	++	u	0.183	0.34,0.162			
	++	u	0.28	0.27			
	++	u	0.186	0.151			
	++	u	0.165	0.29			
6	++	u	0.028	0.52	1220	240-3300	f=50,p=5-15
	++	u	0.127- 0.24	0.032+ 0.189-0.75			
	++	u	0.81, 0.196	0.53,1.04, 0(zero)			Fe low,f=30,p=10-30 Mg low,f=30,p=10-15
7B	++	u	0.42-0.88	0.87-1.47	1960(1510- 2500)	0	
	++	u	0.59-1.02	1.36-1.49			
	++	u	0.52-0.70	0.78-1.36			
20B	++	u	0.179- 0.31+0.40 max	0.20-0.45	1130	1570	f=40. dol.,f=10
<u>Member 3: replacive calcite mosaics (7.2.1.2.;7.2.2.;7.9.)</u>							
7A	++	u	0.085- 0.161	0.41-1.16+ 1.31-2.4	2100	910	f=50-60,p=5
	++	u	0.111	0.58-3.3	1300(1050- 1900)	550	
8	++	u	0.170	0.97-1.45, 1.89-2.2	530	570	Mg high mode,f=75
15	++	u	0.39-1.29	0.53-2.4	1780,1230	2300	dol.,f=5-10,p=<5

			FeCO <sub>3</sub>	K <sub>2</sub> CO <sub>3</sub>	MnCO <sub>3</sub>	SrCO <sub>3</sub>	
<b>Member 3: main calcite suite</b>							(7.1.3.; 7.4.5.; 7.5.5.3.; 7.7.5.; 7.9)
9	++	u	0.26-0.29 +0.50max	0.37-0.46 +3.6max	1210(940- 1300	2000(1300- 3300	f=30-80, p=<5-10
11	++	u	0.32-0.46 +0.50max	0.31-0.55 +1.50-1.97	1020	2600	f=40, p=5-10. dol., f=20 probably originally a cement.
12	++	u	0.41 +0.85max	0.091 +0.63max	3100	1710	f=65; dol., f=10, p=5-10
14	++	u	0.190+ 0.54-0.68	0.26+0.65- 1.5	2000, 1120	700	f=65, p=<5-10 dol., f=15-20, p=<5
	++	u	0.108+ 0.19-0.95	0.114+ 0.21-2.2			
18A	++	u	0.65-0.80	1.15-1.56	2200	940	
	++	u	0.82	1.38	2800	1050	
	++	u			4100	360	
	++	u			4700	620	
18B	++	u	0.8	1.03-1.69	2200	880	
	++	u	1.32	0.93	2700	1200	
	++	u	1.02	1.70			
	++	u	1.15	1.84			
20A	++	u	0.17-0.37 +1.06max	0.25-0.89 +2.3max	1610	1600	f=50+, p=5; dol., f=15, p=<5
22A	++	u	0.57	0.65	1880, 2100	1280	dol, f=<5, p=<5
	++	u	0.79	1.15, 1.59			
23	++	u	0.152 +0.45max	0.166 +0.37-1.17	1480	2200	f=50+, p=<10. dol., f=<5, p=10
	++	u			640	1820	
24A	++	u	0.15-0.32 +0.49-2.2	0.119-0.29 0.43-1.31	850	0	Fe: f=30, p=<10; Mg: f=50+, p=<10
24B	++	u	0.26, 0.39	0.26, 1.24	1330	1280	
25	++	z	0.058, 0.36	0.34-0.68 +1.21	750	1890	high iron areas are later, possibly post-tectonic Mg peaks: f=50, p=5
	++	z	0.087, 0.30	0.56+0.89			
	++	z	0.052- 0.084, 0.32	0.44-0.81+ 0.94-1.07			
30	?	u	0.49(0.37 -0.62	1.03(0.5- 1.83	1250	2600	
	?	u	0.51	1.30			
31	?	u	0.61	1.03	1190	1950	
	?	u	0.59	1.20			
	?	u	0.56	1.16			
<b>Member 3: post-tectonic calcite</b>							(7.8; 7.9)
21	++	z	0.56	0.94-1.37	1620	2500	zoned on luminescence
22B	++	z	0.39-0.59	0.33-0.93	1050-1810	710-820	towards the vein centre Fe, Mg & Mn increase whereas Sr decreases.
26	o	e	0.79-1.43	0.143-0.29	1440	130	zoning seen on staining; results are a combination of 6 scans
	++		0.35	0.41-0.86	1220	130	
	++		0.127	0.141	740	130	
	+		0.70	0.22	?	?	
	+	r	0.29/0.13	0.125	?	?	
<b>Member 4: post-tectonic calcite</b>							(7.8; 7.9)
1A	+	c	?	0.22	790	800	average of two scans
	+		?	0.35	790	800	
	e		0.29	0.24	1350	800	
	+		0.14	0.24	670	800	
	++		0.064	0.24	3500	800	
	o		0.027	0.28	380	800	
	++		0.089	0.25	7400	800	
	o		0.027	0.33/0.37	600/330	800	
	++		0.260	0.29	1900	800	
	++		0.260	0.29	3500	800	
	o	r	0.027	0.39	310	800	

			FeCO <sub>3</sub>	MgCO <sub>3</sub>	CaCO <sub>3</sub>	SrCO <sub>3</sub>	
3A	o	c	0.46	0.57	370	170	average of several scans
	o		0.30-0.33	0.16-0.38 +0.57	370	170	
	o		0.24	0.19	370	170	
	o		0.35	0.063	370	170	
	++		0.46	0.38	2500	170	
	++		0.46	0.45	2500	170	
	++	r	0.46	0.63	2500	170	
3B	o	u	0.36	0.34, 0.44 +1.21, 1.46	700	520	Mn, p= 10. This calcite cut calcite veins of analysis 3A.
	o	u			590	610	
17	++	z	0.039	0.021	1400, 0	600	Mn varies from fibre to fibre. Calcite is in contact metamorphic marble

## DOLOMITES

1	2	3	4 % CaCO <sub>3</sub>	5 % MgCO <sub>3</sub>	6 % FeCO <sub>3</sub>	7 % MnCO <sub>3</sub>	8	9 Note all results are weight %
Fine-grained dolomite, member 4								(Chapter 6)
1	+	u	56.1	43.4	0.38 +0.58- 0.83	0.046	-4	f<10, p<5-15
3	+	u	54.8	44.6	0.53 (0.47- 0.71)	0.034	-4	
Fine-grained dolomite, member 3								(Chapter 6)
5	++	u	60.8	37.6	1.40(0.89- 1.89) +2.3 -5.5	0.164 (0.149- 0.172)	-16	
6	+	u	60.1	37.5	2.2	0.22	-10	
7	++	u	58.6	39.9	0.59 +1.00- 1.96	0.28	-14	f=20, p=5. SrCO <sub>3</sub> =350ppm.
8	++	u	n.d.	38.4-44.1	0.57-0.78 +0.89-1.18, 2.2	0.115-0.23	-8	f=20-60, p=5
9	o	u	n.d.	38.3	2.9-3.3 +3.6-5.1	0.25 (0.21 -0.30)	-10	f=40, p<5
10	o	u	57.9	37.0, 40.5	3.5(2.5- 4.6)	0.21	-7	SrCO <sub>3</sub> not detectable
11A	o	u	n.d.	35.1-43.5	1.53-4.5	0.22	-25	
12A	o	u	n.d.	35.3-37.0	5.7(2.6- 7.9)	0.32-0.36	-6	
13A	o	u	n.d.	36.4-40.6	3.3	0.22	+2	
15	o	u	n.d.	34.1-36.0	5.0-8.2	0.27-0.30	-6	
16	o	u	54.5	41.7	3.6	0.25-0.27	-8	
19A	o	u	57.8	38.9	3.1	0.23-0.28	-3	SrCO <sub>3</sub> =100ppm. luminescent specks have higher Mn:0.35, 0.48.
20A	++	u	59.2	38.7	1.87	0.27	-1	
21A	+	u	55.8	38.8-43.7	2.9(2.7- 3.6)	0.28	-4	
22A	o	u	n.d.	37.0	4.7(4.1 -5.5)	0.35	-13	
23	+	u	58.7	37.6(35.3- 39.8)	2.8-4.5	0.23-0.30	-12	
24A	o	u	n.d.	39.1	2.8	0.23	-9	
25	+	u	54.9	41.5	3.6(1.95- 4.3)	0.173	-11	SrCO <sub>3</sub> =350ppm
26	o	u	57.3	40.3	2.6(2.2- 2.9)	0.150	-10	SrCO <sub>3</sub> =150ppm
-	?	u	60.7	35.9	3.2	0.22	-4	Whole rock analysis (A.A.) of dolostone from bed 23D. Some calcite present.
Member 3: matrix rhombs and intergranular rhombs								(7.2.4.)
11B	++	o	n.d.	38.4-46.9	0.141 3-3.6	0.173 0.215	-23	clean
	++	o	"	"	0.22			
	++	o	"	"	2.5			
	++	o	"	"	0.31			
	++	o	"	"	3-3.6			
	++	o	"	"	0.28			
	o	o	"	"	3.0			
12B	?	o	60.0	39.4	3.1	0.28	-12	cores are inclusion-rich,
		o		31.5	7.5	0.28	-19	rims clean.
		o	60.0	39.4	1.74	0.28	-12	
		o		31.5	2.4	0.28	-19	

			CnCO <sub>2</sub>	FeCO <sub>2</sub>	MgCO <sub>2</sub>	MnCO <sub>2</sub>		
13B	o	c	58.0	38.1	4.3/2.3 3.9	0.172-0.23 0.172-0.23	-5	Rim, and part of core are clean; rest (inner) part of core is inclusion-rich for each rhomb
	o	r	"	"	4.3/2.7 4.4			
	o	c	"	"	4.8/3.3 3.3			
14	o	c	n.d.	36.7	3.4-4.6 5.5-5.8	0.189 0.189	+4	cores are inclusion-rich, rims clean
18	o	u	57.4	33.8-35.4	6.9	0.5	0	rhombs clean
	o	c	"	"	12.2	0.53		
	o	r	"	"	6.5	0.53		
	o	u	"	"	6.8	0.53		
	o	u	"	"	6.8			
	o	u	"	"	7.0			
20B	++	c	n.d.	39.5	1.43 3.3	0.28 0.28	+1	cores are inclusion-rich, rims clean
	++	c	n.d.	39.5	1.05 3.6		+1	
21B	o	c	n.d.	36.1-42.2	0.058	?	-16	clean
	+	"	"	"	1.43-3.6	0.18-0.25	-16	inclusion-rich
	+	"	"	"	1.78	0.22/0.14	-16	inclusion-rich
	o	"	"	"	3.6-4.1	0.28	-16	clean
	o	r	"	"	3.0-3.9	?	-16	clean
	+	c	"	38.8	0.78-4.2	0.34-0.51	-1	inclusion-rich
	+	"	"	"	1.45-2.2	0.51/0.174	-1	inclusion-rich
	o	"	"	"	3.9,4.4	0.35	-1	clean
	o	"	"	"	3.7-4.9	0.35	-1	clean
	o	r	"	"	6.5	0.35	-1	clean
22B	o	u	"	36.8	4.5-5.5	0.31	-2	clean
24B	++	c	"	39.8	0.93-1.6	0.20	-11	inclusion-rich
	o	"	"	"	3.3-3.7	0.25	-11	clean
	o	"	"	"	2.3-3.7	?	-11	clean
	o	r	"	33.2	8.5	?	-7	clean
	+	c	59.3	38.9	2.4	0.14	-19	inclusion-rich
	+	"	"	"	1.0	0.14	-19	inclusion-rich
	++	"	"	"	1.0	0.26	-19	inclusion-rich
	o	"	"	"	3.5	0.26	-19	clean
	o	r	"	"	2.7	0.26	-19	clean
<b>Member 3: post-tectonic rhombs</b>								(7.8.1.)
19B	o	c	n.d.	37.4	7.3	0.091	0	clean. Other rhombs had similar range of iron values, but less well developed zonation
	o	"	"	"	3.0-4.1	0.091	0	
	o	"	"	"	5.6	0.091	0	
	o	r	"	"	3.8-4.8	0.091	0	
	o	e	"	"		0.109	0	
	o	e	"	"		0.168	0	
	o	e	"	"		0.23	0	
<b>Member 1: patchy fine and medium-grained dolomite</b>								(Chapter 6)
27A	z	z	n.d.	40.0-42.1	0.23+1.30- 2.7	0.047- 0.101+0.24 -0.54	0	f=80 for fine-grained dolomite. f=20 for m.gr. dolomite
28A	z	z	n.d.	40.5	0.32-0.38 +0.76-2.20, 3.5	0.063- 0.094 +0.20-0.42	0	as above.
<b>Member 1: equant replacive dolomite</b>								(Chapter 6)
2	z	z	54.3	45.1	0.32	0.048- 0.158+ 0.46, 1.15	-13	f=50, p=5-10. Dolomite is inclusion-rich. Grain boundaries contain impurities (Fe, Si, Ti-rich)
27C	z	z	57.9	41.5	0.156+1.42, 3.6, 5.4	0.043+0.23 0.35, 0.46	0	f=30, p=5-10. Fe, Mn are low at grain boundaries (=later zones). Dolomite is inclusion-rich.
<b>Member 1: zoned dolomite rhombs in mud</b>								(Chapter 6)
27D	++	c	58.3	39.9	0.73-1.51	1.10	-7	1 clean
	+	r	"	"	1.63/0.99	0.96/0.41	-7	2 inclusion-rich/3 clean.
	++	o	"	"	0.54-0.79, 1.6, 1.9		-7	1 clean
	+	r	"	"	1.57/0.89		-7	2 inclusion-rich/3 clean.
	++	o	"	"	0.76	0.79	-7	1A clean
	++	"	"	"	0.92	1.37	-7	1B clean
	+	r	"	"	1.83/1.22	0.94/0.72	-7	2 inclusion-rich/3 clean.

			CaCO <sub>3</sub>	MgCO <sub>3</sub>	FeCO <sub>3</sub>	MnCO <sub>3</sub>		
28B	+	c	n.d.	42.3	0.21-0.60	0.064-0.2%	-24	1 inclusion-rich
	o	"	"	"	0.189-0.26	0.040	-24	2 clean
	++	"	"	"	0.26/0.82	0.67	-24	3 inclusion-rich
	+	"	"	"	0.82-1.43	0.28-0.67	-24	4 clean
	o	"	"	"	17	?		dark line
	o	r	"	"	0.82-1.43	?	-24	5 clean
Member 1: zoned intergranular dolomite								(Chapter 6)
27E	z	z	n.d.	42.3	0.159+1.54, 2.0,2.7	0.080+0.36, 0.53,0.70, 1.04,1.73	-6	f=30-60
28C	z	c	59.5	39.8	0.100-0.137 +0.33-0.81	0.0102- 0.036+ 0.158-0.27	-18	inclusion-rich
	++	"	"	"	0.12	0.27	-18	clean
	+/o	"	"	"	0.12	0.05/ 0.0102	-18	clean
	++	"	"	"	0.12	0.23	-18	clean
	o	r	"	"	9			dark line
29	c	c	56.2	42.0	0.109	0.020	-6	1 inclusion-rich
	++	"	"	"	"	0.348	-6	2 "
	o	"	"	"	"	0.020	-6	3 "
	++	"	"	"	"	0.26	-6	4 "
	o	"	"	"	"	?	-6	5 "
	++	"	"	"	"	?	-6	6 "
	o	"	"	"	"	0.020	-6	7 "
	++	"	"	"	"	0.37	-6	8 "
	o	"	"	"	"	0.020	-6	9 "
	++	"	"	"	0.58	0.70	-6	10 "
	+	"	"	"	0.109	0.188-0.27	-6	11 clean
	o	"	"	"	0.31-0.69	0.020	-6	12 "
	++	"	"	"	0.109-0.86	0.020-0.75	-6	13 inclusion-rich
	o	"	"	"	0.21	<0.348	-6	14 "
	++	"	"	"	0.86	1.46	-6	15 "
	+	"	"	"	0.35-0.86	0.122	-6	16 "
	+	"	"	"	>5.0	0.72	-6	17 clean
	++	"	"	"	0.86	1.11	-6	18 "
	+	r	"	"	2.0-3.6	0.41-1.37	-6	" late replacive zone
Member 1: zoned dolomite fringe (pseudo-vug)								(Chapter 6)
28D	+	c	57.9	39.8	0.069	?	-23	1 inclusion-rich
	++	"	"	"	"	?	-23	2 "
	+	"	"	"	"	0.033	-23	3 "
	o	"	"	"	"	0.033	-23	4 clean
	++	"	"	"	0.086	>0.168	-23	5 "
	o	"	"	"	>0.069	0.033	-23	6 "
	++	"	"	"	>1.48	>0.57	-23	7 inclusion-rich
	+	"	"	"	<0.98	<0.159	-23	8 "
	++	"	"	"	>1.48	>0.93	-23	9 "
	+	"	"	"	0.91/1.37	0.48/0.68	-23	10/11 clean
	+/o	"	"	"	2.4/1.37	1.16/<0.54	-23	12/13 some inclusions
	o/+	"	"	"	1.37/2.4	<0.54/1.16	-23	13/14 some inclusions, becoming clean
	+	r	"	"	1.37/0.78	0.48/0.25	-23	15 clean
Member 1: clean intergranular dolomite								(Chapter 6)
27B	?	u	n.d.	41.2	1.05	0.57	0	
	?	u	"	"	3.3	0.66	0	
	?	u	"	"	1.19	0.66	0	
	++	c	"	"	0.90	0.57	0	
	+	r	"	"	2.9-4.1	0.36	0	
	++	o	56.0	40.8	0.96	0.50	-5	
	+	r	"	"	2.8 +4.4, 5.3,5.9	0.50	-9	
	?	u	"	"	3.0-3.8		-10	

## APPENDIX E: Working methods

### B1: Hand specimens

All specimens were marked in situ with the horizontal, an azimuth, and the way-up. Each specimen was sawn in one or more directions such that one face was perpendicular to both bedding and cleavage. Specimens were reconstructed on thin section examination for measurement of cleavage, quartz fibre, and other orientations.

Polished sawn surfaces were etched in 5% (v/v) HCl and stained for 2-4 minutes in the combined Alizarin Red-S/Potassium Ferricyanide solution of Dickson (1965), but with a lower strength acid (0.5% v/v HCl). Acetate peels were often taken, but these were only used for general descriptions as the dolomite does not etch clearly enough to produce high resolution peels for use in grain fabric studies.

### B2: Thin sections

Rock chips were mounted in epoxy resin to provide a firm base for the production of extra-thin sections (15-25 $\mu$ m) as standard procedure. The sections were hand-ground beyond the normal thickness with successively finer grades of carborundum powder, finishing on 1200 grade. They were stained by the method of Dickson (1965), but in very weak acid (0.25% v/v HCl) as the sections are so thin.

The combined use of extra-thin sections with the staining technique greatly facilitated examination and interpretation of fine-grained lithologies and mixed calcite-dolomite rocks.

Some thin sections were stained for K-feldspar, essentially by the method of Bailey & Stevens (1960).

Thin sections for probe work were polished on mechanical laps, finishing on  $\frac{1}{2}$  $\mu$ m diamond, or aluminium oxide powder. After probe work, the conducting gold coat was removed and

the sections were studied under cathodoluminescence.

Three of the slides used on the microprobe were subsequently ground using 1200 grade carborundum powder to 10-15 $\mu$ m thickness and then polished, using a soft cloth, with 1 $\mu$ m aluminium oxide powder to a final thickness of less than 5 $\mu$ m (= ultra-thin sections). The thickness can be reduced further by etching in 5% HCl (for dolostones).

### B3: X-ray diffraction

This was carried out on a Phillips X-ray spectrometer using Cu K $\alpha$  radiation with slits of 1 $^\circ$ , 1 $^\circ$  and 0.2mm and the results monitored on a chart recorder. The samples were crushed and run as powder or smear mounts; phengites gave an unoriented pattern whichever method was used. The results were made semi-quantitative by running standards of mineral mixtures from rocks in the study area and deriving empirical correction factors (table B1). The peak height of a chosen peak for each mineral was divided by the correction factor and the values recalculated to total 100%.

TABLE B1

#### X.R.D. correction factors

Mineral	peak measured		empirical correction factor	subject to interference from:
	2 $\theta$	d( $\text{\AA}$ )		
Quartz	20.9	4.26	1	microcline
Albite A	27.9	3.19	2.67	muscovite(phengite)
Albite B	23.55	3.77	1.23	muscovite(phengite)
Albite C	24.35	3.66	1.23	microcline
Microcline	27.5	3.24	2	
Calcite	29.5	3.04	5.75	
Dolomite	31.0	2.89	2.58	
Muscovite (phengite)	8.90	10.0	1.8	

#### B4: Atomic Absorption analysis

This was carried out on an EEL 240 atomic absorption spectrometer. When calcite was analysed, 10ml of 50% acetic acid was added to 0.5g of crushed sample; after dissolution the volume was made up to 50ml with de-ionised water. For dolomite, 10ml of 20% HCl was added to 0.5g of sample and after dissolution the sample was evaporated to dryness, 10ml of 50% acetic acid added and the volume made up to 50ml with de-ionised water.

The solutions were diluted as appropriate for analysis of Ca, Mg, Fe, Mn, Sr and Na. Before Sr analysis, 10ml of NaCl solution were added to 40ml of sample solution to prevent ionisation and for Ca and Mg analysis lanthanum chloride solution was added to prevent Al interference.

#### B5: Cathodoluminescence

Earlier work was performed using uncapped thin sections finished on 1200 grade carborundum powder using an apparatus designed and built by Dr. A.A.Mills of Leicester University. The later work was carried out using polished probe slides on an instrument built by Mr. W.Wilson at Nottingham under the direction of Dr. J.A.D.Dickson.

Cathodoluminescence gives a striking demonstration of mineral distribution and of zonation within crystals, particularly in carbonates.

The orange-red luminescence of calcites and dolomites is activated by Mn and quenched by Fe, Co and Ni (Sippel & Glover 1965). Quantification of the relative importance of these effects has only been to order of magnitude concentrations previously (Long & Agrell, 1965). The results of the present study (fig. B1) define the threshold of luminescence much more closely. At concentrations of Fe

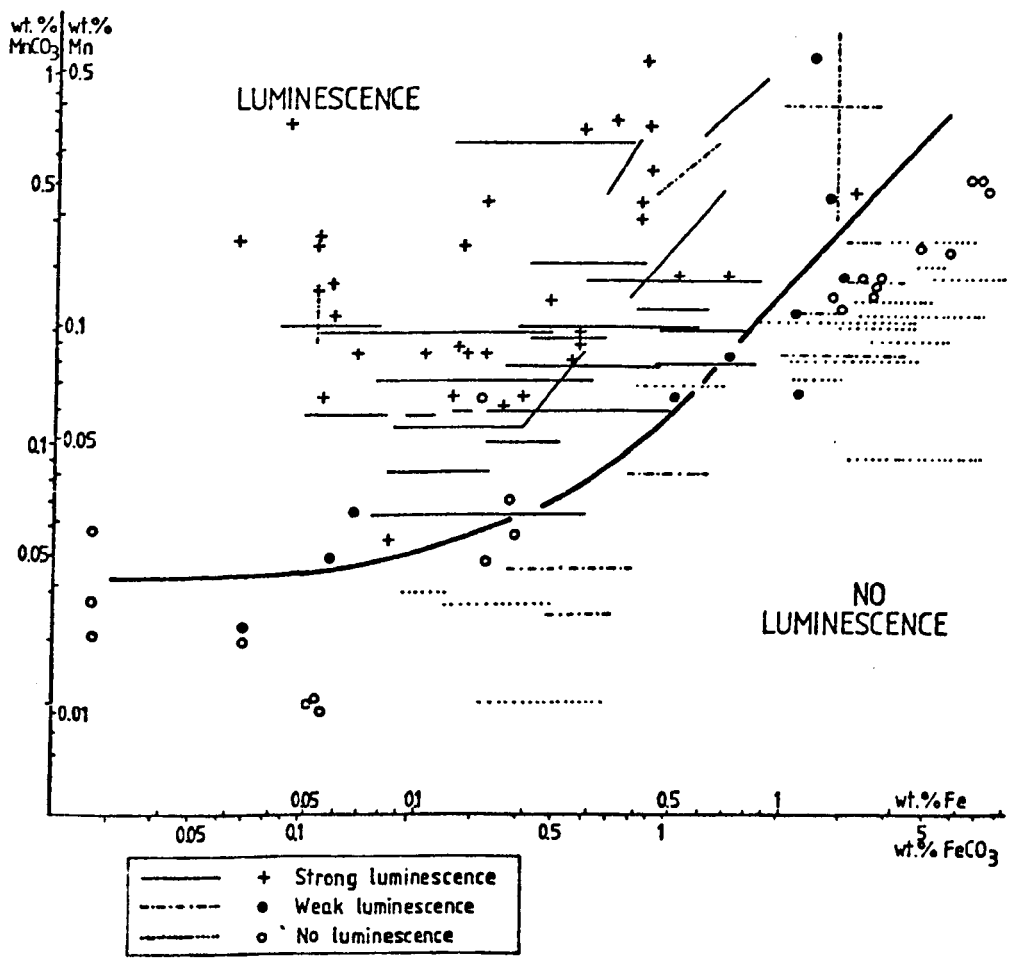


Figure B-1: Luminescence of calcites and dolomites in the Bonahaven Formation in terms of their Fe and Mn concentrations.

below 0.5%  $\text{FeCO}_3$ , luminescence seems to depend on there being sufficient (0.05%)  $\text{MnCO}_3$ . At higher concentrations of Fe, luminescence is seen if the  $\text{MnCO}_3$  concentration is more than about a tenth of the  $\text{FeCO}_3$  concentration. Some analyses lie on the 'wrong' side of the luminescence/ no luminescence boundary: this could be due to variations in the quantity of Co or Ni present, although they will only be present in trace amounts. Another factor is that the distinction between strong, weak and no luminescence is subjective. The possibility of extreme heating leading to mineral luminescence (Sommer, 1972b) does not seem applicable.

There is usually a wavelength shift in luminescence between the typical orange colour of calcite and the more reddish dolomite. This has been explained theoretically by Sommer (1972a). However zoned dolomite in member 1 shows a range of colours from yellow to red of uncertain origin; there is no apparent relation to the concentration of iron and manganese.

Appendix C: Determination of size distributions of spheres from size distributions of their sections

In this Appendix, the procedure is outlined by which, in Chapter 5, the size distribution of spherules was converted to a three-dimensional distribution. The method is based on the paper by Hennig & Elias (1971) in which pairs of size distributions are plotted: one member of each pair representing a particular size distribution of spheres and the other representing the distribution of circles in a section cut through the spheres. They suggest comparing a measured distribution with these standard curves. However, the number of sphere distributions that they present is limited and so it was thought necessary to calculate the spheres' distribution from the measured thin section distribution in the way outlined by Hennig & Elias. Essentially a set of simultaneous equations is generated and solved: the co-efficients of these equations were not given by Hennig & Elias (1971) so had to be derived (see below).

The data is divided into 12 size classes of equal size, the smallest class to include the origin. For spheres of class 12 (the largest), a certain proportion ( $a_{12}$ ) will have size within class 12 when measured in thin section, a proportion ( $a_{11}$ ) will have size within class 11 and so on. For spheres of size class 11,  $b_{11}$  will be in class 11 in thin section,  $b_{10}$  in class 10 and so on.

In thin section, as circles of size class 12 can only be derived from spheres of class 12, their frequency ( $N_{12}$ ) =  $a_{12}C_{12}$ , where  $C_{12}$  is the frequency of spheres in class 12. Circles of size 11 can be derived from class 11 or 12 of the spheres' distribution, so  $N_{11} = a_{11}C_{12} + b_{11}C_{11}$ .



## REFERENCES

Number(s) in parentheses after each reference indicate the page(s) of this thesis where the reference is cited.

- AITKEN, J.D. 1967. Classification and environmental significance of cryptalgal limestones and dolomites with illustrations from the Cambrian and Ordovician of southwestern Alberta. *J. Sedim. Petrol.*, 37, 1163-78. (105)
- AKHTAR, K. & SRIVASTAVA, V.K. 1976. Ganurgarh Shale of southeastern Rajasthan, India: a Precambrian regressive sequence of lagoon-tidal flat origin. *J. Sedim. Petrol.*, 46, 14-21. (80)
- AL-HASHIMI, W.S. 1976. Significance of strontium distribution in some carbonate rocks in the Carboniferous of Northumberland, England. *J. Sedim. Petrol.*, 46, 369-76. (102)
- ALLEN, J.R.L. 1970. Physical processes of sedimentation. George Allen and Unwin, London. (63)
- ALLEN, J.R.L. & BANKS, N.L. 1972. An interpretation and analysis of recumbent-folded deformed cross-bedding. *Sedimentology*, 19, 257-83. (36)
- ALLISON, A. 1933. The Dalradian succession in Islay and Jura. *Q. Jl geol. Soc. Lond.*, 89, 125-44. (5, 16)
- ALTSCHULER, Z.S., CLARKE, R.S. & YOUNG, E.J. 1958. Geochemistry of uranium in apatite and phosphorite. *U. S. Geol. Surv. Prof. Pap.* 314-D, 45-90. (107)
- ANDERTON, R. 1974. Sedimentology of the Middle Dalradian of Argyll with special reference to the Jura Quartzite, Scarba Conglomerate and Craignish Phyllites. Ph. D. thesis, University of Reading. (1, 1A, 7, 10, 85, 86, 87, 198, 200, 205, 206)
- ANDERTON, R. 1975. Tidal flat and shallow marine sediments from the Craignish phyllites, Middle Dalradian, Argyll, Scotland. *Geol. Mag.*, 112, 337-48. (1, 24, 44, 98, 136, 161)
- ANDERTON, R. 1976. Tidal shelf sedimentation: an example from the Scottish Dalradian. *Sedimentology*, 23, 429-58. (1, 10, 34, 85, 87, 198, 203, 206)
- ANDREWS, P.B. 1970. Facies and genesis of a hurricane-washover fan, St. Joseph Island, Central Texas coast. *Rep. Inves. No. 67*, Bur. Econ. Geol. Univ. Texas, Austin, Texas. (43, 44)
- ASHBY, M.F. & VERRALL, R.A. 1973. Diffusion-accommodated flow and superplasticity. *Acta Metall.*, 21, 149-63. (164, 168)
- ASQUITH, G.B. 1967. The marine dolomitization of the Mifflin Member, Plattenville Limestone in southwest Wisconsin. *J. Sedim. Petrol.*, 37, 311-26. (94)
- ATHERTON, M.P. 1976. Crystal growth models in metamorphic tectonites. *Phil. Trans. R. Soc.*, A283, 255-70. (143, 149)
- BADIOZAMI, K. 1973. The Dorag dolomitization model- application to the Middle Ordovician of Wisconsin. *J. Sedim. Petrol.*, 43, 965-84. (92, 93, 94, 95, 104, 105)
- BAILEY, E.B. 1917 (for 1916). The Islay Anticline (Inner Hebrides) *Q. Jl geol. Soc. Lond.*, 72, 132-64. (1A, 4, 7, 16, 19, 20, 20A, 91)
- BAILEY, E.B. & McCALLIEN, W.J. 1937. Perthshire tectonics: Schichallion to Glen Lyon. *Trans. R. Soc. Edinb.*, 59, 79-117. (203)

- BAILEY, E.H. & STEVENS, R.E. 1960. Selective staining of K-feldspar and plagioclase on rock slabs and thin sections. *Am. Miner.*, 45, 1020-25. (215)
- BARWIS, J.H. 1976. Internal geometry of Kiawah Island beach ridges. pp115-26 IN: HAYES, M.O. & KANA, T.W. (eds.). *Terrigenous clastic depositional environments*. Tech. Rpt. 11, Coastal Research Division, Dept. Geol. Univ. S. Carolina, Columbia, S. Carolina. (44)
- BASAHHEL, A.N. 1971. The Dalradian stratigraphy and structure of Southern Islay, Argyll. Ph. D. Thesis, University of Liverpool. (1, 1A, 10, 16, 20, 20A, 21)
- BASKIN, Y. 1956. A study of authigenic feldspars. *J. Geol.*, 64, 132-55. (130, 151)
- BATHURST, R.G.C. 1971. Carbonate sediments and their diagenesis. Elsevier, Amsterdam. (66, 91, 93, 94, 99, 100, 104, 117, 124, 148, 167, 191)
- BAUSCH, W.M. 1968. Clay content and calcite crystal size of limestones. *Sedimentology*, 10, 71-5. (100)
- BEEK, J.L. van & KOSTER, E.A. 1972. Fluvial and estuarine sediments exposed along the Oude Maas (The Netherlands). *Sedimentology*, 19, 237-56. (61)
- BEHRENS, E.W. & LAND, L.S. 1972. Subtidal Holocene dolomite, Baffin Bay, Texas. *J. Sedim. Petrol.*, 42, 155-61. (79, 91, 104)
- BENSON, L.V., ACHAUER, C.W. & MATTHEWS, R.K. 1972. Electron microprobe analyses of magnesium and iron distribution in carbonate cements and recrystallized sediment grains from ancient carbonate rocks. *J. Sedim. Petrol.*, 42, 803-11. (209)
- BENSON, L.V. & MATTHEWS, R.K. 1971. Electron microprobe studies of magnesium distribution in carbonate cements and recrystallized skeletal grainstones from the Pleistocene of Barbados, W. Indies. *J. Sedim. Petrol.*, 41, 1018-25. (209)
- BERNER, R.A. 1971. *Principles of chemical sedimentology*, McGraw-Hill, New York. (107, 145)
- BETRAND-SARFATI, J. 1976. An attempt to clarify Late Precambrian stromatolite microstructures. pp251-9 IN: WALTER, M.R. (ed.). *Stromatolites*. Elsevier, Amsterdam. (66, 68, 71)
- BEUKES, N.J. 1977. Transition from siliciclastic to carbonate sedimentation near the base of the Transvaal Supergroup, northern Cape Province, South Africa. *Sediment. Geol.*, 18, 201-22. (81, 86, 88, 98)
- BICKLE, M.J. & POWELL, R. 1977. Calcite-dolomite geothermometry for iron-bearing carbonates. *Contr. Miner. Petrol.*, 59, 281-92. (103, 191, 208)
- BLATT, H., MIDDLETON, G. & MURRAY, R. 1972. *Origin of sedimentary rocks*. Prentice-Hall, New Jersey. (92, 192)
- BODINE, M.W., HOLLAND, H.D. & BORCSIK, M. 1965. Coprecipitation of manganese and strontium with calcite. pp401-6 IN: *A symposium on problems of postmagmatic ore deposition II*. Prague. (102A)
- BOER, R.B. de 1977. On the thermodynamics of pressure solution-interaction between chemical and mechanical forces. *Geochim. cosmochim. Acta*, 41, 249-56. (93)
- BORCH, C.C. von der & JONES, J.B. 1976. Sperular modern dolomite from the Coorong area, South Australia. *Sedimentology*, 23, 587-91. (91)

- BORCH, C.C. von der & TRUEMAN, N.A. 1974. Dolomitic basal sediments from northern end of ninetyeast ridge. Init. Rept. Deep Sea Drilling Project, 22, 477-83. (129)
- BORRADAILE, G.J. 1973. Dalradian structure and stratigraphy of the northern Loch Awe district, Argyllshire. Trans. R. Soc. Edinb., 69, 1-21. (31, 169)
- BORRADAILE, G.J. 1977. On cleavage and strain: results of a study from West Germany using tectonically deformed sand dykes. J1 geol. Soc. Lond., 133, 146-64. (169)
- BORRADAILE, G.J. & JOHNSON, H.D. 1973. Finite strain estimates from the Dalradian Dolomitic Formation, Islay, Argyll, Scotland. Tectonophysics, 18, 249-59. (6, 17, 18, 20, 20A, 24, 56, 160)
- BOUMA, A.H. & HOLLISTER, C.D. 1973. Deep ocean basin sedimentation. pp79-118 IN: MIDDLETON, G.V. & BOUMA, A.H. (eds.). Turbidites and deep-water sedimentation: lecture notes for a short course. Pacific Section S.E.P.M., Los Angeles, California. (42)
- BRAUN, M & FRIEDMAN, G.M. 1969. Carbonate lithofacies and environment of the Tribes Hill Formation (Lower Ordovician) of the Mohawk Valley, New York. J. Sedim. Petrol., 39, 113-35. (97)
- BRENCHLEY, P.J. & NEWALL, G. 1977. The significance of contorted bedding in Upper Ordovician sediments of the Oslo region, Norway. J. Sedim. Petrol., 47, 819-33. (37)
- BRIDGES, P.H. 1976. Lower Silurian transgressive barrier islands, southwest Wales. Sedimentology, 23, 347-62. (80)
- BRIDGES, P.H. & LEEDER, M.R. 1976. Sedimentary model for intertidal mudflat channels with examples from the Solway Firth, Scotland. Sedimentology, 23, 533-52. (42, 51, 80)
- BROWN, E.H. 1967. The greenschist facies in part of Eastern Otago, New Zealand. Contrib. Mineral. Petrol., 14, 259-92. (183)
- BROWN, P.R. 1972. Incipient metamorphic fabrics in some mud-supported carbonate rocks. J. Sedim. Petrol., 42, 841-7. (98, 185)
- BURST, J.F. 1965. Subaqueously formed shrinkage cracks in clay. J. Sedim. Petrol., 35, 348-53. (57)
- BUTLER, G.P. 1970. Holocene gypsum and anhydrite of the Abu Dhabi sabkha, Trucial Coast: an alternative explanation of origin. pp120-52 IN: RAU, J.L. & DELLWIG, L.F. (eds.). Third symposium on salt. The Northern Ohio Geological Society, Cleveland, Ohio. (137)
- BUTTON, A. 1973. Algal stromatolites of the Early Proterozoic Wolkberg Group, Transvaal sequence. J. Sedim. Petrol., 43, 160-7. (70)
- BUTTON, A. 1976. Iron-formation as an end-member in carbonate sedimentary cycles in the Transvaal Supergroup, S. Africa. Econ. Geol., 71, 193-201. (80, 108, 108A)
- BUYCE, M.R. & FRIEDMAN, G.M. 1975. Significance of authigenic K-feldspar in Cambro-Ordovician carbonate rocks of the Proto-Atlantic shelf in North America. J. Sedim. Petrol., 45, 808-21. (130)
- CAMPBELL, J.D. 1958. En echelon folding. Econ. Geol., 53, 448-72. (21)
- CAREY, S.W. & AHMED, N. 1961. Glacial marine sedimentation. pp865-95 IN: RAASCH, G.O. (ed.) Geology of the Arctic, vol. 2. Univ. Toronto Press. (198)
- CHARLESWORTH, J.K. 1957. The Quaternary Era, vol. 2. Edward Arnold, London. (198)

- CHATTERJEE, N.D. 1966. On the widespread occurrence of oxidized chlorites in the Pennine zone of the Western Italian Alps. *Contr. Miner. Petrol.*, 12, 325-39. (183)
- CHURCH, M. & GILBERT, R. 1976. Proglacial fluvial and lacustrine environments. pp22-100 IN: JOPLING, A.V. & McDONALD, B.C. (eds.) *Glaciofluvial and glaciolacustrine sedimentation. Soc. Econ. Palaeont. Mineral. Spec. Publ.*, 23. (33)
- CLIFTON, H.E. 1969. Beach lamination: nature and origin. *Mar. Geol.*, 7, 553-9. (42).
- CLIFTON, H.E., HUNTER, R.E. & PHILLIPS, R.L. 1971. Depositional structures and processes in the non-barred high energy nearshore. *J. Sedim. Petrol.*, 41, 651-70. (34).
- CLOUD, P.E. & SEMIKHATOV, M.A. 1969. Proterozoic stromatolite zonation. *Am. J. Sci.*, 267, 1017-61. (71, 72).
- COOMBS, D.S., ELLIS, A.J., FYFE, W.S. & TAYLOR, A.M. 1959. The zeolite facies, with comments on the interpretation of hydrothermal syntheses. *Geochim. cosmochim. Acta*, 17, 53-107. (153).
- COSGROVE, J.W. 1976. The formation of crenulation cleavage. *Jl. geol. Soc. Lond.*, 132, 155-78. (169, 180).
- CROW, M.J., MAX, M.D. & SUTTON, J.S. 1971. Structure and stratigraphy of the metamorphic rocks in part of northwest County Mayo, Ireland. *Jl. geol. Soc. Lond.*, 127, 579-84. (204)
- CURRAY, J.R. 1956. The analysis of two-dimensional orientation data. *J. Geol.*, 64, 117-31. (63)
- CURTIS, C.D. & SPEARS, D.A. 1968. The formation of sedimentary iron minerals. *Econ. Geol.*, 258-70. (106, 150)
- DALRYMPLE, D.W. 1966. Calcium carbonate deposition associated with blue-green algal mats, Baffin Bay, Texas. *Publs. Inst. mar. Sci. Tex.*, 10, 187-200. (67):
- DAVIDSON-ARNOTT, R.G.D. & GREENWOOD, B. 1976. Facies relationships on a barred coast, Kouchibouguac Bay, New Brunswick, Canada. pp149-68 IN: DAVIES, R.A. & ETHERINGTON, R.L. *Beach and nearshore sedimentation. Soc. Econ. Palaeont. Mineral. Spec. Publ.* 24. (43)
- DAVIES, D.K., ETHERIDGE, F.G. & BERG, R.R. 1971. Recognition of barrier environments. *Bull. Am. Ass. Petrol. Geol.*, 55, 550-65. (43)
- DAVIES, P.J., FERGUSON, J. & BUBELA, B. 1975. Dolomite and organic material. *Nature, Lond.*, 255, 472-4. (94, 104)
- DAVIS, R.A. 1965. Underwater study of ripples, SE Lake Michigan. *J. Sedim. Petrol.*, 35, 857-66. (49, 51)
- DEER, W.A., HOWIE, R.A. & ZUSSMAN, J. 1962. *Rock-forming minerals. Vol. 3 Sheet silicates. Longmans, London.* (182)
- DEFFEYES, K.S., LUCIA, F.J. & WEYL, P.K. 1965. Dolomitization of Recent and Plio-Pleistocene sediments by marine evaporite waters on Bonaire, Netherlands Antilles. pp71-88 IN: PRAY, L.C. & MURRAY, R.C. (eds.) *Dolomitization and limestone diagenesis. Soc. Econ. Palaeont. Mineral. Spec. Publ.* 13. (92, 104)
- DEWEY, J.F. 1969. Evolution of the Appalachian/Caledonian orogen. *Nature, Lond.*, 222, 124-9. (1, 205)
- DICKSON, J.A.D. 1965. A modified staining technique for carbonates in thin section. *Nature, Lond.*, 205, 587. (215)

- DICKSON, J.A.D. & BARBER, C. 1976. Petrography, chemistry and origin of early diagenetic concretions in the Lower Carboniferous of the Isle of Man. *Sedimentology*, 23, 189-211. (151)
- DOBSON, M.R., EVANS, D. & WHITTINGTON, R. 1975. The offshore extension of the Loch Gruinart Fault, Islay. *Scott. J. Geol.*, 11, 23-35. (22)
- DONOVAN, R.N. & FOSTER, R.J. 1972. Subaqueous shrinkage cracks from the Caithness flagstone series (Middle Devonian) of North-East Scotland. *J. Sedim. Petrol.*, 42, 309-17. (56, 57)
- DOW, D.B. & GEMUTS, I. 1969. Geology of the Kimberley Region, Western Australia. *Bureau Mineral Res. Aust. Bull.*, 106. (197)
- DOWNIE, C, LISTER, T.R., HARRIS, A.L. & FETTES, D.J. 1971. A palynological investigation of the Dalradian rocks of Scotland. *Rep. No. 71/9 Inst. geol. Sci.* (6, 98)
- DUNOYER de SEGONZAC, G. 1970. The transformation of clay minerals during diagenesis and low-grade metamorphism: a review. *Sedimentology*, 15, 281-346. (148, 149)
- DURNEY, D.W. 1972. Solution transfer, an important geological deformation mechanism. *Nature, Phys. Sci.*, 235, 315-7. (165)
- DURNEY, D.W. & RAMSAY, J.G. 1973. Incremental strains measured by syntectonic crystal growths. pp67-96 IN: JONG, K.A. de & SCHOLTEN, R. (eds.) *Gravity and tectonics*. Wiley, New York. (28, 29, 169, 172, 173, 175A, 176, 177, 178, 179)
- DURRANCE, E.M. 1976. A gravity survey of Islay, Scotland. *Geol. Mag.*, 113, 251-61. (22)
- EDMUNDS, W.M. & ATHERTON, M.P. 1971. Polymetamorphic evolution of garnet in the Fanad aureole, Donegal, Eire. *Lithos*, 4, 147-61. (143)
- EDMUNDS, W.M. & THOMAS, P.R. 1966. The stratigraphy and structure of the Dalradian rocks north of Recess, Connemara, Co. Galway. *Proc. R. Ir. Acad.*, 64B, 517-28. (204)
- ELLIOTT, D. 1972. Deformation paths in structural geology. *Bull. geol. Soc. Am.*, 83, 2621-38. (28, 172, 173)
- ELLIOTT, D. 1973. Diffusion flow laws in metamorphic rocks. *Bull. geol. Soc. Am.*, 84, 2645-64. (164, 165, 166)
- ENGELHARDT, W.von 1977. *The origin of sediments and sedimentary rocks*. (translated by JOHNS, W.D.) Halsted Press, John Wiley, New York-Toronto-Sydney. (151, 153)
- ERIKSSON, K.A., McCARTHY, T.S. & TRUSWELL, J.F. 1975. Limestone formation and dolomitization in a Lower Proterozoic succession from South Africa. *J. Sedim. Petrol.*, 45, 604-14. (108, 108A)
- ETHERIDGE, M.A. & LEE, M.F. 1975. Microstructure of slate from Lady Loretta, Queensland, Australia. *Bull. geol. Soc. Am.*, 86, 13-22. (168)
- EUGSTER, H.P. & CHOU, I-M. 1973. The depositional environments of Precambrian banded iron-formations. *Econ. Geol.*, 68, 114-68. (193)
- EVAMY, B.D. 1967. Dedolomitization and the development of rhombohedral pores in limestones. *J. Sedim. Petrol.*, 37, 1204-15. (193, 195)
- EVAMY, B.D. 1969. The precipitational environment and correlation of some calcite cements deduced from artificial staining. *J. Sedim. Petrol.*, 39, 787-93. (102, 106, 123)
- EVANS, G. 1965. Intertidal flat sediments and their environments in The Wash. *Q. Jl. geol. Soc. Lond.*, 121, 209-45. (42)

- FAIRBAIRN, H.W. 1949. Structural petrology of deformed rocks. Addison-Wesley, Cambridge, Mass. (172, 173)
- FAIRBAIRN, H.W. 1950. Pressure shadows and relative movements in a shear zone. *Trans. Am. Geophys. Union*, 31, 914-6. (173)
- FINLOW-BATES, T. 1977. The formation of fibrous texture in some veins. *Geol. Mag.*, 114, 141-4. (179)
- FISCHBECK, R. & MÜLLER, G. 1971. Monohydrocalcite, hydromagnesite, nesquehonite, dolomite, aragonite and calcite in speleothems of the Fraenkische Schweiz, Western Germany. *Contr. Miner. Petrol.*, 33, 87-92. (94)
- FISCHER, A.G. 1961. Stratigraphic record of transgressing seas in light of sedimentation on the Atlantic coast of New Jersey. *Bull. Am. Ass. Petrol. Geol.*, 45, 1656-66. (45)
- FISCHER, A.G. 1975. Tidal deposits, Dachstein limestone of the North-Alpine Triassic. pp235-42 IN: GINSBURG, R.N. (ed.) *Tidal deposits. A casebook of Recent examples and fossil counterparts.* Springer-Verlag, Berlin. (68)
- FOLK, R.L. & LAND, L.S. 1975. Mg/Ca ratio and salinity: two controls over crystallization of dolomite. *Bull. Am. Ass. Petrol. Geol.*, 59, 60-8. (91, 92, 93, 94, 104)
- FOLK, R.L. & SIEDLECKA, A. 1974. The 'schizohaline' environment: its sedimentary and diagenetic fabrics as exemplified by late Palaeozoic rocks of Bear Island, Svalbard. *Sediment. Geol.* 11, 1-15. (91, 93, 94, 98, 104)
- FRIEDMAN, G.M. 1965. Terminology of crystallization textures and fabrics in sedimentary rocks. *J. Sedim. Petrol.*, 35, 643-55. (4)
- FRIEDMAN, G.M. & SANDERS, J.E. 1967. Origin and occurrence of dolostones. pp 267-348 IN: CHILINGAR, G.V., BISSELL, H.J. & FAIRBRIDGE, R.W. (eds.) *Carbonate rocks.* Elsevier, Amsterdam. (91, 93)
- FROST, J.G. 1974. Subtidal algal stromatolites from the Florida backreef environment. *J. Sedim. Petrol.* 44, 532-7. (66)
- FRUTH, I. & SCHERRBICKS, R. 1975. Facies and geochemical correlations in the upper Hauptdolomit (Norian) of the Eastern Lechtaler Alps. *Sediment. Geol.*, 13, 27-45. (107)
- FÜCHTBAUER, H. 1974. *Sediments and sedimentary rocks. Vol. I.* Halsted Press Division, J. Wiley & sons Inc., New York. (2, 91, 94, 141, 149, 151, 160, 189, 192, 194)
- FÜCHTBAUER, H & TISLJAR, J. 1975. Peritidal cycles in the Lower Cretaceous of Istria (Yugoslavia). *Sediment. Geol.*, 14, 219-33. (57, 62)
- GABLINA, I.F. & TSEPIN, A.I. 1975 (for 1974). Isomorphous impurities in calcite as indicators of the genesis of sandstones of the Dzhuzkazgan suite. *Doklady. Akad. Nauk. SSSR.*, 221, 196-8. (208)
- GEBELEIN, C.D. 1969. Distribution, morphology and accretion rate of Recent sub-tidal stromatolites, Bermuda. *J. Sedim. Petrol.*, 39, 49-69. (71)
- GEBELEIN, C.D. Biological control of stromatolite microstructure: implications for Precambrian time-stratigraphy. *Am. J. Sci.*, 274, 575-98. (64)
- GEBELEIN, C.D. 1977. Dynamics of Recent carbonate sedimentation and ecology (Cape Sable, Florida). E.J. Brill, Leiden. (76)
- GEBELEIN, C.D. & HOFFMAN, P. 1973. Algal origin of dolomitic laminations in stromatolitic limestone. *J. Sedim. Petrol.*, 43, 603-13. (69, 94, 104, 125)

- GILL, W.D., KHALAF, F.I. & MASSOUD, M.S. 1977. Clay minerals as an index of the degree of metamorphism of the carbonate and terrigenous rocks in the South Wales coalfield. *Sedimentology*, 24, 675-91. (149)
- GINGERICH, P.D. 1969. Markov analysis of cyclic alluvial sediments. *J. Sedim. Petrol.*, 39, 330-2. (75)
- GOLDBERG, E.D. 1963. The oceans as a chemical system. pp 3-25 IN: *The Sea*. Interscience, New York-London. (103)
- GOLDSMITH, J.R. 1953. A "simplexity principle" and its relation to 'ease' of crystallization. *J. Geol.*, 61, 439-51. (92)
- GOLDSMITH, J.R. & GRAF, D.L. 1958. Structural and compositional variations in some natural dolomites. *J. Geol.*, 66, 678-93. (93, 98)
- GOLUBIC, S. 1973. The relationship between blue-green algae and carbonate deposits. pp 433-72 IN: CARR, N.G. & WHITTON, B.A. *The Biology of blue-green algae*. Blackwell, Oxford. (64)
- GOODWIN, P.W. & ANDERSON, E.J. 1974. Associated physical and biogenic structures in environmental subdivision of a Cambrian tidal sand body. *J. Geol.*, 81, 779-94. (42, 61)
- GRAF, D.L. 1960. Geochemistry of carbonate sediments and sedimentary carbonates. *Illinois State geol. Surv. Circ.* 301. (102)
- GRAF, D.L. 1962. Minor element distribution of sedimentary carbonates. *Geochim. cosmochim. Acta.*, 26, 849-56. (108)
- GRAF, D.L. & LAMAR, J.E. 1950. Petrology of Fredonia Oolite in southern Illinois. *Bull. Am. Ass. Petrol. Geol.* 34, 2318-36. (121)
- GRAHAM, C.M. 1976. Petrochemistry and tectonic significance of Dalradian metabasaltic rocks of the SW Scottish Highlands. *Jl geol. Soc. Lond.*, 132, 61-84. (206)
- GREEN, J.F.N. 1924. The structure of the Bowmore-Portaskaig district of Islay. *Q. Jl geol. Soc. Lond.*, 80, 72-105. (16)
- GREGORY, J.W. 1928. The sequence in Islay and Jura. *Trans. geol. Soc. Glasg.*, 18, 420-41. (16)
- GUSTAVSON, T.C., ASHLEY, G.M. & BOOTHROYD, J.C. 1976. Depositional sequences in glaciolacustrine deltas. pp264-80 IN: JOPLING, A.V. & McDONALD B.C. *glaciofluvial and glaciolacustrine sedimentation*. Soc. Econ. Paleont. Mineral. Spec. Publ. 23. (33)
- GUTSTADT, A.M. 1968. Petrology and depositional environments of the Beck Spring Dolomite (Precambrian), Kingston Range, California. *J. Sedim. Petrol.*, 38, 1280-9. (126, 194)
- HACKMAN, B.D. & KNILL, J.L. 1962. Calcareous algae from the Dalradian of Islay. *Palaeontology*, 5, 268-71. (6)
- HAGAN, G.M. & LOGAN, B.W. 1974. Development of carbonate banks and hypersaline basins, Shark Bay, Western Australia. *Am. Ass. Petrol. Geol. Mem.* 22, 61-139. (80)
- HANSHAW, B.B., BACK, W. & DEIKE, R.G. 1971. A geochemical hypothesis for dolomitization by ground water. *Econ. Geol.* 66, 710-24. (92, 93)
- HARLAND, W.B. & GAYER, R.A. 1972. The Arctic Caledonides and earlier oceans. *Geol. Mag.*, 109, 289-314. (205)
- HARRIS, A.L., BALDWIN, C.T., BRADBURY, H.J., JOHNSON, H.D. & SMITH, R.A. (in press). Basin evolution of the Dalradian Supergroup. (206)
- HARRIS, A.L. & PITCHER, W.S. 1975. The Dalradian Supergroup. pp52-75 IN: *A correlation of Precambrian rocks of the British Isles*. Spec. Rep. geol. Soc. Lond. 6. (1A, 3, 148, 196, 203, 204)

- HAYES, M.O., ANAN, F.S. & BOZEMAN, R.N. 1969. Sediment dispersal trends in the littoral zone; a problem in palaeogeographic reconstruction. pp 290-315 IN: Field Trip Guidebook; coastal environments of NE Massachusetts and New Hampshire, Coastal Research Group, Univ. Mass. (43, 44)
- HAYES, M.O. & KANA, T.W. (eds.) 1976. Terrigenous clastic depositional environments. Tech. Rpt. 11, Coastal Research Division, Dept. Geol. Univ. S. Carolina, Columbia, S. Carolina. (80, 201)
- HEARD, H.C. 1976. Comparison of the flow properties of rocks at crustal conditions. Phil. Trans. R. Soc. A283, 173-86. (163)
- HEMLEY, J.J., MEYER, C. & RICHTER, D.H. 1961. Some alteration reactions in the system  $\text{Na}_2\text{O}-\text{Al}_2\text{O}_3-\text{SiO}_2-\text{H}_2\text{O}$ . U.S. Geol. Surv. Prof. Pap., 424-D, 338-40. (153)
- HENDERSON, J.B. 1975. Archaean stromatolites in the Northern Slave Province, Northwest Territories, Canada. Can. J. Earth. Sci., 12, 1619-30. (67, 70)
- HENDRY, H.E. & STAUFFER, M.R. 1975. Penecontemporaneous recumbent folds in trough cross-bedding of Pleistocene sands in Saskatchewan, Canada. J. Sedim. Petrol., 45, 932-43. (36)
- HENNIG, A. & ELIAS, H. 1971. A rapid method for the visual determination of size distributions of spheres from the size distributions of their sections. J. Microsc., 93, 101-7. (219, 220)
- HILLS, E.S. 1972. Elements of structural geology. Chapman & Hall, London. (169, 173)
- HOBDAY, D.K. & HORNE, J.C. 1977. Tidally influenced barrier island and estuarine sedimentation in the Upper Carboniferous of southern west Virginia. Sediment. Geol., 18, 97-120. (44, 49)
- HOFFMAN, P. 1972. Proterozoic carbonate platform-to-basin facies zonation, Pethi Group, Great Slave Lake, N.W. Territories, Canada. (abs.) Bull. Am. Ass. Petrol. Geol., 56, 627-8. (76)
- HOFFMAN, P. 1975. Shoaling-upward shale-to-dolomite cycles in the Rocknest Formation (Lower Proterozoic) Northwest Territories, Canada. pp257-67 IN: GINSBURG, R.N. (ed.) Tidal deposits. A casebook of Recent examples and fossil counterparts. Springer-Verlag, Berlin. (76)
- HOFFMANN, H.J. 1973. Stromatolites: characteristics and utility. Earth Sci. Rev., 9, 339-73. (72)
- HOFFMANN, H.J. 1975a. Stratiform Precambrian stromatolites, Belcher Islands, Canada: relations between silicified microfossils and microstructure. Am. J. Sci., 275, 1121-32. (70)
- HOFFMANN, H.J. 1975b. Australian stromatolites, an essay review. Geol. Mag., 112, 97-100. (71)
- HOLEYWELL, R.C. & TULLIS, T.E. 1975. Mineral reorientation and slaty cleavage in the Martinsburg Formation, Lehigh Gap, Pennsylvania. Geol. Soc. Am. Bull., 86, 1296-1304. (168)
- HOLLAND, H.D. 1972. The geologic history of sea-water- an attempt to solve the problem. Geochim. cosmochim. Acta., 36, 637-51. (107, 125)
- HOLLISTER, L.S. 1966. Garnet zoning: an interpretation based on the Raleigh fractionation model. Science, N.Y., 154, 1647-51. (143)
- HORODYSKI, R.J. 1975. Stromatolites of the Lower Missoula Group (Middle Proterozoic) Belt Supergroup, Glacier National Park, Montana. Precambrian Res., 2, 215-64. (68)

- HORODYSKI, R.J. 1976. Stromatolites from the Middle Proterozoic Allyn Limestones, Belt Supergroup, Glacier National Park, Montana. pp587-97 IN: WALTER, M.R. Stromatolites. Elsevier, Amsterdam. (67)
- HOWARTH, R.J. 1971. The Portaskaig Tillite succession (Dalradian) of Co. Donegal. Proc. R. Ir. Acad., B71, 1-35. (204)
- HOWARTH, R.J., KILBURN, C. & LEAKE, B.E. 1966. The Boulder Bed succession at Glencolumbkille, County Donegal. Proc. R. Ir. Acad., 65B, 117-56. (204)
- HUBBARD, D.K. & BARWIS, J.H. 1976. Discussion of tidal inlet sand deposits: examples from the South Carolina coast. pp 128-42 IN: HAYES, M.O. & KANA, T.W. (eds.) Terrigenous clastic depositional environments. Tech. Rpt. 11, Coastal Research Division, Dept, Geol. Univ. S. Carolina, Columbia, S. Carolina. (41, 44)
- HUBBARD, J.A.E.B. 1972. Stromatolite fabric: a petrographic model. 24th Int. geol. Congr., 7, 380-396. (66)
- ILLING, L.V., WELLS, A.J. & TAYLOR, J.C.M. 1965. Penecontemporaneous dolomite in the Persian Gulf. pp89-111 IN: PRAY, L.C. & MURRAY, P.C. (eds.) Dolomitization and limestone diagenesis. Soc. Econ. Palaeont. Mineral. Spec. Publ. 13. (92, 93, 98)
- INGERSON, E. 1962. Problems concerning the geochemistry of sedimentary carbonates. Geochim. cosmochim. Acta, 26, 815-47. (125)
- JOHNSON, M.R.W. 1963. Some time relations of movement and metamorphism in the Scottish Highlands. Geologie Mijnb., 42, 121-42. (183)
- JONES, K.A. 1961. Origin of albite porphyroblasts in the rocks of the Ben More-Am Binnein area, western Perthshire, Scotland. Geol. Mag., 98, 41-55. (152)
- KAHLE, C.F. & FLOYD, J.C. 1971. Stratigraphic and environmental significance of sedimentary structures in Caygan (Silurian) tidal flat carbonates, Northwestern Ohio. Bull. Geol. Soc. Am., 82, 2071-98. (76)
- KASTNER, M. 1971. Authigenic feldspar in carbonate rocks. Am. Miner., 56, 1403-42. (130)
- KATZ, A. 1971. Zoned dolomite crystals. J. Geol., 79, 38-51. (106, 123, 124, 141).
- KATZ, A. 1973. The interaction of magnesium with calcite during crystal growth at 25-90°C and one atmosphere. Geochim. cosmochim. Acta, 37, 1563-86. (102A)
- KATZ, A. & MATTHEWS, A. 1977. The dolomitization of CaCO<sub>3</sub>: an experimental study at 252-295°C. Geochim. cosmochim. Acta, 41, 297-308. (102A)
- KATZ, A., SASS, E. & STARINSKY, A. 1972. Strontium behaviour in the aragonite-calcite transformation: an experimental study at 40-98°C. Geochim. cosmochim. Acta, 36, 481-96. (102A)
- KENDALL, C.G. St. C. 1969. An environmental re-interpretation of the Permian evaporite/carbonate shelf sediments of the Guadalupe Mountains. Bull. Geol. Soc. Am., 80, 2503-26. (80, 88).
- KENDALL, C.G.St.C. & SKIPWITH, Sir P.A. d'E. 1968. Recent algal mats of a Persian Gulf lagoon. J. Sedim. Petrol., 38, 1040-58. (72, 79)
- KENNEDY, M.J. 1969a. The metamorphic history of North Achill Island, Co. Mayo, and the problem of the origin of albite schists. Proc. R. Ir. Acad., 67B, 261-80. (152)
- KENNEDY, M.J. 1969b. The structure and stratigraphy of the Dalradian rocks of North Achill Island, Co. Mayo, Ireland. Q. Jl geol. Soc. Lond., 125, 47-81. (204)

- KEPPER, J.C. 1974. Origin of massive banded carbonates with 'Bluebird structures' in the Cambrian of the Eastern Great Basin. *J. Sedim. Petrol.*, 44, 1251-61. (194)
- KERR, S.D. & THOMPSON, A. 1963. Origin of nodular and bedded anhydrite in Permian shelf sediments, Texas and New Mexico., *Bull. Am. Ass. Petrol. Geol.*, 47, 1726-32. (160)
- KILBURN, C., PITCHER, W.S. & SHACKLETON, R.M. 1965. The stratigraphy and origin of the Portaskaig Boulder Bed Series (Dalradian). *Lpool. Manchr. geol. J.*, 4, 343-60. (87, 204).
- KINSMAN, D.J.J. 1969. Interpretation of  $Sr^{2+}$  concentrations in carbonate minerals and rocks. *J. Sedim. Petrol.*, 39, 486-508. (102A, 142)
- KLEIN, G. de V. 1970a. Tidal origin of a Precambrian Quartzite: the Lower Fine-grained quartzite (Middle Dalradian) of Islay, Scotland. *J. Sedim. Petrol.*, 40, 973-85. (1, 6, 7, 34, 35, 35a, 36, 37, 39, 40, 41, 46, 76, 196, 206)
- KLEIN, G. de V. 1970b. Depositional and dispersal dynamics of inter-tidal sand bars. *J. Sedim. Petrol.*, 40, 1095-1127. (34, 36, 44, 61, 63)
- KLEIN, G. de V. 1971. A sedimentary model for determining palaeotidal range. *Bull. geol. Soc. Am.*, 82, 2585-92. (84)
- KNILL, J.L. 1963. A sedimentary history of the Dalradian Series. pp99-121 IN: JOHNSON, M.R.W. & STEWART, F.H. (eds.) *The British Caledonides*. Oliver & Boyd, Edinburgh. (1)
- KOMAR, P.D. 1974. Oscillatory ripple marks and the evaluation of ancient wave conditions and environments. *J. Sedim. Petrol.*, 44, 169-80. (49)
- KRYLOV, I.N. & SEMIKHATOV, N.A. 1976. Table of the ranges of the principal groups of Precambrian stromatolites. pp693-4, IN: WALTER, M.R. (ed.) *Stromatolites*. Elsevier, Amsterdam. (72)
- KUMAR, N. 1973. Modern and ancient barrier sediments: new interpretations based on stratal sequence in inlet-filling sands and on recognition of nearshore storm deposits. *Ann. N. Y. Acad. Sci.*, 220, 247-340. (41, 42, 43).
- KUMAR, N. & SANDERS, J.E. 1974. Inlet sequence: a vertical succession of sedimentary structures and textures created by the lateral migration of tidal inlets. *Sedimentology*, 22, 491-532. (41)
- LAMBERT, R. St. J. & MCKERRROW, W.S. 1976. The Grampian orogeny. *Scott. J. Geol.*, 12, 271-92. (206, 207)
- LAND, L.S. 1973. Contemporaneous dolomitization of middle Pleistocene reefs by meteoric water, North Jamaica. *Bull. mar. Sci.*, 23, 64-92. (93, 94, 105, 129)
- LAND, L.S., SALEM, M.R.I. & MORROW, D.W. 1975. Palaeohydrology of ancient dolomites: geochemical evidence. *Bull. Am. Ass. Petrol. Geol.* 59, 1602-26. (208)
- LAPORTE, L.F. 1967. Carbonate deposition near mean sea level and resultant facies mosaics. Manlius Formation (Lower Devonian) of New York State. *Bull. Am. Ass. Petrol. Geol.*, 51, 73-101. (70, 76, 97)
- LEEDER, M. 1975. Lower Border Group (Tournaisian) stromatolites from the Northumberland basin. *Scott. J. Geol.*, 11, 207-26. (67)
- LEGGO, P.J. & PIDGEON, R.T. 1970. Geochronological investigation of Caledonian history in W. Ireland. *Eclog. geologicae Helveticae*, 63, 207-12. (6)

- LEGGO, P.J., TANNER, P.W.G. & LEAKE, B.E. 1969. Isochron study of Donegal Granite and certain Dalradian rocks of Britain. pp 354-62 IN: KAY, M.(ed.) North Atlantic geology and continental drift., Mem. Am. Ass. Petrol. Geol., 12.
- LIPPMAN, F. 1973. Sedimentary carbonate minerals. Springer-Verlag, Berlin. (92, 98, 104)
- LITHERLAND, M. 1970. The stratigraphy and structure of the Dalradian rocks around Loch Creran, Argyll. Ph. D. Thesis, University of Liverpool. (203)
- LOGAN, B.W., HOFFMAN, P. & GEBELIN, C.D. 1974. Algal mats, cryptalgal fabrics, and structures, Hamelin Pool, Western Australia. pp 140-93 IN: Evolution and diagenesis of Quaternary Carbonate sequences, Shark Bay. Am. Ass. Petrol. Geol. Mem., 22. (65, 71, 80)
- LOGAN, B.W., REZAK, R. & GINSBURG, R.N. 1964. Classification and environmental significance of algal stromatolites. J. Geol., 72, 68-83. (64)
- LONG, J.V.P. & AGRELL, S.O. 1965. Cathode-luminescence of minerals in thin section. Mineralog. Mag., 34, 318-26. (217)
- LOREAU, J-P. & PURSER, B.H. 1973. Distribution and ultrastructure of Holocene ooids in the Persian Gulf. pp279-328 IN: PURSER, B.H. (ed.) The Persian Gulf. Springer-Verlag, Berlin. (79, 88)
- LOVERING, T.S. 1969. The origin of hydrothermal and low temperature dolomite. Econ. Geol., 64, 743-54. (92, 93)
- MCCAVE, I.N. 1971. Discussion of "Tidal origin of a Precambrian Quartzite: the Lower Fine-grained Quartzite of Islay, Scotland". J. Sedim. Petrol., 41, 1147-8. (41)
- MCINTYRE, W.L. 1963. Trace element partition co-efficients - a review of theory and application to geology. Geochim. cosmochim. Acta, 27, 1209-64. (101, 102A, 144, 145)
- MACQUEEN, R.W. & GHENT, E.D. 1970. Electron microprobe study of magnesium distribution in some Mississippian echinoderm limestones from Western Canada. Can. J. Earth Sci., 7, 1308-16. (208)
- MACQUEEN, R.W., GHENT, E.D. & DAVIES, G.R. 1974. Magnesium distribution in living and fossil specimens of the echinoid Peronella lesueri Agassiz, Shark Bay, Western Australia. J. Sedim. Petrol., 44, 60-9. (208)
- MANHEIM, F.T. 1967. Evidence for submarine discharge of water on the Atlantic continental slope of the southern United States, and suggestions for further research. Trans. N.Y. Acad. Sci., 29, 839-53. (105)
- MARDIA, K.V. 1972. Statistics of directional data. Academic Press, London. (63, 99)
- MARSCHNER, H. <sup>(16)</sup> Ca-Mg-distribution in carbonates from the Lower Keuper in NW Germany. pp 128-35 IN: MÜLLER, G. & FRIEDMAN, G.M. Recent developments in carbonate sedimentology in Central Europe. Springer-Verlag, Berlin. (98)
- MASSON, P.H. 1955. An occurrence of gypsum in southwest Texas. J. Sedim. Petrol., 25, 72-7. (136, 137)
- MATHER, J.D. 1970. The biotite isograd and the lower greenschist facies in the Dalradian rocks of Scotland. J. Petrol., 11, 253-75. (183, 184)

- MAZZULLO, S.J. 1976. Significance of authigenic K-feldspar in Cambrian-Ordovician carbonate rocks of the Proto-Atlantic shelf in North America: a discussion. *J. Sedim. Petrol.*, 46, 1035-40. (130)
- MEANS, W.D. 1975. Natural and experimental microstructures in deformed micaceous sandstone. *Bull. geol. Soc. Am.*, 86, 1221-9. (169, 172, 173)
- MEYERS, W.J. 1974. Carbonate cement stratigraphy of the Lake Valley Formation (Mississippian), Sacramento Mountains, New Mexico. *J. Sedim. Petrol.*, 44, 837-61. (123, 141)
- MICHARD, G. 1968. Coprecipitation de l'ion manganoux avec le carbonate de calcium. *C. R. Acad. Sci. Paris (D)* 267, 1685-8. (102A)
- MILLER, J.A. 1975. Facies characteristics of Laguna Madre wind-tidal flats. pp 67-74 IN: GINSBURG, R.N. *Tidal deposits. A casebook of Recent examples and fossil counterparts.* Springer-Verlag, Berlin. (79, 137)
- MILNER, S. 1976. Carbonate petrology and syndepositional facies of the Lower San Andreas Formation (Middle Permian), Lincoln County, New Mexico. *J. Sedim. Petrol.*, 46, 463-82. (58)
- MOBERLY, R. 1968. Composition of magnesian calcites of algae and pelecypods by electron microprobe analysis. *Sedimentology*, 11, 61-82. (208, 209)
- MOBERLY, R. 1970. Microprobe study of diagenesis in calcareous algae. *Sedimentology*, 14, 113-23. (209)
- MONTY, C.L.V. 1967. Distribution and structure of Recent stromatolitic algal mats, eastern Andros Island, Bahamas. *Annls. Soc. geol. Belg.*, 90, 55-100. (64, 72)
- MONTY, C.L.V. 1973. Precambrian background and Phanerozoic history of stromatolitic communities, an overview. *Annls. Soc. geol. Belg.*, 96, 585-624. (72, 126)
- MONTY, C.L.V. 1976. The origin and development of cryptalgal fabrics. pp 193-249 IN: WALTER, M.R. (ed.) *Stromatolites*, Elsevier, Amsterdam. (66, 68)
- MOORE, C.H. 1973. Intertidal carbonate cementation Grand Cayman, West Indies. *J. Sedim. Petrol.*, 43, 591-602. (208)
- MOSHER, S. 1976. Pressure solution as a deformation mechanism in Pennsylvanian conglomerates from Rhode Island. *J. Geol.*, 84, 355-64. (174)
- MUKHERJI, K.K. & YOUNG, G.M. 1973. Diagenesis of the Black River (Middle Ordovician) limestones in southern Ontario, Canada. *Sediment. Geol.*, 9, 21-52. (57)
- MÜLLER, G., IRION, G. & FORSTNER, U. 1972. Formation and diagenesis of inorganic Ca-Mg carbonates in the lacustrine environment. *Naturwissenschaften*, 59, 158-64. (92, 93, 94, 104)
- MÜLLER, G. & TIETZ, G. 1966. Recent dolomitization of Quaternary biocalcarenites from Fuerteventura (Canary Islands). *Contr. Miner. Petrol.*, 13, 89-96. (92, 104)
- ODOM, I.E., DOE, T.W. & DOTT, R.H. 1976. Nature of feldspar-grain size relations in some quartz-rich sandstones. *J. Sedim. Petrol.*, 46, 862-70. (89)
- OLDERSHAW, A.E. & SCOFFIN, T.P. 1967. The source of ferroan and non-ferroan cements in Halkin and Wenlock Limestones. *Geol. J.*, 5, 309-20. (106)
- OOMKENS, E. 1974. Lithofacies relations in the Late Quaternary Niger Delta complex. *Sedimentology*, 21, 195-222. (41)

- ORVILLE, P.M. 1962. Alkali metasomatism and feldspars. *Norsk. geol. Tidsskrift*, 42, 283-316. (153)
- PABST, A. 1931. Pressure shadows and the measurement of orientation of minerals in rocks. *Am. Miner.*, 16, 55-61. (169, 172, 173, 178)
- PARK, R. 1976. A note on the significance of lamination in stromatolites. *Sedimentology*, 23, 379-93. (66)
- PARK, W.C. & SCHOT, E.H. 1968. Stylolites: their nature and origin. *J. Sedim. Petrol.*, 38, 175-91. (147)
- PEACH, B.N. & HORNE, J. 1930. Chapters on the geology of Scotland. Oxford Univ. Press, London. (6, 16)
- PETTIJOHN, F.J. 1975. Sedimentary rocks, Harper & Row, N.Y. (152)
- PETTIJOHN, F.J., POTTER, P.E. & SIEVER, R. 1972. Sand and sandstone, Springer-Verlag, Berlin. (88, 192)
- PHILLIPS, W.E.A., STILLMAN, C.J. & MURPHY, T. 1976. A Caledonian plate tectonic model. *Jl geol. Soc. Lond.*, 132, 579-609. (195, 205, 206)
- PHILLIPS, W.J. 1974. The development of vein and rock textures by tensile strain crystallization. *Jl geol. Soc. Lond.*, 130, 441-8. (178)
- PHILLIPS, W.J. 1975. IN: Discussion of the development of vein and rock textures by tensile strain crystallization. *Jl geol. Soc. Lond.*, 131, 433. (30)
- PITCHER, W.S. & BERGER, A.R. 1972. The geology of Donegal: a study of granite emplacement and unroofing. Wiley Interscience, N.Y. (204)
- POWELL, C.McA. 1969. Intrusive sandstone dykes in the Sianes Slate near Negaunee, Michigan. *Geol. Soc. Am. Bull.*, 80, 2585-94. (169)
- PRICE, N.J. 1975. Rates of deformation. *Jl geol. Soc. Lond.*, 131, 553-75. (163)
- PURSER, B.H. & EVANS, G. 1973. Regional sedimentation along the Trucial Coast, SE Persian Gulf. pp 211-31 IN: PURSER, B.H. (ed.) *The Persian Gulf*. Springer-Verlag, Berlin. (79)
- PURSER, B.H. & SEIBOLD, E. 1973. The principal environmental factors influencing Holocene sedimentation and diagenesis in the Persian Gulf. pp 1-90 IN: PURSER, B.H. (ed.) *The Persian Gulf*. Springer-Verlag, Berlin. (79)
- RAAF, J.F.M. de, BOERSMA, J.R. & GELDER, A. van 1977. Wave-generated structures and sequences from a shallow marine succession, Lower Carboniferous, County Cork, Ireland. *Sedimentology*, 24, 451-83. (40, 49)
- RAMDOHR, P. 1969. The ore minerals and their intergrowths (English edition). Pergamon Press, Oxford. (157)
- RAST, N. & LITHERLAND, M. 1970. The correlation of the Ballachullish and Perthshire (Iltay) successions. *Geol. Mag.*, 107, 259-72. (1, 21)
- RAYBOULD, J.G. 1975. Tectonic control on the formation of some fibrous quartz veins, Mid-Wales. *Geol. Mag.*, 112, 81-90. (176, 178)
- READ, J.F. 1974. Carbonate banks and wave-built platform sedimentation, Edel Province, Shark Bay, Western Australia. *Am. Ass. Petrol. Geol. Mem.*, 22, 1-60. (80)
- READING, H.G. & WALKER, R.G. 1966. Sedimentation of Eocambrian tillites and associated sediments in Finnmark, Northern Norway. *Palaeogeogr. Palaeoclim. Palaeoecol.*, 2, 177-212. (198)
- REED, S.J.B. 1973. Principles of X-ray generation and quantitative analysis with the electron microprobe. IN: ANDERSON, C.A. (ed.) *Microprobe Analysis*, Wiley, N.Y. (213)

- REES, M.N., BRADY, M.J. & ROWELL, A.J. 1976. Depositional environment of the Upper Cambrian John Wash Limestone (Howes Range, Utah). *J. Sedim. Petrol.*, 46, 38-47. (80, 81).
- REINECK, H-E. 1967. Layered sediments of tidal flats, beaches and shelf bottoms of the North Sea. pp 191-206 IN: LAUFF, F.H. (ed.) *Estuaries. Am. Ass. Adv. Sci.*, Washington D.C. (34, 40)
- REINECK, H-E. 1969. Tidal flats (abs.) *Am. Ass. Petrol. Geol. Bull.*, 737. (63)
- REINECK, H-E. & SINGH, I.B. 1972. Genesis of laminated sand and graded rhythmicity in storm-sand layers of shelf mud. *Sedimentology*, 18, 123-8. (34, 40, 84)
- REINECK, H-E. & SINGH, I.B. 1973. *Depositional sedimentary environments.* Springer-Verlag, Berlin-Heidelberg-New York. (5)
- REINECK, H-E. & WUNDERLICH, F. 1968. Classification and origin of flaser and lenticular bedding. *Sedimentology*, 11, 99-104. (37)
- RICHTER, D.K. 1974. Entstehung und diagenese der devonischen und permotriassischen Dolomite in der Eifel. *Contr. Sedimentol.* 2, Schweizerbart, Stuttgart. (189)
- ROBERTS, J.D. 1976. Late Precambrian dolomites, Vendian glaciation, and synchronicity of Vendian glaciations. *J. Geol.*, 84, 47-63. (126)
- ROBERTS, J.L. 1974. The structure of the Dalradian rocks in the SW Highlands of Scotland. *Jl geol. Soc. Lond.*, 130, 93-124. (17, 20, 20A, 22, 26, 31)
- RUSNAK, G.A. 1960. Sediments of the Laguna Madre. pp 153-96 IN: SHEPARD, F.P., PALEGER, F.B. & ANDEL, T.H. van *Recent sediments Northwest Gulf of Mexico. Am. Ass. Petrol. Geol. Tulsa, Oklahoma.*
- RUTTER, E.H. 1976. The kinetics of rock deformation by pressure solution. *Phil. Trans. R. Soc. Lond.* A283, 203-19. (162, 162A, 164).
- SANDBERG, P.A. 1975. New interpretations of Great Salt Lake ooids and of ancient non-skeletal carbonate mineralogy. *Sedimentology*, 22, 497-538. (125)
- SCHENK, P.E. 1967. The Macumber Formation of the Maritime Provinces, Canada - a Mississippian analogue to recent strand-line carbonates of the Persian Gulf. *J. Sedim. Petrol.*, 37, 365-76. (76)
- SCHERER, M. 1977. Preservation, alteration and multiple cementation of aragonitic skeletons from the Cassian Beds (U. Triassic, Southern Alps): petrographic and geochemical evidence. *Neues. Jahrbuch Geol. Paläont. Abh.*, 154, 213-62. (112, 121)
- SCHERMERHORN, L.J.G. 1974. Late Precambrian mictites: glacial and/or non-glacial? *Am. J. Sci.*, 274, 673-824. (126)
- SCHWARTZ, R.K. 1975. Nature and genesis of some storm washover deposits. *Tech. Mem. No. 61, U.S. Coastal Eng. Res. Center, Ft. Belvoir, Va.* (42, 43, 44)
- SCHWARZ, H-U. 1975. Sedimentary structures and facies analysis of shallow marine carbonates (Lower Muschelkalk, Middle Triassic, SW Germany). *Contr. Sedimentology. 3.* Schweizerbart, Stuttgart. (58, 101)
- SCHWARZACHER, W. 1975. *Sedimentation models and quantitative stratigraphy.* Elsevier, Amsterdam. (75)
- SEREBRYAKOV, S.N. 1976. Biotic and abiotic factors controlling the morphology of Riplean stromatolites. pp 321-36 IN: WALTER, M.R. (ed.) *Stromatolites.* Elsevier, Amsterdam. (66)

- SHEARMAN, D.J. 1966. Origin of marine evaporites by diagenesis. *Trans. Inst. Min. Metall.*, 75, B208-15. (160)
- SHEARMAN, D.J., MOSSOP, G., DUNSMORE, H. & MARTIN, M. 1972. Origin of gypsum veins by hydraulic fracture. *Trans. Int. Min. Metall.*, 81, B149-55. (28, 178)
- SHELTON, J.W. 1962. Shale compaction in a section of Cretaceous Dakota Sandstone, Northwestern North Dakota. *J. Sedim. Petrol.*, 32, 873-7. (56)
- SHINN, E.A. 1968. Practical significance of birdseye structures in carbonate rocks. *J. Sedim. Petrol.*, 38, 215-23. (58)
- SIDDANS, A.W.B. 1976. Deformed rocks and their textures. *Phil. Trans. R. Soc. Lond. A*, 283, 43-54. (168)
- SILLÉN, L.G. 1965. Oxidation state of earth's ocean and atmosphere I: a model calculation on earlier states. The myth of the 'probiotic soup'. *Arkiv Kemi*, 24, 431-56. (107)
- SILLÉN, L.G. 1966. Oxidation state of earth's ocean and atmosphere II. The behaviour of Fe, S and Mn in earlier states. Regulating mechanisms for O<sub>2</sub> and N<sub>2</sub>. *Arkiv Kemi*, 25, 159-76. (107)
- SIPPEL, R.F. & GLOVER, E.D. 1965. Structures in carbonate rocks made visible by luminescence petrography. *Science, N.Y.* 150, 1283-7. (217)
- SMITH, A.G. 1976. Plate tectonics and orogeny: a review. *Tectonophysics*, 33, 215-85. (206)
- SOMMER, S.E. 1972a. Cathodoluminescence of carbonates, 1. Characterization of cathodoluminescence from carbonate solid solutions. *Chem. Geol.*, 9, 257-73. (218)
- SOMMER, S.E. 1972b. Cathodoluminescence of carbonates 2. Geological applications. *Chem. Geol.*, 9, 275-84. (218)
- SPENCER, A.M. 1969. Discussion of 'Late Precambrian glaciation in Scotland'. *Proc. geol. Soc. Lond.*, 1657, 177-98. (98, 160, 197, 198)
- SPENCER, A.M. 1971a. Late Precambrian glaciation in Scotland. *Mem. geol. Soc. Lond.* 6. (1, 7, 10, 13, 18, 32, 33, 34, 86, 87, 160, 197, 198, 204)
- SPENCER, A.M. 1971b. Discussion of 'Tidal origin of a Precambrian Quartzite: the Lower Fine-grained Quartzite of Islay' by G. de V. Klein. *J. Sedim. Petrol.*, 41, 884-5. (7, 38, 39)
- SPENCER, A.M. 1975. Late Precambrian glaciation in the North Atlantic region. pp217-40 IN: WRIGHT, A.E. & MOSELEY, F. *Ice ages: ancient and modern*. Seel House Press, Liverpool. (87)
- SPENCER, A.M. & PITCHER, W.S. 1968. Occurrence of the Port Askaig Tillite in north-east Scotland. *Proc. geol. Soc. Lond.*, 1650, 195-8. (203)
- SPENCER, A.M. & SPENCER, M.O. 1972. The late Precambrian/Lower Cambrian Bonahven Dolomite of Islay and its stromatolites. *Scott. J. Geol.*, 8, 269-82. (2, 4, 5, 6, 7, 8, 10, 11, 12, 15, 38, 55, 56, 64, 71, 91)
- SPRY, A. 1969. *Metamorphic textures*. Pergamon Press, Oxford. (145, 157, 169, 173)
- STASHCHUK, M.F. 1972. *The oxidation-reduction potential in geology (English translation)*. Consultants Bureau, New York-London. (107)
- STEWART, A.D. 1975. 'Torridonian' rocks of western Scotland. pp 43-51 IN: *A correlation of the Precambrian rocks in the British Isles*. *Spec. Rept. Geol. Soc. Lond.* 6. (1A)

- STRAATEN, L.M.J.U. van 1954a. Sedimentology of Recent tidal flat deposits and the Psammites du Condroz (Devonian). *Geologie Mijnb.*, 16, 25-47. (56)
- STRAATEN, L.M.J.U. van 1954b. Composition and structure of recent marine sediments in the Netherlands. *Leid. geol. Medel.*, 19, 1-110. (41, 56, 63)
- SWEENEY, R.E. & KAPLAN, I.R. 1973. Pyrite framboid formation: laboratory synthesis and marine sediments. *Econ. Geol.*, 68, 618-34. (150)
- SWETT, K. 1965. Dolomitization, silicification and calcitisation patterns in Cambro-Ordovician oolites from Northwest Scotland. *J. Sedim. Petrol.*, 35, 928-38. (159, 194)
- SWETT, K. 1968. Authigenic feldspars and cherts resulting from dolomitization of illitic limestones: a hypothesis. *J. Sedim. Petrol.*, 38, 128-35. (130)
- TANNER, W.F. 1960. Shallow-water ripple mark varieties. *J. Sedim. Petrol.*, 30, 481-5. (51)
- TANNER, W.F. 1967. Ripple mark indices and their uses. *Sedimentology*, 9, 75-88. (49)
- TANNER, W.F. 1971. Numerical estimates of ancient waves, water depth and fetch. *Sedimentology*, 16, 71-88. (44, 49)
- TEICHMÜLLER, M. & TEICHMÜLLER, R. 1968. Geological aspects of coal metamorphism. pp 233-67 IN: MURCHISON, D. & WESTOLL, T.S. (eds.) *Coal and coal-bearing strata*. Oliver & Boyd, Edinburgh & London. (148)
- TERWINDT, J.H.J. 1971. Litho-facies of inshore estuarine and tidal inlet deposits. *Geologie Mijnb.*, 50, 515-26. (41)
- THOMPSON, J.B. & NORTON, S.A. 1968. Palaeozoic regional metamorphism in New England and adjacent areas. pp 319-27 IN: ZEN, E.A., WHITE, W.S., HADLEY, J.B. & THOMPSON, J.B. *Studies of Appalachian Geology*, Wiley Interscience, N.Y. (184)
- THRAILKILL, J. 1968. Dolomite cave deposits from Carlsbad Caverns. *J. Sedim. Petrol.*, 38, 141-5. (94)
- TRUSWELL, J.F. & ERIKSSON, K.A. 1975. A palaeoenvironmental interpretation of the Early Proterozoic Malmani Dolomite from Zwarktops, South Africa. *Precambrian Res.*, 2, 277-303. (80, 81)
- TUCKER, M.E. 1976. Replaced evaporites from the late Precambrian of Finnmark, Arctic Norway. *Sediment. Geol.*, 16, 193-204. (161)
- TUCKER, M.E. 1977. Stromatolite biostromes and associated facies in the late Precambrian Porsanger Dolomite Formation of Finnmark, Arctic Norway. *Palaeogeogr. Palaeoclim. Palaeoecol.*, 21, 55-83. (81, 88, 159)
- TUCKER, M.E. & KENDALL, A.C. 1973. The diagenesis and low-grade metamorphism of Devonian stylolinitid-rich pelagic carbonates from W. Germany: possible analogues of recent pteropod oozes. *J. Sedim. Petrol.*, 43, 672-87. (167)
- TULLIS, T.E. & WOODS, D.S. 1975. Correlation of finite strain from both reduction bodies and preferred orientation of mica in slate from Wales. *Bull. geol. Soc. Am.* 86, 632-8. (168)
- TUREKIAN, K.K. 1968. *Oceans*. Prentice-Hall, New Jersey. (103)
- VEIZER, J. 1974. Chemical diagenesis of belemnite shells and possible consequences for paleotemperature determination. *Neues. Jb. Geol. Palaont. Abh.*, 147, 91-111. (102A)

- VEIZER, J. 1977a. Geochemistry of lithographic limestones and dark marls from the Jurassic of southern Germany. *Neues. Jb. Geol. Palaont. Abh.*, 153, 129-146. (102A, 103)
- VEIZER, J. 1977b. Diagenesis of pre-Quaternary carbonates as indicated by tracer studies. *J. Sedim. Petrol.*, 47, 565-81. (190)
- VEIZER, J., LEMIEUX, J., JONES, B., GIBLING, M.R. & SAVELLE, J. 1977. Sodium: palaeosalinity indicator in ancient carbonate rocks. *Geology*, 5, 177-9. (98)
- VERNON, R.H. 1968. Microstructures of high-grade metamorphic rocks at Broken Hill, Australia. *J. Petrol.*, 9, 1-22. (157)
- WALKER, F. 1960. The Islay-Jura dyke swarm. *Trans. geol. Soc. Glasg.*, 24, 121-33. (8, 186).
- WALTER, M.R. 1972. Stromatolites and the biostratigraphy of the Australian Pre-Cambrian and Cambrian. *Spec. Pap. Palaeont.*, 11. (64)
- WALTER, M.R. (ed.) 1976. *Stromatolites*. Elsevier, Amsterdam. (64, 71)
- WEAVER, C.E. 1960. Possible uses of clay minerals in the search for oil. *Bull. Am. Ass. Petrol. Geol.*, 44, 1505-18. (149)
- WEBER, J.N. 1964. Trace element composition of dolostones and dolomites and its bearing on the dolomite problem. *Geochim. cosmochim. Acta*, 28, 1817-68. (102, 108A).
- WEBER, K. 1972. Note on determination of illite crystallinity. *Neues. Jb. Miner. Mh.*, 267-76. (149)
- WHITE, S. 1973. Syntectonic recrystallization and texture development in quartz. *Nature, Phys. Sci.*, 244, 276-8. (163)
- WHITE, S. 1976. The effects of strain on the microstructures, fabrics, and deformation mechanisms in quartzites. *Phil. Trans. R. Soc. Lond. A283*, 69-86. (162, 162A, 163, 164)
- WHITE, W.A. 1961. Colloid phenomena in the sedimentation of argillaceous rocks. *J. Sedim. Petrol.*, 31, 560-70. (56, 57)
- WICKHAM, J. & ANTHONY, M. 1977. Strain paths and folding of carbonate rocks near Blue Ridge, central Appalachians. *Bull. geol. Soc. Am.*, 88, 920-4. (30)
- WILKINSON, S.B. 1907. The geology of Islay. *Mem. geol. Surv. U.K.* (4, 5, 16, 20A)
- WILLIAMS, G.E. 1975. Late Precambrian glacial climate and the earth's obliquity. *Geol. Mag.*, 112, 441-65. (126)
- WILLIAMS, P.F. 1972a. Development of metamorphic layering and cleavage in low grade metamorphic rocks at Bermagui, Australia. *Am. J. Sci.*, 272, 1-47. (169, 180)
- WILLIAMS, P.F. 1972b. 'Pressure shadow' structures in foliated rocks from Bermagui, New South Wales. *J. geol. Soc. Aust.*, 18, 371-7. (169, 170)
- WILSON, J.L. 1975. *Carbonate facies in geological history*. Springer-Verlag, Berlin. (91)
- WILSON, R.C.L. 1966. Silica diagenesis in Upper Jurassic limestones of Southern England. *J. Sedim. Petrol.*, 36, 1036-49. (133)
- WINKLER, H.G.F. 1976. *Petrogenesis of metamorphic rocks*. (4th edition) Springer-Verlag, Berlin. (2, 148, 149, 152, 163, 182, 183)
- WOODLAND, A.W. 1938. Petrological studies in the Harlech Grit Series of Merionethshire. II. *Geol. Mag.*, 75, 440-54. (171)
- WRIGHT, A.E. 1976. Alternating subduction directions and the evolution of the Atlantic Caledonides. *Nature Lond.*, 264, 156-60. (206)

- YOUNG, G.M. 1973. Origin of carbonate-rich early Proterozoic Espanola Formation, Ontario, Canada. Geol. Soc. Am. Bull., 84, 135-60. (108A, 109)
- ZENGER, D.H. 1972. Significance of supratidal dolomitization in the geological record. Bull. geol. Soc. Am., 83, 1-11. (76, 91, 98)
- ZENGER, D.H. 1973. Syntaxial calcite borders on dolomite crystals, Little Falls Formation (Upper Cambrian), New York. J. Sedim. Petrol., 43, 118-24. (129, 194)

\* \* \*



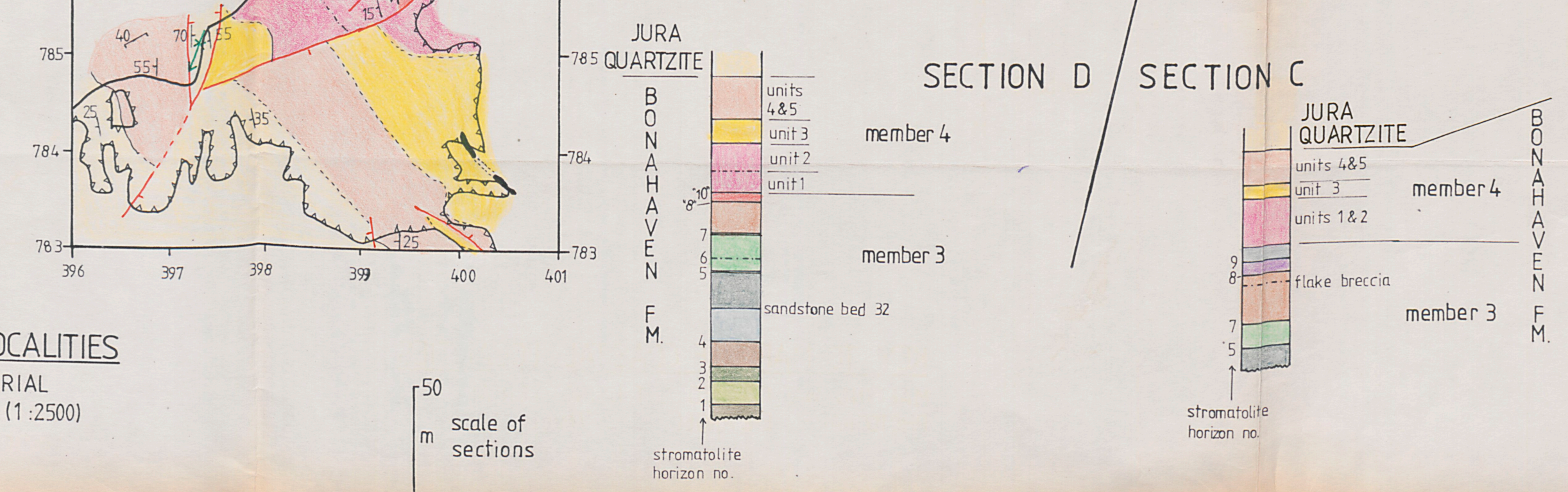
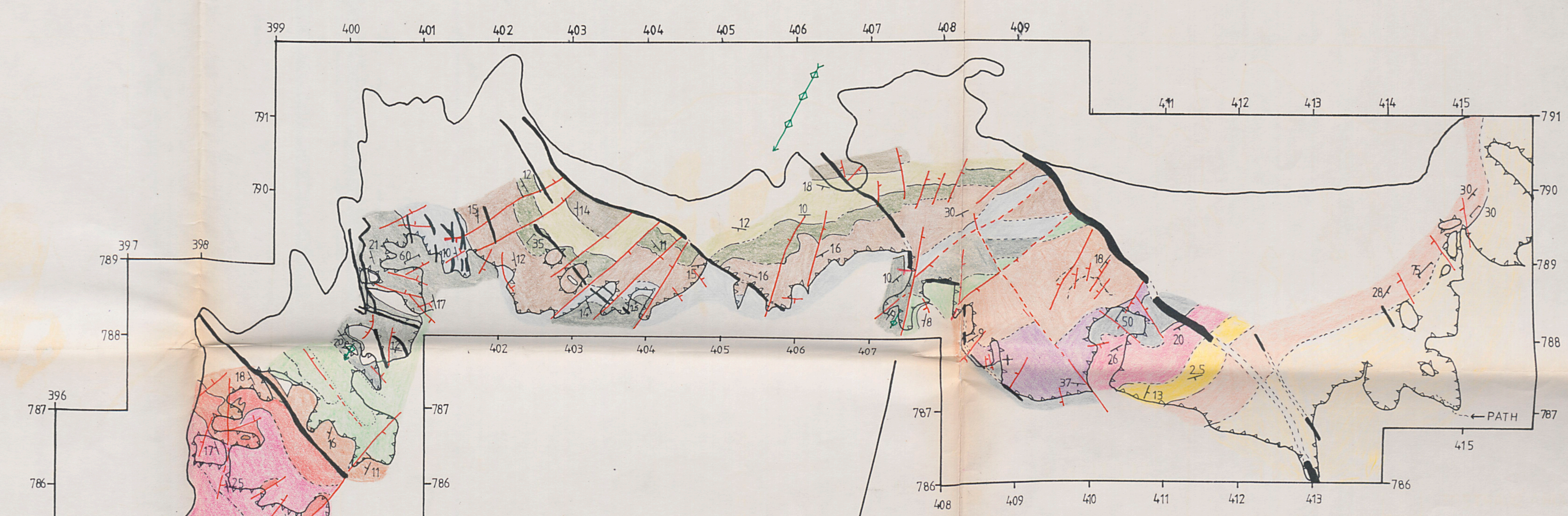
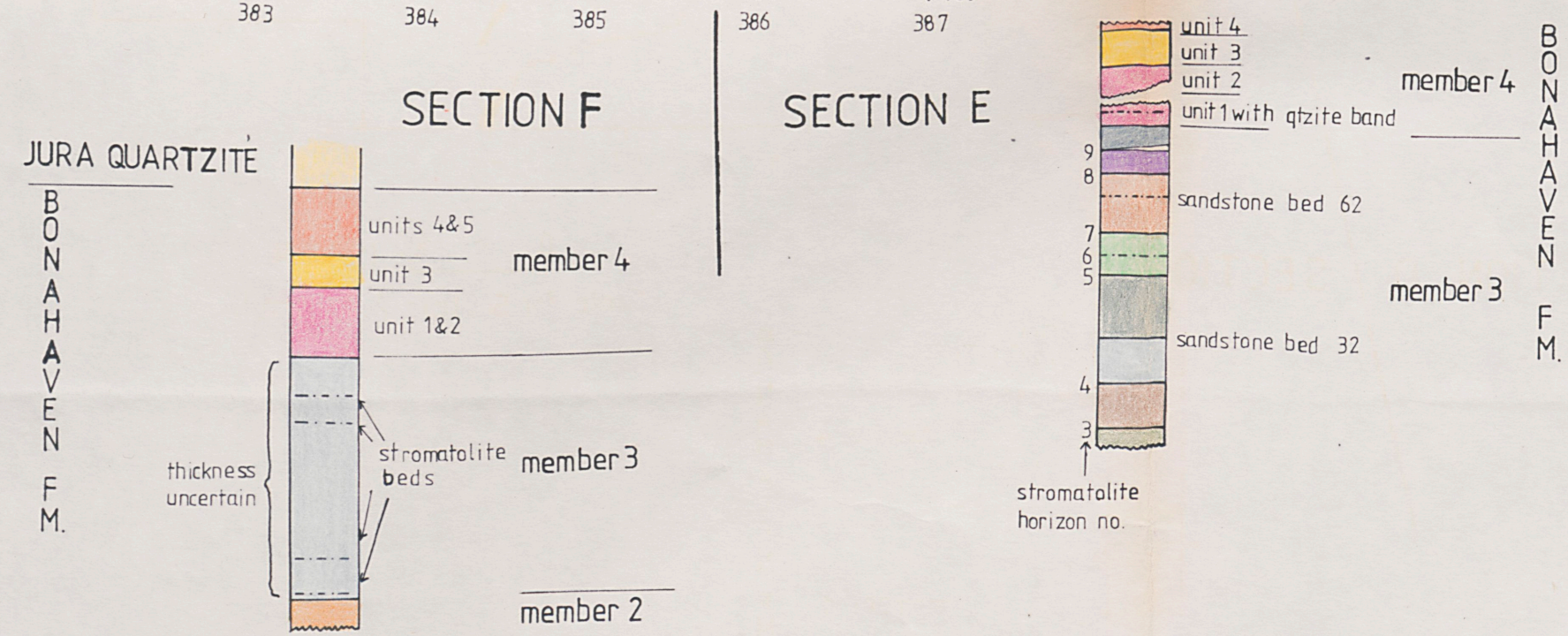
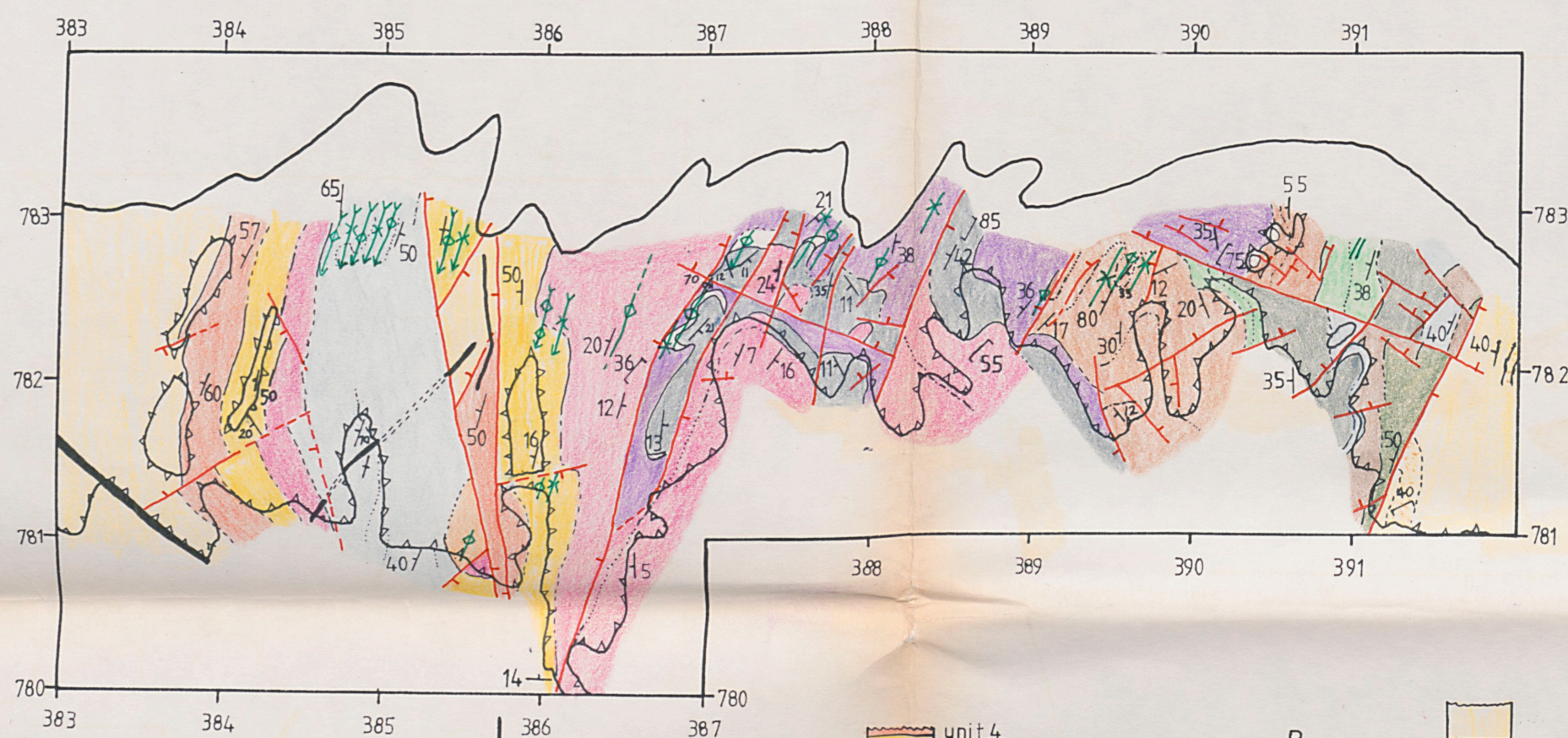
## IMAGING SERVICES NORTH

Boston Spa, Wetherby  
West Yorkshire, LS23 7BQ  
[www.bl.uk](http://www.bl.uk)

# CONTAINS MAPS

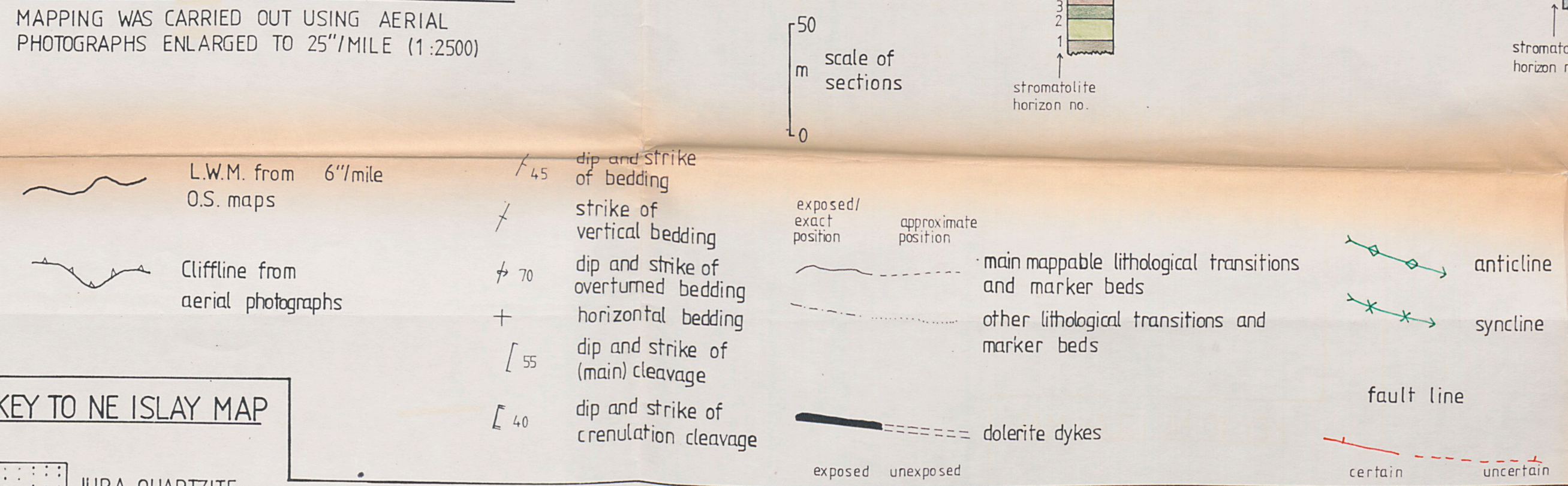
ENCLOSURE 1: GEOLOGICAL MAPS

Scale for Sections E and F  
0 m 100 (1:4000)

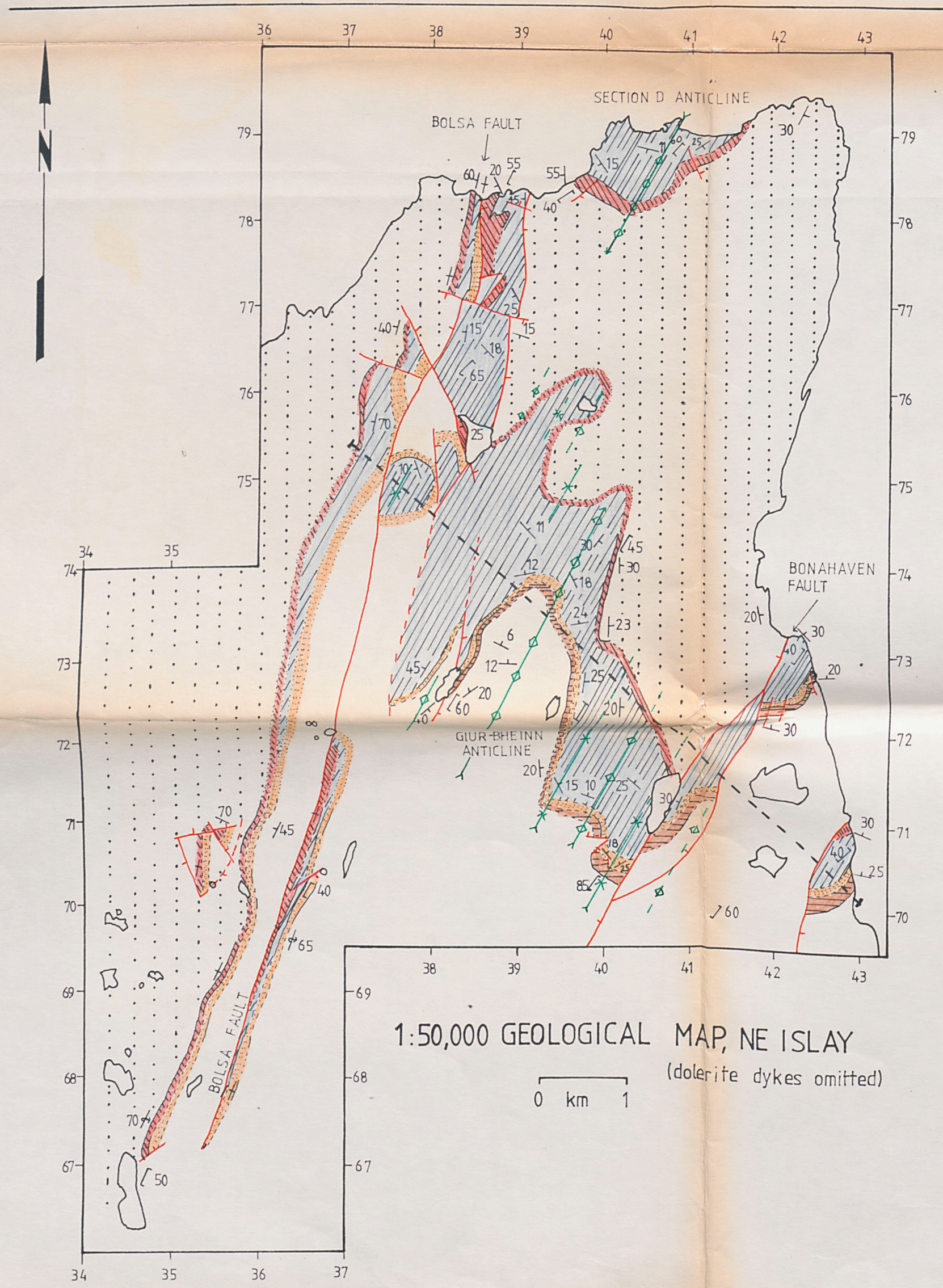
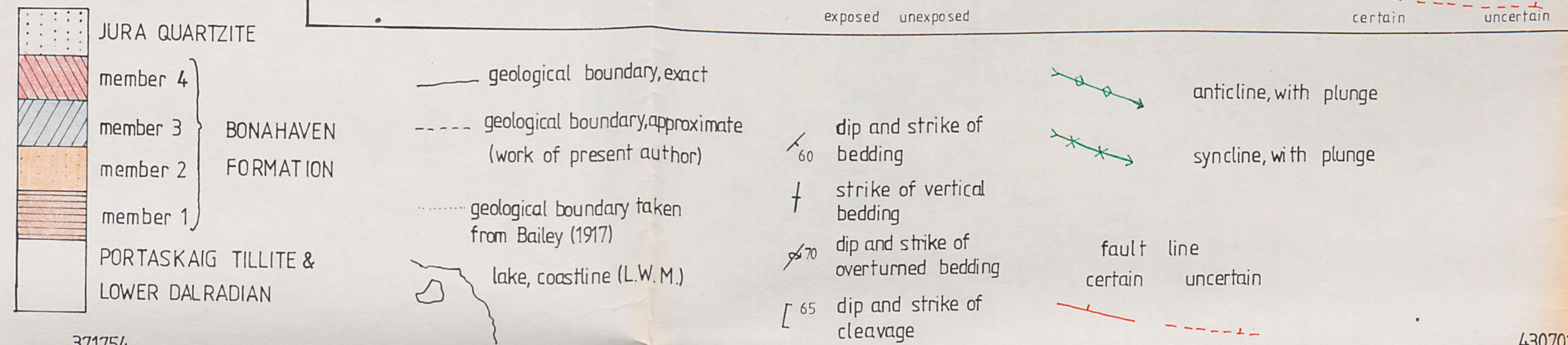


KEY TO MAPS OF COASTAL LOCALITIES

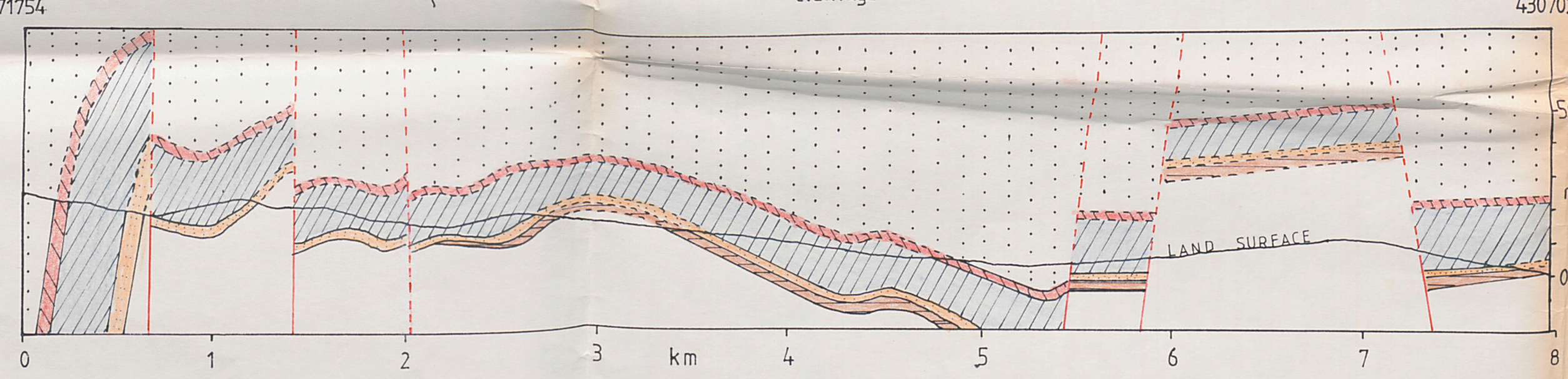
MAPPING WAS CARRIED OUT USING AERIAL PHOTOGRAPHS ENLARGED TO 25"/MILE (1:2500)



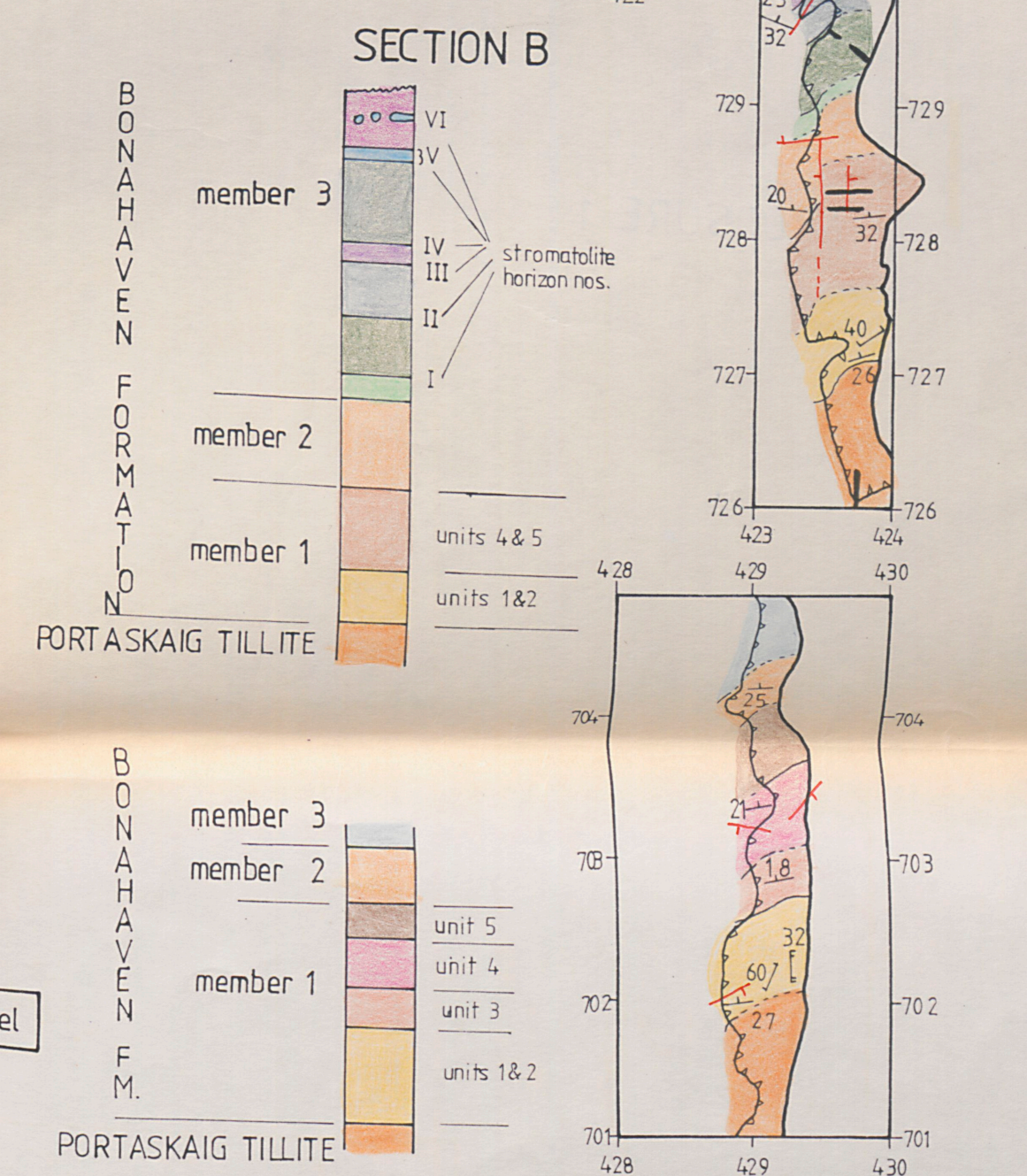
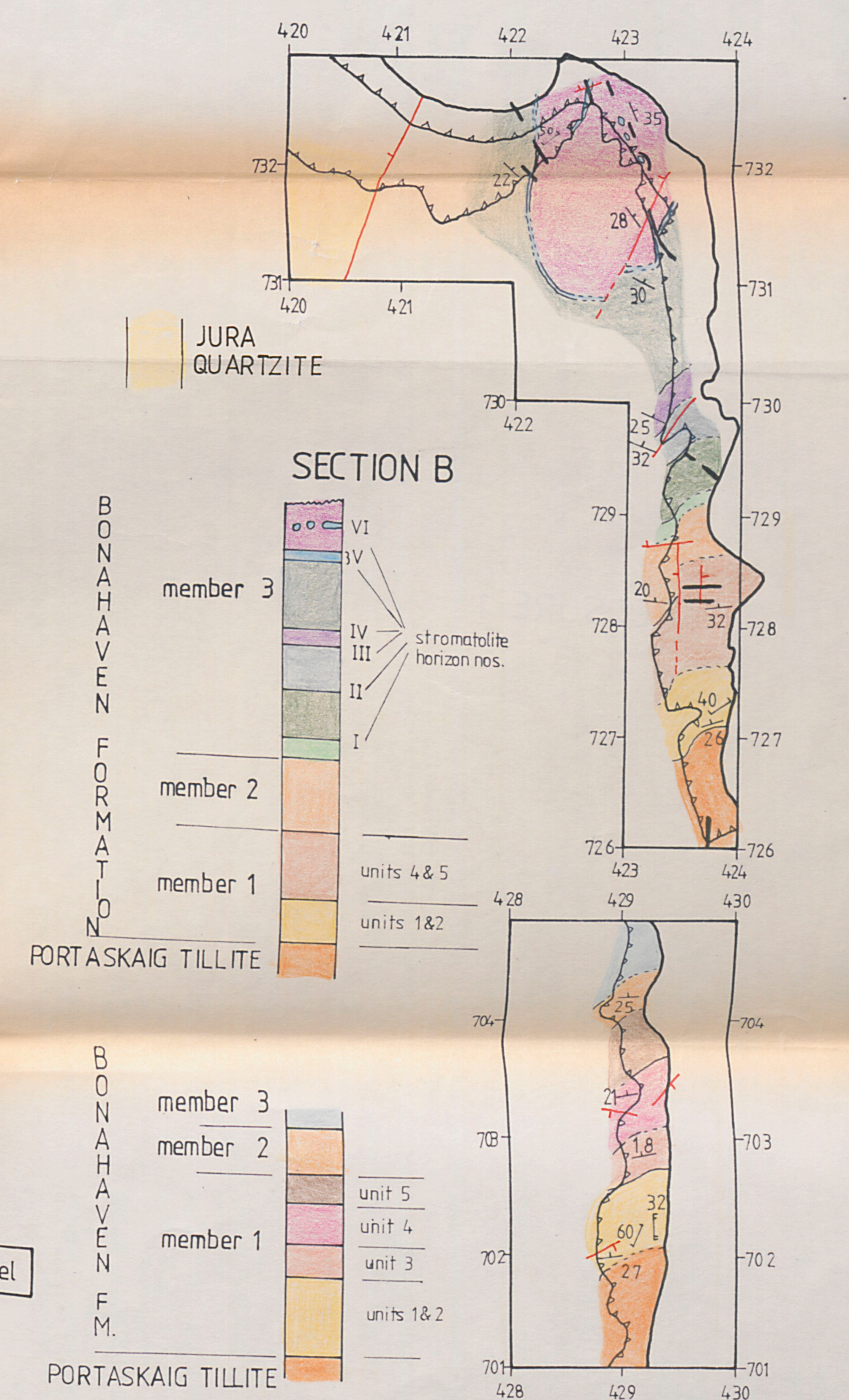
KEY TO NE ISLAY MAP



1:50,000 GEOLOGICAL MAP, NE ISLAY (dolerite dykes omitted)

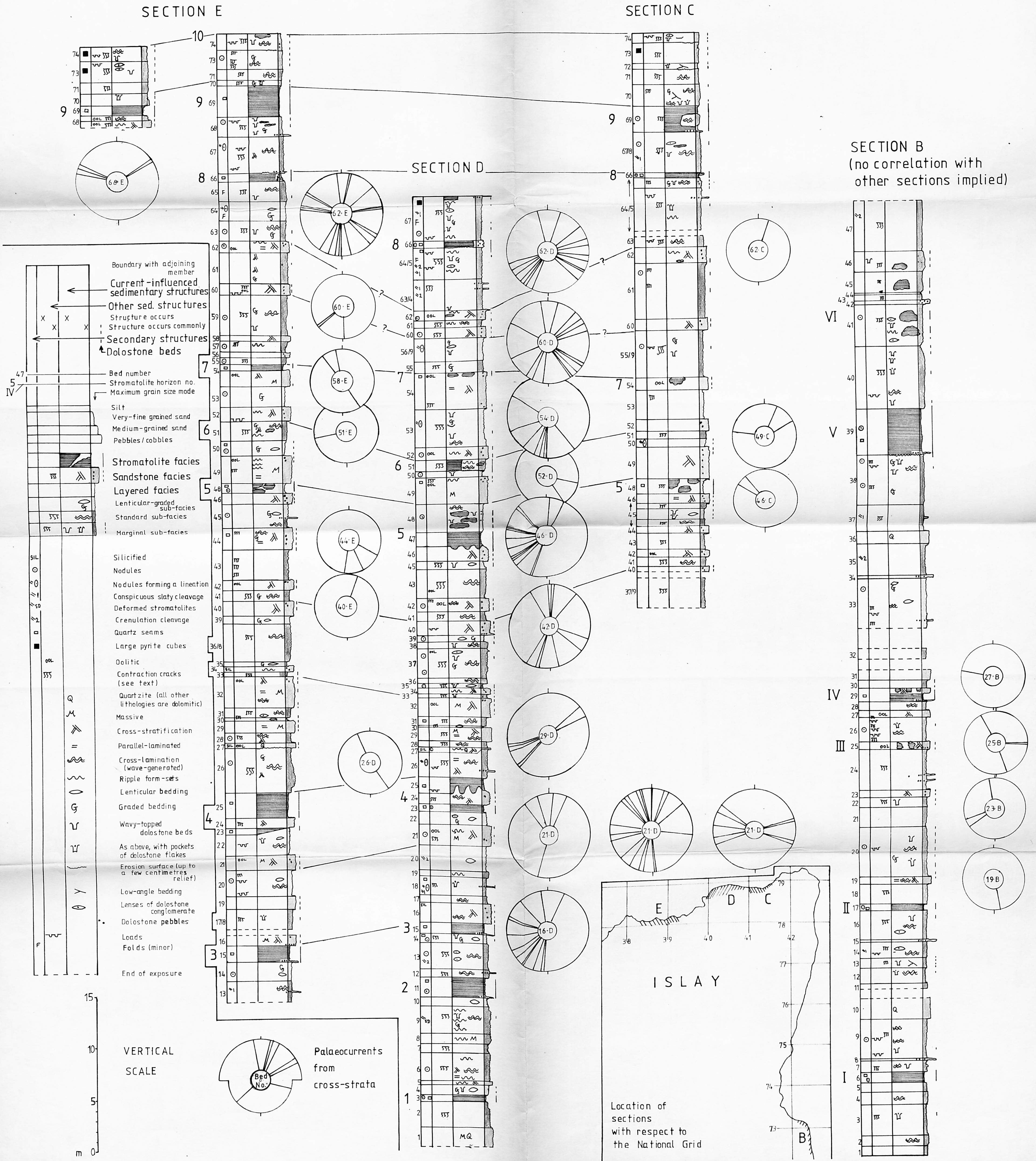


SECTION ALONG DASHED LINE OF 1:50,000 MAP



SECTION A (base only)

ENCLOSURE 2 : MEMBER 3 SECTIONS AND PALAEOCURRENTS FROM CROSS-STRATA



# ENCLOSURE 3: LATERAL VARIATIONS IN MEMBER 3 FACIES ALONG THE NORTH COAST OF ISLAY

